Non-enzymatic regeneration of ergothioneine after reaction with singlet oxygen

Inaugural-Dissertation

zur Erlangung des Doktorgrades
der Mathematisch-Naturwissenschaftlichen Fakultät
der Heinrich-Heine-Universität Düsseldorf

vorgelegt von

Mhmd Oumari
aus Hasaka / Syrien

Düsseldorf, Juli 2019

aus dem Institut für Pharmakologie
der Universität zu Köln

Gedruckt mit der Genehmigung der
Mathematisch-Naturwissenschaftlichen Fakultät der
Heinrich-Heine-Universität Düsseldorf

Berichterstatter:

1. Prof. Dr. Peter Proksch

2. Prof. Dr. Dirk Gründemann

Tag der mündlichen Prüfung: 18.09.2019

Eidesstattliche Versicherung

Ich versichere an Eides Statt, dass die Dissertation von mir selbstständig und ohne unzulässige fremde Hilfe unter Beachtung der "Grundsätze zur Sicherung guter wissenschaftlicher Praxis an der Heinrich-Heine-Universität Düsseldorf" erstellt worden ist. Gedankengut oder Daten, die aus fremden Quellen entliehen wurden, sind kenntlich gemacht. Diese Dissertation ist von mir noch an keiner anderen Stelle vorgelegt worden.

Ich habe vormals noch keinen Promotionsversuch unternommen.

Düsseldorf, Juli 2019 ……

(Mhmd Oumari)

Acknowledgments

First of all, I would like to profoundly thank Professor Dr. Dirk Gründemann for awarding me the project, the friendly support and the opportunity to do my PhD in his work group. It has been an honor to be his student.

I am very grateful to Professor Dr. Peter Proksch for his support and allowing me to do my PhD thesis at the University of Düsseldorf.

I would like to thank our co-operation partners, Professor Dr. Bernd Goldfuss for his support through Density Functional Theory (DFT) computations, and Professor Dr. Hans-Günther Schmalz for the synthesis of endoperoxide ($DHPNO_2$).

I would also like to thank the members of the work group of Professor Dr. Dirk Gründemann and my colleagues Kathi, Samira, Simone, Julia, Julian, Chih-hsuan and Lea, as well as previous colleagues, Peter and Christopher for the great working atmosphere and their support.

I would like to thank my family, parents, siblings and friends for their support and motivation during my PhD and in all aspects of life.

Publications

1) Oumari, M., B. Goldfuss, C. Stoffels, H.G. Schmalz and D. Grundemann, *Regeneration of ergothioneine after reaction with singlet oxygen.* Free Radic Biol Med, 2019. **134**: p. 498-504.

2) Stoffels, C., M. Oumari, A. Perrou, A. Termath, W. Schlundt, H.G. Schmalz, M. Schafer, V. Wewer, S. Metzger, E. Schomig and D. Grundemann, *Ergothioneine stands out from hercynine in the reaction with singlet oxygen: Resistance to glutathione and TRIS in the generation of specific products indicates high reactivity.* Free Radic Biol Med, 2017. **113**: p. 385-394.

Abstract

Ergothioneine (ET) is a histidine betaine derivative with a sulfur atom attached to the position two of the imidazole ring. As established, ET eradicates singlet oxygen ($^1O_2$) and has been considered an antioxidant. Various functions of ET regarding reactive oxygen species (ROS) have been proposed and much progress concerning ET has been attained. However, no mechanism for the regeneration of ET after a reaction with ROS has been determined. In fact, if ET is an important antioxidant, like ascorbate, glutathione (GSH), ubiquinol and vitamin E, and if the benefit of ET in living organisms is continual and does not lose its capacity to eradicate oxidants after a single chemical reaction, then the ET should be regenerated from its oxidized product so as to be an efficient antioxidant. In this work, a non-enzymatic mechanism for the regeneration of ET after reaction with $^1O_2$ was discovered. For this mechanism, four molecules of GSH are needed to detoxify $^1O_2$ into water and oxidized GSH (GSSG) as a by-product. Clean $^1O_2$ was generated by thermolysis at 37 °C of the endoperoxide $DHPNO_2$. Addition of 1 mM ET to 10 mM $DHPNO_2$ and 10 mM GSH increased the production of GSSG by factor of 26 (in water) and 28 (D_2O), respectively, measured by means of LC-MS/MS. The ring of ET was responsible for the whole reaction cycle and the zwitterionic amino acid backbone was not involved, since only the ring of ET, and 4-methyl ET ring significantly generated GSSG, with equally high intensity as ET. According to the results from the production of GSSG in the present work, the data suggest that ET reacts with $^1O_2$ 150-fold more efficiently than GSH, and ET reacts at least 4-fold faster than ascorbic acid towards $^1O_2$. The necessary thiol foundation (GSH) exists naturally in all mammalian and vertebrate cells as well as in all species that produce ET, such as cyanobacteria, mycobacteria, and fungi with relatively high intracellular concentrations (5 - 10 mM). The byproduct GSSG, regenerates to GSH in living organisms by glutathione reductase, utilizing a NADPH dependent-enzyme. Based on that, ET must now be viewed as closely linked with the redox couple GSH/GSSG. These findings prove the importance of ET over other reactive compounds, that are non-recoverable, for the detoxification of noxious $^1O_2$.

Table of Contents

List of figures

List of Tables

List of abbreviations

AA	Ascorbic acid
α	Alpha
AF2	Excitation energy
APCL	Atmospheric pressure chemical ionization
β	Beta
°C	Celsius scale
CE	Collision energy
CI	Chemical ionization
cps	Counts per second
cm	Centimetre
CXP	Collision cell exit potential
Cys	Cysteine
Da	Dalton
δ	Delta
DFT	Density functional theory
DHIT	1,3-Dihydroimidazole-2-thione
DHPN	N,N`-di(2,3-dihydroxypropyl)-1,4-naphthalenedipropanamide
$DHPNO_2$	N,N`-di(2,3-dihydroxypropyl)-1,4-naphthalenedipropanamide 1,4-endoperoxide
D_2O	D_2O
DNA	Deoxyribonucleic acid
DP	Declustering potential
ESI	Electrospray ionization
ET	Ergothioneine
ETT	Ergothioneine transporter
F	Phenylalanine
$^1\Delta$	First excited state
FS	Full scan
γ	Gamma
Ge	Germanium

GR	Glutathione reductase
GSH	Glutathione
GSSG	Glutathione disulfide
G-6-P	Glucose 6-phosphate dehydrogenase enzyme
h	Plank constant
$t_{1/2}$	Half-life
His	Histidin
HPLC	High-performance liquid chromatography
k	Reaction rate coefficient
kcal	Kilocalorie
kJ	Kilojoule
*K*m	Michaelis-Menten constant
k_q	Physical quenching rate constant
k_r	Chemical reaction rate constant
L	Leucine
LC	Liquid chromatography
LC-MS	LC coupled with mass spectrometry (Q1)
LC-MS/MS	LC coupled with mass spectrometry (Q1-Q3)
LipDH	Lipoamide dehydrogenase
M	Molar concentration
max.	Maximum
Me-	Methyl group
µg	Microgram
mg	Miligram
min	Minutes
µl	Microliter
µM	Micromol
mM	Millimolar
mRNA	Messenger ribonucleic acid
ms	Millisecound
MS	Mass spectrometry

MS^2	Product ion scan
MS^3	Ion trap
MSO	Methionine sulfuxide
m/z	mass-to-charge ratio
n	Natural number
NaCl	Sodium chloride
NDP	3,3`-(1,4-Naphtyl)-dipropionic acid
ng	Nanogram
NADH	Nicotinamide adenine dinucleotide (Reduced form)
NADPH	Nicotinamide adenine dinucleotide phosphate (Reduced form)
NS	No signal
8OG	8-Oxoguanine
π	Pi
PCR	Polymerase chain reaction
pH	Potential hydrogen
pD	Potential deuterium
PKa	Negative common logarithm of acidity constant
Rb	Rose bengale
RNA	Ribonucleic acid
ROS	Reactive oxygen species
rpm	Rotation per minute
RT-PCR	Real-time quantitative polymerase chain reaction
sec	second
SEM	Standard error of the mean
Sen	Photosensitizer
Ser	L-Serine
$^3\Sigma$	Second excited state
$^1O_2$	Singlet oxygen
SLC	Solute carrier
SR	Scan rate
sRGB	Standard red green blue
SRM	Selected reaction monitoring

T	Temperature
t	Time
TMPyP	Tetrakis (N-methyl-4-pyridyl)-21,23H-porphyrin tetratosylat
TrxR-1	Thioredoxin reductase
$^3O_2$	Triplet oxygen
TRIS	Tris(hydroxymethyl)aminomethane
NDMOL	1,4-Naphthalene dimethanol
UV	Ultraviolet
V	Volume
v	Frequency
vs.	Versus
λ	Lambda

Summary

Ergothioneine (ET) eradicates singlet oxygen ($^1O_2$) and has been considered an antioxidant. Various functions of ET regarding reactive oxygen species (ROS) have been proposed and much progress concerning ET has been attained. However, so far, no mechanism for the regeneration of ET after a reaction with ROS has been determined. In fact, if it is an important antioxidant, like ascorbate, glutathione (GSH), ubiquinol and vitamin E, and if the benefit of ET in living organisms is continual and does not lose its capacity to eradicate oxidants after a single chemical reaction, then the ET should be regenerated from its oxidized products so as to be an efficient antioxidant. Therefore, the aim of this project was to investigate whether ET can be regenerated from its oxidized products after reaction with $^1O_2$.

In this project, a non-enzymatic mechanism for the regeneration of ET after reaction with $^1O_2$ was discovered. Several experiments regarding to the regeneration mechanism of ET were performed in the laboratory and could describe a novel ET regeneration mechanism after the reaction with noxious $^1O_2$ by LC-MS/MS. Additionally, the DFT computations could also support all the steps of the proposed ET regeneration mechanism after reaction with $^1O_2$.

For the ET regeneration mechanism, 4 molecules of GSH are needed to detoxify $^1O_2$ into water and GSSG as a by-product. GSH exists naturally in all mammalian cells with relatively high intracellular concentrations (5 - 10 mM). The byproduct GSSG regenerates to GSH in living organism by glutathione reductase, utilizing NADPH as an electron donor. Thus, the discovered mechanism of ET regeneration after the reaction with $^1O_2$ occurs without loss of ET.

In this discovered regeneration mechanism, the ring of ET (1,3-dihydroimidazole-2-thione) is not only responsible for the reaction of ET with $^1O_2$, but also supports the ET regeneration mechanism from its reaction products means a thiol group of other compound like GSH that is present in all mammalian cells. In addition, the zwitterionic amino acid backbone of ET is not involved in the regeneration cycle.

The GSSG production data in the present work suggest that ET reacts with $^1O_2$ 150-fold more efficiently than GSH. In addition, ET reacts at least 4-fold faster than ascorbic acid towards $^1O_2$.

Based on that, ET must now be viewed as closely linked with the redox couple GSH/GSSG. These findings prove the importance of ET over other reactive compounds, that are non-recoverable, for the detoxification of noxious $^1O_2$.

Moreover, for further research projects, the finding of the ET regeneration mechanism should be tested and confirmed in living cells to be relevance for humans.

Zusammenfassung

Ergothionein (ET) ist ein Antioxidans und ist als solches in der Lage reaktiven Singulettsauerstoff ($^1O_2$) abzufangen. Im Zusammenhang mit reaktiven Sauerstoffspezies (ROS) wurden viele verschiedene Eigenschaften von ET untersucht und viele Erkenntnisse gewonnen. Allerdings ist bisher kein Mechanismus zur Regeneration von ET nach einer Reaktion mit ROS bekannt. Damit ET ein wichtiges Antioxidans für den Organismus darstellen kann, welches mit der Bedeutung von bekannteren Substanzen, wie Ascorbat, Glutathion (GSH), Ubichinol und Vitamin E gleichzusetzen ist, muss ein Regenerationsmechanismus existieren, um eine kontinuierliche antioxidative Wirkung gegenüber ROS zu garantieren. Aufgrunddessen war das Ziel dieser Arbeit die Untersuchung, ob ET nach einer Oxidation mit $^1O_2$ regeneriert werden kann.

Im Rahmen dieses Projekts konnte ein nicht-enzymatischer Mechanismus zur Regeneration von ET nach einer Reaktion mit $^1O_2$ nachgewiesen werden. Dazu wurden verschiedene Experimente bezüglich der Wiedergewinnung von ET durchgeführt, wodurch die einzelnen Reaktionsschritte mittels LC-MS/MS aufgeklärt werden konnten. DFT-Berechnungen konnten den neu entdeckten Regenerationsmechanismus zusätzlich belegen.

Bei der Regeneration von ET werden vier Moleküle GSH zur Detoxifizierung eines Moleküls $^1O_2$ benötigt, dabei werden zwei Moleküleoxidiertes GSH (GSSG) als Nebenprodukt gebildet. Physiologisch liegt GSH in allen Säugerzellen in relativ hohen intrazellulären Konzentrationen (5 bis 10 mM) vor. Das gebildete GSSG wird im Organismus unter Verbrauch von NADPH über das Enzym Glutathion-Reduktase zu GSH reduziert. Somit erfolgt der Regenerationsmechanismus nach einer Reaktion mit $^1O_2$ ohne Verlust von ET.

Bei der Regeneration von ET ist die Ringstruktur (1,3-dihydroimidazol-2-thion) nicht nur entscheidend für die Reaktion von ET mit $^1O_2$, sondern führt mithilfe von Thiolgruppen anderer physiologischer Substanzen beispielsweise GSH zu einer

Regeneration der entstandenen ET-Produkte. Dabei ist der zwitterionische Aminosäurerest nicht beteiligt.

Die Ergebnisse des durchgeführten GSSG-Generationsassays weisen darauf hin, dass die Reaktion von ET mit $^1O_2$ im Verhältnis zu GSH 150-fach effizienter abläuft. Des Weiteren reagiert ET mit $^1O_2$ viermal schneller verglichen mit Ascorbinsäure.

Anhand der Ergebnisse muss von einer engen Beziehung zwischen ET und dem Redoxpaar GSH/GSSG ausgegangen werden. Die im Rahmen dieser Arbeit erlangten Erkenntnisse belegen die Bedeutung von ET bei der Entgiftung von schädlichem $^1O_2$ gegenüber Substanzen, die über keinen Regenerationsmechanismus verfügen.

Zur Bestätigung, ob der ermittelte *in vitro* Regenerationsmechanismus von ET für den menschlichen Organismus überhaupt von Relevanz ist, müssen weitere Experimente in lebenden Zellen durchgeführt werden.

1 Introduction

1.1 Ergothioneine

Ergothioneine (ET), a naturally occurring compound, is considered as a powerful antioxidant [1, 2]. Charles Tanret discovered ET in 1909 and it was first purified from the ergot fungus (Claviceps purpurea) [3, 4]. Several functions of ET have been suggested, however its precise physiological purpose is still unresolved. Moreover, numerous studies have been proposed that polymorphisms in the SLC22A4 gene, which cods for the ergothioneine transporter (ETT) [5], are associated with susceptibility to inflammatory diseases such as ulcerative colitis, Crohn´s disease, gout and type I diabetes [1, 6]. Several studies have provided potential effects of ET against neurodegenerative diseases [7]. Recently, ET was proposed to be a possible vitamin [8, 9]. Overall, most of our food contains very little ET [10], however, some mushrooms contain around 1 mg/g of dried material [11]. In humans, ET is received exclusively from the food. After ingestion, ET is removed from the circulation and stored in the body with very little metabolism [12]. Furthermore, the ergothioneine transporter (ETT) is expressed in some human tissues so as to import ET into the cells in order to protect them from oxidative damage [13]. Therefore, ET accumulates in high concentration in cells and tissues which are exposed to injury by oxidative stress e.g. erythrocytes, bone marrow, kidney and eyes [14, 15].

1.1.1 Properties of ergothioneine

Ergothioneine is a histidine betaine derivative with a sulfur atom attached to position four of the imidazole ring [16]. ET is synthesized in micro-organisms starting from histidine [17]. Due to the weakness of double bond C=S in the planar imidazole ring and the high stability of the aromatic heterocyclic five-membered ring, a second zwitterionic resonance structure is formed [18]. ET is a highly hydrophilic structure

and it is very soluble in aqueous solutions [13]. In addition, ET is relatively resistant in acidic and in warm environments [1].

Ergothioneine is a tautomer in nature, in other words, it can be found in the thiol or thione form, however, the thione form (Figure 1) predominates under the physiological pH and this is an important distinguishing feature over other intracellular sulfur-containing molecules [1].

Figure 1. The structure of thione-thiol tautomers of ET. The thione form (left) predominates under physiological conditions at neutral pH.

Humans and other vertebrates can not produce ET, however, cyanobacteria [19], mycobacteria [20] and certain fungi such as Asperigillus oryzae and Streptomyces species [11, 21] are capable of synthesizing high levels of ET (0.1 - 2 mg/g of dried material). The absorption of ET in the human body takes place in the small intestine and ET is recovered almost completely in the kidney. Therefore, the detection of proposed ET metabolites is very low in the urine (< 4% of administered ET) [5, 22, 23].

The free energy from the oxidation of ET to ET-disulfide is low in comparison to the energy released from the production of other alkyl disulfides from thiol compounds, which exist in biological organisms such as glutathione (GSH) and Cysteine. Thus, the thione structure of ET is thermodynamically more stable [24]. Moreover, ET is not autoxidized like GSH under physiological conditions, because of its special

structure that includes the thione group [25]. ET is present in many if not all, human cells, but it accumulates to high levels (0.1 – 2 mM) in the erythrocytes, bone marrow, kidneys and lenses of the eye [26, 27].

1.1.2 The ergothioneine transporter

The ergothioneine transporter (ETT; human gene symbol SLC22A4) was discovered by Gründemann et al. in 2005 [5]. Before then, it was not known how ET was transferred into the cells, due to the fact that ET has a very hydrophilic zwitterion structure and cannot cross on its own the phospholipid bilayers of the cell plasma membrane.

ETT is a membrane protein that belongs to the solute carrier (SLC) family 22. SLC transporters currently content 395 human transporters with 52 families [28]. The structure of most SLC transporters has 12 transmembrane segments with a length of 400-800 amino acids. Moreover, the family SLC22 consists of 23 transporters and due to their function and localization they are drug targets [29]. ETT is composed of 551 amino acids and it is highly specific for the uptake of ET, which has a low K_m value (20 μM) [5, 23].

ETT is a powerful sodium-driven uptake transporter of the cell membrane [30, 31]. Moreover, ETT is present in humans and in all vertebrates and it provides the opportunity to transfer ET into the cells. The accumulation of ET exclusively depends on the activity of ETT [32, 33].

Cells missing ETT are not able to accumulate ET, which was shown in humans, ETT-knockout zebra fish and ETT-knockout mice [5, 34, 35]. The distribution of ETT in human tissues was analyzed by real-time quantitative polymerase chain reaction (RT-PCR) to determine ETT mRNA levels (Figure 2). The data showed high levels of ETT mRNA in bone marrow, cord blood and fetal liver. Furthermore, the content of ET in the tissues of wild-type and ETT-knockout zebra fish was examined (Figure 3). In addition, data from Figure 3 show high ET levels in the intestine, kidney, eye,

liver, brain and gills of the wild-type control, whereas ET was hardly measurable in the knockout ETT zebrafish.

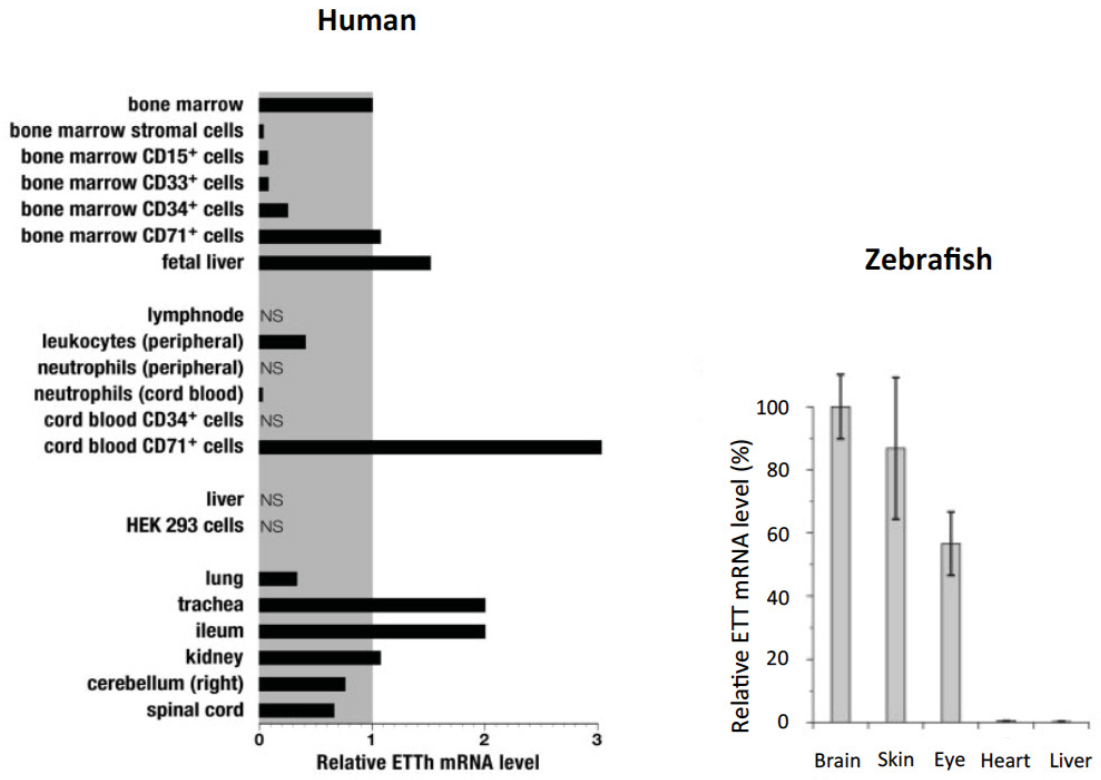

Figure 2. Various tissues and their ETT mRNA content in humans (left) and in zebrafish (right) were analyzed by real-time PCR. Left: a relative expression of ETT mRNA in the selected tissues in relation to the ETT mRNA of bone marrow. Right: a relative expression of ETT mRNA relative to the level of ETT mRNA in the brain. Data shown are mean ± SEM (n = 3), NS = No signal. Modified from [5, 36].

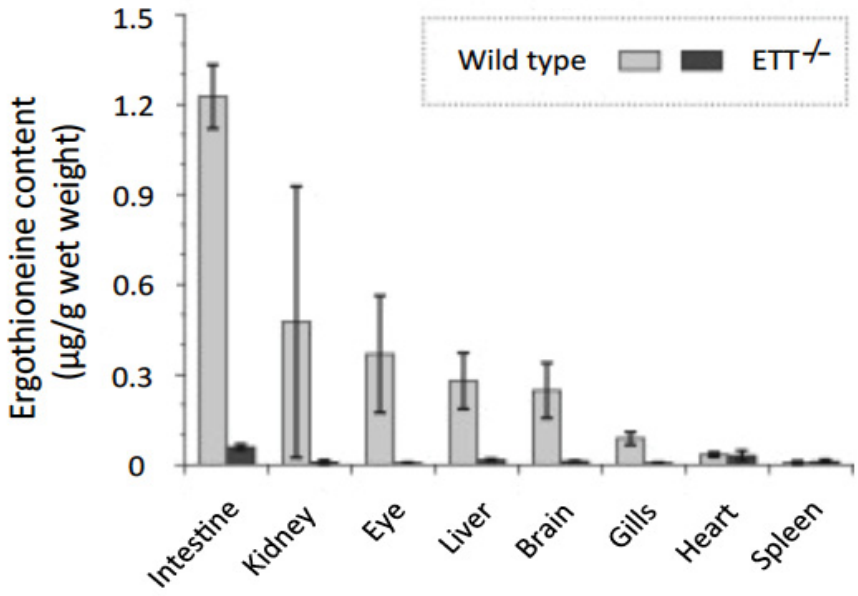

Figure 3. ET content in the tissues of wild-type and ETT-knockout adult zebrafish. ET content of tissue lysates was determined by LC-MS/MS. Data shown are mean ± SEM (n = 2 or 3). Modified from [36].

Mutations in the gene SLC22A4, that is responsible for expression of ETT, are associated with susceptibility to type I diabetes and chronic inflammatory diseases such as ulcerative colitis, Crohn´s disease and gout [36, 37]. In patients with Crohn´s disease, the concentration of ET and the ETT mRNA levels in the small intestine was relatively elevated in comparison to healthy human [38]. Moreover, the 503F variant of the SLC22A4 gene that is associated with Crohn´s disease has about 50% higher transport efficiency than the non-mutated variant 503L [39]. In addition, the concentration of ET in the blood of patients with crohn´s disease was much reduced compared to healthy volunteers [34]. It is currently unknown how this mutation promotes disease [1, 6].

Earlier studies demonstrated the effect of ET on type I diabetes, particularly in pregnant women, since type I diabetes in pregnancy is very common due to their altered metabolism. Moreover, the glucose-mediated free radical dependent embryo malformation can be inhibited by the combination of ET and vitamin E and this could

manage the diabetic embryopathy [40], because free radicals have an important role in the diabetic teratogenic effect [41-43].

1.1.3 Physiological role and therapeutic potential of ergothioneine

Although various functions of ET have been proposed, the exact physiological function is still unresolved [12]. Numerous studies considered ET as an antioxidant and its activity is attributable to the thiol group and double bond in the imidazole ring [1, 2]. In vitro, Motohashi and Mori showed the scavenge effect of ET against the highly reactive hydroxyl radicals (HO·), and they suggested that ET might react as a radical scavenger in pathological systems [44]. Furthermore, ET acts as a chelator for copper ions by forming a redox-inactive ET-copper-complex to prevent copper-induced DNA oxidative damage [45], and further inhibits HO· that are generated from reactions of transition metal ions with H_2O_2 [46]. In fact, copper ions oxidize hemoglobin [47], NADH/ NADPH [48] and erythrocyte plasma membrane [49]. In addition, ET protects alpha1-Antiproteinase against inactivation by peroxynitrite ($ONOO^-$) [50] and hypochlorous acid (HOCl) [46]. ET can reduce ferrylmyoglobin 4 (Mb^{IV}) to ferrylmyoglobin 3 (Mb^{III}). The Mb^{IV} itself is produced from the oxidation of myoglobin (Mb) by H_2O_2 [51, 52].

The protection of ET against radicals was performed in cells. For instance, the cytoprotection of ET towards H_2O_2 and superoxide anion generated by pyrogallol was examined in HeLa cells with and without ETT. The HeLa cells without ETT had a lower viability in comparison to cells including ETT [31]. Deiana et al. reported that ET protects the organs of rats against lipid peroxidation [53].

Pfeiffer et al. have investigated the role of ET in zebrafish, and reported that the skin of unstressed ETT knockout zebrafish contained 4-fold more 8-oxoguanine than in the wild-type [36]. 8-oxoguanine is produced from the reaction of guanine with $^1O_2$ or hydroxyl radicals. In fact, 8-oxoguanine reacts 100 times faster than guanine towards

$^1O_2$ and the ring of 8-oxoguanine is similar to the ring of ET [54]. Interestingly, hydroxyl radicals react with all DNA bases (guanine, adenine, cytosine and thymine) but ET reacts only with guanine [55]. Therefore, it was proposed that the specific function of ET might be to eradicate $^1O_2$.

The reaction of ET towards $^1O_2$ was compared with other compounds that contain thiol groups such as GSH, cysteine, 2-mercaptopropionyl-glycine, and mercaptoethanol. Moreover, in the experiments that were performed in vitro, ET was more reactive towards $^1O_2$ than other above-mentioned compounds [56].

Johanna Krüger [57], and Christopher Stoffels [58], from the work group of professor Dr. D. Gründemann did compare the reaction of ET and GSH with $^1O_2$ *in vitro* as well as intracellularly, and both of them confirm that ET is more reactive towards $^1O_2$ than GSH.

1.2 Reactive oxygen species

Reactive oxygen species (ROS) are a group of unstable and chemically reactive molecules that contain oxygen such as the hydroxyl radical, singlet oxygen, superoxide anion and hydrogen peroxide (Figure 4) [59, 60]. However, the reactivity, lifetime and diffusion distance of the different ROS vary strongly.

The hydroxyl radical has the highest reactivity of the aforementioned ROS, which explains its very low diffusion and lifetime; therefore, its reaction takes place at the site of generation. Other ROS have longer lifetimes and can diffuse further from their site of production [61].

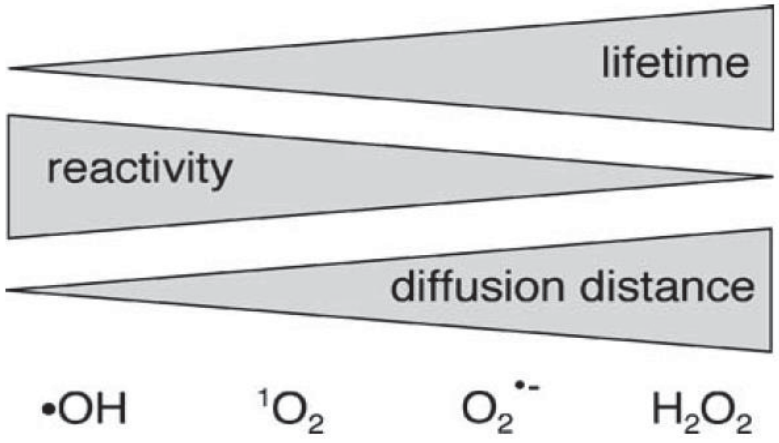

Figure 4. Lifetime, reactivity and diffusion distance of ROS in cells. The highest reactivity of hydroxyl radical (·OH) explains why it reacts with almost everything available in living organisms; whereas $^1O_2$ is relatively less reactive than ·OH, has a longer lifetime and a longer diffusion distance that make it a unique molecule and may provide the opportunity for $^1O_2$ to select its reaction partner. Modified from [59].

ROS are considered to be toxic byproducts of metabolism and they can be responsible for cell damage and death. Furthermore, ROS can damage DNA, lipids, proteins and many important molecules in the cells and tissues [62]. Moreover, many human diseases are associated with oxidative stress related to ROS [63].

Due to the variability in reactivity, lifetime and diffusion distance of ROS, each of them has specific properties e.g. hydroxyl radicals react with all compounds that are available in the biological system [64], however, singlet oxygen selectively chooses its reaction partner. For example, hydroxyl radicals react with all DNA and RNA bases, but singlet oxygen reacts only with guanine [65].

Furthermore, while hydroxyl radicals react with all amino acids, singlet oxygen reacts with only five of them, which are; methionine [66], histidine [67], cysteine [68], tryptophan [69], and tyrosine [70].

1.3 Singlet oxygen

Singlet oxygen is an oxygen species with extra energy; hence, it is a highly reactive molecule that can damage living organisms. In fact, the oxygen molecule in its ground state is called dioxygen (O_2 or $^3O_2$) and has two electrons with parallel spins in two separate orbitals ($\pi-$orbitals) [71]. The symbol $^3\Sigma$ of the ground state oxygen indicates that O_2 exists as a triplet molecule. In addition, dioxygen needs energy to react with other molecules and this activation energy is relatively high (96 kJ/mole).

The first excited state has two electrons with opposite spins in the single orbital in a singlet state and this indicates $^1\Delta$ state (Figure 5). However, the second excited state $^1\Sigma$ has only a lifetime of 1 x 10^{-11} s and converts immediately to the $^1\Delta$ state [72, 73]. Moreover, there is no evidence that the second excited state exists under the physiological conditions [72]. Therefore, singlet oxygen or the symbol $^1O_2$ that is used in this work refers to oxygen in the $^1\Delta$ state.

Oxygen molecule	Symbol	Energy	Orbital occupancy
Second excited state	$^1\Sigma$	37 kcal	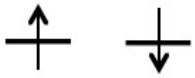
First excited state	$^1\Delta$	22 kcal	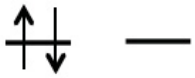
Ground state	$^3\Sigma$		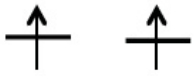

Figure 5. Oxygen molecule types according to energy level. The singlet oxygen in the first excited state ($^1\Delta$) is indicated as singlet oxygen ($^1O_2$). Modified from [72].

The energy difference between singlet oxygen and ground state oxygen is very specific; therefore, singlet oxygen can be detected by its chemiluminescence at 1270 nm [74, 75].

1.3.1 Generation of singlet oxygen

In the human body, $^1O_2$ is produced by photosensitizers in the skin and eye when activated by sunlight and as a by-product of enzymatic oxygen conversions by hemoglobin and peroxidases [12].

Several methods such as using photosensitizers or endoperoxides were improved in order to generate singlet oxygen experimentally.

1.3.1.1 Photosensitizers

Photosensitizers are compounds that absorb light of a specific wavelength from an electromagnetic radiation source to produce an excited state in other compounds by photochemical processes [76]. Photosensitizers such as tetrakis (N-methyl-4-pyridyl)-21,23H-porphyrin tetratosylat (TMPyP) and rose bengal are frequently used in vitro and cells experiments in order to produce $^1O_2$. In addition, photosensitizers require only light as energy and dioxygen that is dissolved in aqueous solutions as the oxidizing agent, in order to produce $^1O_2$ [77].

The advantages of this approach are that photosensitizers can easily enter the cells due to their specific structure. For instance, TMPyP is positively charged and may penetrate through the cell membrane by the process so called self-promoted uptake, and then accumulates in the cell´s nucleus where the negative charge exists (Figure 6A) [78, 79], and rose bengal has a specific non-polar structure and it accumulates in the plasma membrane (Figure 6B) [80].

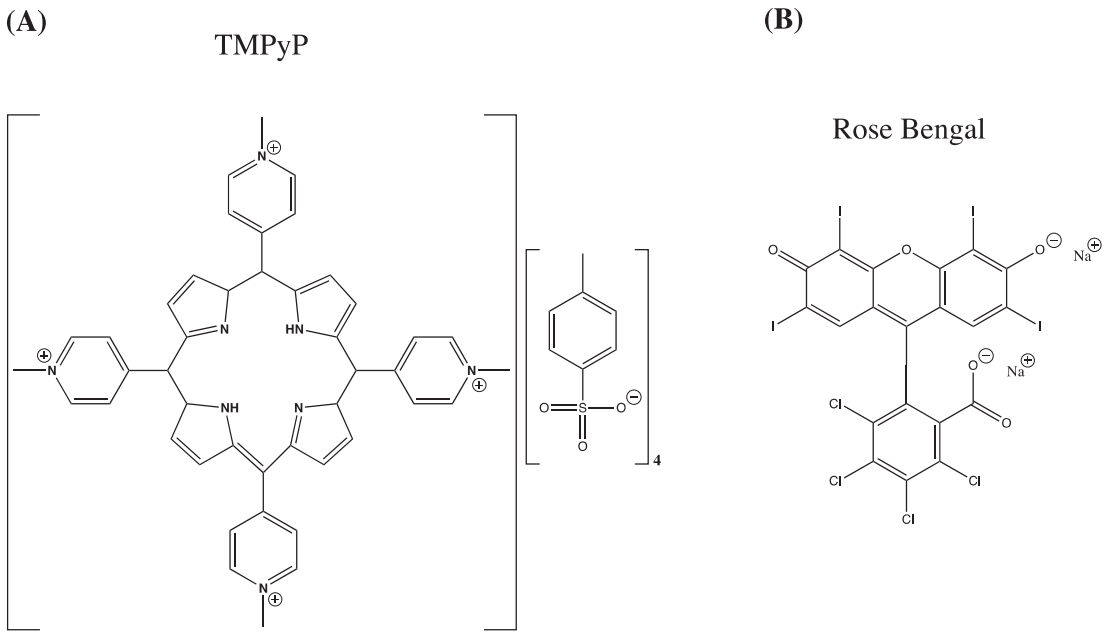

Figure 6. The Structure of the photosensitizers TMPyP and rose bengal. (A) The structure of TMPyP shows a positively charged compound. (B) The non-polar structure of rose bengal represents a negatively charged molecule. Modified from [77].

Photosensitizers such as TMPyP, rose bengal and methylene blue can rapidly absorb energy from the ultraviolet or visible section of the light spectrum and transform from their ground state to an excited state, where they become unstable (^{3}Sen*) (Figure 7).

Moreover, the formation of singlet oxygen needs not only a photosensitizer and light but also needs triplet oxygen that is dissolved in an aqueous solution. The excited photosensitizer (^{3}Sen*) can react via two mechanisms, Type I or II. In the type I reaction, ^{3}Sen* attracts an electron from another molecule (X) to form photosensitizer radical ($Sen^{\cdot -}$) and substrate radical ($X^{\cdot +}$). After that, the photosensitizer radical transfers this electron to the ground state oxygen dissolved in the aqueous solution forming superoxide anion and returns to its ground state (Sen). Afterwards, the superoxide anion reacts with water, forming hydrogen peroxide and hydroxyl radical. In the type II reaction, ^{3}Sen* transfers its energy to the ground state oxygen dissolved in solution, resulting in $^1O_2$ [81].

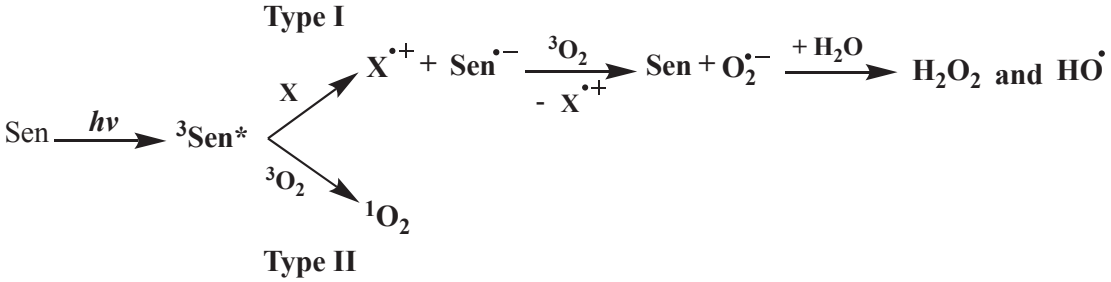

Figure 7. Formation of reactive oxygen species through two major pathways of photosensitization processes. Photosensitizers capture the energy of light and turn from their ground state (Sen) to the excited state (^{3}Sen*). Then there are two possibilities to react further; in the Type I, ^{3}Sen* attracts an electron from another molecule (X) to form photosensitizer radical (Sen·$^-$) and substrate radical (X·$^+$). Next, the photosensitizer radical transfers an electron to the ground state oxygen dissolved in aqueous solution forming superoxide anion (O_2·$^-$) and then returns to its ground state (Sen). Afterwards, superoxide anion (O_2·$^-$) reacts with water forming hydrogen peroxide (H_2O_2) and hydroxyl radical (OH·). In the type II, ^{3}Sen* transfers its energy to ground state oxygen dissolved in solution, resulting in singlet oxygen ($^1O_2$). The * is a symbol of an excited state. Modified from [82].

Photosensitizers generate a large amount of $^1O_2$ and it can be used multiple times. Moreover, they are light dependent, which means that they can form $^1O_2$ from triplet oxygen only in the presence of light. The disadvantages of using a photosensitizer is that not only $^1O_2$ can be generated, but also hydroxyl radicals, superoxide anions and hydrogen peroxides will be produced at the same time and this might affect the results. Thus, the results can be ambiguous, since it cannot be distinguished whether the results were yielding from $^1O_2$ or from some other ROS. Therefore, the best alternative is an endoperoxide such as N,N`-di(2,3-dihydroxypropyl)-1,4-naphthalenedipropanamide 1,4-endoperoxide ($DHPNO_2$) in order to produce pure $^1O_2$.

1.3.1.2 Endoperoxide ($DHPNO_2$)

The naphthalene derivative N,N`-di(2,3-dihydroxypropyl)-1,4-naphthalenedipropanamide 1,4-endoperoxide ($DHPNO_2$) is a compound that has very specific properties, which make it an essential tool to apply in this work. $DHPNO_2$ is well soluble in aqueous solutions and produces pure $^1O_2$ by heating to 37 °C, which

means that it is the ideal compound for generating $^1O_2$ by thermolysis at physiological temperature [12]. Moreover, $DHPNO_2$ generates 59% $^1O_2$ and 41% $^3O_2$ (Figure 8) and the half-life of $DHPNO_2$ is 23 min at 37 °C [83].

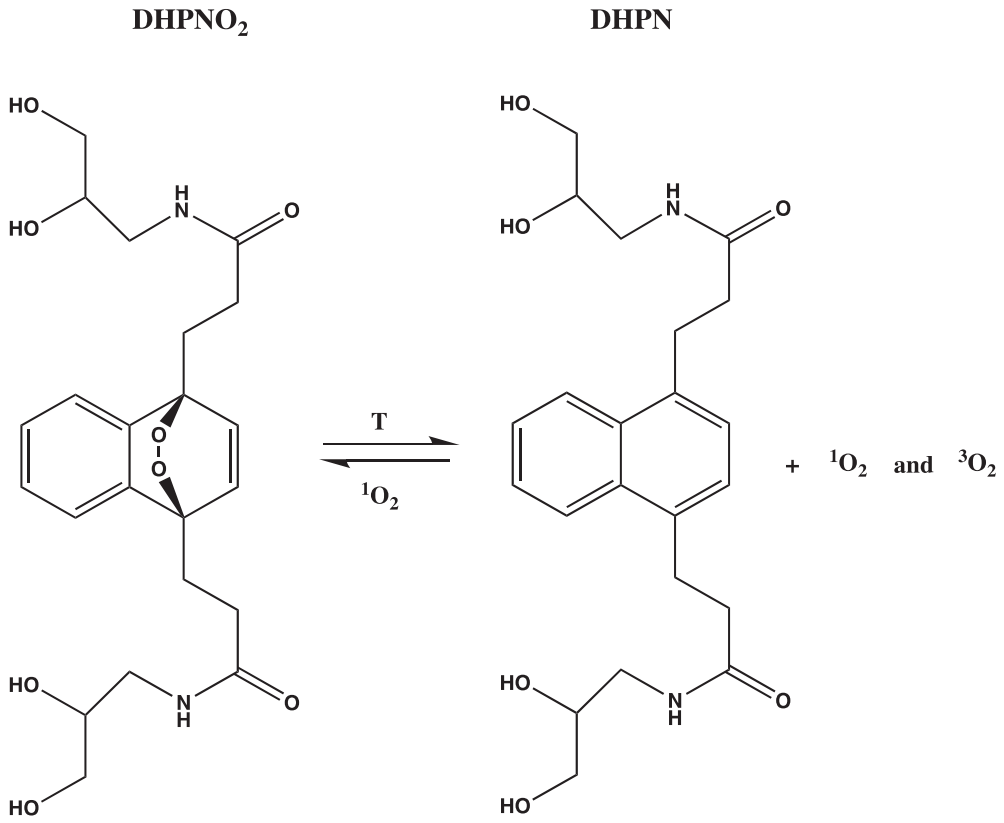

Figure 8. Generation of $^1O_2$ from $DHPNO_2$ by thermolysis. $DHPNO_2$ converts to DHPN and generates 59% $^1O_2$ and 41% $^3O_2$ at 37 °C [83]. The reverse reaction occurs under an $^1O_2$ source, such as photosensitizer and light at 4 °C [12].

The biggest advantage of $DHPNO_2$ is that it generates clean $^1O_2$ without production of any other ROS; therefore, one can be sure that the observed reactions occur only with $^1O_2$ when $DHPNO_2$ is used. In contrast, photosensitizers produce, besides $^1O_2$, all other ROS (hydroxyl radical, super oxide anion and hydrogen peroxide). Interestingly, $DHPNO_2$ is not able to generate $^1O_2$ at $\leq$4 °C, which is the second big

advantage of $DHPNO_2$, as it provides the opportunity to control the experiment concerning starting or stopping the reaction.

The disadvantage of $DHPNO_2$ in comparison to photosensitizers is that once $^1O_2$ is released from $DHPNO_2$, no further $^1O_2$ can be produced from this molecule. In other words, the generation of $^1O_2$ by $DHPNO_2$ is limited to its concentration and can be used only once. By contrast, photosensitizers are able to produce ROS in the form of multiple turnovers when activated by light and in the presence of triplet dissolved oxygen in the solution. $DHPNO_2$ can diffuse through the plasma membrane of cells and releases $^1O_2$ in the cytosolic space; therefore, it is the most suitable compound for $^1O_2$ generation for cellular experiments [84].

1.3.2 Properties and reactions of singlet oxygen

Singlet oxygen ($^1O_2$) belongs to the reactive oxygen species. Although temperature has a significant effect on oxygen in its ground state, it has less effect on singlet oxygen. In addition, the oxidation effect of singlet oxygen is dependent on the nature of the reaction environment and the nature of the compounds that $^1O_2$ can react with [82]. The half-life of $^1O_2$ is solvent-dependent. In water, the half-life of $^1O_2$ is 3 μs with a maximum diffusion distance of 155 nm [85, 86]. However, the half-life of $^1O_2$ in deuterated solvents (D_2O) increases to 68 μs [87]. This feature makes $^1O_2$ distinctive in comparison to other ROS, and such solvents are usually used to show the specificity of singlet oxygen.

In fact, all molecules attempt to exist with minimal energy, therefore, $^1O_2$ that has a high excess of energy has to be rid of its extra energy and this can be achieved via physical or chemical quenching. In physical quenching, $^1O_2$ moves from its excited state to its ground state, without any change in its structure and the excess energy is transformed into heat. Examples of physical quenchers are azide, beta-carotene and lycopene [88, 89]. In chemical quenching, compounds with a specific function react with $^1O_2$ and a covalent bond will build between them. In other words, the $^1O_2$

molecule will transform into another molecule and there will be less or no more $^1O_2$ in the solvent or system.

Singlet oxygen reacts with compounds that have high electron density such as double bonds or amino acids, which contain a sulfur atom, like methionine and cysteine [66, 68, 90, 91]. Based on that, $^1O_2$ can react with unsaturated lipids, nucleic acids that include the guanine base, anions, amines, sulfides, and carbon-carbon double bonds [71]. Thus, $^1O_2$ will attack proteins (68%), Ascorbate (16,5%), RNA (6,9%), DNA (5,5%), Beta-carotene (>1%) as well as GSH (>1%) [58, 92].

Singlet oxygen reacts selectively with many compounds available in biological systems. However, these compounds must have specific properties.

First of all, $^1O_2$ reacts with double bonds via three main additions reaction mechanisms (Figure 9):

(1) The “ene” type reaction [90]; this occurs when singlet oxygen reacts with olefins and results in the formation of Alkyl hydro peroxides e.g. reaction of singlet oxygen with unsaturated lipids or with cholesterol in the biological systems [93].

(2) The [2+2] cycloaddition type reaction [94]; In this case, $^1O_2$ is attached to activated double bonds, forming a dioxetane intermediate which is unstable and decomposes into hydroxyl or ketone structures [95].

(3) The [4+2] cycloaddition type reaction (Diels-alder-addition) [96, 97]; in this reaction type, $^1O_2$ will entrench itself across double bonds of cyclic conjugated dienes, yielding an endoperoxide.

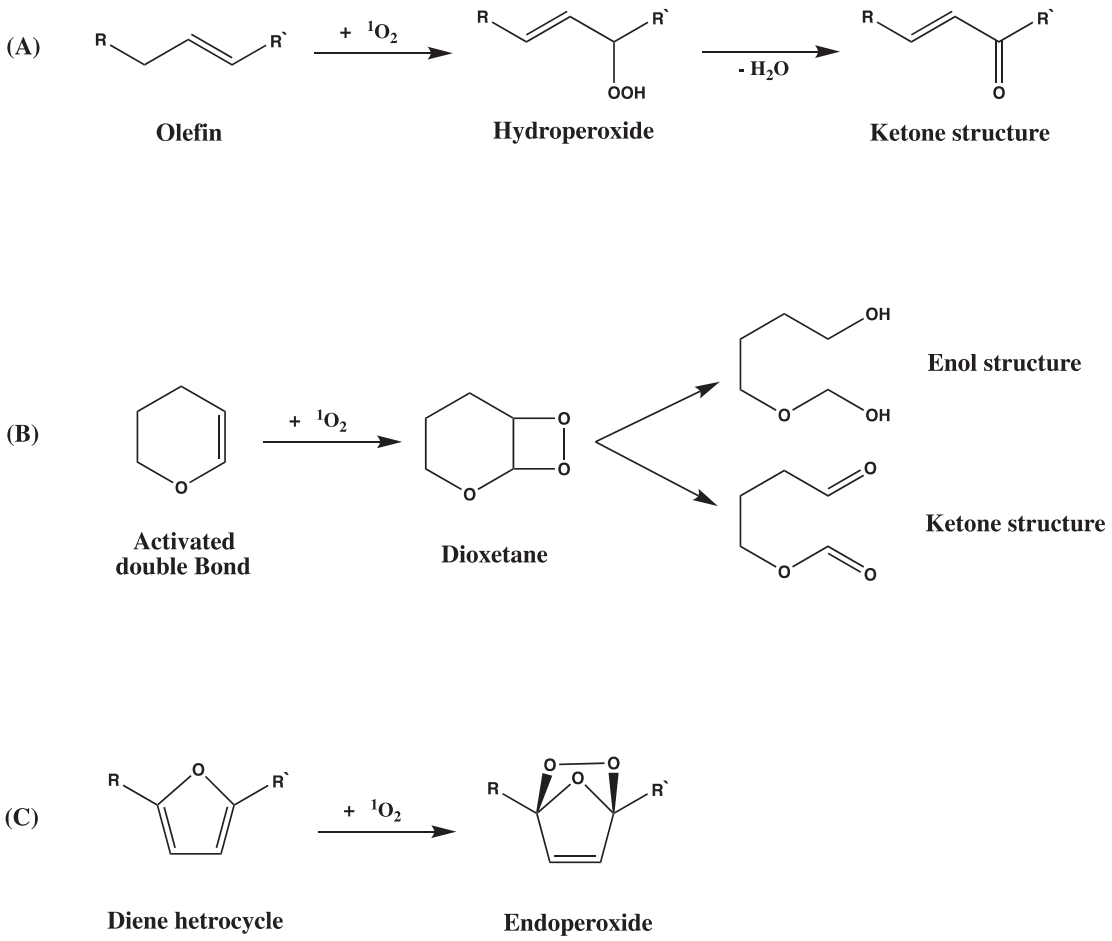

Figure 9. The three main addition reaction types of singlet oxygen to double bonds. (A) The "ene" type reaction yielding hydroperoxide. (B) The [2+2] cycloaddition type reaction resulting in a dioxetane, which decomposes to either enol or ketone structures. (C) The [4+2] cycloaddition type reaction, yielding an endoperoxide. R and R` are alkyle moieties.

Secondly, $^1O_2$ reacts also with molecules that contain heteroatoms, such as sulfur e.g. methionine. In this case, sulfides are oxidized by $^1O_2$ to sulfoxides (Figure 10). [72].

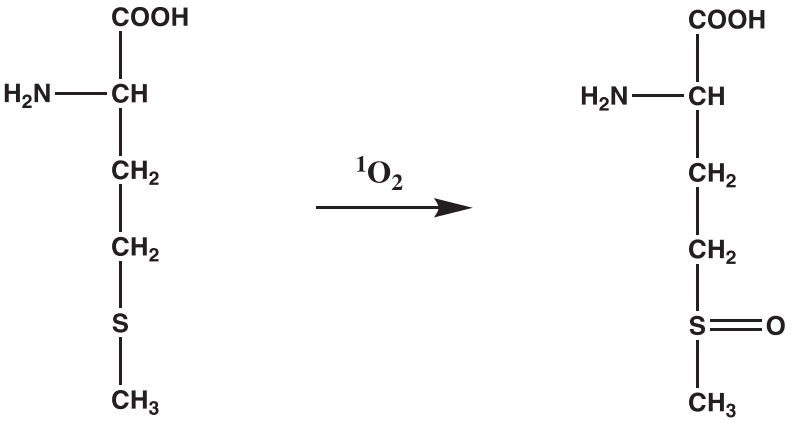

Figure 10. Singlet oxygen reacting with heteroatomic molecules. Oxidation reaction of methionine by singlet oxygen, yielding methionine-sulfoxide.

Moreover, $^1O_2$ can react with reducing agents via electron transfer reaction, without building a covalent bond with these agents. For instance, $^1O_2$ receives one or two electrons from ascorbic acid and converts to superoxide anions that react with protons to form hydrogen peroxide, but then, ascorbic acid (AA) is oxidized to dehydroascorbic acid (DHA) (Figure 11) [89].

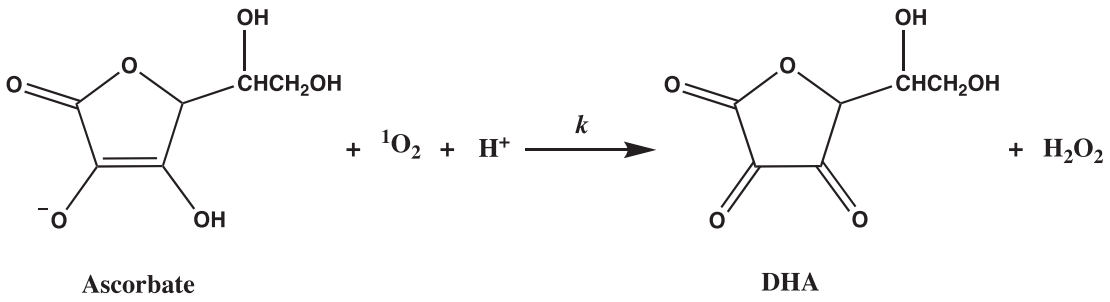

Figure 11. Reaction of singlet oxygen with ascorbic acid via electron transfer reaction. An electron-reducing agent (Ascorbate) reduces $^1O_2$ to H_2O_2, and the reduced form of agent (Ascorbate) is transformed to the oxidized form (DHA). The reaction is rapid and k (reaction rate coefficient) is 3 x 10^8 M^{-1} s^{-1} [98].

The reactivity of AA towards $^1O_2$ is also much greater at the physiological pH due to the deprotonation of AA (pKa = 4.0) [98]. Furthermore, Bisby et al. suggested that AA is the most efficient quencher of $^1O_2$, and the reaction of ascorbate monoanion with $^1O_2$ is very fast ($k = 3 \times 10^8\ M^{-1}\ s^{-1}$). Moreover, the concentration of AA in the cells is high (2-4 mM), therefore, it has been proposed that AA could be an important chemical quencher for $^1O_2$ in vivo [98].

1.4 Antioxidants

Antioxidants are compounds that prevent or delay oxidation (chemical reaction) via their ability to be oxidized more easily and effectively than the protected material [99]. The oxidation itself is a process that can lead to production of ROS. Antioxidants are powerful substances that protect living organisms and cellular components from injury or damage caused by free radicals. Antioxidants differ in their selectivity for various classes of molecules. There are many types of antioxidants, some produced in the body and others not. The ones produced in the body are called endogenous antioxidants and they include glutathione, ubiquinol and uric acid. The antioxidants which cannot be synthesized in the human body are called exogenous and need to be provided through our diet. Examples of these are ascorbic acid and vitamin E. Furthermore, antioxidants provide several benefits due to their properties. For example, ascorbic acid and glutathione are soluble in aqueous solutions and can scavenge oxidants in the blood plasma and cytosolic space of the cells, whereas ubiquinol and vitamin E are fat-soluble and protect the plasma membrane of cells from damage [61].

1.4.1 Regeneration of antioxidants

The concentration of an antioxidant in living organisms is very important in providing the ability for defense against oxidants. However, in the absence of regeneration, the antioxidant´s efficiency will be limited by their intracellular concentration and the

purpose will be lost after a single chemical reaction with oxidants. In addition, the protection of cells and tissues from ROS must be continuous in order for them to be sheltered. Therefore, all-important antioxidants, such as ascorbic acid, GSH, vitamin E, ubiquinol and uric acid, have the capacity to be regenerated from their oxidized form [100-103]. Clearly, the capacity of an antioxidant effect without regeneration provides less physiological meaning, whereas, antioxidants that are able to be regenerated from their oxidized form provide a continuous protection which is of prime physiological importance. [103].

1.4.1.1 Regeneration of ascorbic acid

Ascorbic acid (AA), also known as vitamin C, is a highly important and powerful antioxidant and it has several functions that include the prevention of cellular and tissue damage, as well as treating the scurvy disease [104-107]. AA reacts with ROS and is oxidized into dehydroascorbic acid (DHA). AA is required in the human body not only for its function as an antioxidant but also for activating many enzymes and acting as a co-factor in some enzymatic reactions, such as collagen synthesis [108].

Furthermore, both AA and ascorbate, the deprotonized form of AA under physiological condition, exist in the human body depending on the respective pH value. Moreover, AA can act as a hydrogen donor and it recycles vitamin E from its oxidized product Fig [109].

AA regenerates from its oxidized form DHA by GSH. In this mechanism, two molecules of GSH are needed and one molecule of GSSG is produced per cycle as a by-product (Figure 12) [89, 109].

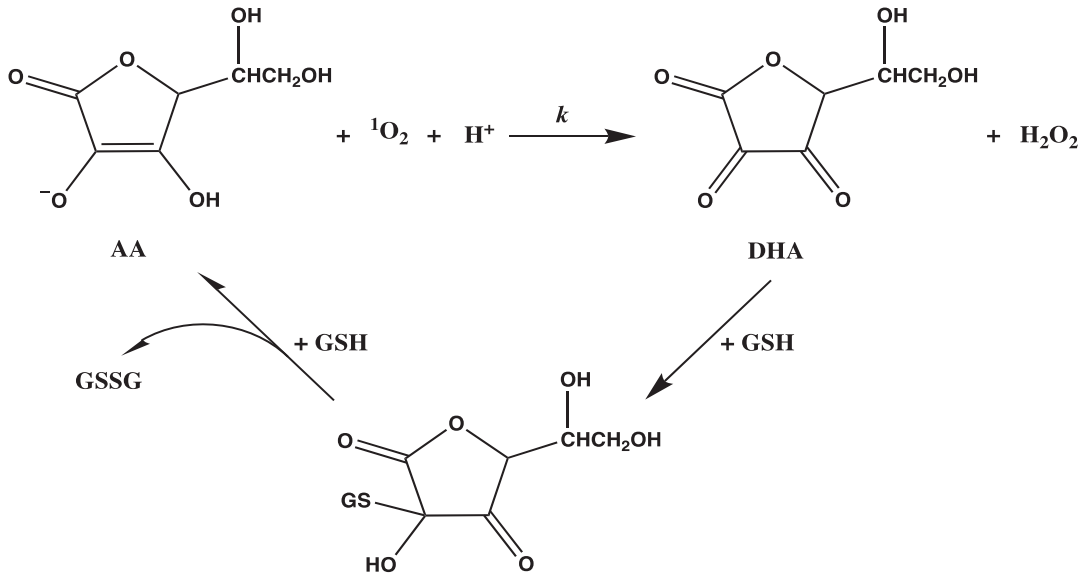

Figure 12. Regeneration of ascorbic acid (AA) from its oxidized form dihydroascorbic acid (DHA) by glutathione (GSH). Two molecules of GSH are needed to regenerate AA from DHA and produce one molecule GSSG per cycle [109].

1.4.1.2 Regeneration of glutathione

Glutathione (GSH) is an important compound that has several functions in living organisms [110-112]. It is a major antioxidant due to its ability to protect cells from a variety of free radicals. GSH is found in all mammalian cells with relatively high intracellular concentration (5 - 10 mM) and it is also found in almost every compartment of the cell [113, 114]. Moreover, GSH synthesized from glutamate, cysteine and glycine, yielding the peptide (GSH) that is relatively stable in the cells. The γ–carboxyl group of glutamate rather than α–carboxyl group is linked with amino group of cysteine and providing a specific peptide bond, because α–carboxyl peptide bonds are common linkage in proteins. Therefore, this unusual peptide bond keeps the GSH away from being hydrolyzed by peptidases [114].

The property of GSH as a reducing agent is related to the thiol group of the cysteine residue in its structure. Moreover, GSH as an electron donor is able to reduce disulfide bonds that are formed in the cells and during this process GSH is oxidized into glutathione disulfide (GSSG). For example, GSH breaks the disulfide bonds of

proteins to cysteine residues by a reduction reaction. Furthermore, GSH as an electron donor is also able to regenerate AA from its oxidized product DHA and it is converted in this reaction to its oxidized product GSSG.

The ratio of GSH to GSSG within living organisms is usually used to measure oxidative stress [115, 116]. GSH is regenerated from its oxidized form by the enzyme glutathione reductase (GR), utilizing NADPH as an electron donor in the cells [109, 117]. In this case, NADPH is converted to NADP, however, NADP is reduced to NADPH again with the aid of glucose 6-phosphate dehydrogenase (Figure 13) [118].

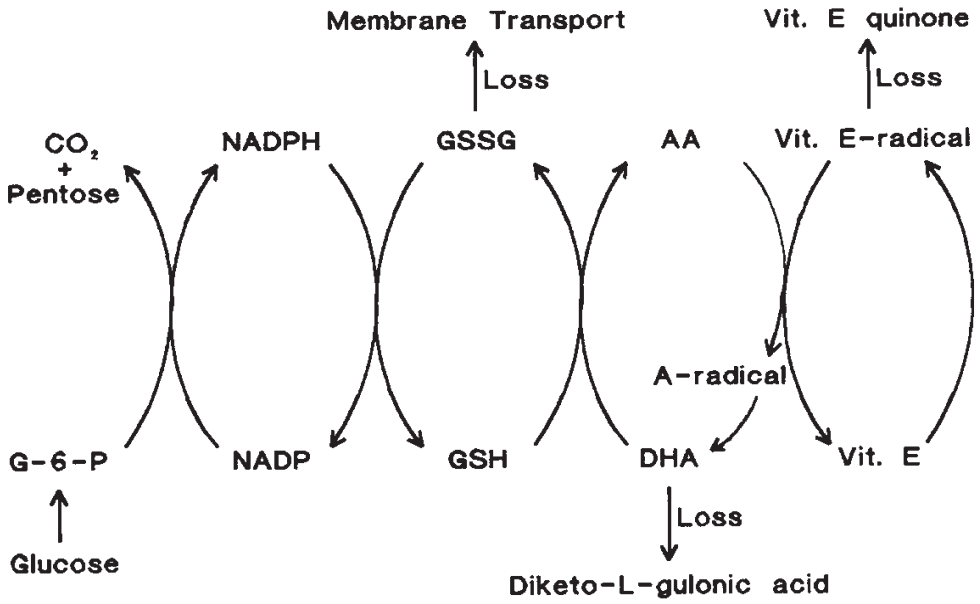

Figure 13. Regeneration mechanism of some important antioxidants from their oxidized products in the cell. Vitamin E regenerates from its oxidized form E-radical with the aid of ascorbic acid (AA) and AA non-enzymatically regenerates from its oxidized product dehydroascorbic acid (DHA) through glutathione (GSH). GSH is recycled from its oxidized form glutathione disulfide (GSSG) through NADPH-dependent enzyme and glutathione reductase. Some oxidized forms of those compounds may be lost from the cycles; therefore, the regeneration of those antioxidants is not complete ($<$ 100%). DHA may degrade to diketo-L-gulonic acid, GSSG may transfer from the cells, and E-radical may be converted to less reactive E quinone. Vit. = Vitamin, G-6-P = Glucose 6-phosphate dehydrogenase enzyme [109].

1.4.1.3 Regeneration of vitamin E

Vitamin E ($\alpha-, \beta-, \gamma-, \delta-$tocopherol and $\alpha-, \beta-, \gamma-, \delta-$tocotrienol) is a fat-soluble antioxidant which is incorporated into the plasma membrane of cells and has various biological functions [119]. In order to inhibit the damaging effect of oxidants, vitamin E can donate a hydrogen atom from its hydroxyl group of the phenol structure to free radicals to scavenge or detoxified them, because the covalent bond between the hydrogen- and oxygen atom (O-H) in vitamin E is weak in comparison to other phenols [120]. After the donation of hydrogen atoms from vitamin E, the oxidized form of vitamin E, which is tocopheryl radical, will be formed.

Vitamin E is regenerated from its oxidized product with the aid of ascorbic acid via a redox reaction. In this process, the ascorbic acid acts as a hydrogen donor (Figure 13) [108, 109].

1.4.1.4 Regeneration of ubiquinol

Ubiquinol is a highly effective and only fat-soluble antioxidant that is synthesized in the human body [121]. Ubiquinol can reduce free radicals and is converted to its oxidized form ubiquinone (coenzyme Q_{10}).

The function of ubiquinol is related to its ability to exchange two electrons which will move between reduced and oxidized forms [122]. Its ability to be regenerated from its oxidized form makes it unique [102]. Moreover, ubiquinol can be recycled from ubiquinone in the redox process with the aid of lipoamid dehydrogenase, glutathione reductase and thioredoxin reductase (Figure 14).

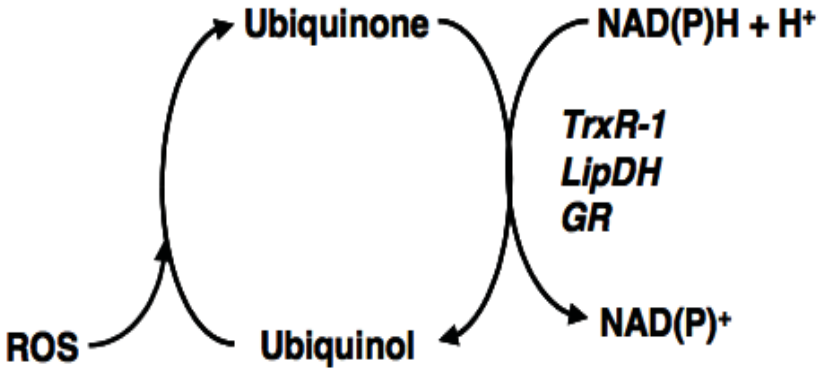

Figure 14. Regeneration of ubiquinol after reaction with reactive oxygen species (ROS). Ubiquinol is recycled from its oxidized form ubiquinone through thioredoxin reductase (TrxR-1), lipoamide dehydrogenase (LipDH) and glutathione reductase (GR) [102].

Consequently, all-important antioxidants, which are oxidized in living organisms, need to be regenerated to be capable of a sustained effect. Ergothioneine is considered a powerful antioxidant, however, it is unclear whether this is of physiological significance. Because all significant antioxidants can be regenerated from their respective oxidized products, this leads to the question whether ergothioneine can be regenerated as well.

1.5 The aim of this project

Ergothioneine (ET) is readily oxidized in aqueous solutions by singlet oxygen. Stoffels et al. did identify *in vitro* the reaction products of ergothioneine with singlet oxygen [12]. Several molecules such as 246 (respective numbers in this thesis represent *m/z* ratios of parent ions), 262 and 264 as reaction products of ET with $^1O_2$ were found by means of LC-MS/MS. However, in the presence of GSH, the products 551 and 553 were produced (Figure 15).

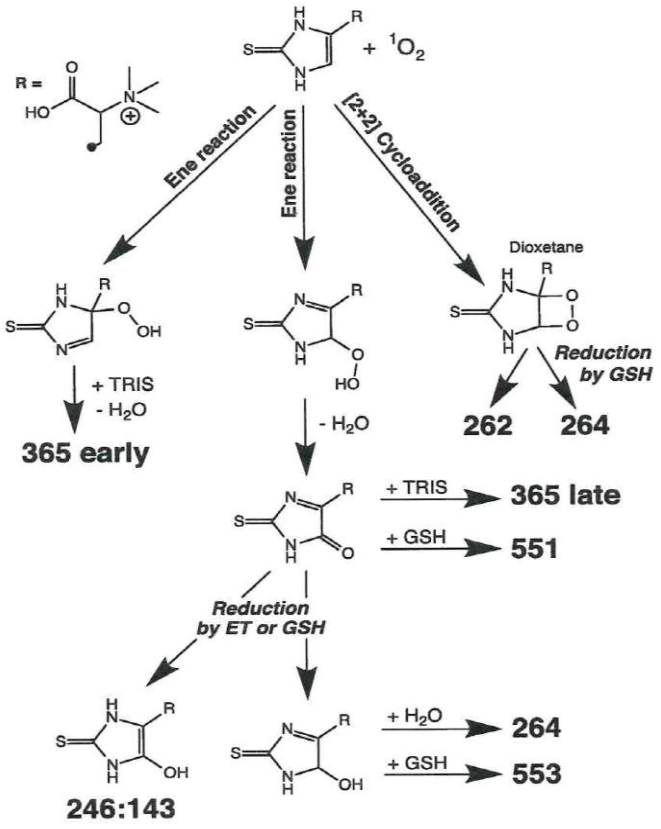

Figure 15. The proposed reaction pathway of ET with $^1O_2$ in water or Tris. The scheme provides the reaction products of ET with $^1O_2$ in the presence of GSH [12].

Building on this previous work, the aim of the present work was originally to analyse the stability of the reaction products of ET with $^1O_2$ both in the presence and absence of various concentrations of GSH and to investigate whether those products (551, 553, 246 and 264) could react further or decompose to other compounds over time.

ET has been considered as an antioxidant because it eradicates reactive oxygen species and particularly $^1O_2$. However, it is unclear whether ET is of physiological significance, since, as mentioned above, all-important antioxidants such as ascorbic acid, glutathione, vitamin E (tocopherols and tocotrienols), uric acid and ubiquinol are regenerated from their main oxidized products, yet there is still no mechanism of regenerating ET after the reaction with a ROS. Therefore, the core target of this project was to elucidate whether ET regenerates from its oxidized products, which arise from the reaction of ET with $^1O_2$, using GSH as a reducing agent (thiol compound).

In the absence of regeneration, the efficiency of ET as a powerful antioxidant will be limited by its intracellular concentration and the benefit will be lost after a single chemical reaction with ROS. Moreover, the protection of cells and tissues in the human body from oxidants must be continuous in order for them to remain intact. Obviously, the capacity of an antioxidant effect without regeneration provides less physiological meaning, whereas antioxidants that can be regenerated from their oxidized form provide a continuous protection which is of prime physiological importance.

2 Materials and Methods

All experiments carried out for this work were performed in the center for pharmacology of the University hospital of Cologne in the work group of professor Dr. Dirk Gründemann.

The endoperoxide $DHPNO_2$ was synthesized by members of the work group of professor Dr. Hans-Günther Schmalz at the Institute of organic chemistry of the University of Cologne.

Density functional theory (DFT) computations were performed by professor Dr. Bernd Goldfuss at the institute of organic chemistry of the University of Cologne.

2.1 Materials

The commerical compounds used in this work are the following: Ergothioneine (THD-201, Tetrahedron, France), Glutathione (G4251, Sigma-Aldrich, Munich, Germany), Methimazole, L-Ascoric acid, Deuterium oxide, L-Serine and Ammonium hydrogen carbonate (M8506, A92902, 151882, S4500 and 09830, respectively, Sigma-Aldrich, Darmstadt, Germany), 2-Thiohydantoin and (L)-Dehydroascorbic acid (T30406 and 261556, Sigma-Aldrich Chemie GmbH, Schnelldorf, Germany), 3-(5-Oxo-2-thioxo-4-imidazolidinyl)-propanoic acid (CDS002303, Sigma-Aldrich Chemie GmbH, Steinheim, Germany), 2-Sulphanyl-1H-imidazole (OR8823, Apollo Scientific, Bredbury, Stockport, United Kingdom), 1,3 Dihydro-imidazol-2-one (sc-357477A, Santa Cruz Biotechnology, Inc, Heidelberg, Germany), 4-Methyl-1H-imidazole-2-thiol (ST02626, Synthon Chemicals GmbH & Co. KG, Bitterfeld-Wolfen, Germany), L-Cysteine Separopore 6B-CL (201811581, bioWORLD, Dublin, OH, USA; particle size range: 52 – 180 µm), L-Serine Separopore 6B-CL (201811621, bioWORLD, Dublin, OH, USA; particle size range: 52 – 180 µm), pH test strips (92125, 92150, Carl Roth GmbH & Co, Karlsruhe, Germany), Sodium

chloride (92652, Carl Roth GmbH + Co. KG, Karlsruhe, Germany). All other chemicals were at least of analytical grade.

Plastic- and glass wares were obtained from the companies Becton Dickinson (Heidelberg, Germany), VWR international (Darmstadt, Germany) and Sarstedt (Nümbrecht, Germany). Non-sterile materials were autoclaved by means of autoclave from company of H + P Labortechnik (Oberschleissheim, Germany) at 121 °C and 1.2 bar for 20 min. All glasswares were sterilized in a sterilizer (type T12, Heraeus Instruments, Düsseldorf, Germany) at 200 °C.

2.2 Solutions and buffers

The solutions and buffers were prepared with deionized water from the Milli-Q Advantage A10 water treatment plant (Merck Millipore, Darmstadt, Germany) at room temperature and sterile filtered (Sterile Syring Filter w / 2.2 µm polyethersulfone membrane, VWR International, Leuven, Netherlands).

In assays without buffer, all solutions were checked for neutral pH and adjusted if necessary by adding small amounts of concentrated ammonia solution.

2.3 Generation of singlet oxygen ($^1O_2$)

In order to generate $^1O_2$ in aqueous solution in the present project, the photosensitizer TMPyP and endoperoxide $DHPNO_2$ were utilized.

2.3.1 Generation of singlet oxygen through the photosensitizer TMPyP

The photosensitizer TMPyP is frequently used in literatures to generate $^1O_2$ [80], because TMPyP has considerable advantages, such as generating a high amount of $^1O_2$, and beeing light dependent, which means that the photosensetizer TMPyP can produce $^1O_2$ from triplet oxygen only in the presence of light, and in the absence of light, no $^1O_2$ will be generated. Therefore, this can helpe to control the reaction of the experiments by starting and stopping the production of $^1O_2$ by switching on or off the light. However, the disadvantages of using the photosensitizer TMPyP for $^1O_2$ production is that the other reactive oxygen species, such as hydroxyl radical, superoxide anion and hydrogen peroxide are produced alongside the $^1O_2$ production [123].

The optimal excitation UV-wavelength of the photosensitizer TMPyP is at 422 nm, however, a wavelength at 365 nm was applied because this was available from the UV-device in our laboratory and this is still within the stimulation range of TMPyP.

In the experiments where TMPyP was used as a $^1O_2$ generator, the 6 and 12 well-plats with a radious of 30 mm and depth of 20 mm without cover were utilized to allow the reaction solution to recieve the UV-light. The total volume of the reaction solution for each sample was 300 µl with 100 µM end concentration of TMPyP in H_2O, D_2O or buffer. The samples were incubated in a waterbath at 37 °C. The light was applied for 20 min or for time cross between 0 and 20 min. The distance between the UV-light device and the samples was 14 cm.

The negative control for the experiments with photosensitizer TMPyP were always the identical reaction conditions but in the absence of light (Figure 16). The reactions were stopped by turning the light off, and then diluting the samples 1:100 with ice-cold water or buffer. Afterwards, the samples were put in a closed box that included ice to avoid any effect of light outside the dark room and temperature, and then the samples were directly analyzed by LC-MS/MS.

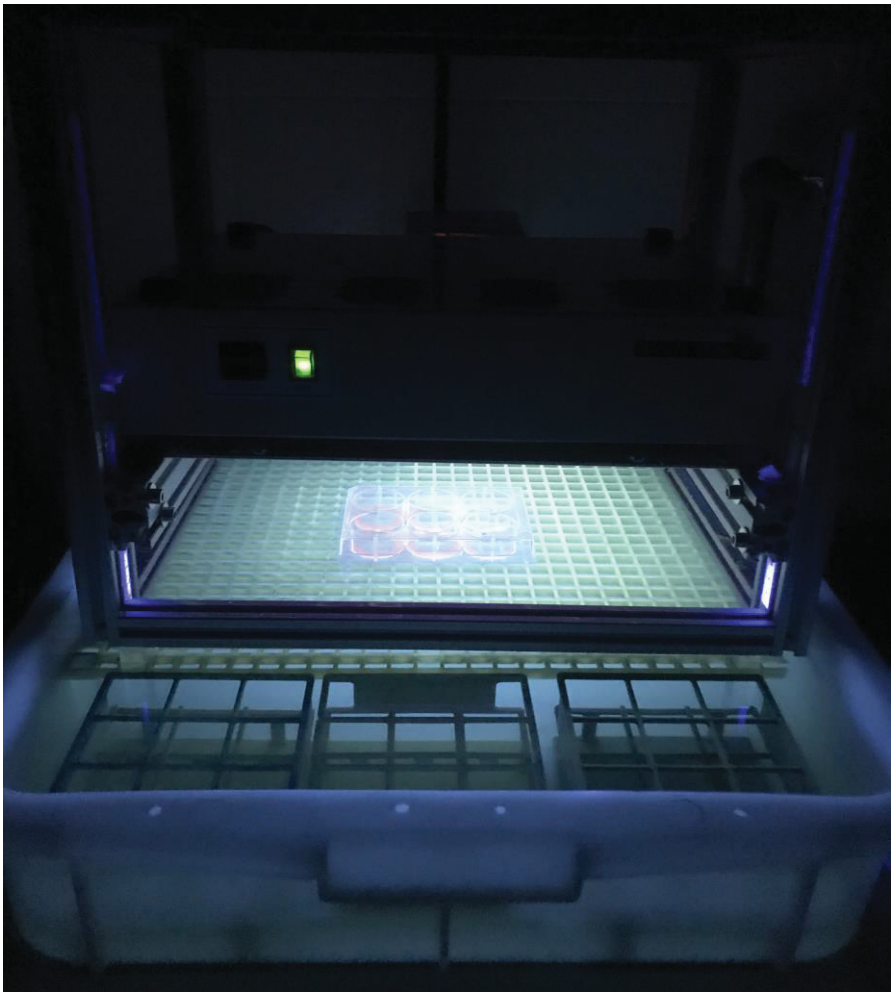

Figure 16. Picture of an experiment using the photosensitizer TMPyP as $^1O_2$ generator. The reaction in this example took place in 6-well plats in a 37 °C water bath. The UV-light source which was responsible for the production of $^1O_2$ and started the reaction was at a height of 14 cm.

The disadvantages of using a photosensitizer is that not only $^1O_2$ can be generated, but also hydroxyl radicals, superoxide anions and hydrogen peroxides will be produced at the same time and this will affect the results. Thus, the results can be ambiguous, since they cannot solely be attributed to $^1O_2$. Based on that, the best alternative $^1O_2$ generator in order to produce pure $^1O_2$ is an endoperoxide, such as $DHPNO_2$. Therefore, the results from the experiments that utilized TMPyP as a $^1O_2$ generator had to be confirmed by experiments that were performed with $DHPNO_2$ as a $^1O_2$ generator, since $DHPNO_2$ produces a clean $^1O_2$ and the results cannot be ambiguous [12].

2.3.2 Generation of singlet oxygen through the endoperoxide $DHPNO_2$

Since the endoperoxide $DHPNO_2$ is not available, as it cannot be commercially obtained, it was synthesized for previous projects and also for this work by the work group of prof. Dr. Schmalz (University of Cologne, Institute of organic chemistry). $DHPNO_2$ is stored at -80 °C and it is stable for a longe time (months). The $DHPNO_2$ is inactive at temperatures of ≤ 4°C and the generation of $^1O_2$ can only occur through warming. In addition, the $DHPNO_2$ dissolves very well in water (39 mmol/l at 20 °C) and it has a half-life of 23 min at 37 °C to release 59% $^1O_2$ and 41% $^3O_2$ [83]. In fact, the synthesis of $DHPNO_2$ proceeded through various steps to produce the compound DHPN, and then, DHPN was incubated with the photosensitizer methylene blue at 4 °C under a suitable wavelength of light to provide oxygen for DHPN to react with. Furthermore, the $^1O_2$ reacted with double bonds of the DHPN ring through [4+2] cycloaddition reaction to produce $DHPNO_2$ (Figure 8). In addition, this experement was performed in D_2O in order to increase the yield [12].

The advantages of this approach are that $DHPNO_2$ on the one hand, produces pure $^1O_2$ and not other ROS, like photosensitizers, and on the other hand, $DHPNO_2$ is well soluble in water and not highly polar. In other words, $DHPNO_2$ is the best choice for cell experiments among other endoperoxides, such as NDP [84] and NDMOL [124] which have more ionic groups like 3,3 '- (1,4-naphthyl) -dipropionic acid and 1,4-naphthalenedimethanol, respectively, to generate pure $^1O_2$ in cells [58].

In the experiments that were performed utilizing $DHPNO_2$ as $^1O_2$ generator, the reactions were started by adding ice-cold $DHPNO_2$ to the reaction solution at 37 °C, and the reactions were stopped by adding ice-cold water or buffer (depending on the reaction condition), and then moving the reaction solution directly into the ice.

2.4 The reaction of ergothioneine with singlet oxygen in the presence and absence of glutathione

Various conditions were tested for the *in vitro* reaction of ET with $^1O_2$ in the presence and absence of GSH. For the reactions that utilized $DHPNO_2$ as $^1O_2$ generator, all experiments were performed with an end volume of 50 or 100 µl in brown polypropylene Eppendorf tubes (Sarstedt, Nümbrecht, Germany) in buffered water (10 mM ammonium hydrogen carbonate at pH 7,4 or 8,0). 10 µM of ET reacted with 10 mM $DHPNO_2$ with and without (control) 10 mM GSH, in the time range 0 to 16 min at 37 °C on a shaker (300 rpm). After the indicated times, 10 µL of each sample were diluted with ice-cold buffered water in a ratio of 1:2, 1:10 or 1:100. Afterwards, the samples were immediately analyzed by LC-MS/MS for ET and ET-products.

For some experiments, additional conditions were tested. For instance, 100 µM of ET reacted with 10 mM $DHPNO_2$ and (0, 0.1, 0.3, 1, 3, 10, 30 or 100) mM GSH as a function of GSH concentration in 10 mM ammonium hydrogen carbonate at pH 7,4 for 10 min at 37 °C on a shaker (300 rpm). After the indicated times, samples were diluted with ice-cold buffered water in a ratio of 1:10 and then immediately analyzed by LC-MS/MS for the compounds 551:244, 551:200, 553:246, 553:308, 264:188, 246:202 and 246:125.

2.5 The assay of oxidized glutathione (GSSG)

In order to analyze and quantify the glutathion disufide (GSSG) in the present work, numerous experiments were performed. The mixture (V = 100 µl) of 10 mM GSH and 10 mM $DHPNO_2$ in the presence and absence (control) of 1 mM of the respective substance (Ergothioneine, L-Ascorbic acid, Methimazol, 3-(5-Oxo-2-thioxo-4-imidazolidinyl)-propanoic acid, 2-Sulphanyl-1H-imidazole, 1,3 Dihydro-imidazol-2-one, 4-Methyl-1H-imidazole-2-thiol and 2-Thiohydantoin) in D_2O were incubated in the time range of 3 to 12 min at 37 °C and 300 rpm on a shaker. As a second control, a reaction of 10 mM GSH and 1mM ET was also performed under the same condition

but without $DHPNO_2$. Samples of 10 µl were taken at the indicated time-points and diluted with ice-cold water to a ratio of 1:100 and then put on ice. Afterwards, the samples were immediately analyzed by LC-MS/MS for the GSSG: the compounds 307:130, 613:355 and 613:484.

In the case of GSSG generation as a function of GSH concentration, a solution of 0,1 mM of ET, 10 mM DHPNO2 and (0, 0.1, 0.3, 1, 3, 10, 30 or 100) mM GSH in 10 mM ammonium hydrogen carbonate pH 7,4 were incubated for 10 min at 37 °C. The production of GSSG was immediately analyzed by LC-MS/MS.

Parallel experiments of GSSG production from the reaction of GSH with TMPyP as $^1O_2$ generator, with and without ET (control) were performed. For all reactions that utilized TMPyP as $^1O_2$ generator, the mixture (V = 300 or 1000 µl) of 10 mM GSH and 100 µM TMPyP in D_2O was incubated in the time range of 5 to 20 min at 37 °C in the presence of UV-light at 365 nm. The controls were made under the same reaction conditions but in the absence of UV-light. The reaction was started by switching the UV-light on. In addition, the reaction took place in the 6 or 12 well polystyrene plates (Sarstedt, Nümbrecht, Germany). Samples of 10 µl were taken at the indicated time-points and diluted with ice-cold water to a ratio of 1:100 and then put on ice. Subsequently, the samples were immediately analyzed by LC-MS/MS for GSSG.

2.6 Capturing the reaction intermediates that arise from the reaction of ergothioneine and singlet oxygen

In order to prove the mechanism of ET regeneration, the reaction intermediates that arose from the reaction of ET with $^1O_2$ were captured by using cross-linked agarose beads that were covered with free thiol groups. In the solution (V = 50 µl), 1 mM ET + 0.1 mM GSH in buffer (10 mM ammonium hydrogen carbonate pH 8.0) with and without (control) 10 mM $DHPNO_2$ were mixed with 100 µl of sedimented cysteine (8-fold molar excess of thiol groups versus ET) or serine cross-linked agarose beads

(201811581, 201811621, bioWORLD, Dublin, OH, USA; particle size range: 52 – 180 µm; approx. 4 nmol L-cysteine/ L-serine per µl of gel) in polypropylene reaction tubes (72.690.001, Sarstedt, Nümbrecht, Germany).

The samples were incubated for 10 min at 37 °C and 1200 rpm in a shaker, then the beads were transfered into polypropylene microliter tips (70.762.010, Sarstedt, Nümbrecht, Germany) that were already plugged with very small pieces of cotton. Subsequently, the beads were washed three times with 500 µl 100 mM NaCl in buffer. In the next step, 100 µl buffer, 100 µl 10 mM serine in buffer and 100 µl 10 mM GSH in buffer were added to the bead columns at room temperature consecutively. The respective flowthrough fractions were immediately analyzed by LC-MS/MS for ET.

2.7 The assay of oxidized ascorbic acid

In order to analyze the oxidized ascorbic acid, the main oxidized products of AA were identified after the reaction with $^1O_2$ and they were compared with the relevant literature. For this analysis, the full scan method was used in which the reaction solutions of 1 mM AA and 10 mM $DHPNO_2$ were incubated in H_2O or D_2O for 0 and 12 min at 37 °C in a shaker (300 rpm). When the time point was at 0 minutes, the samples were incubated directly on ice. The data from the full scan measurement of MS were analyzed by the difference shading method (Figure 43). The main products 209:191 and 191:147 that were mentioned in the literature [125], were indeed found during a full scan, therefore, these compounds were analyzed through the SRM method as oxidized products of AA, since the major oxidized product DHA, hydrolyses in aquious solutions.

After identifying the oxidized products of AA, experiments of 1mM AA and 1 mM $DHPNO_2$ in the presence and absence (control) of 1mM ET or 1 mM His in D_2O were incubated in the time range of 3 to 12 min at 37 °C and 300 rpm in a shaker. As an

additional control, a reaction under the same conditions but without $DHPNO_2$ was also performed. Samples of 10 µl were taken at the indicated time-points and diluted with ice-cold water to a ratio of 1:100 and then put on ice, and then, the samples were immediately analyzed by LC-MS/MS for compounds 209:191 and 191:147.

2.8 High-performance liquid chromatography coupled with tandem mass spectrometry

The combination of liquid chromatography (HPLC or LC) and mass spectrometry (MS) is one of the most important analytical techniques that is utilized for the characterization of organic and inorganic compounds. This tandem (LC-MS) provides the opportunity to separate many compounds in mixtures by LC and identify the molecular structure of the individual compounds qualitatively and quantitatively with high sensitivity by MS according to their mass-to-charge ratio (*m/z*) [126, 127].

The LC-MS device that was used in this work was a combination system of HPLC (SLC-20AD Prominance, Shimadzu, Duisburg, Germany) and MS (Q Trap 4000, AB Sciex, Darmstadt, Germany).

2.8.1 High-performance liquid chromatography

High-performance liquid chromatography (HPLC) is a technique that is frequently utilized in the analytic researches to separate and identify each compound in a sample mixture [128]. The mixture moves through a column which included a solid adsorbent material called stationary phase, by mobile phase. Each molecule in the mixture interacts slightly with the stationary phase according to its chemical structure, the nature of the adsorbent material and the composition of the mobile solvents, leading to the difference in the flow rates for various molecules [129]. Thus, compounds will be separated as they flow out of the adsorbent material. The time that each compound

needs to elute from the column is called retention time and this is important in identifing the analyte.

The several types of columns that were filled with many different adsorbent materials which have different particle sizes are used in this work (Table. 1).

Table 1: Several types of HPLC columns.

Column	Producer	Precolumn	Dimensions
ZIC-HILIC	Dichrom, Marl, Germany	No precolumn	Particle size 5µm, Ø 2,1 x 100 mm
HILIC	Waters, Dublin, Irland	Particle size 5 µm, Ø 3,9 x 20 mm	Particle size 5µm, Ø 3 x 50 mm
DC18	Waters, Dublin, Irland	Particle size 5 µm, Ø 3,9 x 20 mm	Particle size 5µm, Ø 3 x 100 mm
ZIC-pHILIC	Dichrom, Marl, Germany	No precolumn	Particle size 5µm, Ø 2,1 x 100 mm
xBridge Shield RP18	Dichrom, Marl, Germany	Particle size 5,3 µm, Ø 3 x 20 mm	Particle size 5µm, Ø 3 x 100 mm

Usually, small particle sizes (3-10 µm) are used for HPLC in order to receive sufficient chromatographic resolution, therefore, high pressure has to be applied on the column [130]. On the other hand, the mobile phase is made of a combination of water and organic solvents, such as acetonitrile and methanol, with or without additives. In addition, in some cases fomic acid, acetic acid or salts, such as ammonium formiat and ammonium acetat, are added to the mobile solvents to assist the separation of molecules in the mixture [129]. Moreover, the composition of the mobile solvents in some operations are changed during the elution (gradient method)

or kept steady (isocratic elution) for molecules that are different in their assinity to adsorbent material.

In order to detect a method which provides a sufficent separation, a series of analytic measurement were performed in this Project. For instance, the mobile solvents and their composition were changed by varying the gradient conditions.

After performing experiments and diluting the samples, a 10 or 20 µL of each sample was analyzed by means of HPLC, according to the condition below (Table. 2-10).

After the separation, the compounds are moved directly to the mass spectrometer for the analysation, since a coupling of HPLC with MS analysis are utilized.

Table 2: HPLC conditions for ET, ET-product and GSSG. This table shows the HPLC condition for the compounds 230:127, 230:186, 551:244 , 551:200, 553:246, 553:308, 246:202 , 246: 225, 264:188, 262:245, 613:355, 613:484 and 307:130.

Compounds	ET, ET-product and GSSG
Column	ZIC-HILIC
Eluent A	0,1 Formic acid in H_2O
Eluent B	0,1 Formic acid in acetonitrile
Flow rate	0,2 mL/min
Flow	Gradient: 90% B at 0 min, 90% B at 0,5 min, 10% B at 9 min, 10% B at 10 min, 90% B at 14 min, 90% at 15 min
Running time	15 min
Injection volume	20 µL
Temperature	35 °C

Table 3: HPLC conditions for oxidized products of ascorbic acid by $^1O_2$ (209:191 and 191:147 for negative polarity).

Compounds	209:191 and 191:147
Column	ZIC-pHILIC
Eluent A	10 mM Ammonium acetate pH 8,9
Eluent B	Acetonitrile
Flow rate	0,3 mL/min
Flow	Isocratic: 70% B
Running time	4,5 min
Injection volume	20 µL
Temperature	40 °C

After the separation, the compounds are moved directly to the mass spectrometer for the analysis, since a coupling of HPLC with MS analysis are utilized.

2.8.2 Mass spectrometry

Mass spectrometry (MS) is one of the most powerful analytical techniques that is employed for the identification of substances qualitatively and quantitatively in a pure sample or complex mixtures [131]. The principle of MS is to produce ions from compounds to separate these ions by their mass-to-charge ratio (*m/z*) and then analyse them by a detector with high sensitivity.

Morover, the MS consists of three units: an ion source, a mass analyzer and a detector. In the first stage, ions are produced by an appropriate method, such as electrospray ionization (ESI), chemical ionization (CI) and atmospheric pressure chemical ionization (APCL), depending on the analytical method and the nature of the

compounds, whether hard or soft ionization is needed for the ion generation. In the second stage of MS, the ions that are produced in the ionization unit will be separated by the quadrupole filters (mass analyzer) according to their mass-to-charge ratio and moved towards the detector. In addition, specific ions can be selected and fragmented in this stage. The last stage of MS is the detector that generates an electrical current proportional to the frequency of the incident ions which pass through the mass analyzer [132].

2.8.2.1 Electrospray ionisation process

Electrospray ionization (ESI) is one of many techniques utilized in mass spectrometry in order to generate ions. In this process, a high voltage will be applied to scatter the liquid containing the analytes under atmospheric pressure and transfer the drops into a fine aerosolized form [133].

The solvent of drops evaporates increasingly with the aid of high temperature and heated inert gas, such as nitrogen, forming charged droplets which explod upon reaching their Rayleigh limit, producing smaller and more stable microdrops. Thus, the increasing charge in the microdrops leads to further explosion, creating a stream of positive or negative charge that transfers to the mass analyzer (Figure 17) [134, 135].

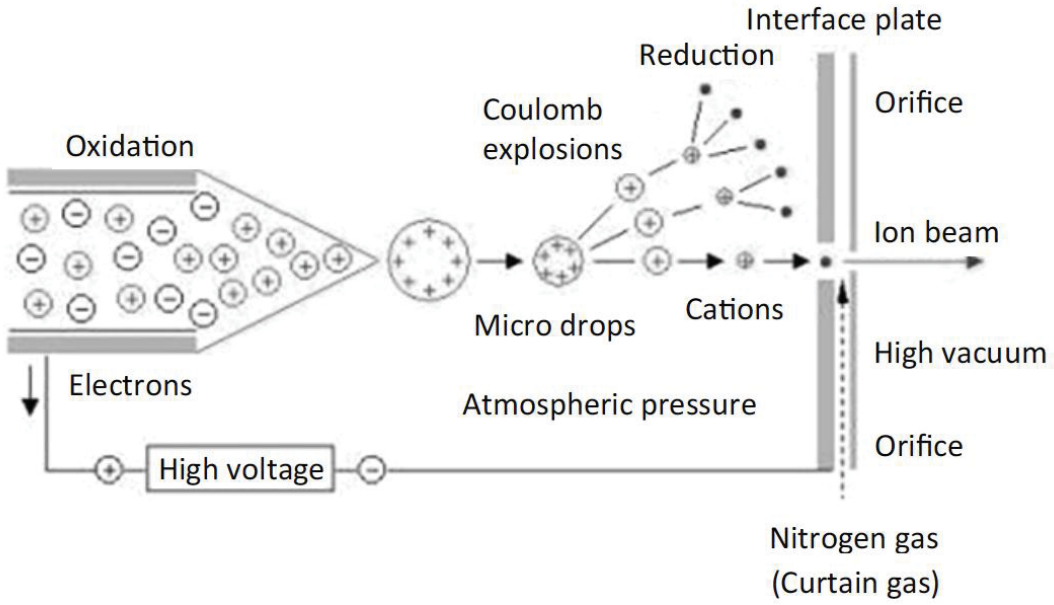

Figure 17. Schematic diagram of electrospray ionization in positive mode. After the eluents are arrived at the ionization unit, high voltage and temperature are applied. Thus, the Taylor cone emits droplets of liquid that gradually evaporate, so that they are charged progressively. When the charge density in the drops are increases, the droplets explode and leave a stream of charged ions (positive ions for positive mode). Modified from [136].

2.8.2.2 The quadrupole filters of the mass spectrometry

The charged analytes that are generated in the ionization unit flow to the quadrupole filters of MS that consist of four parallel cylindrical metal rods with the same diagonal distance from the center axis (Z). The diagonally-opposite poles receive a voltage and an opposite voltage polarity is applied on the adjacent poles. Therefore, an electric field with very fast varying phases is produced inside the quadrupole part and oscillates ions in the X and Y directions to stabilize their paths towards the detector. Particular ions with a specific *m/z* pass though the quadrupole, when specific voltage is applied. In addition, all other ions with a different *m/z* shift from the right direction and collide with the metal rods and become discharged (Figure 18).

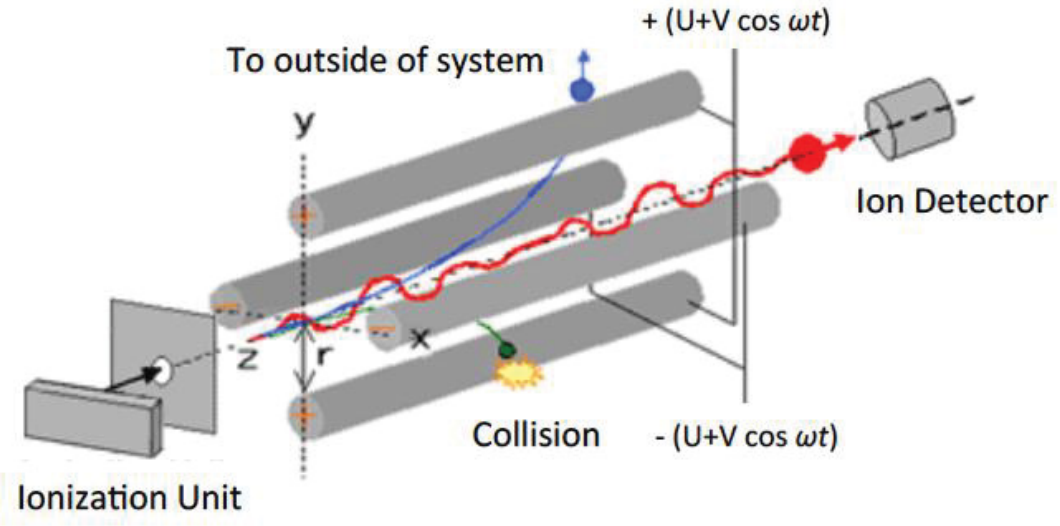

Figure 18. Schematic diagram of Quadrupole MS. The quadrupole MS includes four parallel cylindrical metal rods inside a vacuum chamber, placed equidistantly from the center line. Ions will be produced in the ionization unit and then accelerated in the Z-direction towards the quadrupole sector. The diagram shows how voltage is applied to diagonally-opposite poles and an opposite voltage polarity is applied on the adjacent poles. Thus, an electric field with very fast varying phases is created inside the quadrupole part and this is oscillates ions in the X and Y directions. Particular ions in a specific *m/z* pass though the quadrupole towards the detector when specific voltage is applied. Modified from [137].

The purpose of the first filter (Q1) is to permit only selected molecules with certain *m/z* to pass and move towards the detector. In the second quadrupole (Q2), the only selected molecules with a specific *m/z*, so-called parent ions, will be fragmented. The fragmentation process occurs by breaking the parent ions by applying the required energy through nitrogen gas, producing specific fragment patterns (daughter ions) that are different for each selected ion (parent ion) in the Q1. Afterwards, the specific fragments pass the second mass filter (Q3) to reach and hit the detector, creating an electron current that is converted into a digital signal (Figure 19) [138]. The measurement of the produced fragments can be compared with their respective parent ion and this helps achieve a precise identification and quantification analysis of the selected ion.

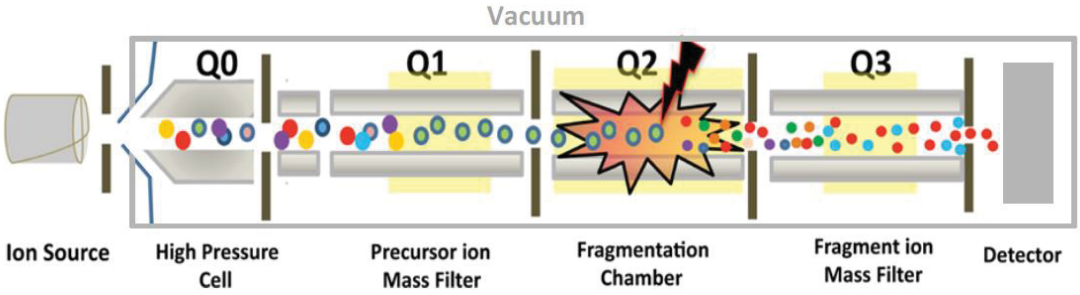

Figure 19. Schematic diagram of detecting a specific *m/z* molecule in a triple quadrupole mass spectrometer. Charged compounds will be accelerated in the Q0 after ionization in the ionization unit, and then specific ions (parent ions) will pass through the filter in Q1 towards Q2. In the Q2 chamber, the parent ions will be fragmented by nitrogen gas. Only the produced fragments of the preselected ions with a specific *m/z* will pass through the second mass filter in the Q3 chamber to reach the detector, and then an electron current will be released, converted into a digital signal. Modified from [139].

2.8.2.3 Fullscan process

Full scan (FS) is a method in mass spectrometry that is utilized in order to detect all molecules in a reaction mixture. In this process, all reactants and reaction products are analyzed in Q1 after becoming charged in the ionization unit. In other words, Q2 and Q3 are not involved in this analysis. This method indicates only the intensities of each *m/z* compound (parent ions) without fragmentation and provides an overview of the molecular mass of the contained sample mixture. This method is less sensitive, since many compounds may have similar molecular *m/z*. Therefore, the FS method is followed usually by selected reaction monitoring (SRM) (2.8.2.7) to analyze each indicated parent ion further, individually

In this work, the range analysis of *m/z* compounds was between 50 and 500 *m/z* for a scan time of 2 sec. In the work group of Prof. Gründemann, five columns with different adsorbent material and various mobile solvents were tested. In addition, the FS method can be performed in a positive or negative mode (Table 4 and 5).

Table 4: HPLC conditions of the fullscan analysis for positive mode

Column	ZIC-HILIC	HILIC	DC18
Eluent A	Ammonium formate pH 3,75	0,1 Formic acid in H_2O	0,1 Formic acid in H_2O
Eluent B	Methanol	0,1 Formic acid in acetonitrile	0,1 Formic acid in acetonitrile
Flow rate	0,2 mL/min	0,3 mL/min	0,3 mL/min
Flow	Gradient: 70% B at 0 min, 70% B at 0,5 min, 30% B at 9 min, 30% B at 10 min, 70% B at 14 min	Gradient: 90% B at 0 min, 90% B at 0,5 min, 10% B at 9 min, 10% B at 10 min, 90% B at 14 min	Gradient: 10% B at 0 min, 10% B at 0,25 min, 80% B at 6 min, 10% B at 9 min
Running time	15 min	15 min	11 min
Injection volume	20 µL	10 µL	20 µL
Temperature	40 °C	40 °C	35 °C

Table 5: HPLC conditions of the fullscan analysis for negative mode

Column	ZIC-pHILIC	xBridge Shield RP18
Eluent A	10 mM Ammonium acetate pH 8,9	10 mM Ammonium acetate pH 8,9
Eluent B	Acetonitrile	Methanol
Flow rate	0,2 mL/min	0,2 mL/min
Flow	Gradient: 70% B at 0 min, 70% B at 0,5 min, 30% B at 9 min, 30% B at 10 min, 70% B at 14 min	Gradient: 30% B at 0 min, 30% B at 0,5 min, 70% B at 9 min, 70% B at 10 min, 30% B at 14 min
Running time	15 min	15 min
Injection volume	10 µL	10 µL
Temperature	40 °C	40 °C

After measurement of the intensity for all compounds in the sample mixture by MS, the data are analyzed with the aid of difference shading.

2.8.2.4 Difference shading

The data that were obtained from the measurement with the aid of the full scan method in MS were transferred into jdx-files using the program analyst 1.6.3 (AB Sciex, Darmstadt, Germany). Afterwards, the data were converted into BD-files through the program DS DataConvert (version 1.6) in order to render their evaluation compatible with the DS FullView program.

Both programs, DS DataConvert DS and FullView were discovered by Prof. Dr. Gründemann (Center for pharmacology, University Hospital of Cologne) [5]. Consequently, the data show in three dimentional mass spectra which the intensity (y-axis), retention time (x-axis) and *m/z* (z-axis) are (Figure 20).

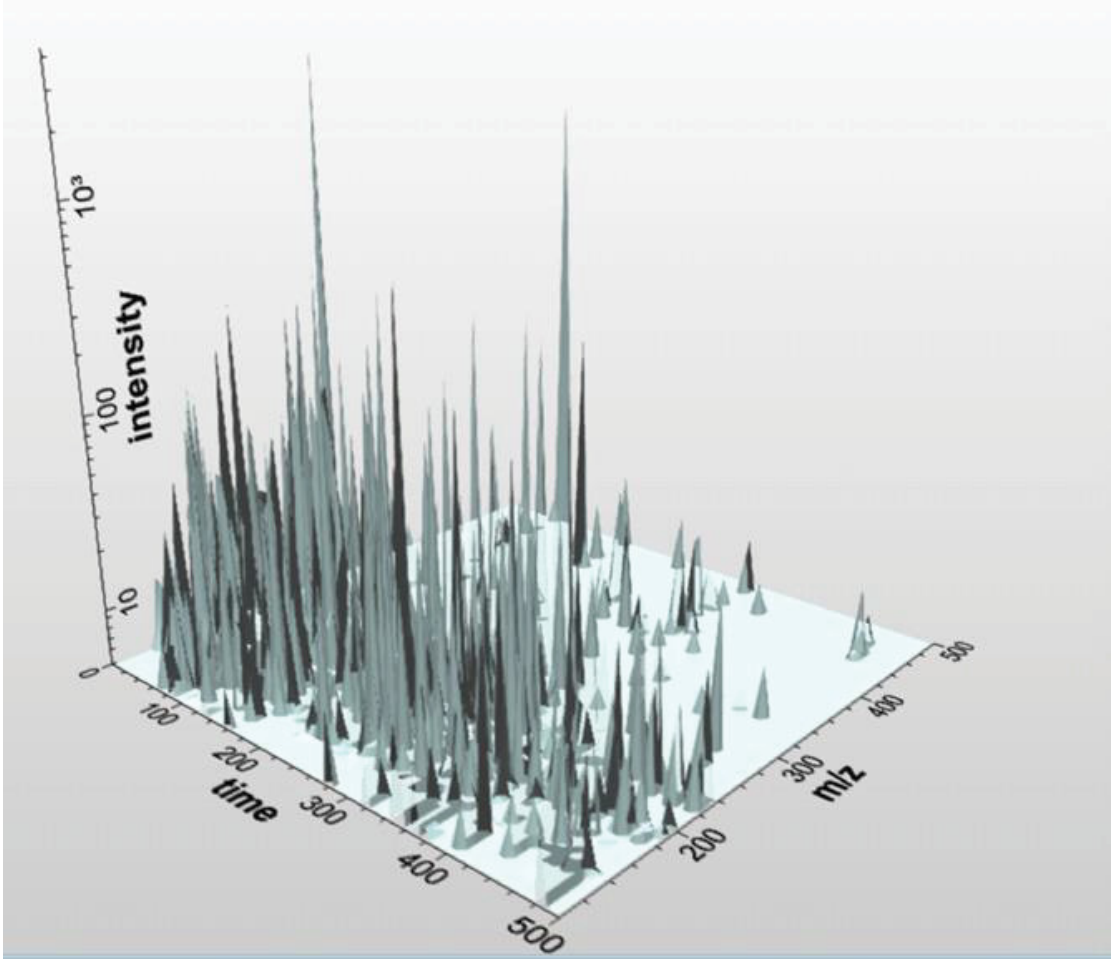

Figure 20. Schematic of 3D ion chromatogram resulting from the analysis of full scan experiment. This raw data show full scan mass spectra obtained at consecutive times and provide the retention time, intensity and the mass-to-charge ratio (*m/z*) [140].

Moreover, the intensities from the measured samples (effect and control), are compared in the 8-bit color mode of the sRGB color space. The overlap of images provides a gradiant of color between white for high intensities and black for low or no

intensities. The difference of intensities between the effect and control samples leads to gray shades which can be analyzed and show either a red or a cyan signal (Figure 21 and 22).

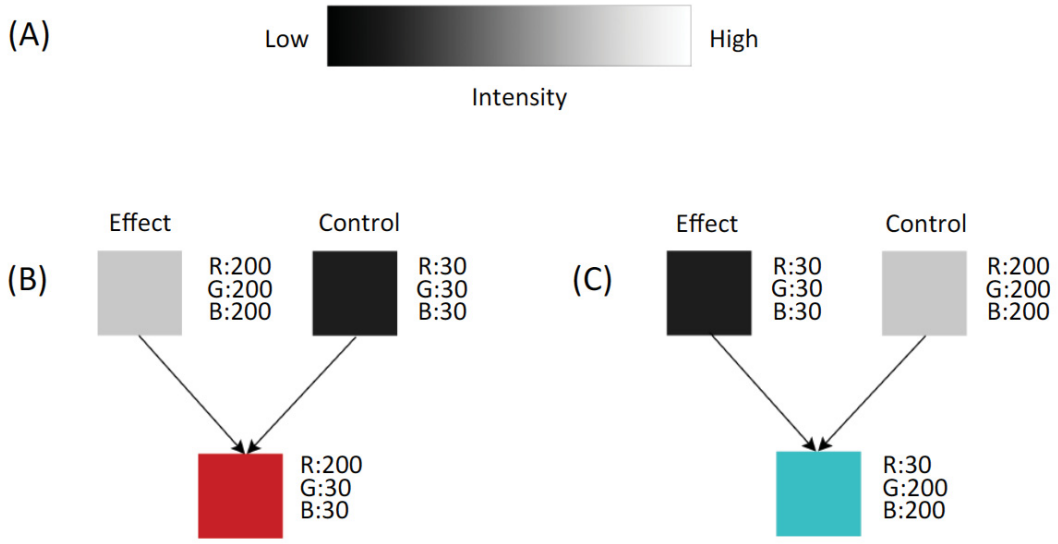

Figure 21. Schematic of the intensities calculation in the difference shading. (A) Show the intensity in the sRGB color range for each mass spectrum. Dark color indicates low intensity or no peak, whereas light is for high intensities. (B) Red signals are displayed when the intensity from the effect sample is higher than the intensity from the control sample. (C) Cyan signals show up when the intensities from the control are higher than the intensity from effect. Modified from [29].

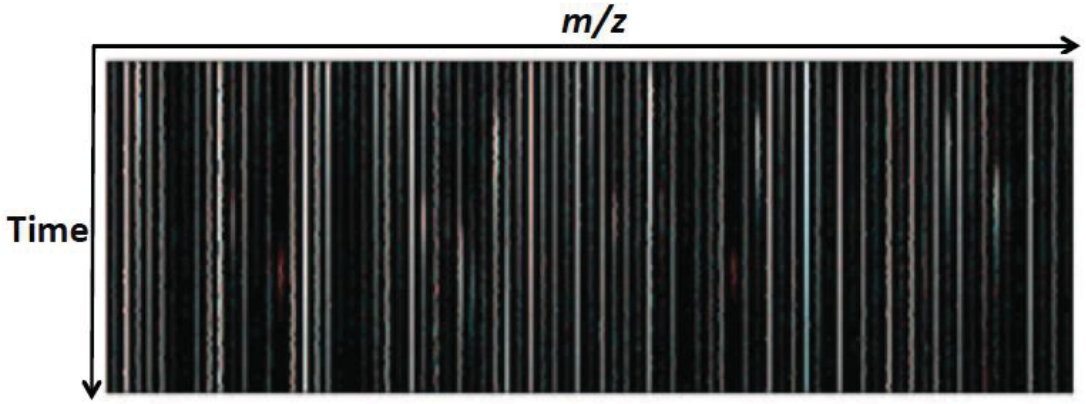

Figure 22. Schematic of results yielded through LC-MS difference shading. The compounds which are presented in the effect or control samples, show in red or cyan, respectively. The white color appears when the intensities from the effect and control samples are the same. Black indicates low intensities. Modified from [5].

An example of difference shading analysation in this work is the detection of the reaction product of ascorbic acid (AA) and singlet oxygen ($^1O_2$) (Figure 43). In this case, samples from the reaction of AA with $DHPNO_2$ ($DHPNO_2$ generates $^1O_2$ through warming) for 12 min at 37 °C were the effect samples, and samples taken at 0 min were the control samples, since $DHPNO_2$ produces no $^1O_2$ at 0 min. The red signals were obtained from the reaction products of AA with $^1O_2$ (effect samples). In addition, each red signal provides the *m/z* of a parent ion (reaction product) at a specific retention time.

Moreover, this results (*m/z* and retention time for each parent ion) from difference shading can be used for futher and more sensitive analysation with the aid of product ion scan.

2.8.2.5 Product ion scan

The product ion (MS/MS or MS^2) scan is a method used for the accurate identification of compounds. In this process, a specific molecule (parent ion) with a certain *m/z* (*m/z* could be obtain from a signal in the full scan of an unknown compound) will be selected in the first MS chamber (Q1) and only then can this selected molecule pass to the second MS chamber (Q2). In the Q2, a specific energy will be applied on the selected molecule and break it, forming certain fragments called daughter ions that are move towards the detector. In addition, all fragments that are produced in the Q2 can be analyzed by the detector or the Q3 can be set to allow only one fragment to pass the Q3 filter to reach the detector (Figure 19). The molecular structure can be determined by comparison with a data bank, such as MassBankjapan.de [141] or Metlin [142]. Furthermore, if the fragments can not be found in any databases, then possible molecular structures can be postulated by interpreting the resuting fragments. Moreover, the identified fragments can be transferred into a selected reaction monitoring (SRM) method (2.3.4) which provides

more accurate analysation, since the quantification in this method is based on a specific molecule (parent ion) and its specific fragment (daughter ion).

2.8.2.6 Tuning process

The tuning process is a method that identifies the optimal conditions to measure a specific material. In this method, a pure substance is injected directly into the mass spectrometry by means of a syringe. This process provides the information about the *m/z* of a parent ion of the substance and its respective fragments (daughter ions), forming after appling an energy on the parent ion in the fragmentation chamber (Q2) of the MS. In addition, the method itself changes automatically the applied energy and selects a suitable energy to determine the optimum fragmentation conditions. Afterwards, the data obtained from the tuning will be merged into an appropriate method and tested through various columns with a different HPLC conditions method to become significant signal for the substance after moving through the colums.

Moreover, the tune method was utilized in this work to find the best condition for LC-MS/MS to measure the substances oxidized GSH (GSSG) and dehydroascorbic acid (DHA).

2.8.2.7 Selected reaction monitoring (SRM)

Selected reaction monitoring (SRM) is a sensitive method that used in the LC-MS/MS to identify substances. In this method, a certain parent ion that already has a charge or becomes a specific charge (positive or negative) in the ionization unit (Q0) (Figure 19) will be selected in the first quadrupole (Q1) and only this parent ion will be allowed to pass to the fragmentation chamber (Q2). In the Q2, the parent ion receives a suitable energy (collision energy) which breaks it up into fragments. The specific fragment or all fragments (daughter ions) which belong to the parent ion can then pass

through the Q3 towards the detector to be analyzed. This process can be performed on triple quadrupole mass spectrometers.

Thus, specific molecules can be exactly identified by means of a calibration series of pure substances. For instance, for ET and GSSG quantification, a calibration series of the concentrations 0, 50, 100, 200, 400 and 800 ng were prepared in respective solutions of this experiment and then used. However, in some cases where no calibration series can be made, the data from the integration of the peak areas were demonstrated in order to identify the products. The data presented in this work were analyzed with the aid of the program called Analyst 1.6.3. Table 4 shows various substances which were identified through the SRM method.

Table 6: Analysis and quantification for the *m/z* compounds by MS via SRM. The fragmentation was performed by collision with nitrogen at Q2. DP: declustering potential, CE: collision energy, CXP: collision cell exit potential, and the scan time for all fragments was 150 ms.

Compound	Parent ion (*m/z*)	Fragment (*m/z*)	DP (V)	CE (V)	CXP (V)
ET	230	127	41	27	8
ET	230	186	41	27	8
ET + $^1O_2$	262	245	60	30	10
ET + $^1O_2$ ± GSH	264	188	60	30	10
ET + $^1O_2$ ± GSH	246	202	60	25	10
ET + $^1O_2$ ± GSH	246	125	60	25	10
ET + $^1O_2$ + GSH	551	244	60	40	10
ET + $^1O_2$ + GSH	551	200	60	40	10
ET + $^1O_2$ + GSH	553	246	60	25	10
ET + $^1O_2$ + GSH	553	308	60	25	10
GSSG	613	355	71	33	14
GSSG	613	284	60	25	10
GSSG	307	130	56	21	6
AA + $^1O_2$	209	191	-30	-10	-25
AA + $^1O_2$	191	147	-30	-10	-25

2.8.2.8 Ion trap (MS^3)

The ion trap (MS^3) process is a fail-safe method that can only be performe with ion-trap-based mass spectrometry [138]. In this method, a certain fragment (daughter ion) that was produced in Q2 from a selected ion in Q1 (parent ion) will be collected in the Q3 chamber and fragmented further by applying a specific collision energy to it, yielding further fragments which hit the detector and are analyzed (Figure 23). This process is often used and performed in order to distinguish between two or many molecules which have the same mass-to-charge ratio and both or all of them produce a fragment that has identical *m/z* value. In other words, it demonstrates information about further fragmentation of the desired fragment ions [138]. MS^2 can analyze only the parent ions and the respective daughter ions, whereas the MS^3 method can identify the fragments of the daughter ion as well.

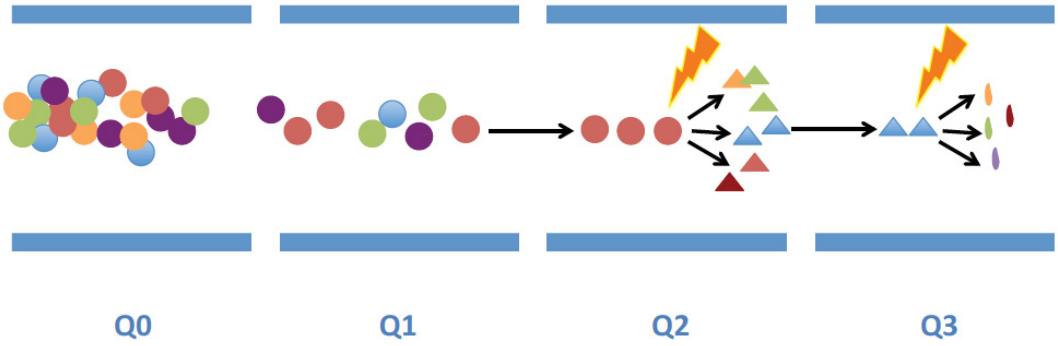

Figure 23. Schematic diagram of MS^3 for quantitative analysis by LC-MS. Charged compounds will be accelerated in the Q0, and then, a specific analyte ione is selected in Q1 and fragmented in the Q2. Specific fragment ions from Q2 are trapped in Q3 and fragmented further to generate product ions which are analyzed by the detector. Modified from [143].

In the present work, the MS^3 method was performed to analyze the compound 264 in order to distinguish between its two variants, both of which are ET and include two hydroxyl functional groups, which occupy either vicinal at position 4 and 5 (vicinal hydroxyls) or both hydroxyl functional groups bond to the same carbon atom at position 5 (geminal 5-diol). The MS^2 could not distinguish between them, since both

variants produce the same fragment 188 arising after the loss of thiourea form either a vicinal enediol or an acrylic acid structure, respectively. The MS^3 experiment was able to collect the fragment 188 itself and fragmented it further to identify its product. The fragmentation of 188 produced a robust signal at 160 (Figure 28), which must correspond to the loss of CO. Thus, this robust fragment at 160 can only agree with the vicinal enediol. Therefore, the compound 264 contains hydroxyl groups at position 4 and 5 separately, resulting from an attack of water at position 4 of the enol structure 246:202 and not from an attack at position 5 of the imidazole ring.

The condition of the MS^3 method that were used in the analyzation of the compound 264 were showed in Table 7.

Table 7: Analysis and quantification for the compound 264 by MS via MS^3. The first and second fragmentations were performed at Q2 and Q3, respectively. The parameters in the Q1 are DP: declustering potential, CE: collision energy, CXP: collision cell exit potential, and the scan time. The parameters in the Q3 are AF2: Excitation energy, SR: Scan rate, ET: Excitation time, DFT: Dynamic fill time.

Parent ion	264
Fragment (Q2)	188
DP (V)	60
CE (V)	30
CXP (V)	10
Scan time (ms)	150
Fragment (Q3)	160
AF2	45
SR (Da/s)	1000
ET (ms)	75
Fill time (ms)	DFT

2.9 Calculations and statistics

Results are presented, if not indicated otherwise, as the arithmetic mean ± SEM with at least n = 3 replicates. All assays were performed at least twice, on separate days. For each experiment the substances were freshly prepared.

The area of the intensity vs. retention time was integrated for each analyte. Linear calibration curves from six standards were prepared for ET and GSSG, in the respective solvent of each experiment and were analyzed with a weighting of $1/y^2$.

Linear regression slopes were compared (in two groups each, control and sample) utilizing GraphPad Prism version 8.0.1 for macOS, GraphPad Software, San Diego, California, USA. The P values (two-tailed) indicate the possibility that randomly selected data points would have slopes as different as (or more different than) observed. P values < 0.05 were considered significant.

Density functional theory (DFT) computations were performed with the Gaussian 16 package [144]. All minima and transition structures were fully optimized and characterized by frequency computations using the B3LYP/6-31G*-GD3-BJ method. Gibbs-energies (unscaled, 298.150 K, 1 bar) were used to assess relative stabilities and reaction barriers [103]

3 Results

3.1 The reaction of ergothioneine with singlet oxygen in the presence and absence of glutathione

Many experiments of ET with $^1O_2$ in both the presence and absence of GSH were performed in this work in order to analyse the stability of their reaction products and investigate whether those products could react further over time or decompose to other compounds. The compound 246:202 (respective numbers in this thesis represent *m/z* ratios of parent ions and their respective fragments) produced much faster than other products formed from ET and $^1O_2$. However, it was observed that the addition of 10 mM glutathione (GSH) prevented the loss of ET almost completely (Figure 24A) and nearly all ET-products disappeared or decreased, despite the fact that the reactivity of ET toward $^1O_2$ is about fifty-fold faster than GSH [12].

In the control assay made of ET and singlet oxygen, the content of compound 246:202 decayed and follow the decrease of ET over time in the absence of GSH, whereas in the assay including GSH, the compound 246:202 was markedly reduced, but literally unchanged (Figure 24B). This could indicate that GSH reacts with the product 246:202 in order to form a new compound or that GSH is able to minimize the production of 246:202.

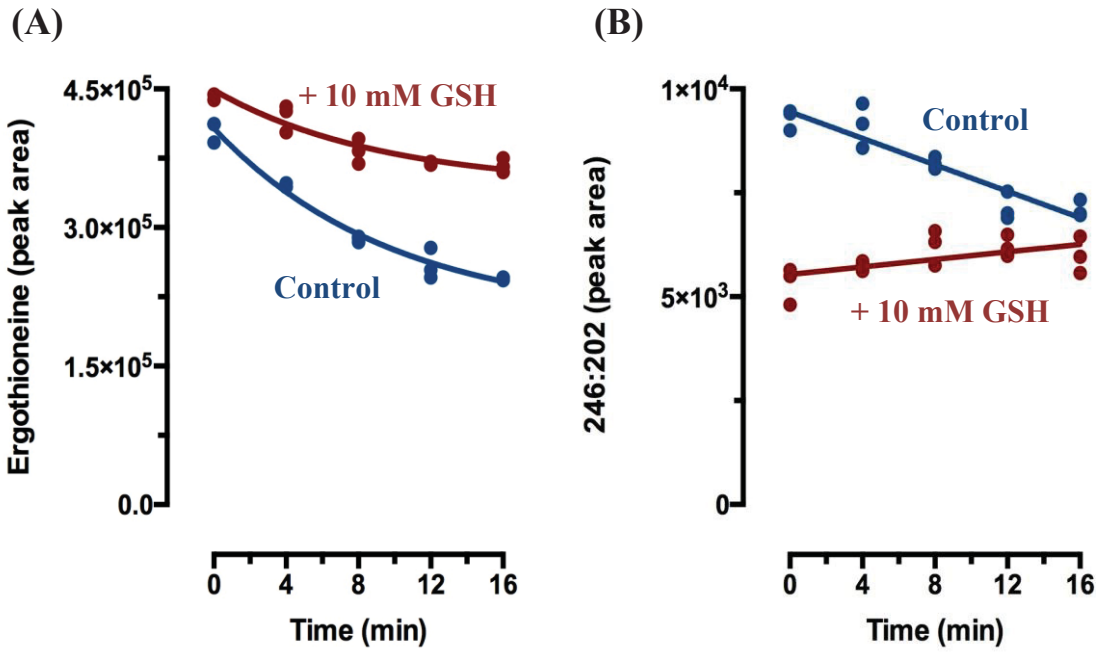

Figure 24. Addition of GSH prevents the loss of ET during the reaction with $^1O_2$. 10 µM ET and 10 mM $DHPNO_2$ without (Control) or with 10 mM GSH in 10 mM ammonium hydrogen carbonate, at pH 7.4, were incubated (V = 50 µl) for the indicated times at 37 °C. All samples were diluted 1:100 and analyzed immediately by LC-MS/MS for ET (A) and for the compound 246:202 (B). Exponential decay functions and linear regression (GSH in B) were used to describe the data.

Singlet oxygen can be added to the double bond of the imidazole ring of ET and generates a hydroperoxide (compound 262), which decomposes yielding a lactam intermediate (Figure 25). This lactam intermediate (244) can be reduced to the compound 246 with the aid of ET and yields the by-product ET-disulfide. The compound 262 is a side product that arises from water attacking the compound 244 on the position 4 of the imidazole ring. However, in the presence of GSH, the position 4 of compound 244 will likely be attacked by GSH and the intensity of the compound 262 will be declined (Figure 26).

In addition, the compound 551 is produced after the attack of one molecule of GSH. Afterwards, the compound 551 will be reduced to 246 by a second molecule of GSH and the oxidized GSH (GSSG) appears as a side reaction.

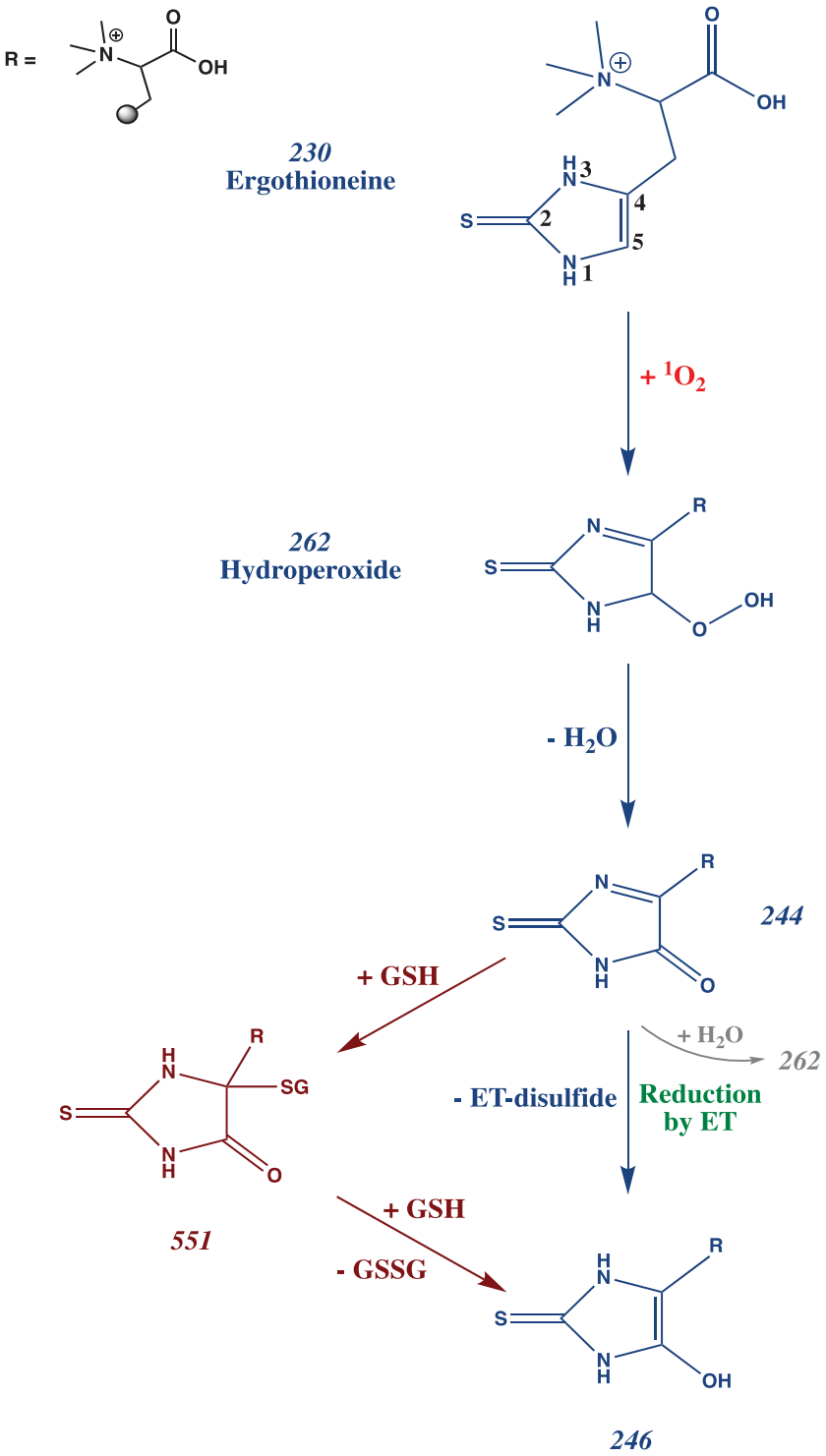

Figure 25. The proposed reaction of ET with $^1O_2$ with and without GSH. In the first step of the reaction of ET with $^1O_2$, singlet oxygen is added to the double bond of ET, yielding a hydroperoxide which decomposes to the intermediate compound 244, which is reduced by ET to an enol structure 246 and ET-disulfide as a by-product (blue). The compound 244 can also be attacked by water, yielding a second by-product 262. In the presence of GSH (brown), the intermediate compound 244 will be attacked by a GSH molecule producing the compound 551, which is reduced by a second GSH molecule, yielding the enol structure 246 and GSSG as a by-product.

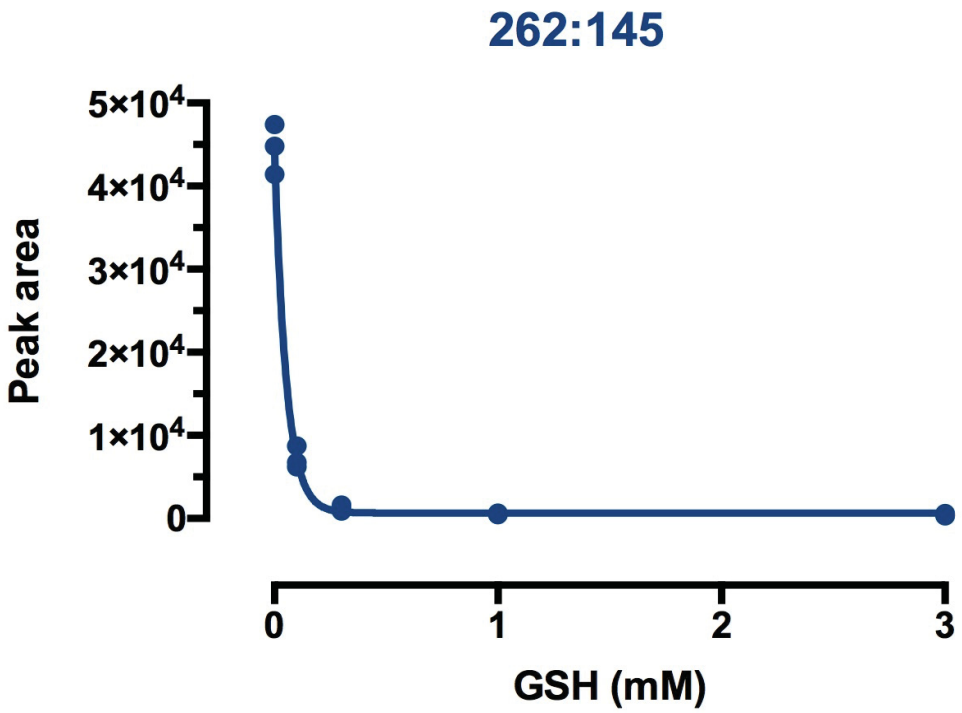

Figure 26. Declining the intensity of 262:145 through increasing the concentration of GSH. 100 µM ET, 10 mM $DHPNO_2$, and GSH as indicated in 10 mM ammonium hydrogen carbonate, pH 7.4, were incubated (V = 100 µl) for 10 min at 37 °C. The diagram shows how the compound 262:145 decays and then stays constant when the concentration of GSH increases. Samples were diluted 1:10 and directly analyzed by LC-MS/MS for the compound 262:145. Exponential decay function was used to describe the data. Each dot represents a sample.

The compound 246 can react with GSH or H_2O yielding the compounds 553 or 264 respectively (Figure 27) [12]. However, the exact mechanism of this addition reaction is unknown.

In fact, the enol structure of the compound 246 has a corresponing ketone form that is more stable (Figure 27) according to the density functional theory (DFT) computations that were performed by Professor Dr. B. Goldfuss from the Department of Organic Chemistry of the University of Cologne. The LC-MS/MS cannot make a distinction between enol and ketone form, since both of them have the same mass-to-charge ratio (246). Moreover, it is also unknown whether the attack of GSH on the compound 246 will be at the position 4 or 5, because the results from both reactions have the same mass-to-charge ratio (553).

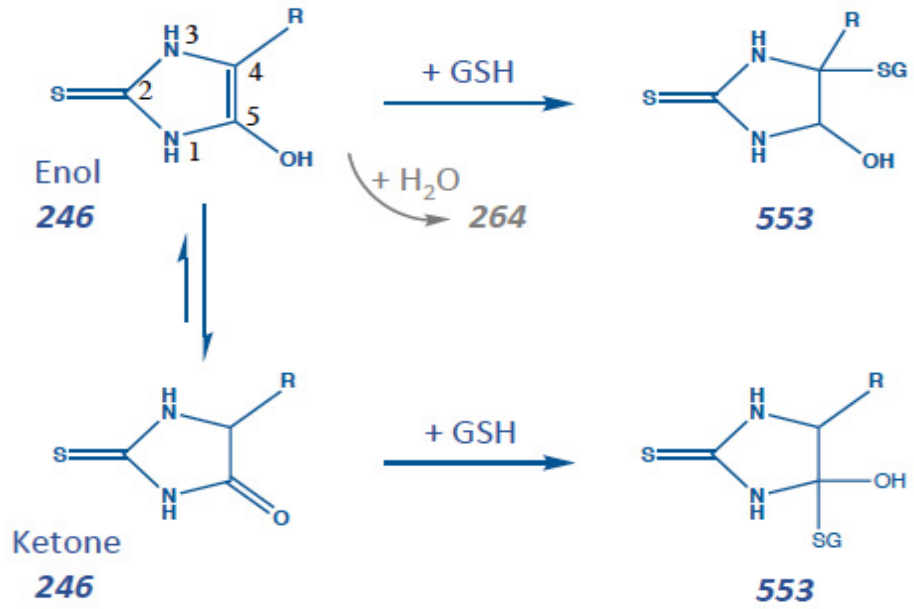

Figure 27. The proposed reaction of GSH with the compound 246. GSH can react with the compound 246, yielding the compound 553. GSH can attack the position 4 of the imidazol ring of the enol structure 246 or it can attack the position 5 of the ketone structure 246. The reaction products yielded from the attack of GSH on the position 4 or 5 cannot be distiguished by LC-MS/MS. H_2O can also react with the compound 246 yielding the compound 264 as a by-product.

The fragmentation data of compound 553 by LC-MS/MS cannot resolve the question of whether GSH prefers position 4 or 5 of the imidazol ring for the attachment [12]. In addition, DFT computation showed that the barriers for the addition of methanethiol to the enol C(4)=C(5)-OH function are similar for the Me-S-C-C(H)-OH (38.9 kcal/mol) or HC-C(SMe)-OH (32.9 kcal/mol) products. Thus, the DFT computation could not indicate which position (4 or 5) is favored.

Subsequently, the idea came from the side reaction 264 that an ET included two hydroxyl functional groups which occupy either vicinal at position 4 and 5 (vicinal hydroxyls) or both hydroxyl functional groups bond to the same carbon atom at position 5 (geminal 5-diol). Although on the one hand the MS^2 could not distinguish between the vicinal hydroxyls and geminal 5-diol, because both variants produce the same fragment 188 arising after the loss of thiourea to form either a vicinal enediol or

an acrylic acid structure, respectively, on the other hand, the MS^3 experiment was able to solve this issue (Figure 28).

In this process (MS^3), the fragment 188 itself was collected and fragmented further in ion trap mode (see 2.8.2.8) to check what could be produced. The fragmentation of 188 produced a robust signal at 160 (Figure 29), which must correspond to the loss of CO in this case.

Thus, this robust fragment at 160 can only agree with the vicinal enediol. Therefore, the compound 264 contains hydroxyl groups at position 4 and 5 separately, resulting from an attack of water at position 4 of the enol structure 246:202 and not an attack at position 5 of the imidazole ring. Thus, GSH molecules can attack at the position 4 of the enol structure 146:202, by analogy. However, this cannot completely rule out an attack at position 5 of the ketone structure 246:202.

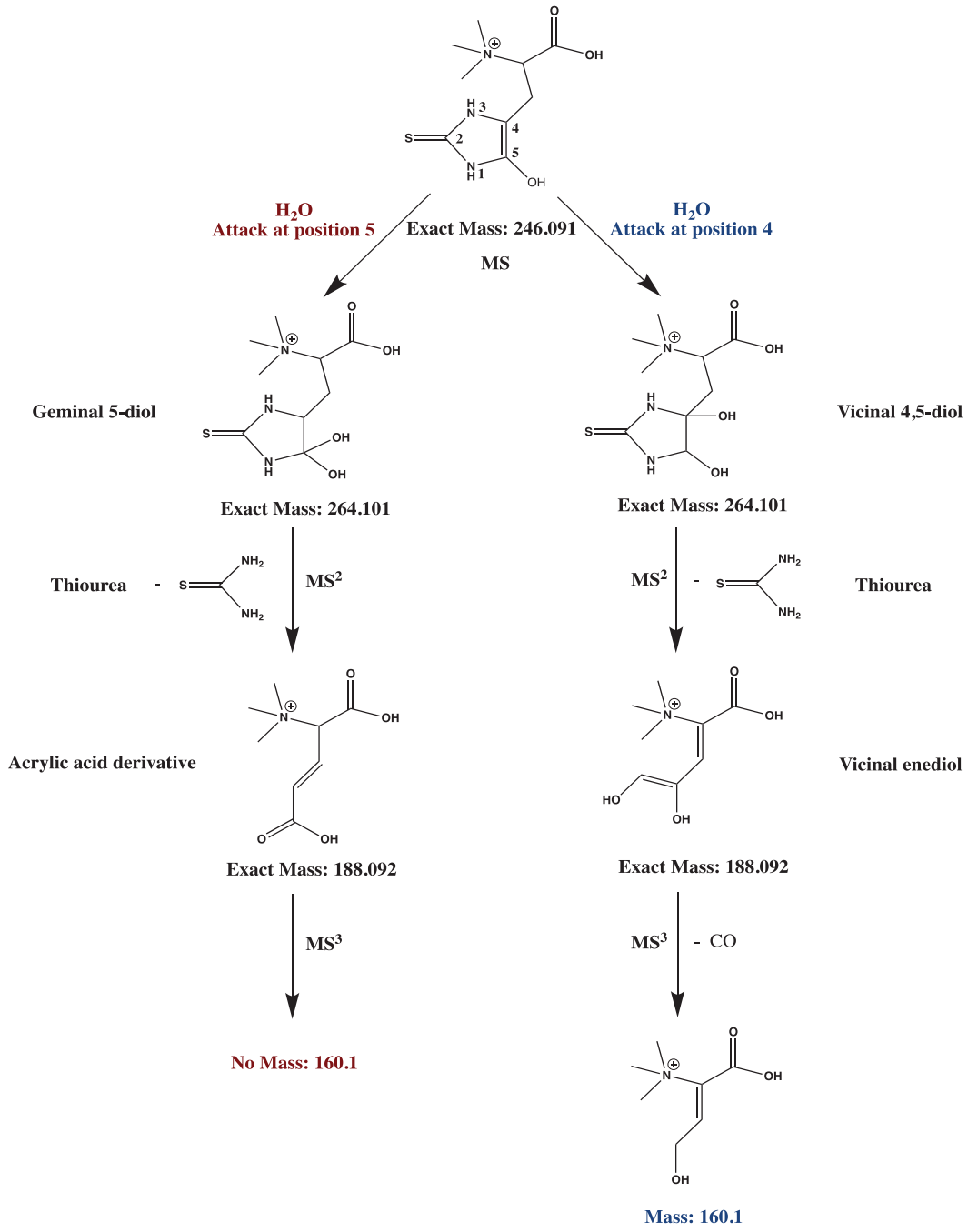

Figure 28. The MS^3 experiment of the proposed reaction of H_2O with the compound 246:202. H_2O can react with the compound 246:202, yielding the product 264:188. H_2O can attack at the position 4 of the imidazol ring yielding a vicinal hydroxyl (one hydroxyl group on the position 4 and one on the position 5) or H_2O can attack at the position 5 producing the geminal 5-diol (two hydroxyl groups on the position 5). MS^2 produces the main fragment 188 which is the same fragment for both variants (Geminal 5-diol and vicinal 4,5-diol), arising after loss of thiourea. In the MS^3, the main fragment 188 is further fragmented and the compound 160 was produced after loss of CO, which can only be produced from water attacking at the position 4 of the imidazole ring.

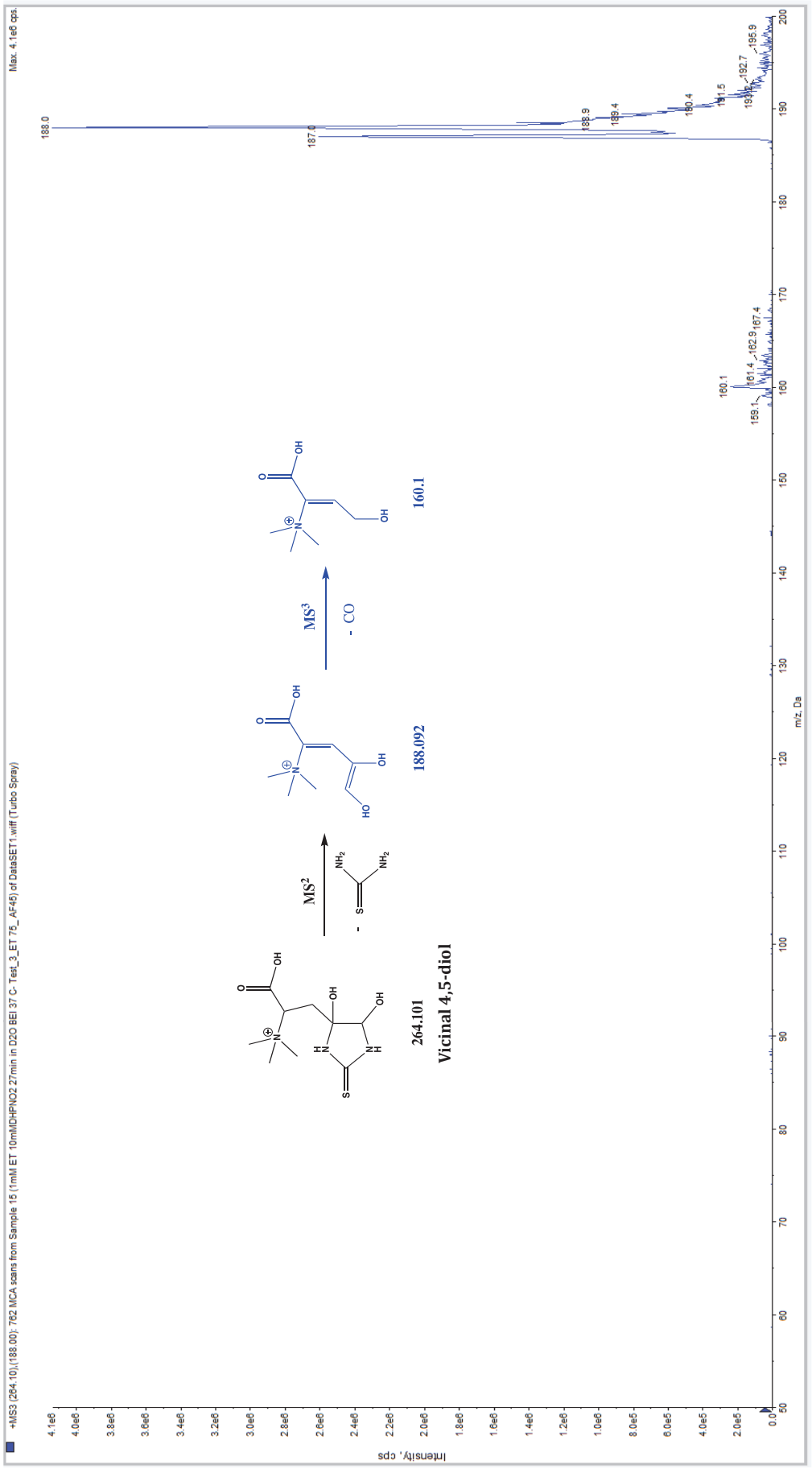

Figure 29. MS^3 process for the compound 264. In this experiment the main fragment 188 of the compound 264 was collected and fragmented in ion TRAP mode. A robust signal at 160 was produced from the fragmentation of 188, which must correspond to the loss of CO from the compound vicinal enediol (Figure 28).

Previously, the products from the reaction of ET and $^1O_2$ in the presence of GSH, i.e. compounds 551:244 and 553:308 were identified [12]. The compounds 551:244 and 553:308 are produced from an attack of the GSH molecule at the intermediate compound 244 and an attack of GSH at the compound 246:202, respectively (Figure 25 and Figure 27). In this project, both compounds were further analyzed in order to investigate what could change when the concentration of GSH changes. Therefore, the accumulation of both compounds 551:244 and 553:308 were measured as a function of GSH (Figure 30A).

It is obvious from (Figure 30A) that the amounts of both compounds that are formed are dependent on the concentration of GSH. In fact, the data show that the compound 551:244 predominates at low concentrations of GSH (0.1 - 1 mM), but gradually disappears when the concentration of GSH progressively increases. Moreover, the compound 551:244 completely disappears at a concentration of around 10 mM of GSH or higher. By contrast, the production of compound 553:308 depends on a higher concentration of GSH; it increases by increasing the concentration of GSH and it accumulates maximally around 10 mM GSH and then declines.

This diagram (Figure 30A) supposes that the compound 551:244 reacts with GSH if it is available in sufficient concentration. Moreover, the generation of compound 553:308 perhaps follows the transformation of 551:244, however, it is less efficient than 551:244, since around 100-fold higher concentrations of GSH are needed to make the compound 553:308 appear. In addition, the compound 553:308 decreases at very high concentrations of GSH and it might react with GSH as well. On the other hand, the diagram of the compound 246:202 shows a decline in its intensity by increasing the concentration of GSH and then stays constant (Figure 30B). The decrease of the compound 246:202 in this case also supports the idea (Figure 24B) that either GSH reacts with the compound 246:202 or decreases the production of it. The compound 264:188 (Figure 30C) that is a product of ET and $^1O_2$ is still in the measurement levels even at very high GSH concentration and this shows the efficiency of ET over GSH towards $^1O_2$. If GSH would merely capture most of the $^1O_2$ in this experiment, then all compounds made from ET and $^1O_2$ should decline at high GSH. This was not the case for compounds 264:188 (Figure 30C) and 246:202 (Figure 30B) up to a 1000-fold excess of GSH over ET.

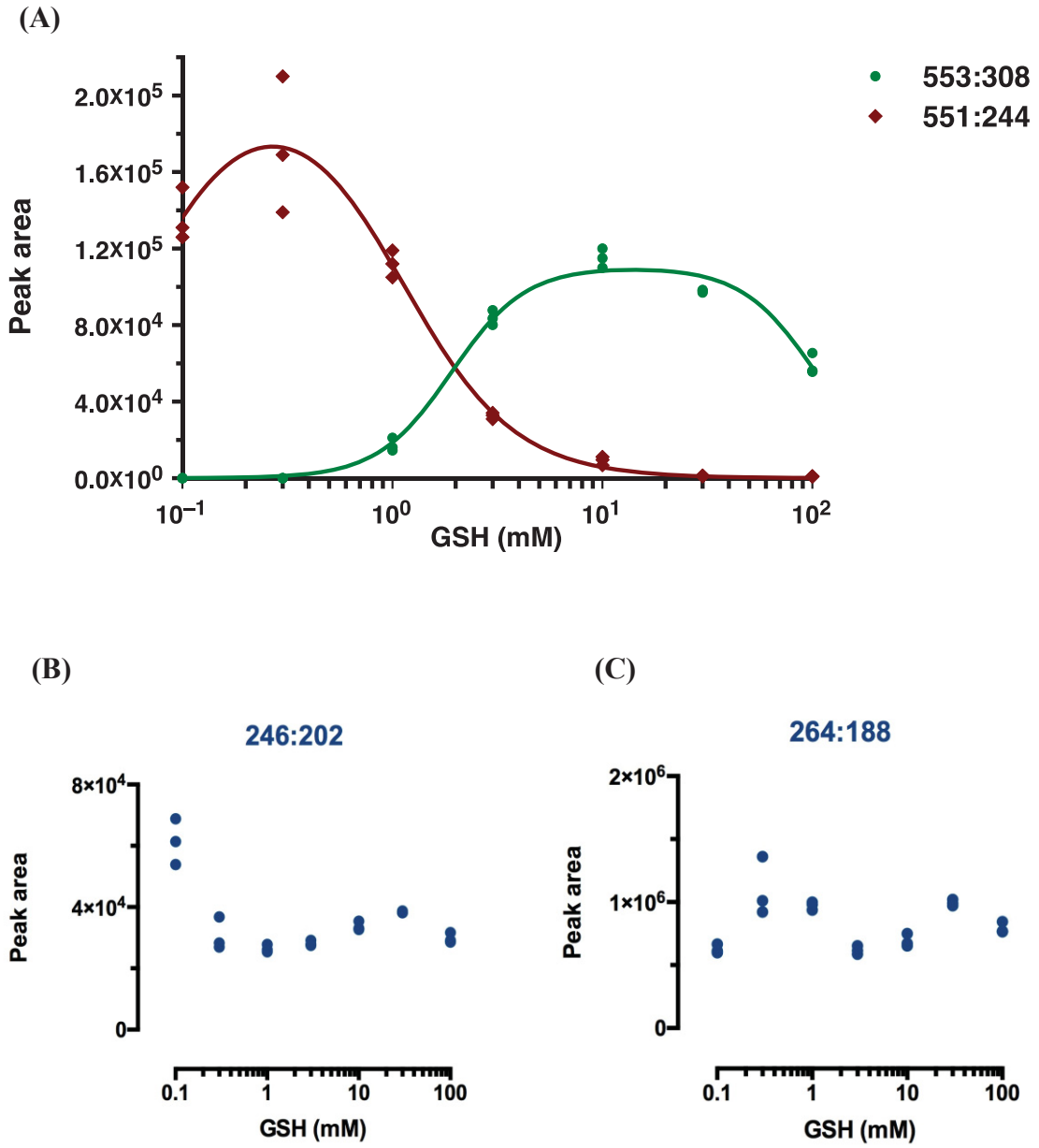

Figure 30. Production of compounds 551 and 553 from the reaction of ET, $^1O_2$ and GSH as a function of GSH concentration. 100 µM ET, 10 mM $DHPNO_2$, and GSH as indicated in 10 mM ammonium hydrogen carbonate, pH 7.4, were incubated (V = 100 µl) for 10 min at 37 °C. (A) Data show how the generation of compounds 551 and 553 is affected by changing the concentration of GSH. (B) The data represent how the compound 246 decays and then stays constant when the concentration of GSH increases. (C) The data show that the compound 264:188 produced from ET and $^1O_2$ is stable. Samples were diluted 1:10 and directly analyzed by LC-MS/MS for compounds 551:244, 553:308, 246:202 and 264:188. Results from a single experiment are shown; each dot represents a sample.

Based on that, GSH molecules can react with the compound 246:202, producing the compound 553:308 that can be reduced by another GSH molecule to obtain ET and the by-products GSSG (oxidized GSH) as well as H_2O (Figure 31).

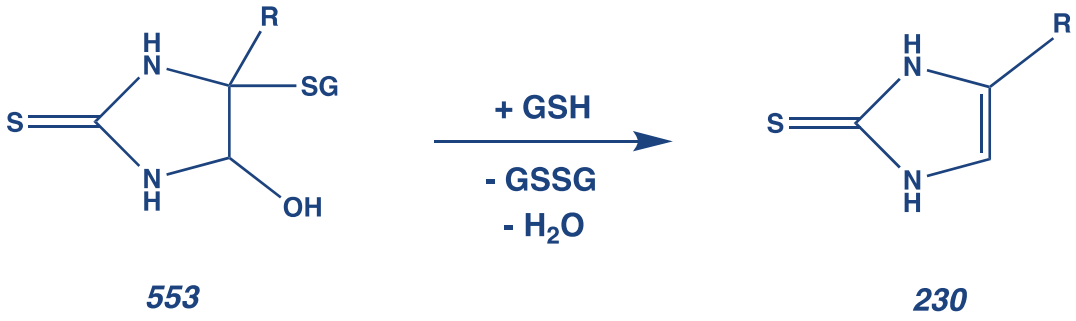

Figure 31. The proposed reaction of GSH with the compound 553. GSH can react with the compound 553, yielding the compound 230 (ET).

In agreement with these findings (Figure 25, 27, and 31), a non-enzymatic multi-step cycle for the regeneration of ET after reaction with $^1O_2$ was proposed (see discussion, Figure 46). This proposed mechanism of regeneration of ET consumes four molecules of GSH and produces two molecules of oxidized glutathione (GSSG) and two molecules of water per cycle.

In order to prove this mechanism, a series of procedures were performed independently: various experiments on the assays of GSSG and isolating the reaction intermediates.

First of all, the by-product GSSG (oxidized GSH) is a stable and quantifiable product in the absence of coenzyme NADPH and the enzyme glutathione reductase (*in vitro*). Therefore, if ET regenerates from its oxidized product in the presence of GSH, then the concentration of GSSG must be increased in this mechanism experiment.

3.2 The assay of oxidized glutathione (GSSG)

GSSG is an oxidized form of GSH and it is a disulfide compound that is produced from two glutathione molecules after reducing another compound. Moreover, the disulfide bond that connects both GSH molecules is stable in the absence of enzymes (Figure 32) [109]. In this work, the concentration of GSSG was measured in order to prove the proposed regeneration mechanism of ET after reacting with $^1O_2$, since the proposed regeneration cycle is dependent on the GSH that is oxidized to GSSG. For each regeneration cycle, four molecules of GSH are required to regenerate one molecule of ET from its oxidized product, arising after reaction with $^1O_2$. The four molecules of GSH that are needed are oxidized to two molecules of GSSG after reducing the intermediate compounds which are involved in the proposed mechanism. Therefore, the concentration of GSSG in this experiment has to increase in line with this proposed regeneration cycle.

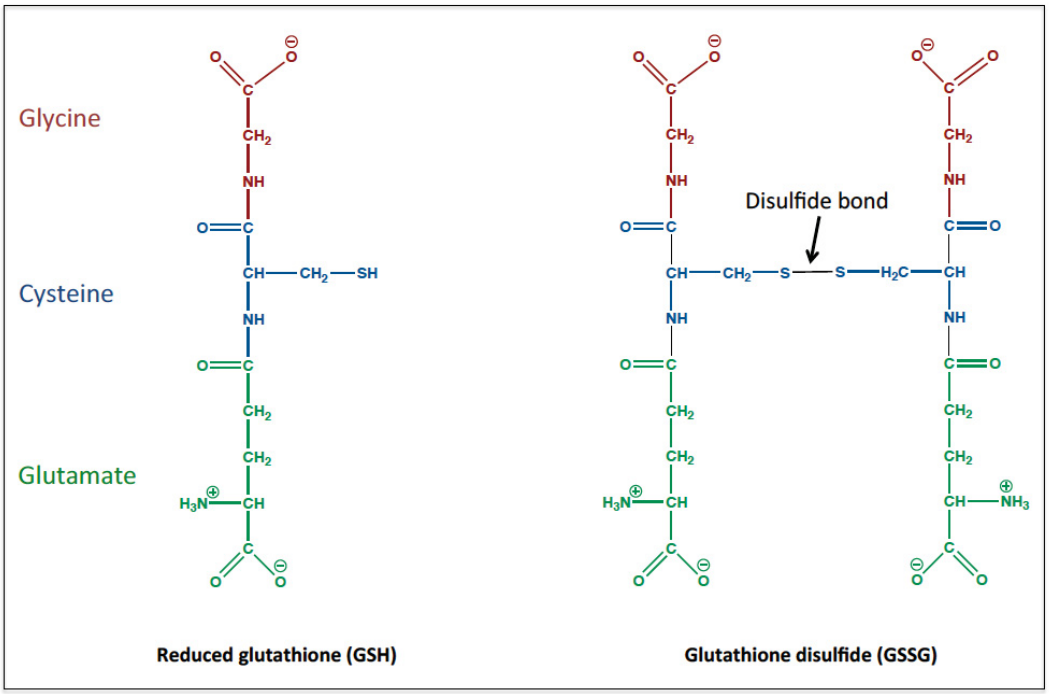

Figure 32. The structures of glutathione (GSH) and its oxidized form glutathione disulfide (GSSG) that are used and discussed throughout this work. Colors in structures display the amino acids that are included in GSH. The arrow shows the disulfide bond in the structure of GSSG.

In order to measure GSSG, an LC-MS/MS method had to be developed to detect the mass-to-charge ratios of the compound GSSG and its fragments. Therefore, the substance GSSG was tuned and fragmented by means of MS/MS and then the results were confirmed by comparing the results with a data bank such as, MassBank [141]. Furthermore, to be sure that the GSSG from the experiments in this work has the same parent ions and identical fragments, the GSSG and its fragments were measured by LC-MS/MS using the method of selected reaction monitoring (SRM) for the samples from the experiment made of 10 mM GSH and 10 mM $DHPNO_2$ that generates pure $^1O_2$. Moreover, this experiment was performed in D_2O for 12 min at 37 °C and then samples were diluted 1:100 and immediately measured by LC-MS/MS for GSSG (Table 8).

The two highest intensities from the peak area of the GSSG generated by the tuned method were 307:130 and 613:355 respectively. In addition, these were similar to the first two intensities that were yielded from oxidized GSH by $^1O_2$ experimentally. Therefore, in this work, the primary focus was on both of these ions to investigate the oxidized GSH in the experiments as well as the other fragment ions of GSSG which are listed in the Table below and which were also measured for comparison to confirm and further support the results.

Table 8: Measurement and fragmentation of oxidized GSH. The method tuning was used for material GSSG through MS/MS to examine its *m/z* of the parent ion and the corresponding fragments. The parent ion and fragments of oxidized GSH (GSSG) were compared and verified through oxidized 10 mM GSH by $^1O_2$ (generated by 10 mM $DHPNO_2$) for 12 min at 37 °C in D_2O and were measured by LC-MS/MS using the SRM method. In this table, the parent ions are listed with their fragments, retention time, exact masses, intensities and the reaction mixtures. Cps = counts per second.

Parent ion (*m/z*)	Fragment (*m/z*)	Retention time (min)	Exact mass (g/mol)	Intensity (cps)	Reaction mixture
613	355	8.0	612.152	164000	800 ng GSSG
613	231	8.0	612.152	149500	800 ng GSSG
613	484	8.0	612.152	105000	800 ng GSSG
307	130	8.0	612.152	331500	800 ng GSSG
307	274	8.0	612.152	3870	800 ng GSSG
613	355	8.0	612.152	196000	GSH + $^1O_2$
613	231	8.0	612.152	168000	GSH + $^1O_2$
613	484	8.0	612.152	135666	GSH + $^1O_2$
307	130	8.0	612.152	743333	GSH + $^1O_2$
307	274	8.0	612.152	9576	GSH + $^1O_2$

The production of GSSG (compounds 613:355 and 307:130) was measured by LC-MS/MS in an experiment using 10 mM GSH and 10 mM $DHPNO_2$ with and without ET in water. In the control assay made with 10 mM GSH and 10 mM $DHPNO_2$, the production of GSSG in the time range of 3 to 12 min was very low, at 0.6 ± 1.3 μM min^{-1}. The addition of 1 mM ET markedly increased the production of GSSG to 14 ± 4 μM min^{-1} (Figure 33).

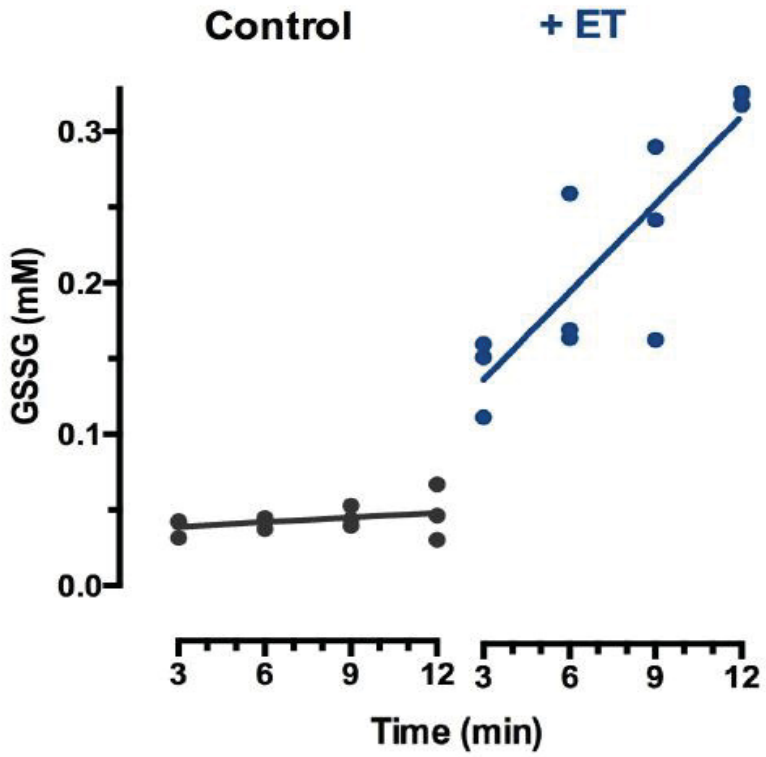

Figure 33. GSSG generation assay in H_2O. The diagram shows the effect of ET regarding the GSSG generation. The control assay contains 10 mM GSH and 10 mM $DHPNO_2$ in H_2O. ET was added to a final concentration of 1 mM. Samples were incubated at 37 °C for 3 to 12 min, diluted 1:100, and then immediately analyzed by LC-MS/MS for GSSG. This data is representative and is derived from a single experiment; each dot represents a sample. Data were analyzed by linear regression; the slopes represent GSSG production rates.

When water was replaced by deuterium oxide (D_2O) in the GSSG generation assay, both rates increased significantly due to the longer $^1O_2$ lifetime in D_2O [85]. Values reached 4.5 ± 1.1 µM min^{-1} for the control and 125 ± 14 µM min^{-1} in the presence of ET (Figure 34). However, the ratio of rates was similar whether in H_2O (factor = 26) or in D_2O (factor = 28). ET was compared with AA, because AA regenerates from its oxidized form dehydroascoric acid (DHA) by GSH and generates one molecule of GSSG per turn [109]. As a negative control, L-histidin (His) was added to the control in this assay (Figure 34), since His does not regenerate from its product after a reaction with $^1O_2$ [92]. The addition of His had, as expected, no effect, because no improvement in GSSG production was observed (2.3 ± 1.9 µM min^{-1}). However, a relatively low stimulation of GSSG was observed by the addition of AA (19.2 ± 1 µM min^{-1}) (Figure 34).

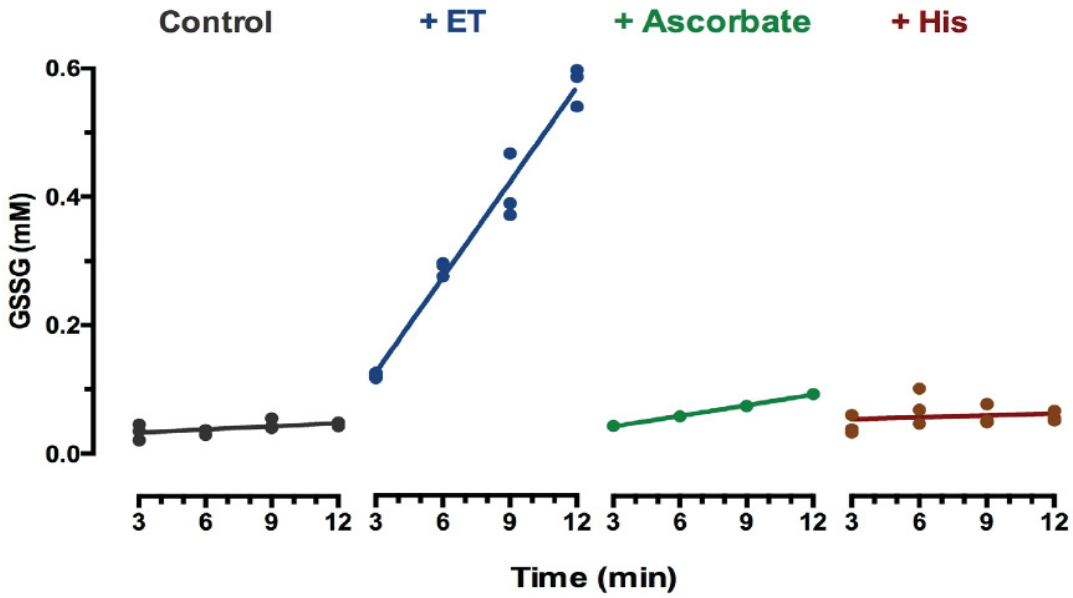

Figure 34. GSSG generation assay in D_2O. The graph demonstrates the efficiency of ET regarding GSSG production in comparison with AA and His. The control assay contained 10 mM GSH and 10 mM $DHPNO_2$ in D_2O. ET, AA and His were added to a final concentration of 1 mM. Samples were incubated at 37 °C for 3 to 12 min, diluted 1:100, and then analyzed immediately by LC-MS/MS for GSSG. This data was derived from a single representative experiment; each dot represents a sample. Data were analyzed by linear regression; the slopes represent GSSG production rates.

To distinguish the reaction efficiency of ET versus AA towards $^1O_2$, the production of GSSG in both was compared. After the subtraction of the GSSG production from the control assay, it turned out that the production of GSSG with ET was eight times higher than with AA. Since the regeneration of AA from DHA produced only one GSSG per turn [109], ET reacts at least 4-fold faster than AA with $^1O_2$, under the assumption that the ET cycle does not operate faster than AA cycle.

In the proposed ET regeneration mechanism, the whole reaction solely depends on the imidazole ring of ET. In order to verify this claim and investigate the importance of sulfur atom on the position 2 and nitrogen atoms within the imidazole ring of ET, ET was compared to several other imidazole derivatives (Figure 35) in the GSSG generation assay.

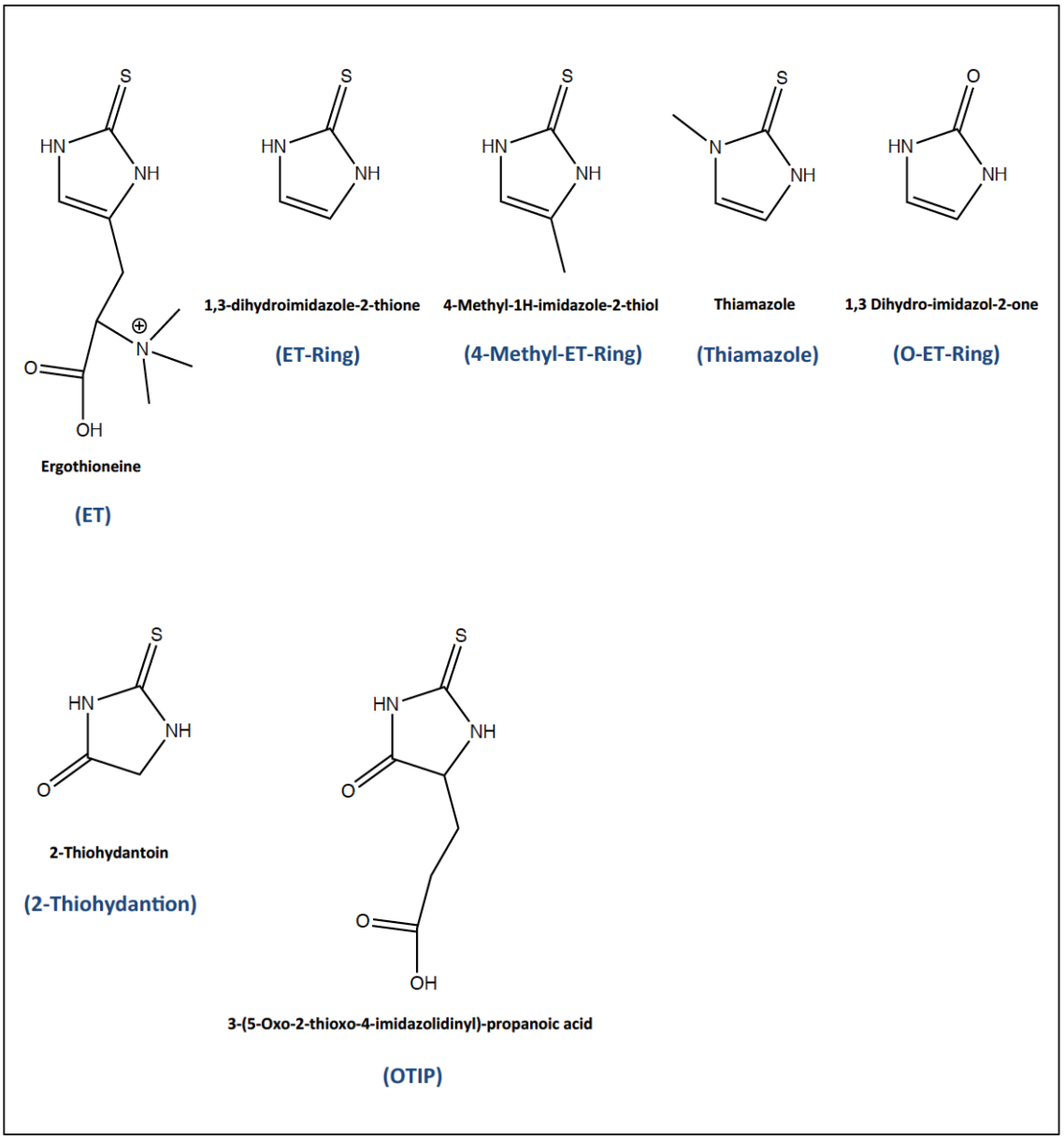

Figure 35. The structures of ET and several imidazol derivatives with their abbreviations used in the text.

Moreover, the experiment made of 10 mM GSH and 10 mM $DHPNO_2$ (control) with and without 1 mM ET, as well as the control with and without 1 mM of many compounds (Figure 35) was performed at least 3 times in order to verify whether the ketone form of the intermediate 246:202 (Figure 27) might be a part of the regeneration mechanism of ET or not, and also to find out the effect of the sulfur and nitrogen atoms within the imidazole ring of ET in the regeneration cycle. In each

experiment, assays with ET (average relative rate = 1 ± 0.13) and without ET (control, 0.03 ± 0.02) were carried out in parallel (Figure 36).

An additional control shows that the combination of 10 mM GSH + 1 mM ET without $^1O_2$ barely generates any GSSG. The addition of His in the assay with $^1O_2$ had no measurable effect (0.02 ± 0.04), whereas a small stimulation by AA (0.15 ± 0.02) was observed as expected, because AA reacts with $^1O_2$, yielding DHA which can be regenerated to AA by GSH, producing GSSG as a by-product. However, the regeneration mechanism of AA from DHA requires only two molecules of GSH producing just one molecule of GSSG per cycle.

The results from this investigation were in agreement with the notion that the ring of ET is responsible for the whole reaction cycle, because the ring of ET, 1,3-dihydroimidazole-2-thione (DHIT) and also 4-methyl-1H-imidazole-2-thiol (4-methyl ET ring) generated GSSG, equally significant as ET.

In line with that, the methylation of the ET ring on the position 4 of the imidazol ring (4-methyl ET ring) had no effect on the generation of GSSG. This confirms the point that the rest of the ET that is bound to position 4 of the ET ring was not involved in the reaction of ET with $^1O_2$. However, the methylation of the ET ring on one of the two nitrogens (drug names: INN thiamazole, USAN methimazole) reduced the production of GSSG (0.58 ± 0.09) by around 50%. Furthermore, the substitution of sulfur with oxygen in the ET ring markedly decreased the production of GSSG (0.29 ± 0.08).

Thus, it was demonstrated that the ring of ET is the sole important part of the ET structure in the proposed regeneration mechanism. Moreover, it could be demonstrated that both the sulfur and nitrogen atoms in the ET-ring have a significant function.

As explained above, the MS^3 suggested that GSH attacks the enol structure of the compound 246:202 in the proposed regeneration cycle of ET and it was proven that the corresponding ketone was not involved (Figure 27). In order to confirm that the

ketone form of the compound 246:202 does not form a part of the regeneration cycle via GSSG assay, two compounds that included a ketone function and similar to the ET ring were compared with the ET in the GSSG generation assay.

The compounds 2-thiohydantoin and 3-(5-Oxo-2-thioxo-4-imidazolidinyl)-propanoic acid that contain a ketone function on the position 5 of the ET ring, instead of a hydroxyl function in the intermediate compound 246:202 (Figure 27), generate the GSSG on the control level (0.05 ± 0.03) and (0.09 ± 0.02), respectively (Figure 36). Therefore, the intermediate molecule including a ketone function can not be a part of the regeneration mechanism of ET and this supports the third addition of GSH at the position 4 of the imidazol ring of ET as well (Figure 27 and 28).

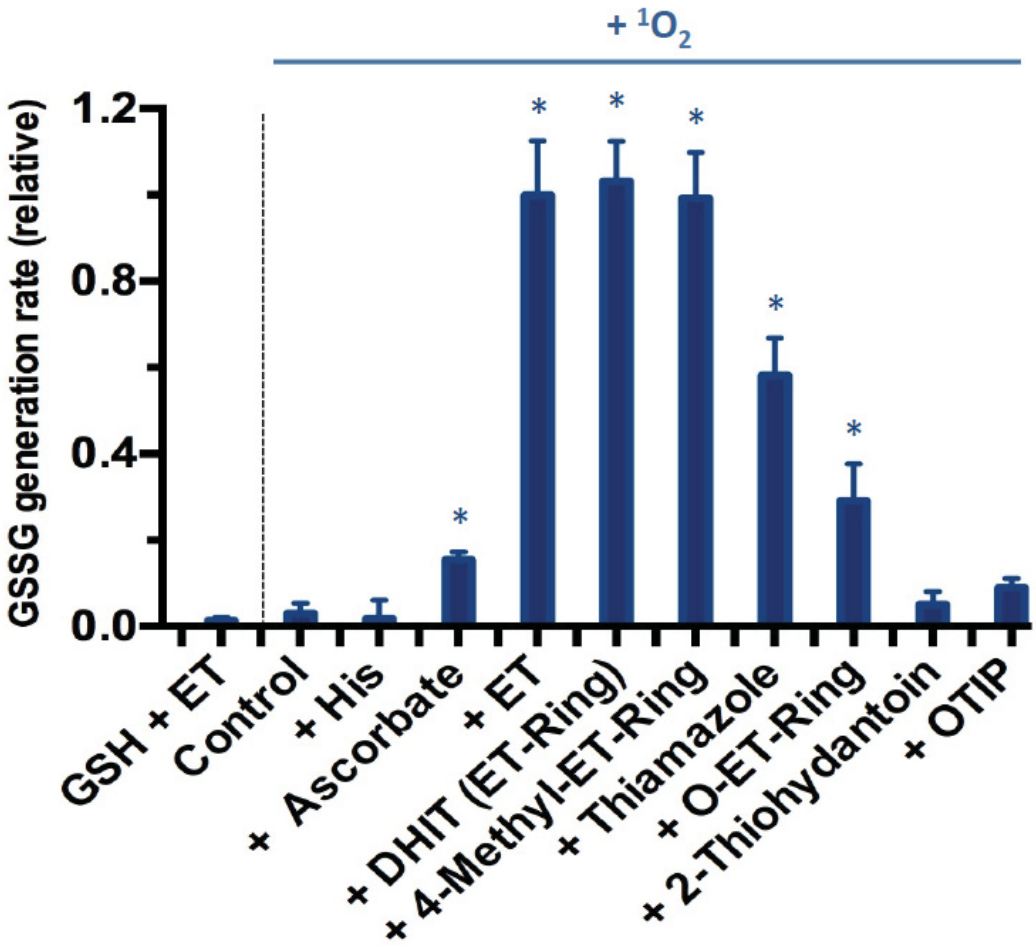

Figure 36. GSSG generation assay in D_2O. This graph represents the combined results from several experiments. The effectiveness of ET regarding GSSG production was compared to various compounds. The control assay contains 10 mM GSH and 10 mM $DHPNO_2$ in D_2O. The compounds were added as indicated to a final concentration of 1 mM. Samples were incubated at 37 °C for 3 to 12 min, diluted 1:100, and then immediately analyzed by LC-MS/MS for GSSG. Rates were normalized to the GSSG production rate in the presence of ET and then averaged (each point is the average of at least 3 experiments). GSH + ET represent 10 mM GSH plus 1 mM ET without $DHPNO_2$ as an additional control. Error bars indicate the SEM; an asterisk denotes that the slope of the sample group was significantly different from the respective control group.

The production of GSSG as a function of GSH concentration could be described by a simple hyperpola (Figure 37). The half-maximal rate was at 1.8 mM (95% confidence interval, 1.5-2.2).

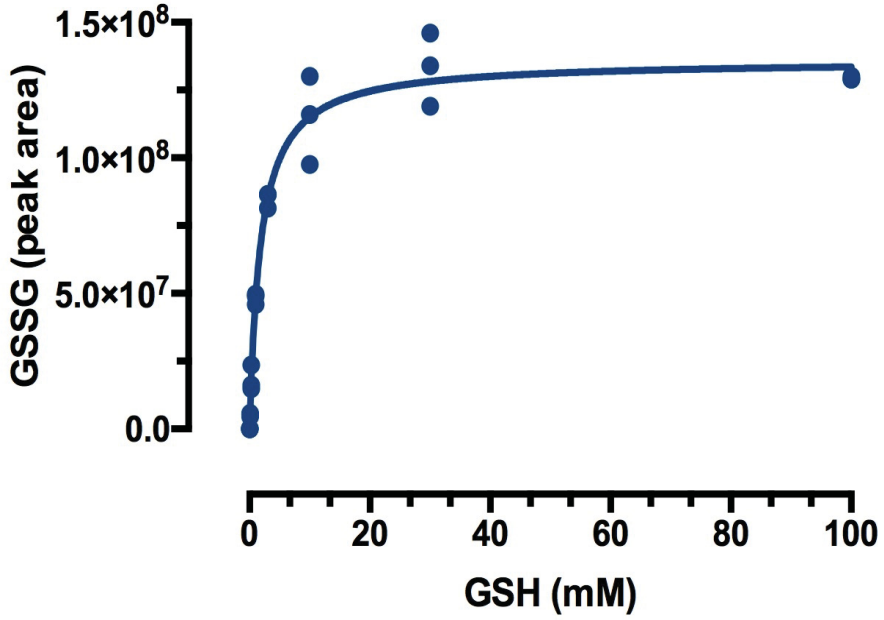

Figure 37. GSSG generation assay as a function of GSH concentration. The assay contains 0.1 mM ET, 10 mM $DHPNO_2$ and GSH as shown in the water buffer (10 mM ammonium hydrogen carbonate in H_2O, pH 7.4). Samples were incubated for 10 min at 37 °C, diluted 1:10, and then immediately analysed by LC-MS/MS for GSSG content. These data come from a single experiment; each dot represents a sample. The data were analysed by non-linear regression, using a hyperpola analogous to the Michaelis-Menten equation.

3.2.1 Using photosensitizer as a singlet oxygen generator in the GSSG generation assay

Parallel to the experiments with $DHPNO_2$ as a $^1O_2$ generator, some experiments with TMPyP were also performed. TMPyP is a photosensitizer and it is a commonly used material in publications as a $^1O_2$ generator. The GSSG generation assay for 10 mM GSH with 100 μM TMPyP without ET (control) and with 1 mM ET in D_2O were performed in both the presence and absence of UV light, since photosensitizers absorb light at a specific wavelength to generate $^1O_2$ (Figure 38).

The optimal excitation wavelength of TMPyP is 422 nm [58], however, in our laboratory, the wavelength of 365 nm was available to apply, which is still within the range of excitation of this photosensitizer.

The data from graph (Figure 38A) represents the efficiency of ET concerning GSSG production in comparison with the control that contains 10 mM GSH and 100 μM TMPyP in D_2O.

The data of the experiment in the presence of light shows that the generation of GSSG was strongly increased (29 ± 0.1 μM min^{-1}) exactly as expected when ET was added to the control to a final concentration of 1 mM, as indicated (Figure 38A). However, the production of GSSG from the control assay made up of 10 mM GSH and 100 μM TMPyP increased slightly (5 ± 0.2 μM min^{-1}), and this was to be expected, since TMPyP generates not only $^1O_2$ but also all other reactive oxygen species (hydroxyl radical, superoxide anion and hydrogen peroxide), which can also oxidize GSH and affect the results. Therefore, the data from the experiments that were performed using $DHPNO_2$ as $^1O_2$ generator were more precise (Figure 34), since $DHPNO_2$ produces pure $^1O_2$ and confirms that the reactions occur only with the use of $^1O_2$.

As a negative control, 1 mM ET and 10 mM GSH were mixed without TMPyP (GSH + ET + Light) and the data showed no measurable effect (0.4 ± 0.1 μM min^{-1}), which confirmed the data from the experiment with $DHPNO_2$.

In the absence of light, no effect was observed, as expected, since ROS are not produced from photosensitizer compounds without light and at a suitable wavelength (Figure 38B). Furthermore, the slopes in the absence of light showed no improvement and they were calculated for the control (GSH + TMPyP), control + ET and the second control (GSH + ET) at 2 ± 0.01 μM min^{-1}, 2 ± 0.05 μM min^{-1} and 0.2 ± 0.1 μM min^{-1}, respectively.

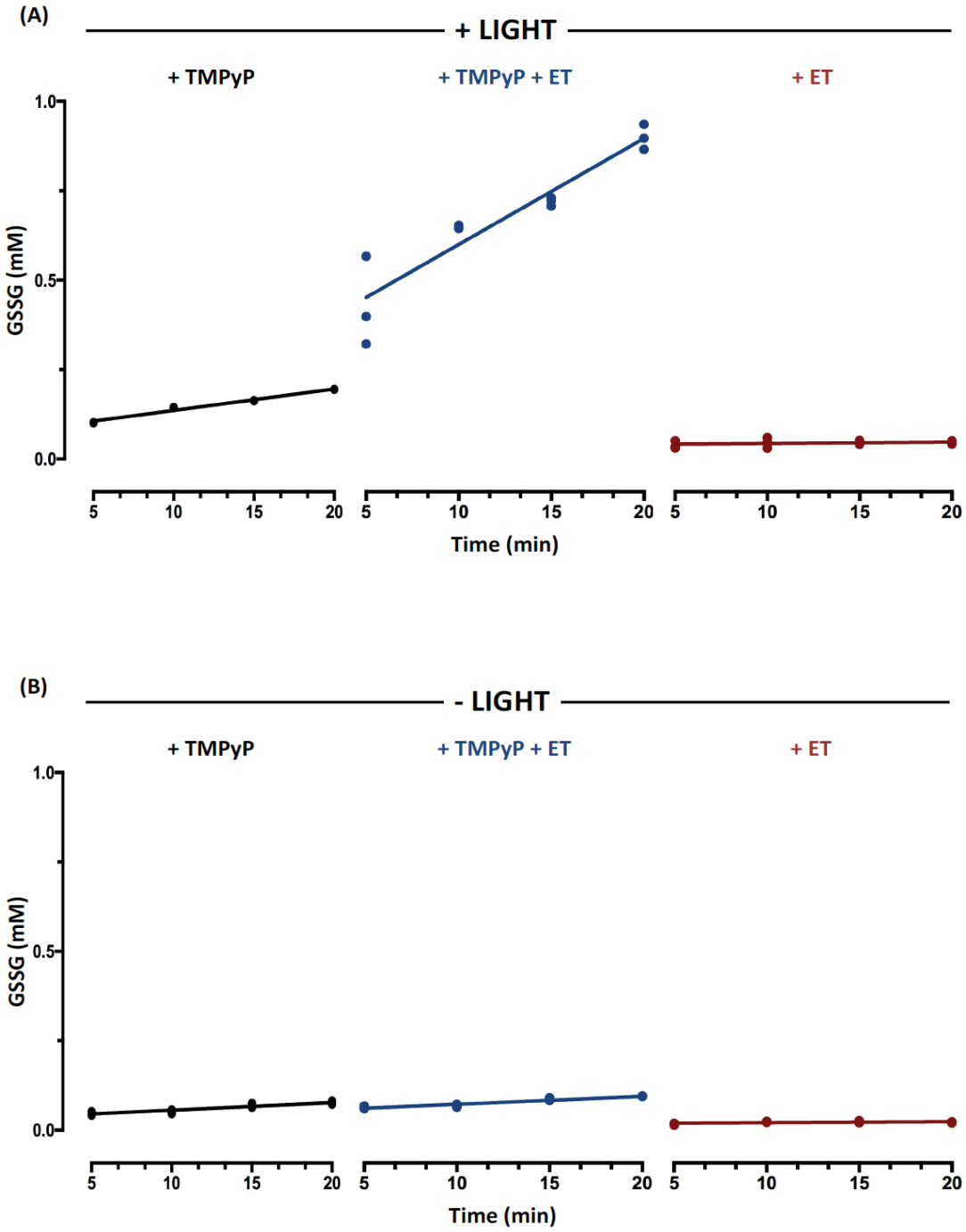

Figure 38. GSSG generation assay for GSH with and without ET in D_2O in the presence of ROS. 10 mM GSH was present in all samples. (A) The graph represents the efficiency of ET concerning to GSSG production in comparison with the control. The control assay contains 10 mM GSH and 100 µM TMPyP in D_2O. ET was added as indicated to a final concentration of 1 mM. As a second control, 1 mM ET and 10 mM GSH were mixed without TMPyP. Samples were incubated at 37 °C for 3 to 12 min under the UV light at 365 nm. (B) The graph shows GSSG production in the absence of light as a control. All samples were diluted 1:100, and then immediately analyzed by LC-MS/MS for GSSG. These data come from a single experiment; each dot represents a sample. Data were analyzed by linear regression; the slopes represent GSSG production rates.

In fact, the generation of $^1O_2$ from $DHPNO_2$ decreases exponentially with the half-life of 23 min and follows the equation for radioactive decay: $N(t) = N_0 * \exp(- \lambda * t)$ with N = amount / time [103]. Definite integration gives the sum of released $^1O_2$ as a function of time: $n = n_{max} * (1 - \exp(- \lambda * t))$. In addition, the production of GSSG is proportional to the total amount of released $^1O_2$. Moreover, the (Figure 39A) represents the accumulation of GSSG in the presence of ET to explain that there is no deviation from using linear regression instead of non-linear curve. The accumulation of GSSG from (Figure 39B) is supposed to be non-linear, however, the linear rate was applied because there is no significant deviation from linearity for the short time used.

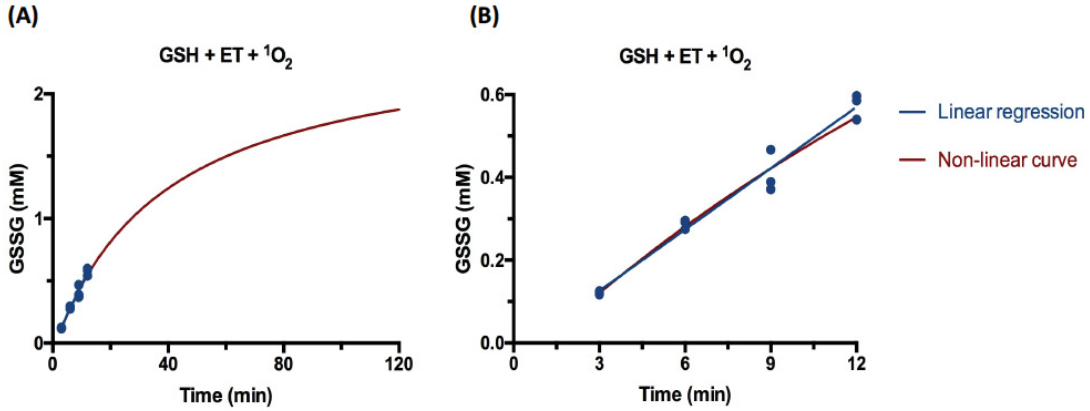

Figure 39. Illustration using linear regression instead of non-linear curve for short time cross. The data used are 10 mM GSH + 1mM ET in the presence of 10 mM $DHPNO_2$ and represent the production of GSSG. (A) The brown curve shows the fit from non-linear regression. (B) The enlarged section of (A) shows that the deviation from linearity is very slight.

The secound series of procedures performed in this work in order to prove the proposed regeneration mechanism of ET, involved capturing the reaction intermediates that arise from the reaction of ET with $^1O_2$

3.3 Capturing the reaction intermediates arising from the reaction of ergothioneine with singlet oxygen

The proposed regeneration mechanism of ET after the reaction with $^1O_2$ was, on the one hand, supported by the GSSG production assay described before (3.2). On the other hand, regarding the proof of the proposed mechanism, an approach was found. What was necessary to clarify the regeneration was whether isolating one of the products from the reaction of ET with $^1O_2$ and then adding GSH to the isolated product (product of ET + $^1O_2$) would stimulate the reaction and continue the regeneration cycle and yield ET. Therefore, if this hypothesis could be proven, the proposed mechanism of ET regeneration after reaction with $^1O_2$ would be strongly supported and would ascertain that GSH regenerates ET from its oxidized product.

In many experiments in the present work, it was attempted to isolate the reaction products of ET with $^1O_2$ through several kinds of thin-layer chromatography according to their polarity. In addition, several different detector materials with high selectivity were used to visualize the ET products. However, isolating this compounds was really challenging due to their instability and sensitivity.

From another standpoint and in order to prove the suggested mechanism of ET regeneration, it was attempted to capture the reaction intermediates that arise from the reaction of ET with $^1O_2$ by using cross-linked agarose beads that were covered with free thiol groups. The hypothesis behind this idea is that the thiol groups of the compound that are bound to the beads should react with the product of ET and $^1O_2$ reaction at the position where the thiol group of GSH would attack (Figure 25). In this case, unreacted ET will be removed after washing the beads, and only the reaction product of ET with $^1O_2$ should remain bound to the beads. Furthermore, the added GSH to the beads should react with the oxidized product of ET which is bound to the beads, and the mechanism cycle will be stimulated towards ET.

In the experiment made of 0.1 mM ET with and without 10 mM $DHPNO_2$, the reaction mixture was incubated on a shaker (1200 rpm) for 10 min at 37 °C in the presence of 100 µl of sedimented beads. These were covered with thiol groups of the

amino acid L-cysteine or, as negative control, with the hydroxyl groups of the amino acid serine. The amino acids were covalently linked via their amino groups to the insoluble, cross-linked agarose beads. In this experiment, 100 µL bead-gel were used; This corresponds to an 8-fold molar excess of thiol groups versus ET (Figure 40A). In the reaction solution, 0.1 mM GSH was present to diminish disulfide formation between ET and the Cys ligands (Figure 41). Afterwards, the beads were transferred into polypropylene microliter tips, wich were plugged with small pieces of cotton (Figure 40B).

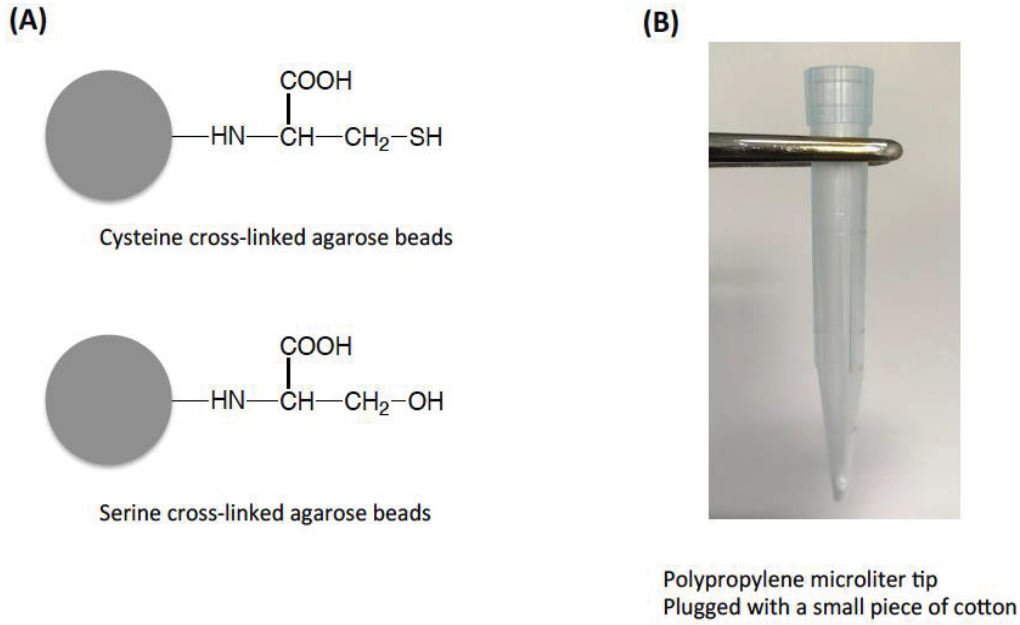

Figure 40. Cysteine/serine cross-linked agarose beads and the column used for capturing the oxidized product of ET. (A) The Figure shows how the amino groups of cysteine and serine are covalently linked to the insoluble cross-linked agarose beads. (B) The picture shows a polypropylene microliter tip plugged with a small pieces of cotton and used as a column to isolate the oxidized products of ET which are formed after the reaction of ET with $^1O_2$.

After washing the beads three times with 100 mM NaCl in buffer, the removal of unreacted ET was complete, since the washing buffer contained no ET (Figure 42). In the assay without $^1O_2$ (as a negative control), 100 µl buffer, 100 µl 10 mM L-serine in buffer and 100 µl 10 mM GSH in buffer were added to the bead columns in room temperature, consecutively.

The respective flowthrough fractions were immediately analyzed by LC-MS/MS for ET. Moreover, the data showed that in the assay without $^1O_2$ (as a negative control), a small amount of ET was released from the columns by GSH. However, in the presence of $^1O_2$, large amounts of ET were released by washing the beads with GSH. This suggests that products from the reaction of ET and $^1O_2$ were indeed captured by the beads. There is relatively no detection of ET when simply adding buffer and serine to the beads, respectively. However, adding GSH stimulated a further reaction towards ET and an impressive amount of ET was detected. In parallel controls, the cross-linked agarose beads that carry L-serine also captured some reaction intermediates, but the amount of ET released from the cys beads was almost 3-fold higher than the amount of ET from serine beads (after subtraction of the background in $^1O_2$-negative assays). In fact, these data strongly suggest that ET is regenerated from Cys-attached intermediates by the thiol function of GSH.

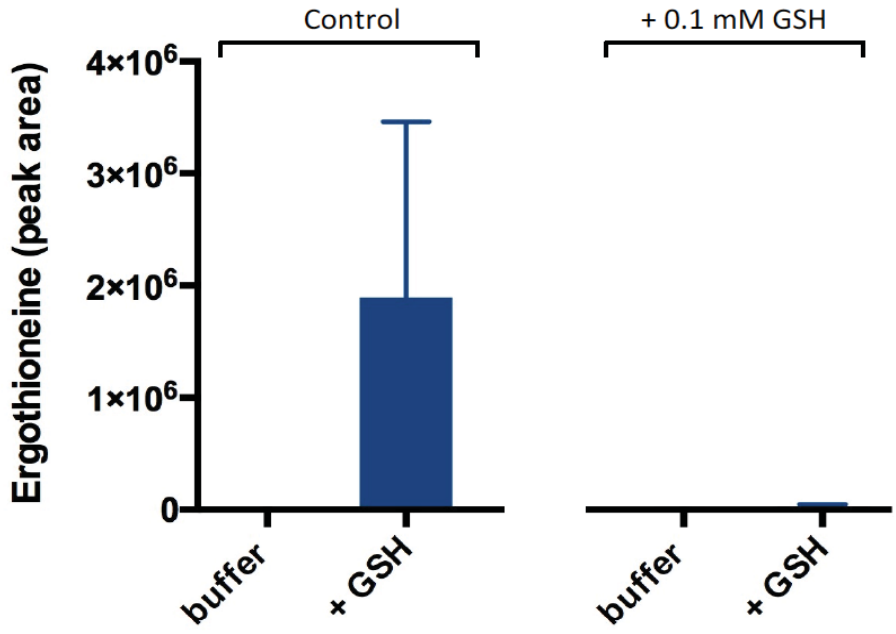

Figure 41. GSH diminish disulfide formation between ET and Cys ligands of the beads. The control reaction mixture contained 1 mM ET and 50 µl of sendimented cys beads in 10 mM ammonium hydrogen carbonate pH 8.0 buffer (V = 50 µL) in the polypropylene reaction tubes. GSH was added to a final concentration of 0.1 mM. The reactions were incubated for 10 min at 37 °C on a shaker (1200 rpm), then the beads were transferred into polypropylene microliter tips which were plugged with small pieces of cotton. After 3 washes, each with 500 µl of 100 mM NaCl buffer, 100 µl buffer and 100 µl 10 mM GSH in buffer, were applied in succession to the columns (at room temperature). The eluates were directly analyzed by LC-MS/MS for ET content. Error bars indicate the mean ± SEM.

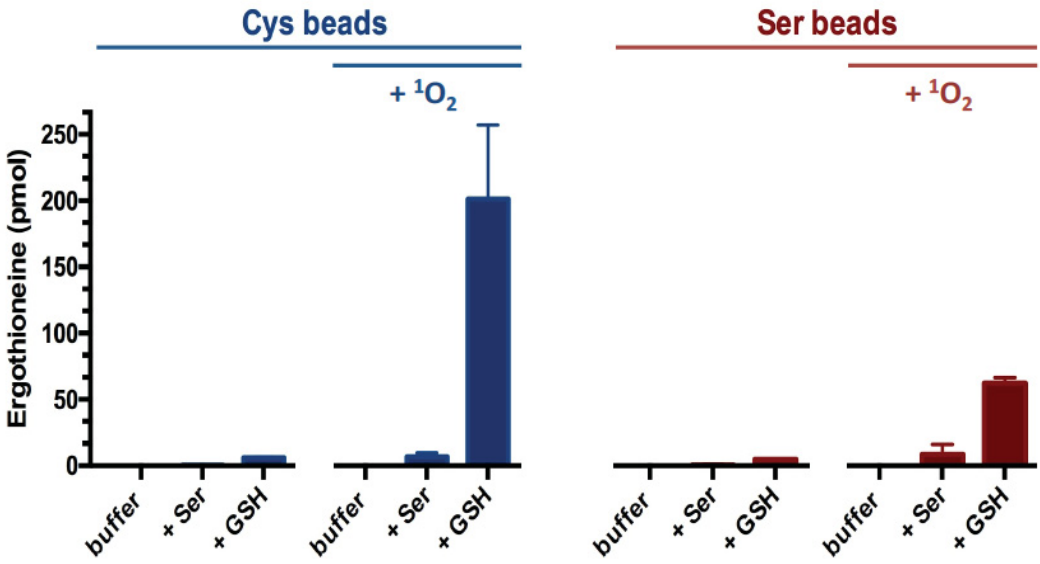

Figure 42. GSH regenerates ET from its oxidized products that were captured by cysteine or serine agarose beads. In the polypropylene reaction tubes, the reaction mixture made of 1 mM ET ± 10 mM $DHPNO_2$ in 10 mM ammonium hydrogen carbonate pH 8.0 buffer (V = 50 µL) was mixed with 100 µl of sendimented cys or ser beads that corresponds to an 8-fold molar excess of thiol groups vrsus ET. 0.1 mM GSH was present in the reaction mixture to diminish the disulfide formation between ET and the Cys ligands (not shown). The reactions were incubated for 10 min at 37 °C on a shaker (1200 rpm), then the beads were transferred into polypropylene microliter tips which were plugged with small pieces of cotton. After 3 washes, each with 500 µl of 100 mM NaCl buffer, the following solutions were applied in succession to the columns (100 µl each, at room temperature): buffer, 10 mM L-serine in buffer, and 10 mM GSH in buffer. The eluates were directly analyzed by LC-MS/MS for ET content. Data shown are median ± median absolute deviation.

3.4 The assay of oxidized ascorbic acid

In this work, the oxidized form of glutathione (GSSG) was quantitatively measured in order to prove the mechanism of ET regeneration after reaction with $^1O_2$. As ET was regenerated from its oxidized product, accourding to the proposed mechanism (see discussion, Figure 46), the production of GSSG was markedly increased, since the regeneration mechanism of ET requires the reducing agent GSH that oxidized to GSSG (Figure 34).

Here, it was examined whether AA is able to regenerate ET from its oxidized product or not, since AA is also a reducing agent and is present at 1-2 mM in human cells

after absorbtion from food. The hypothesis behind this experiment is that the oxidized form of AA should be increased if AA is able to regenerate ET from its oxidized product.

3.4.1 Oxidized ascorbic acid

In fact, DHA (dehydroascorbic acid) is an oxidized form of ascorbic acid (AA) which is produced after reducing another compound. DHA can be regenerated to AA in the presence of GSH (Figure 12). In the absence of GSH, however, DHA is hydrolyzed to other oxidized forms in aqueous solutions [125]. Therefore, the measurement of DHA as an oxidized form of AA by LC-MS/MS in this case would not be precise. In order to find out the most stable and measurable product of AA oxidation, a full scan of all products arising from the oxidation of AA with the use of $^1O_2$ was performed. In this experiment, 1 mM AA and 10 mM $DHPNO_2$ were incubated for 0 and then 12 min at 37 °C in water. Then, all reaction products from both samples were measured by LC-MS and analyzed by the difference shading method (2.8.2.4).

In the reaction of AA with $^1O_2$, red signals were identified at 209, 191 and 147 with a retention time of 3.6 min (Figure 43). In this case, the red signals indicate that the measured intensity in the effect sample (12 min at 37 °C) is higher than the intensity from the control sample (0 min at 37 °C). Moreover, at 0 min and 37 °C, no $^1O_2$ is produced and no oxidation of AA occurs, whereas after 12 min at 37 °C, $^1O_2$ was being produced for 12 min.

The windows at the top left of the figure 43 show the signal 209 in the replicates of two more identical samples at the same retention time of 3.6 min. These experiments were performed in H_2O and D_2O and provided similar results, however, the intensities were higher in the experiment in D_2O, since $^1O_2$ has a longer lifetime in D_2O.

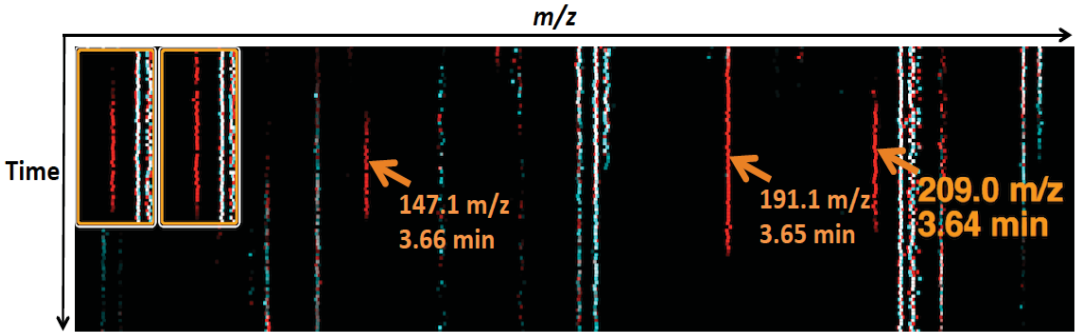

Figure 43. Difference shading image of the reaction of AA with $^1O_2$. AA was incubated with $DHPNO_2$ for 0 or 12 min at 37 °C. The reaction mixtures were measured with the full scan analysis method by LC-MS. The two windows at the top left show replicates of signal 209. Both signals at 191 and 147 are the signal from two fragments of parent ion m/z. Red signals show higher intensities in the effect samples and turquoise signals show higher intensities in the control samples. White color represents signals where the intensities from the effect and the control samples are the same; black represents no signal.

Generally, the detected signals are fragmented by a product ion scan and based on the fragments, the molecular structure can be determined by comparison with a data bank or the literature. Furthermore, if the fragments can not be found in any databases, then possible molecular structures can be postulated by interpreting the resuting fragments. In order to analyze and fragment the detected signals in full scan (209, 191 and 147), the experiment of 1 mM AA with 10 mM $DHPNO_2$ that generates clean $^1O_2$, was performed in water for 12 min at 37 °C and then samples were diluted 1:100 with H_2O and immediately measured by LC-MS/MS for 209 and 191. The fragmentation of compounds 209 and 191 yielded the fragments 191/147 and 147, respectively (Table 9).

Table 9: Measurement and fragmentation of oxidized AA. The parent ion and the fragments of oxidized products of AA by $^1O_2$ were measured by LC-MS/MS using the method SRM. Samples made of 1 mM AA and 10 mM $DHPNO_2$ were incubated for 12 min at 37 °C in D_2O or H_2O. In this table, the parent ions are listed with their fragments, retention time, exact masses, intensities and the reaction mixtures. Cps = counts per second.

Parent ion (*m/z*)	Fragment (*m/z*)	Retention time (min)	Exact mass (g/mol)	Intensity (cps)	Reaction mixture
209	191	0.9	176.124	200933	AA + $^1O_2$
209	147	0.9	176.124	12873	AA + $^1O_2$
191	147	0.9	176.124	9103333	AA + $^1O_2$

The data were compared to the relevant literature and it was found that the relatively stable oxidized product of AA is the compound 209, called monohydrated diketogulonate (Figure 44) [125]. Therefore, in this work, the compound 209:191 and 209:147 were measured with a selected reaction monitoring (SRM) method to obtain a specific measurement of the compounds 209:191 and 209:147 by LC-MS/MS. In contrast, the compound DHA was not used as an oxidized AA indicator for subsequent experiments, due to its hydrolysis after a couple of minutes in aqueous solution.

Monohydrated diketogulonate (*m/z* = 209)

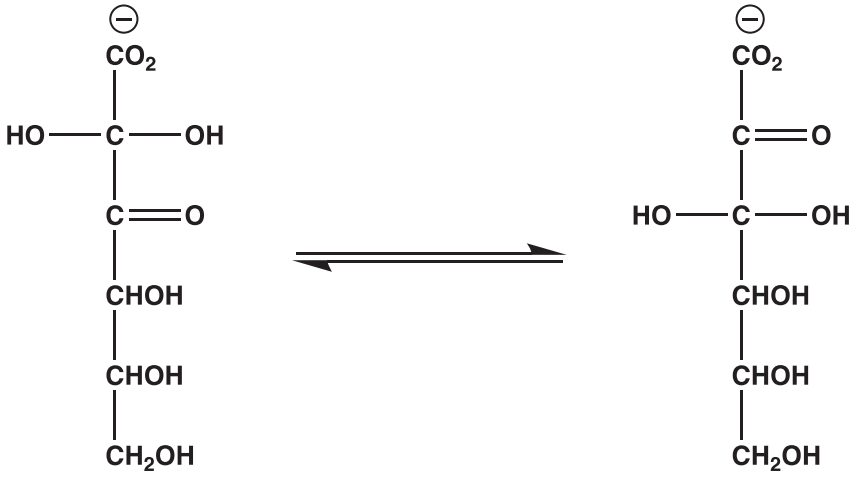

Figure 44. The structures of DHA hydrolysis at neutral pH after oxidizing AA. The compound 209 is relatively stable and measurable by LC-MS/MS. Data shows the structure of monohydrated diketogulonate with hydroxyl groups on the position 2 or 3, and both of them have the same mass to charge ratio (209). Modified from [125].

3.4.2 Does Ascorbic acid regenerate ergothioneine from its oxidized form?

In order to answer this question, the hypothesis behind it should be clarified. As mentioned above (3.3.1), if ascorbic acid (AA) can regenerate ET from its oxidized product, then the oxidized product of AA must be increased exactly like increasing the oxidized form of GSH. Therefore, the production of oxidized AA (209:191 and 209:147) in an experiment of 1 mM AA and 1 mM $DHPNO_2$ with and without ET in D_2O was measured by LC-MS/MS. In the control assay made by AA and $DHPNO_2$, the production of 209:191 in the time range 3 to 12 was at 16.2 ± 0.2 mM min^{-1}.

The addition of 1 mM ET to the control assay markedly decreased the production of 209:191 (reduced for more than 50%) to 6.8 ± 0,1 mM min^{-1} (Figure 45A), and that demonstrates that the production of the oxidized product of AA did not increase and AA is not able to regenerate ET from its oxidized form. In contrast, this data show and prove that ET is more reactive than AA towards $^1O_2$, since ET could protect AA from $^1O_2$ and reduces its oxidation.

The addition of His could also slightly reduce the production of 209:191 (10.1 ± 0,1 mM min^{-1}), since His is also one of the $^1O_2$ quenchers, however, it is not as potent as ET (Figure 45B). As an additional control (ET + AA), AA and ET were incubated in the same experiment in the time range 3 to 12 min without $^1O_2$, however, the data showed no effect (0.4 ± 0.2 mM min^{-1}).

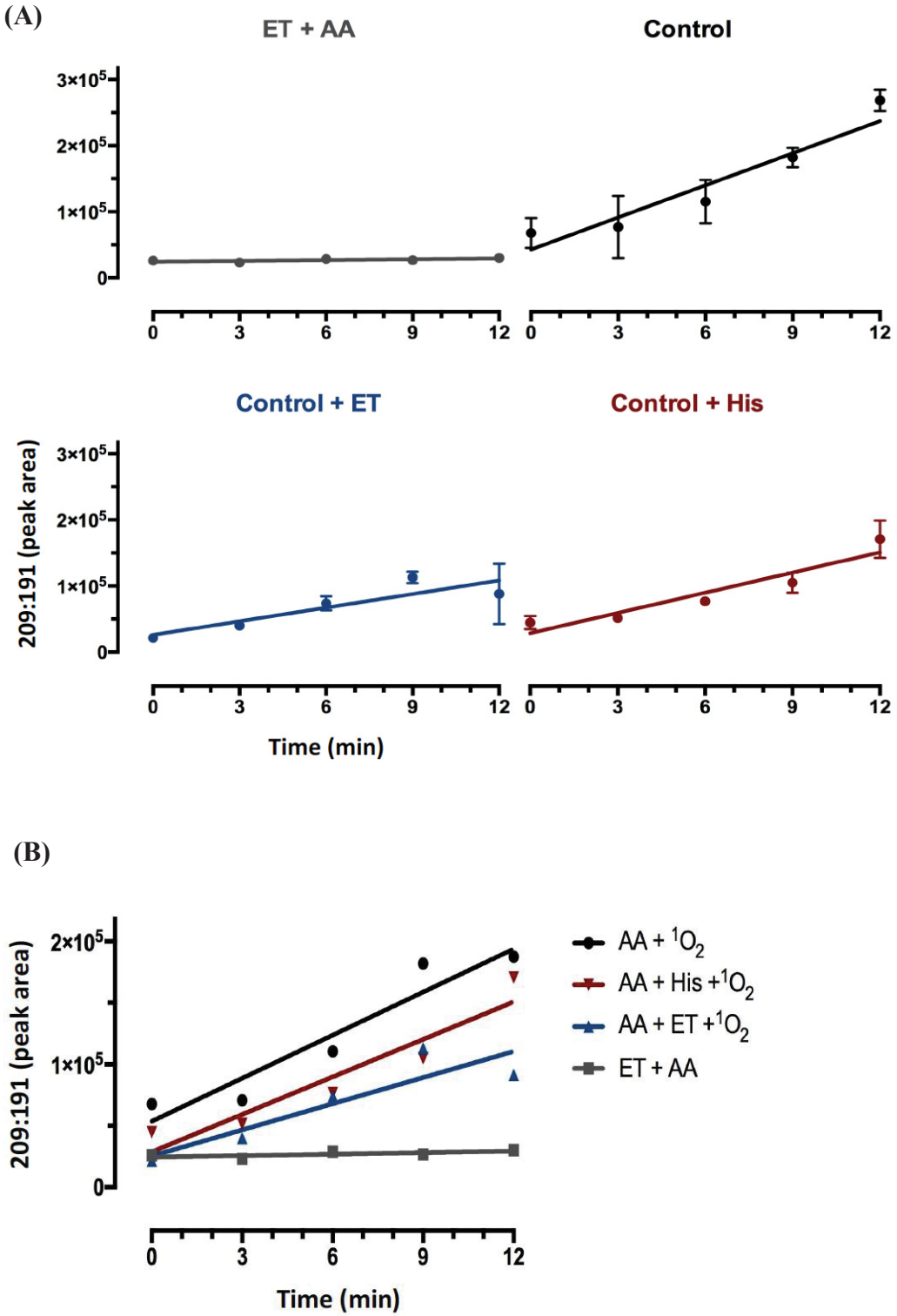

Figure 45. Generation of compound 209:191 over time arising from the reaction of AA with $^1O_2$ in D_2O. (A) The graph shows the efficiency of ET regarding the protection of AA from $^1O_2$. The control assay contains 1 mM AA and 1 mM $DHPNO_2$ in D_2O. ET and His were added as indicated to a final concentration of 1mM. Samples were incubated at 37 °C for 0 to 12 min, diluted 1:100, and then analyzed immediately by LC-MS/MS for compound 209:191. These data come from a single experiment. Data were analyzed by linear regression; the slopes represent the production rates of compound 209:191. (B) The graph shows an overlap of slpoes from (A), a median was applied.

4 Discussion

As established, ergothioneine (ET) eradicates singlet oxygen ($^1O_2$) and has been considered an antioxidant [1, 2]. Moreover, various functions of ET regarding reactive oxygen species (ROS) have been proposed and much progress concerning ET has been attained [36, 45, 46, 50-53]. However, no mechanism for the regeneration of ET after a reaction with ROS has been determined. In fact, if it is an important antioxidant, like ascorbate, glutathione (GSH), ubiquinol, vitamin E and so on, and if the benefit of ET in living organisms is continual and does not lose its capacity to eradicate oxidants (e.g. $^1O_2$ in this project) after a single chemical reaction, then the ET should be regenerated from its oxidized product so as to be an efficient antioxidant. Therefore, the aim of this project was to investigate whether ET can be regenerated from its oxidized products after reaction with $^1O_2$.

In this project, a non-enzymatic mechanism for the regeneration of ET after reaction with $^1O_2$ was discovered. This finding is supported by evidence. For this mechanism, 4 molecules of GSH are needed to detoxify $^1O_2$ into water and GSSG as a by-product. GSH exists naturally in all mammalian cells with relatively high intracellular concentrations (5 - 10 mM) [113, 114]. The byproduct GSSG regenerates to GSH in living organism by glutathione reductase, utilizing NADPH as an electron donor [109, 117]. Thus, the discovered mechanism of ET regeneration after the reaction with $^1O_2$ occurs without loss of ET. However, in the assays that were performed *in vitro* in this work, the recovery of ET after the regeneration from its oxidized products was slightly reduced by side reactions.

4.1 Generation of singlet oxygen

For the generation of $^1O_2$ in aqueous solution in the present work, the photosensitizer TMPyP and the endoperoxide $DHPNO_2$ were used.

4.1.1 Photosensitizer (TMPyP)

The photosensitizer TMPyP is frequently used in the literature to generate $^1O_2$. However, the main drawback of this approach is that other ROS, such as hydroxyl radical, superoxide anion and hydrogen peroxide are produced alongside $^1O_2$ production [123]. Thus, the results will be affected and can be ambiguous, since they cannot solely be attributed to $^1O_2$. Based on that, the best alternative $^1O_2$ generator in order to produce pure $^1O_2$ is an endoperoxide, such as $DHPNO_2$. Therefore, the results from the experiments that utilized TMPyP as a $^1O_2$ generator had to be confirmed by experiments that were performed with $DHPNO_2$ as a $^1O_2$ generator, since $DHPNO_2$ produces a clean $^1O_2$ and the results cannot be ambiguous [12].

4.1.2 Endoperoxide ($DHPNO_2$)

In order to study the reaction of ET with $^1O_2$, a production system of $^1O_2$ was needed. In this work, $^1O_2$ generated from endoperoxide ($DHPNO_2$) was used in order to produce pure $^1O_2$. The advantages of endoperoxide ($DHPNO_2$) are not only the clean production of singlet oxygen by heating at 37 °C, but also its stability at low temperatures ≤ 4 °C [145]. $DHPNO_2$ produces 59% $^1O_2$ and 41% unreactive triplet oxygen ($^3O_2$) only once [83], and the number of produced $^1O_2$ molecules is limited to the concentration of $DHPNO_2$ that is used. Therefore, the produced amount of $^1O_2$ in each experiment can be calculated.

The $DHPNO_2$ that was used in this work was synthesized and verified *in vitro* in the work group of Professor H. Schmalz and it was also tested in the work group of Professor D. Gründmann [58]. Indeed, the half-life of $^1O_2$ was determined through time course and it was 26 min at 37 °C [58], which approximated the value of 23 min in the literature [83].

4.2 Reaction of ergothioneine with singlet oxygen in the presence and absence of glutathione

Stoffels et al. did identify, on the one hand, the reaction products that arise from the reaction of ET with $^1O_2$ in the absence of GSH, which are 246:202, 262:245, and 264:188, and on the other hand, the reaction products of ET with $^1O_2$ in the presence of GSH, which are 551:244 and 553:308, analyzed by LC-MS/MS [12].

In the present work, several experiments of ET with $^1O_2$ in both the presence and absence of GSH were performed in order to analyse the stability of their reaction products through changing the concentration of GSH and performing time course experiments to investigate whether those products could further react over time or, conversely, decompose to other compounds. The results from many experiments suggested that the main reaction product of ET with $^1O_2$ is the compound 246:202, since it is produced much faster than the other observed products. Moreover, when 10 mM GSH was added to the reaction of ET with $^1O_2$, it was observed that the loss of ET was prevented almost completely, although the reaction product of ET + $^1O_2$ (The compound 264:188) is still measurable by LC-MS/MS (Figure 30C).

Consequently, the regeneration mechanism of ET from its oxidized product by GSH was developed (Figure 46). In fact, ET was considered as a powerful antioxidant and all-important antioxidants are regenerated from their oxidized products in order to protect living organisms from damaging ROS, it is essential not to lose this function after a single chemical reaction with oxidants.

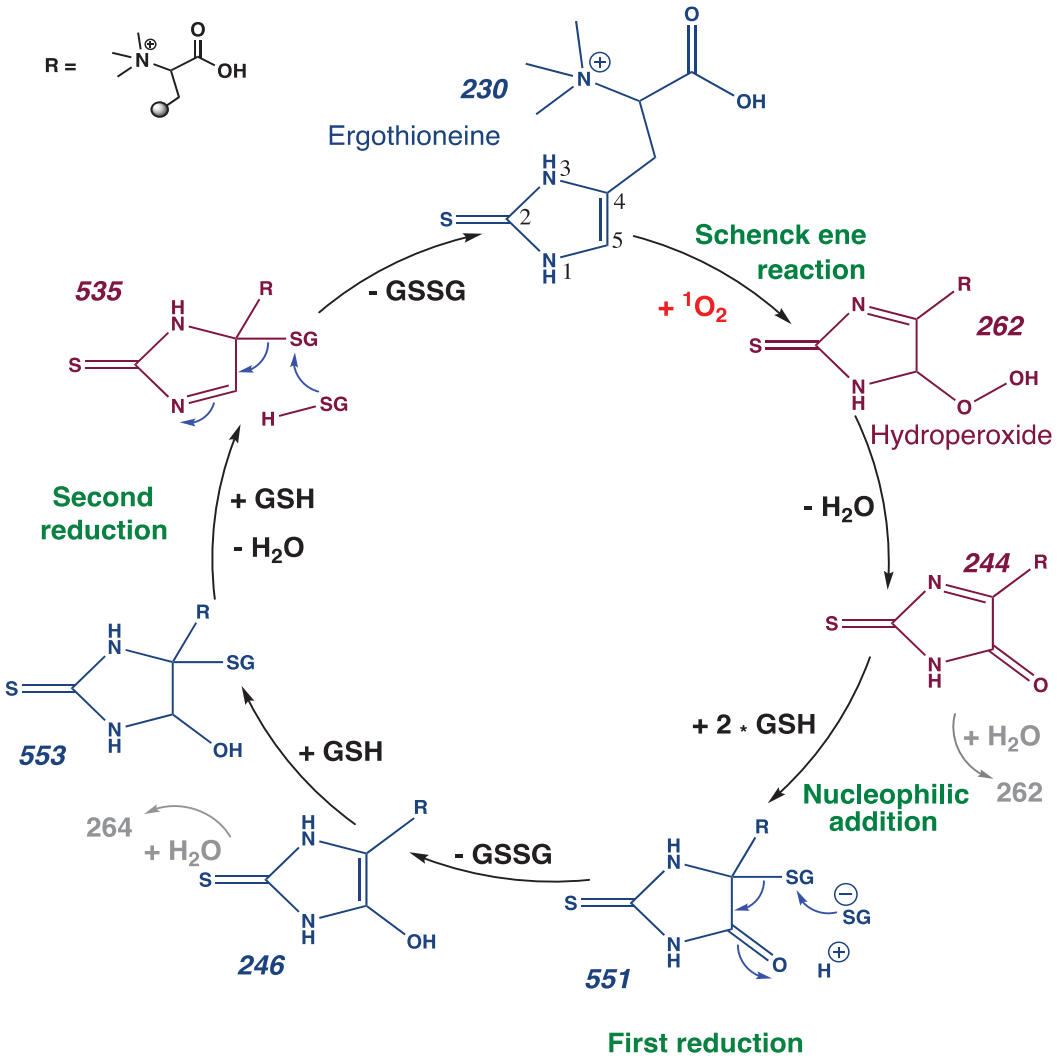

Figure 46. The proposed mechanism cycle of ET after the reaction with singlet oxygen. The scheme represents the products that were detected by LC-MS (blue), and the proposed reaction intermediates (maroon), and the potential side reactions (gray). The *m/z* values (italic numbers) correspond to acidic LC conditions.

The proposed mechanism of ET regeneration after reaction with $^1O_2$ was clarified and experimentally proven step by step in this work (Figure 46). The first step of this regeneration cycle is a reaction of ergothioneine with $^1O_2$ that can be easily described by a Schenck ene addition of $^1O_2$ to the double bond of ET which generates the hydroperoxide 262, which decomposes, yielding the lactam intermediate 244 after the loss of one molecule of water [12]. This step demonstrates the importance of the proton of the nitrogen atom within the ET ring. This proton allows the double bond in the ET ring to move to the neighboring position, when $^1O_2$ is added to the double

bond at position 5. The compound 244, a lactam intermediate, can react with one GSH molecules forming the compound 551:244 which is reduced by another molecule of GSH, yielding the compound 246:202 and the oxidized GSH (GSSG) as a by-product. These two reaction steps of GSH with the intermediate compound 244 produce the compound 551:244 and then, reducing the compound 551:244 to the compound 246:202 by GSH is similar to the reaction (Figure 12) of GSH with dihydroascorbic acid (DHA) in the regeneration mechanism of ascorbic acid (AA) from its oxidized form (DHA) by GSH [109]. In addition, the reaction of the lactam intermediate compound 244 with GSH can be considered as a highly efficient nucleophilic addition to an electron-deficient imine substructure. Moreover, the S=C – N=C (N-thioacylimine) system resembles α,β –unsaturated ketones in the Michael additions [103, 146, 147]. Furthermore, the position 4 of the imidazole ring represents a soft electrophilic site which is generally a target for thiols, which are the softest biological nucleophiles [103, 148].

Afterwards, addition of a third GSH molecule to the compound 246:202 involved a lot of discussion about how to explain and prove this step, because there were two possibilities of adding the GSH molecule to the compound 246:202, and both ways could produce the same compound 553:308. On the one hand, GSH can attack position 4 of the imidazole ring of the enol structure 246:202 (Figure 27), producing the compound 553:308. On the other hand, GSH can attack position 5 of the imidazole ring of the ketone structure 246:202, yielding the compound 553:308.

In fact, the enol structure of the compound 246:202 has a corresponding ketone tautomer that is relatively more stable, but the LC-MS/MS could not distinguish between the enol and ketone structures, since both of them have the same mass-to-charge ratio (246:202). Moreover, it was also unknown whether the attack of GSH at the compound 246:202 would be on position 4 or 5, because the results from both reactions have the same mass-to-charge ratio (553:308).

Analyzing the fragments of the compound 553:308 by LC-MS/MS could not resolve the question of whether GSH prefers position 4 or 5 of the imidazole ring of the compound 246:202 [12]. As a posibility, it was suggested that the density functional theory (DFT) method might confirm the addition of GSH to the compound 246:202.

Therefore, DFT computation was performed and showed that the barriers for the addition of methanethiol to the enol C(4)=C(5)-OH function are similar for the Me-S-C-C(H)-OH (38.9 kcal/mol) or HC-C(SMe)-OH (32.9 kcal/mol) products [103]. Based on that, the DFT computation could not specify which position (4 or 5) is favorable. Afterwards, and in order to answer the question, the idea originated from the side reaction 264 [12] that an ET included two hydroxyl functional groups, occupying either vicinal at position 4 and 5 (vicinal hydroxyls) or both hydroxyl functional groups bound to the same carbon atom at position 5 (geminal 5-diol). Even though, on the one hand the MS^2 experiments could not distinguish between the vicinal hydroxyls and geminal 5-diol, since both variants produce the same fragment 188 arising after the loss of thiourea to form either a vicinal enediol or an acrylic acid structure, respectively, on the other hand, the MS^3 experiment achieved solving this issue (Figure 28). In this process, the fragment 188 itself was collected in ion trap mode and further fragmented in order to check potential products. The fragmentation of 188 produced a robust signal at 160 (Figure 29), which clearly corresponds to the loss of CO in this case. Thus, this fragment at 160 can only agree with the vicinal enediol. Therefore, the compound 264 contains hydroxyl groups at position 4 and 5 separately, as a result of attack water at position 4 of the enol structure 246:202 and not an attack at position 5 of the imidazole ring. Thus, by analogy, GSH molecules should prefer to attack at the position 4 of the enol structure 146:202. This, however, cannot completely exclude an attack at position 5 of the compound 246:202.

Based on that, the addition of a third GSH molecule to the C=C-function of the enol structure 246:202 produces the compound 553:308, which is assisted by GSH to eliminate water, forming the compound 535, which includes an imino function (S=C−N=C system that is called N-thioacyl imine). Finally, the compound 535 is reduced by a fourth molecule of GSH, yielding ET and the by-product GSSG.

The DFT computations that was performed by Professor B. Goldfuss from the Department of Organic Chemistry of the University of Cologne could also support all the steps of the proposed ET regeneration mechanism and explained the details of the final step of the regeneration mechanism as follows: the second reduction by GSH, producing an enamide anion and the protonated disulfide GSSG, and then the proton transfer, yielding ET and GSSG as a by-product (Figure 47).

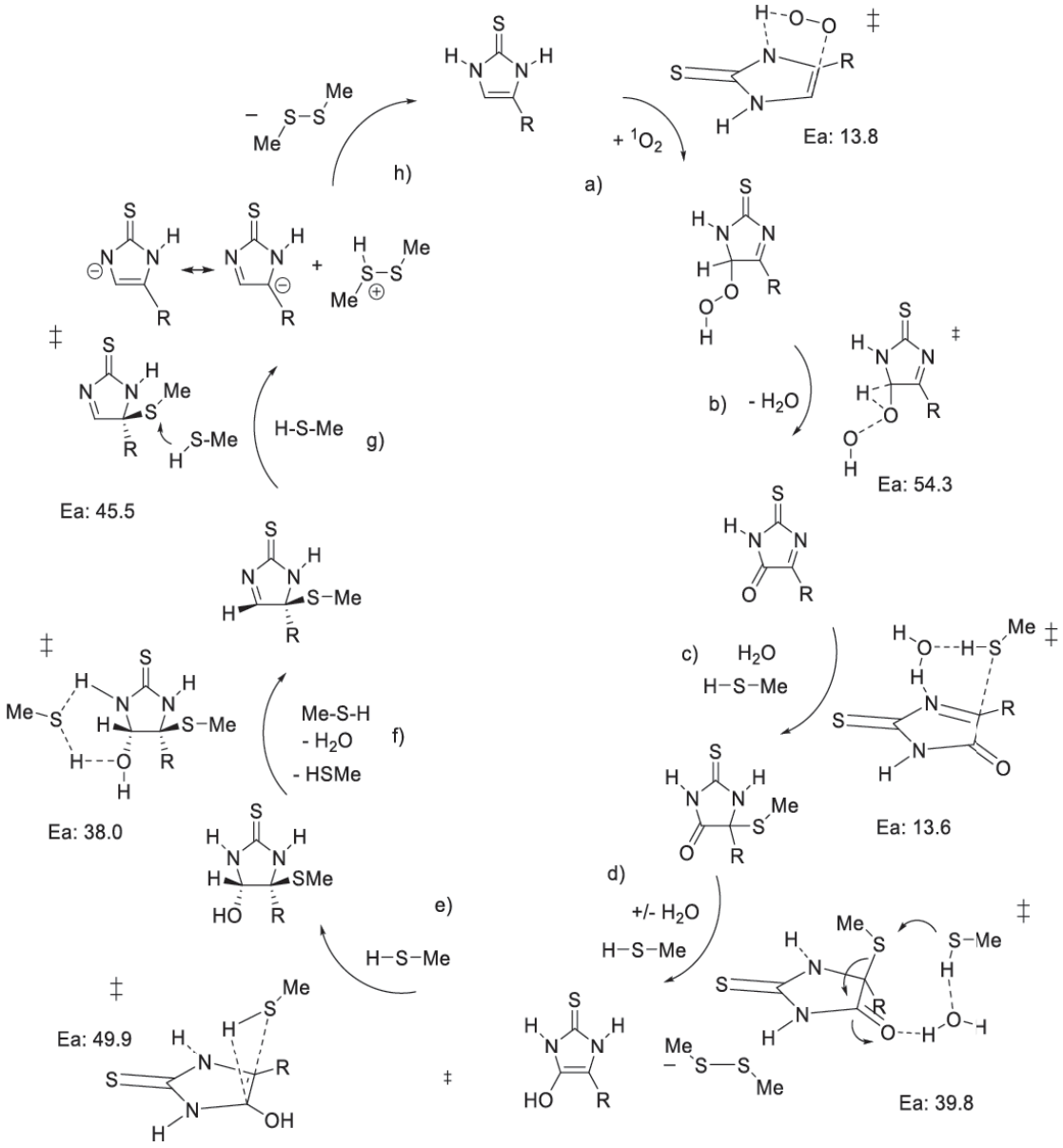

Figure 47. Detailed reaction cycle of ET after the reaction with $^1O_2$. The reaction of ergothioneine with $^1O_2$ and the subsequent regeneration with GSH was computed by employing the B3LYP/6-31G*-GD3-BJ method. A Schenck ene addition of $^1O_2$ to ET generates an alkylhydroperoxide (a), which decomposes, yielding a lactam intermediate (b). Addition of HSMe (as a GSH model) to the N=C-function of this lactam yields an adduct (c), which is subsequently reduced by reaction with a second HSMe molecule via a SN2(S) reaction, yielding an enol structure and the disulfide Me-S-S-Me byproduct (d). Addition of a third HSMe molecule to the C=C-function of the enol generates an adduct (e), which (assisted by MeSH or water) eliminates water, forming an imino function (f). The second reduction proceeds via reaction with HSMe, yielding an enamide anion (g) and the protonated disulfide Me-S(H+)S-Me. Proton transfer yields Me-S-S-Me and ergothioneine (h). Text passages mostly cited from [103].

The potential side reaction 262:145 (gray) could be produced by the attack of water to the N=C-function of the lactam intermediate 244. However, the compound 262:145 completely disappears when the concentration of GSH is up to 0.3 mM (Figure 26). At high concentrations of GSH (up to a 1000-fold excess of GSH over ET), the potential side reaction 264:188 (Figure 46, gray) produces.

4.3 GSSG generation assay

In this work, the concentration of GSSG was measured and quantified in order to prove the proposed ET regeneration cycle after reaction with $^1O_2$ (Figure 46), since this regeneration mechanism occurs only in the presence of GSH. For each regeneration cycle, four molecules of GSH are needed to regenerate one molecule of ET from its oxidized products which arise after the reaction with $^1O_2$. The four molecules of GSH which are required are oxidized to two molecules of oxidized glutathione (GSSG) after reducing the intermediate compounds (oxidized products of ET), which are involved in the proposed regeneration cycle. Thus, the concentration of GSSG in this case must be increased with every regeneration cycle. In the reaction experiments that were performed *in vitro* in this project, no enzymes were present. Therefore, the disulfide bond that is formed in the disulfide compound (GSSG) is stable and in this case the GSSG is not able to be reduced back to GSH in the absence of enzymes (Figure 13 and Figure 32) [109].

The results from the reaction of GSH with $^1O_2$ (Figure 34) demonstrate that there was a slight production of GSSG from 10 mM GSH (control), although in the literature the production of GSSG accounts for 63% of the $^1O_2$ reaction products [149]. In fact, the GSH molecule and other cystein-based thiols were less efficient towards $^1O_2$ than ET, however, the differences were not as marked as in the present work. The ratio of rate constants (f) for ET and GSH, was 13 [149] or 3 (at pH 7.4; GSH was represented here by 2-mercaptopropionyl glycine) [56]. Stoffels et al. suggested that ET is at least 50-fold more reactive than GSH towards $^1O_2$ [12]. However, the GSSG production data in the present work (Figure 34) suggest f = 30 / 2 * 10 = 150; in other words ET reacts with $^1O_2$ 150-fold more efficiently than GSH. Furthermore, the methods that

were utilized in the mentioned literature [56, 149] were completely different from the method used in this project: both groups [56, 149] have measured chemiluminescence at 1270 nm, since the energy differential between $^1O_2$ and ground state oxygen ($^3O_2$) is very specific [74, 75], and based on that, their measurement is proportional to the available $^1O_2$. Devasagyam et al. determined the rate constants from Stern-Volmer plots, which in turn were based on only two points: the initial steady-state chemiluminescence (S_0) and the end-point chemiluminescence (S), after ET or thiol had completely reacted (Figure 48 and 49) [149]. This method did not observe the initial rates of the reaction; if ET reacts further with initial ET-$^1O_2$ products as suggested in the present work, then the efficiency of ET will be underestimated. Moreover, Rougee et al. have utilized a photosensitizer as a $^1O_2$ generator [56], however, other ROS (such as hydroxyl radical, superoxid anion and hydrogen peroxide) were produced alongside the $^1O_2$ generation simutaneously and possibly affected their results.

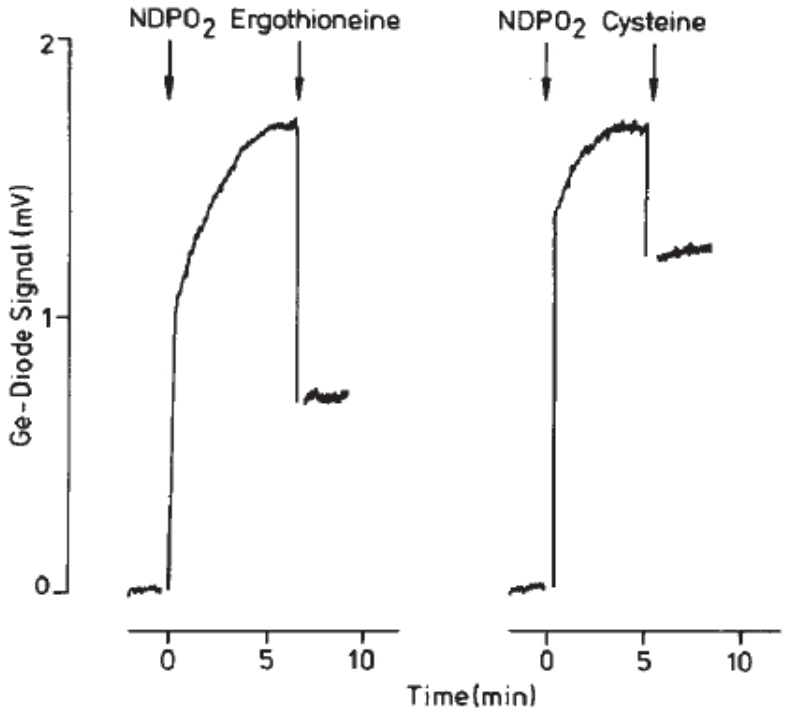

Figure 48. Quenching of the $NDPO_2$-generated $^1O_2$ monomol emission signal at 1270 nm by 1 mM ET and 1 mM cysteine at 37 °C (Figure from Devasagyam et. al [149]). 5 mM $NDPO_2$ was added to 50 mM sodium phosphate buffer in D_2O (pD 7.4). At the peak of monomol emission, the thiol dissolved in the above buffer was injected. The graph shows the efficiency of ET and cysteine through their ability to quench $^1O_2$ [149].

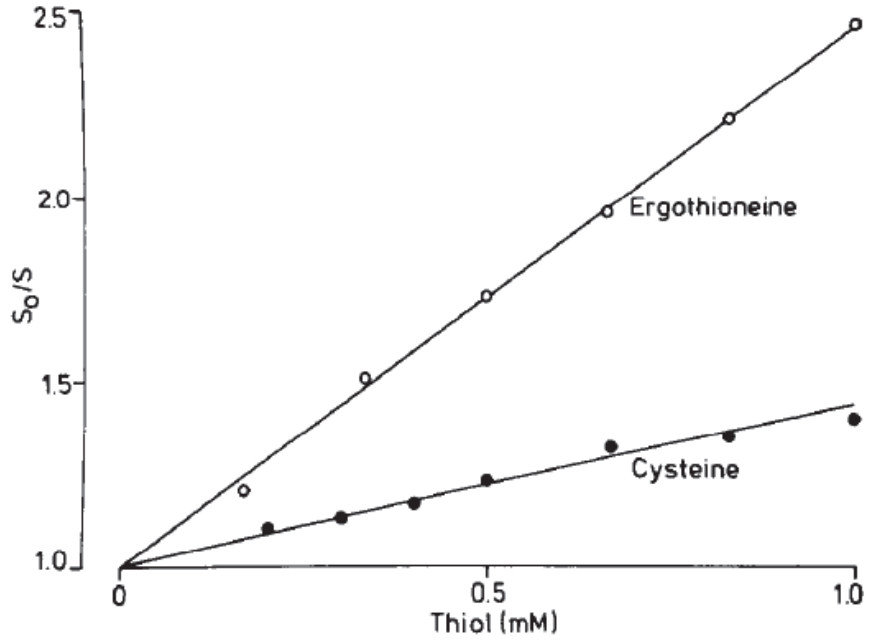

Figure 49. Stern-Volmer plot for the overall Quenching (k_q + k_r) of $^1O_2$ by ET and cysteine at 37 °C in 50 mM sodium phosphate buffer in D_2O (pD 7.4) (Figure from Devasagyam et. al [149]). The diagram shows that the overall quenching ability was markedly decreased by cysteine in comparison with ET. S_0 and S are the chemiluminescence intensities in the absence and presence of the quencher respectively, k_q is the physical quenching rate constant, k_r is the chemical reaction rate constant [149].

The ET regeneration cycle by GSH after the reaction with $^1O_2$ bears a striking resemblance to the non-enzymatic regeneration of ascorbic acid (AA) from its oxidized form dehydroascorbic acid (DHA) by GSH. Moreover, the mechanism of reducing DHA back to AA needs two molecules of GSH, which are oxidized to one molecule of GSSG per turn (Figure 12). The by-product GSSG is reduced to GSH by NADPH-dependent enzymes in living organisms [109].

In fact, the concentration of AA in the cytosol of the cells is high (2-4 mM) and the reaction of the ascorbate monoanion with $^1O_2$ is rapid, $k = 3 \times 10^8\ M^{-1}\ s^{-1}$. It has been suggested, therefore, that ascorbate is the most effective chemical quencher of $^1O_2$ and could play a significant role *in vivo* [98]. However, the data of the present work demonstrate that ET is a superior interceptor of $^1O_2$ than AA [103].

According to the GSSG generation assay, the production of GSSG from the reaction of GSH + $^1O_2$ (control) (Figure 34) in the presence of 1 mM ET is 8-fold higher than

the production of GSSG from the reaction of control + 1 mM AA, after the subtraction of GSSG levels in the control. Therefore, the number of ET molecules that reacted with $^1O_2$ was at least 4 times higher than the number of ascorbate molecules, since the regeneration of AA from its oxidized form (DHA) produces only one GSSG molecule per cycle [109], whereas the regeneration of ET from oxidized products of ET produces two molecules of GSSG per turn. Thus, and under the assumption that the loss of AA (from the DHA hydrolysis in aqueous solution) and ET (from the potential side reaction) are nearly similar, then ET reacted at least 4-fold faster than ascorbic acid towards $^1O_2$. Furthermore, if the ET cycle took more time than the AA cycle, then the difference would be even larger. Note that, the reaction of ET with $^1O_2$ followed by the regeneration cycle entirely deactivates $^1O_2$, whereas the reaction of AA with $^1O_2$ produces not only dehydroascorbic acid (DHA), but also stoichiometric levels of H_2O_2 [89], which provides further oxidative challenges for cells and tissues. Therefore, the ET reaction is not only faster than the AA towards $^1O_2$ but also more efficient and less harmful than AA. In fact, it should be taken into consideration that DHA, depending on the reaction condition, may not be completely reduced back to AA *in vitro* [109]. Moreover, in the ET regeneration mechanism, although some side reactions are possible *in vitro*, the results that are presented in this work demonstrate that ET levels are virtually stable in the presence of 10 mM GSH (Figure 24A).

According to the GSSG generation assay, the efficiency of ET as an interceptor of $^1O_2$ can be clearly estimated. The endoperoxide ($DHPNO_2$) that was utilized in the experiments of this project decays at 37 °C with a half-life of 23 min, to release 59% of $^1O_2$ [83]. Moreover, the decay of $DHPNO_2$ follows the equation $N(t) = N_0 * \exp(-\text{lambda} * t)$ with $\text{lambda} = \ln(2) / t_{1/2}$, which shows that after 12 min $DHPNO_2$ has decayed by 30% to release 10 mM * 0.30 * 0.59 = 1.8 mM $^1O_2$ [103]. With the 2 molecules of GSSG that were produced per ET regeneration cycle, it follows from the difference in the rates (see results) that in 12 min in D_2O, 0.72 mM ET was regenerated, after the reaction with $^1O_2$, and that means that ET chemically quenched an impressive 40% of the released $^1O_2$. Furthermore, the rest of $^1O_2$ was surely quenched physically by non-toxic, unreactive collisions with the solvent or other molecules.

In accordance with the addition reaction of $^1O_2$ to ET (Schenck ene reaction), the double bond in the imidazole ring of ET is responsible for the reaction mechanism. The GSSG generation assay completely agrees and supports the suggested reaction mechanism and demonstrates that the aromatic ring of ET (compound DHIT) is entirely sufficient for the complete regeneration mechanism of ET (Figure 36); in other words, the zwitterionic amino acid backbone is definitely not involved. Moreover, the GSSG production for the compound thiamazole (= DHIT with an additional methyl group, on either one of the nitrogen atoms at positions 1 or 3 in the ring) was only at the half level of the compound DHIT. Furthermore, this is in accordance with the Schenck ene reaction (first step), which needs a proton on the nitrogen atom at the position 3 of the ET ring. However, if the residual GSSG produced from an attack of $^1O_2$ on the other side of the ring (position 5), then the proton on the nitrogen atom at position 1 of the ET ring will be used. Therefore, blocking one of the two nitrogen atoms in the ET ring by using the methyl group, halved the production of GSSG. This demonstrates the importance of both nitrogen atoms with their protons in the ET ring.

The GSSG generation assay could illuminate the second attack of GSH in the proposed regeneration mechanism of ET which was already clarified in this work by means of MS^3.

In fact, the results from the MS^3 method (Figure 29) clearly indicated that the enol structure 246:202 is a part of the ET regeneration cycle (Figure 46) and the corresponding ketone (Figure 27) is not involved, although the ketone is a more stable tautomer according to the DFT computations (not shown). In order to support these results, the compounds 2-thiohydantoin and 3-(5-oxo-2-thioxo-imidazolidin-4-yl)-propionic acid (Figure 35), which have a ketone function on the position 5 of the imidazole ring, were tested in the GSSG generation assay. Both model compounds failed to drive the generation of GSSG (Figure 36). Therefore, the enol structure 246:202 is the crucial intermediate compound in order to initiate the second reduction of the ET regeneration cycle (Figure 46). Moreover, the ET ring promotes this step via its ability to form a zwitterionic resonance structure with a positive charge on the nitrogens (Figure 50) [150], and in this case, the imidazole-2-thiols may activate the C=C bond by decreasing the electron density of the double bond, since a simple enol

C=C-OH is similar to simple C=O functions [148] and it would not readily react with a thiol function under physiological conditions. Therefore, the compound 1,3-dihydroimidazol-2-one (= Compound DHIT with an oxygen instead of sulfur at position 2) produced GSSG 3-fold lower than the compound DHIT in the GSSG generation assay (Figure 36), since the activation of the double bond C=C by decreasing the electron density in imidazole-2-thiones may be better than in imidazole-2-ones.

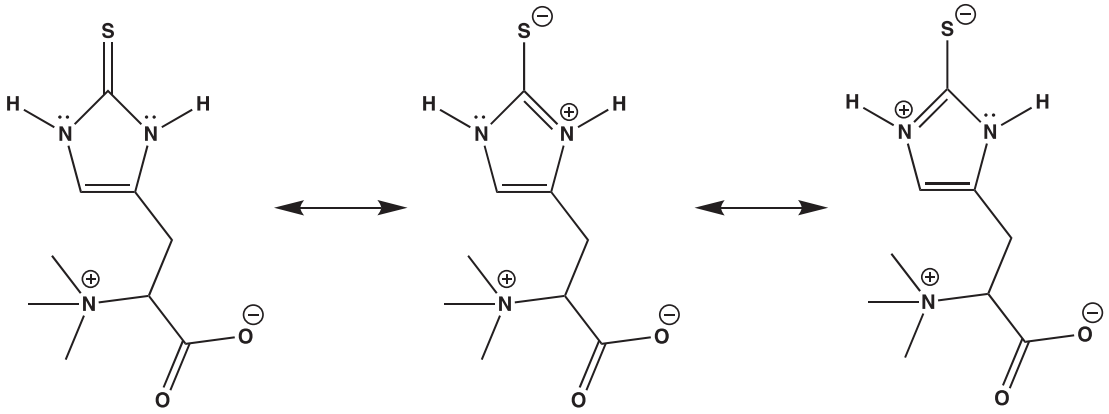

Figure 50. Three possible resonance structures for ET. The ring of ET is able to form a zwitterionic resonance structure with a positive charge on the nitrogens. Modified from [150].

Thus, the results show that the thione on position 2 of the ET ring is important. Furthermore, alkyl substitution at position 4 of the ET ring (DHIT) does not influence the reaction, because the 4-methy-1H-imidazol-2-thiol (= 4-methyl ET ring) was as effective as ET and DHIT to drive the production of GSSG (Figure 36).

Based on that, the ring of ergothioneine (1,3-dihydroimidazole-2-thione) is not only responsible for the reaction of ET with $^1O_2$, but also supports the ET regeneration mechanism from its reaction products by means of a thiol group of other compounds such as GSH, which is present in all mammalian cells. Apparently, every single element in this ring has its own unique importance and is irreplaceable for the production of desired results.

4.4 Capturing the oxidized product of ET after the reaction with singlet oxygen

The suggested ET regeneration cycle after reaction with $^1O_2$ (Figure 46) was supported not only by the GSSG generation assay described above (3.2), but also by capturing the reaction intermediate of the regeneration mechanism by sedimented agarose beads. Agarose beads are usually used for protein purification and they are insoluble, crosslinked, pressure-stable and immediately submersible.
In this section of the present project, the oxidized product that arose after the reaction of ET with $^1O_2$ was isolated by means of beads that were covered with thiol groups. The thiol groups are provided by the amino acid L-cysteine, which was covalently linked to insoluble cross-linked agarose beads via its amino group.

The point behind this strategy is that the thiol group on the beads´ surface should react and bind with the oxidized products of ET, exactly at the position where the thiol group of GSH should attack (Figure 46), and then, after washing the beads and removing the whole reactants, the oxidized products of ET that were bound to the thiol group of cysteine should be reduced towards ET by adding the GSH to the beads. Therefore, the proposed mechanism of ET regeneration after reaction with $^1O_2$ was strongly supported and proven after successfully reducing the oxidized ET product to ET by GSH, and thus it was confirmed that GSH regenerates ET from its oxidized product.

In the experiment made of 0.1 mM ET with and without 10 mM $DHPNO_2$, the reaction mixture included 100 µl of sedimented beads. This experiment was performed in 10 mM ammoniumhydrogen carbonate buffer at pH 8.0 to activate the nucleophilic addition of thiol via deprotonation. Moreover, the concentration of L-cysteine that was utilized in this experiments was approximately 4 nmol per µl of gel; this corresponds to an 8-fold molar excess of thiol groups vs. ET to minimize the intervention that could occur by the thiol group of ET. In addition, the reaction of the amino acid cysteine with $^1O_2$ produces the cysteine disulfide (Figure 51) [92], which means that ET can react with cysteine to yield disulfide compounds. Therefore, 0.1

mM GSH was added to the reaction solution in order to avoid the disulfide formation from ET (see results).

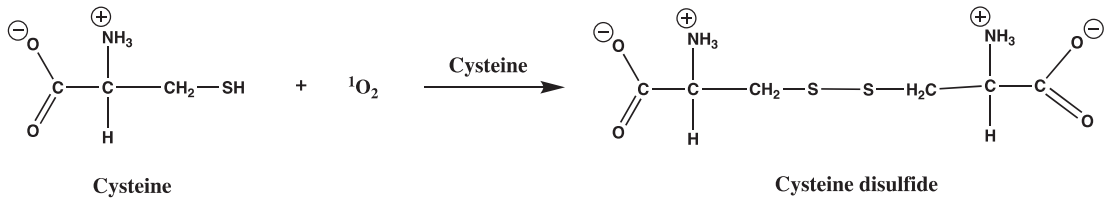

Figure 51. The reaction of the amino acid cysteine with $^1O_2$ producing cysteine disulfide. In the presence of 0.1 mM GSH, the formation of the disulfide bond will be avoided [12, 92].

After the reaction mixture was incubated on a shaker (1200 rpm) for 10 min at 37 °C, the whole reaction solution with beads was transfered immediately into the column. Afterwards, the reaction solution was removed, including all the reactants, while the oxidized product of ET that would bind itself to the beads should remain in the column.

In addition, the beads were washed three times with 100 mM sodium chloride to avoid any possible interaction of the initial ET with the beads (not shown). Furthermore, the removal of unreacted ET from the column was complete, since no ET was detected by LC-MS/MS from eluted buffer (10 mM ammoniumhydrogen carbonate) collected after addition to the beads (Figure 42). Moreover, there was also no detection of ET by addition of 10 mM amio acid L-serine (in buffer) to the beads.

In the assay without $^1O_2$ (as a negative control), no ET was detected from the eluted buffer and 10 mM amio acid L-serine that were added to the beads, respectively, and then, a very small amount of ET was released from the columns by adding 10 mM GSH. However, in the case of an presence $^1O_2$, a large amount of ET was released by adding GSH. This suggests that products of oxidized ET were indeed captured by the beads, since there was no detection of ET by addition of the buffer and serine to the beads, respectively; However, adding 10 mM GSH stimulated the reaction mechanism towards ET and a huge amount of ET was detected by LC-MS/MS.

In parallel controls, the cross-linked agarose beads that carry L-serine (beads that were covered with hydroxyl groups of the amino acid serine instead of thiol groups of the amino acid cysteine) also captured some reaction intermediates but the amount of ET released from serine beads was almost 3-fold lower than the amount of ET obtained from cysteine beads (after subtraction of the background in $^1O_2$-negative assays).
In fact, these results strongly suggest that ET is regenerated from Cys-attached intermediates by the thiol function of GSH.

4.5 The reaction of ascorbic acid with singlet oxygen

In order to find evidence for the proposed ET regeneration cycle after the reaction with $^1O_2$, the analyzation of the oxidized form of glutathione (GSSG) proved the regeneration mechanism of ET, since the regeneration of ET requires the reduced agent GSH which is oxidized to GSSG. The results of the experiments did show that GSSG markedly increased when the ET regenerated from its oxidized product. Therefore, the question arose here of whether the AA can regenerate ET from its oxidized products back to ET. It was examined whether ascorbic acid is able to regenerate ET from its oxidized products or not, since AA is also a reducing agent and can be found at 2-4 mM in human cells after absorption from food [103]. The hypothesis that led to this experiment is that the oxidized form of AA should be increased if AA is able to regenerate ET from its oxidized product.

Obviously, if we look at the regeneration mechanism (Figure 46), it would be apparent that the mechanism cycle needs a thiol group compound and although AA is a reducing agent, however, it includes no thiol function. In addition, if AA should be able to regenerate ET from it oxidized product, then the AA must be oxidized and the oxidized form of AA should increase.

In a process similar to the GSSG generation assay (see 3.2), the oxidized products of AA (arising after the reaction with $^1O_2$) were analyzed by LC-MS/MS. In fact, the oxidized form of AA is dehydroascorbic acid (DHA) [109], however, DHA

hydrolyses into other oxidized forms in aqueous solvents over time (Figure 52) [125]. Furthermore, the degradation of DHA depends on various factors, such as the amount of dissolved oxygen in the solution, pH, temperature, and light exposure [125, 151]. For instance, in acidic solutions, DHA is stable in a biocyclic hemiketal (monohydrated) form [152], whereas it hydrolyses fast in neutral or basic solutions [153]. Therefore, the measurement of DHA as an oxidized product of AA by LC-MS/MS in H_2O would not be accurate.

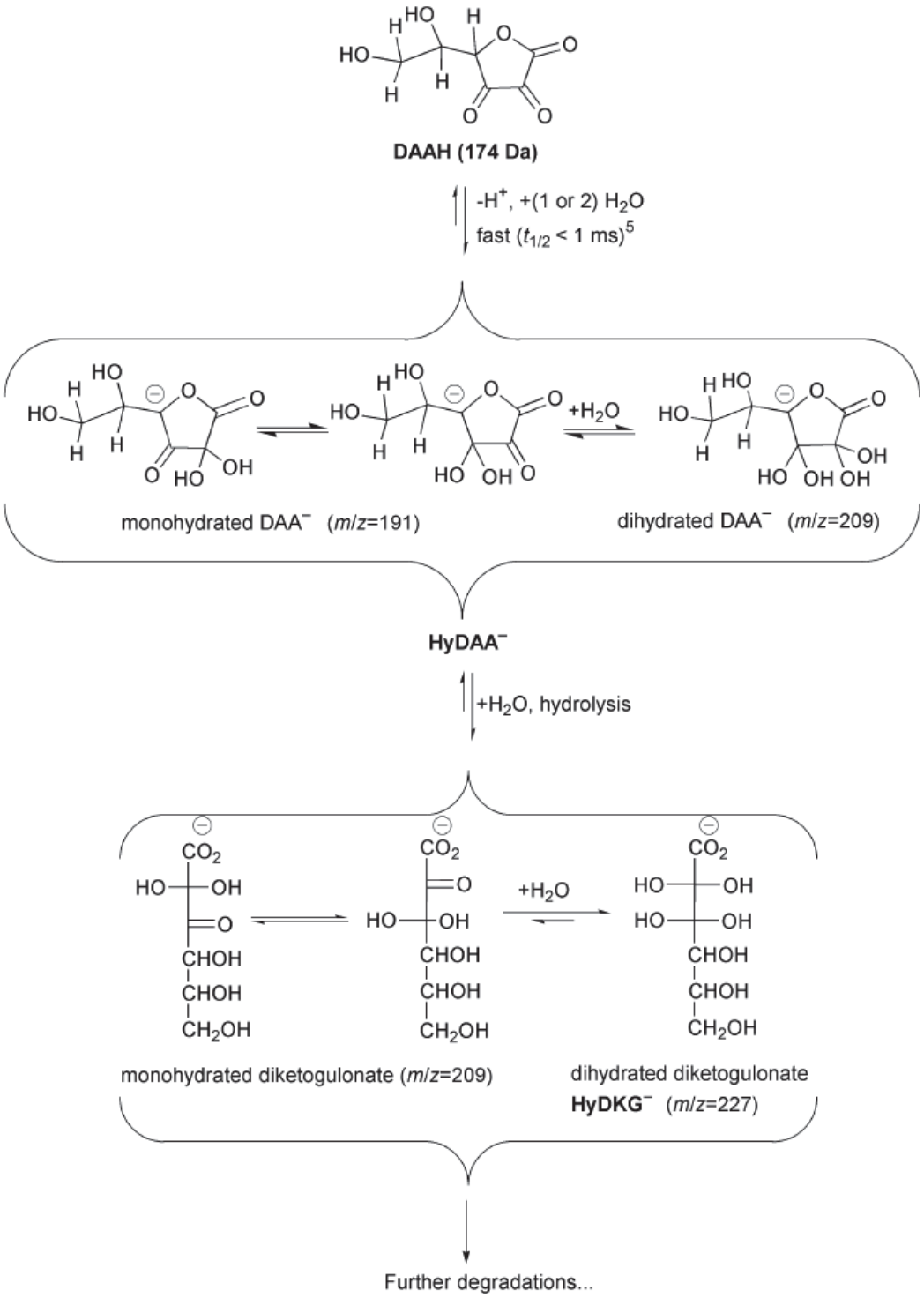

Figure 52. First steps of the degradation of the dehydroascorbic acid at neutral pH in aqueous solution. The measurement was done in buffered water (50 mM ammonium acetate, pH 7.0 ± 0.1) after different incubation times at 27 °C. DAAH = dihydroascorbic acid (DHA). Modified from [125].

In order to find a stable and measurable oxidized product of AA in water (pH was adjusted to 7.4 by adding a small amount of ammonia solution), a full scan of all products arising from the AA oxidation by $^1O_2$, was performed. The compounds with high intensity which were identified by LC-MS and analyzed by the difference shading method [5], were 209, 191 and 147, produced from an oxidation of AA with $^1O_2$ (Figure 43).

These results were confirmed by comparing the identified oxidized products of AA with the literature [125], and the relatively stable oxidized products of AA were identified as the compounds 209 (monohydrated diketogulonate) and 191 (monohydrated DHA) (Figure 52). Therefore, in the present work, both the compounds 209:191 and 209:147 were analyzed with a selected reaction monitoring (SRM) method to obtain a specific measurement of the 209:191 and 209:147 by LC-MS/MS so as to indicate the oxidized product of AA. In contrast, DHA (compound 173) was not used as an oxidized AA indicator for subsequent experiments, due to its ability to hydrolyse over time in aqueous solvents (Figure 53) [125].

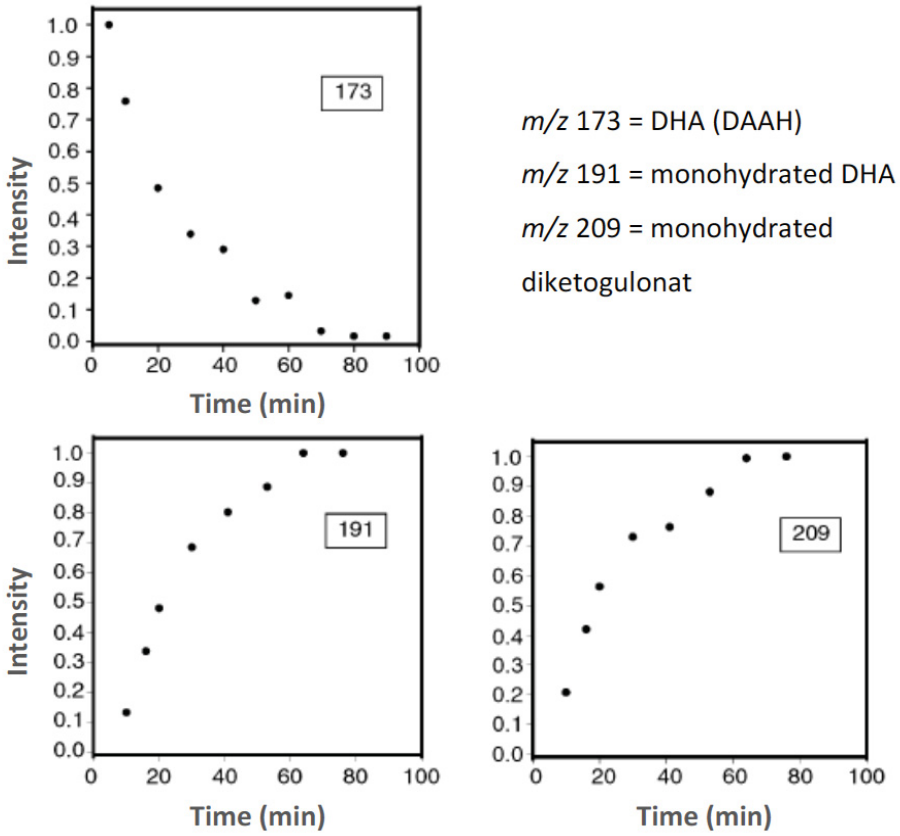

Figure 53. The intensity of compounds 191 and 209 forming in the process of DHA hydrolysis (173) measured by LC-MS/MS. Data show that the intensity of DHA (173) decreases with time and then disappears, whereas the intensity of the compounds 209 and 191, which were relatively stable intermediate compounds in the degradation process, increases. Modified from [125].

The results (Figure 45) demonstrate that AA is not able to regenerate ET from its oxidized product; there was an increasing production of oxidized AA (the compound 209:191) over time from 1 mM AA and 1 mM $DHPNO_2$ (control). The addition of 1 mM ET to the control did not increase the production rate of 209:191, however, the production of 209:191 markedly decreased to around 50% compared to the control assay. Based on that, AA is not able to regenerate ET from its oxidized products, since the production of oxidized forms of AA did not increase.

Furthermore, ET was able to eliminate a large amount of $^1O_2$ and left a small part of $^1O_2$ in the solution for AA to react with. Moreover, ET could protect AA from $^1O_2$ and decrease its oxidation, although the reaction of AA with $^1O_2$ is rapid, $k = 3 \times 10^8$ M^{-1} s^{-1} and AA was considered one of the best $^1O_2$ quenchers. In other words, these

results suported the data from the GSSG production assay (Figure 34) and proved that ET is more efficient than AA towards $^1O_2$.

The addition of His to the control assay could also slightly reduce the production of 209:191, since His is also one of the $^1O_2$ quenchers, however, it is not as effective as ET (Figure 45). Furthermore, the data from the additional control (ET + AA without $^1O_2$) showed no effect.

Based on that, and according to the results that were demonstrated in the present work, ET must now be viewed as closely linked with the redox couple GSH/GSSG. Moreover, the necessary concentration of 5-10 mM GSH is present in humans and all mammalians as well as vertebrate cells [114]. Furthermore, GSH and mycothiol are present in all species that synthesize ET, such as cyanobacteria [154], mycobacteria [155], and fungi [156]. At the time of the establishment of the syntheses of ET in cyanobacteria for the first time [157], built-in auto-recycling obviated the necessity to develop an extra regenerative enzyme. It is obvious now that the ET regeneration mechanism, after the reaction with $^1O_2$, requires high levels of GSH and can only operate in concert with GSH. However, in the absence of GSH, it could be expected that ET, by its nucleophilic thiol tautomer, functions like GSH, so that ET dimers are produced and it consumes itself. Nevertheless, in the presence of only 0.1 mM GSH, ET disulfide production is totally inhibited [12].

It is uncertain at present whether the two proposed [12] alternative initial reactions between ET and $^1O_2$ have any effect on the suggested regeneration mechanism of ET, because the large amount of ET is regenerated from its oxidized product though the cycle shown in this project.

In the present project, on the one hand, several experiments regarding to the regeneration mechanism of ET were performed in the laboratory and could prove this regeneration mechanism via LC-MS/MS and LC-MS/MS/MS. On the other hand, the DFT computations could also support all the steps of the proposed ET regeneration mechanism after reaction with $^1O_2$.

5 Prospect

In this project, a non-enzymatic mechanism for the regeneration of ET after reaction with $^1O_2$ was discovered. This regeneration mechanism needs a thiol group of the reduced agent glutathione that is present in all mammalian cells, to occur. Thus, for further research projects, it is important to investigate whether this regeneration mechanism could operate with the aid of other compounds which include a thiol group in their structures such as mycothiol, N-(2-mercaptopropionyl)glycine or dithiothreitol.

Moreover, it is interesting to find out whether ET can be regenerated from its oxidized products after the reaction with other reactive oxygen species such as hydroxyl radical, superoxid anion and hydrogen peroxide.

Furthermore, this finding of the ET regeneration mechanism should be tested and confirmed in living cells to be relevance for humans.

The *in vitro* experiments performed in order to find a stable and measurable oxidized product of ascorbic acid, the compounds 209:191 (monohydrated diketogulonate) and 191:147 (monohydrated DHA), which were identified in this work through difference shading method, were analyzed by LC-MS/MS. In addition, although these compounds are relatively more stable than DHA, the hydrolysis process in aqueous solutions is continiual, therefore, further research in order to identified all reaction products of AA and $^1O_2$, and investigate their stability over time could be important.

6 Reference list

1. Cheah, I.K. and B. Halliwell, *Ergothioneine; antioxidant potential, physiological function and role in disease.* Biochim Biophys Acta, 2012. **1822**(5): p. 784-93.
2. Aruoma, O.I., J.P.E. Spencer and N. Mahmood, *Protection against oxidative damage and cell death by the natural antioxidant ergothioneine.* Food and Chemical Toxicology, 1999. **37**(11): p. 1043-1053.
3. Franzoni, F., R. Colognato, F. Galetta, I. Laurenza, M. Barsotti, R. Di Stefano, R. Bocchetti, F. Regoli, A. Carpi, A. Balbarini, L. Migliore, et al., *An in vitro study on the free radical scavenging capacity of ergothioneine: comparison with reduced glutathione, uric acid and trolox.* Biomed Pharmacother, 2006. **60**(8): p. 453-7.
4. Tanret, C., *Sur une base nouvelle retiree du seigle ergote, l'ergothioneine.* Compt. Rend., 1909. **149**: p. 222-224.
5. Grundemann, D., S. Harlfinger, S. Golz, A. Geerts, A. Lazar, R. Berkels, N. Jung, A. Rubbert and E. Schomig, *Discovery of the ergothioneine transporter.* Proc Natl Acad Sci U S A, 2005. **102**(14): p. 5256-61.
6. Grundemann, D., *The ergothioneine transporter controls and indicates ergothioneine activity--a review.* Prev Med, 2012. **54 Suppl**: p. S71-4.
7. Nakamichi, N., K. Nakayama, T. Ishimoto, Y. Masuo, T. Wakayama, H. Sekiguchi, K. Sutoh, K. Usumi, S. Iseki and Y. Kato, *Food-derived hydrophilic antioxidant ergothioneine is distributed to the brain and exerts antidepressant effect in mice.* Brain Behav, 2016. **6**(6): p. e00477.
8. Ames, B.N., *Prolonging healthy aging: Longevity vitamins and proteins.* Proc Natl Acad Sci U S A, 2018. **115**(43): p. 10836-10844.
9. Paul, B.D. and S.H. Snyder, *The unusual amino acid L-ergothioneine is a physiologic cytoprotectant.* Cell Death & Differentiation, 2009. **17**(7): p. 1134-1140.
10. Halliwell, B., I.K. Cheah and R.M.Y. Tang, *Ergothioneine - a diet-derived antioxidant with therapeutic potential.* FEBS Lett, 2018. **592**(20): p. 3357-3366.
11. Kalaras, M.D., J.P. Richie, A. Calcagnotto and R.B. Beelman, *Mushrooms: A rich source of the antioxidants ergothioneine and glutathione.* Food Chem, 2017. **233**: p. 429-433.
12. Stoffels, C., M. Oumari, A. Perrou, A. Termath, W. Schlundt, H.G. Schmalz, M. Schafer, V. Wewer, S. Metzger, E. Schomig and D. Grundemann, *Ergothioneine stands out from hercynine in the reaction with singlet oxygen: Resistance to glutathione and TRIS in the generation of specific products indicates high reactivity.* Free Radic Biol Med, 2017. **113**: p. 385-394.

13. Deiana, M., *?-Ergothioneine modulates oxidative damage in the kidney and liver of rats in vivo: studies upon the profile of polyunsaturated fatty acids.* Clinical Nutrition, 2004. **23**(2): p. 183-193.
14. Kobayashi, D., S. Aizawa, T. Maeda, I. Tsuboi, H. Yabuuchi, J. Nezu, A. Tsuji and I. Tamai, *Expression of organic cation transporter OCTN1 in hematopoietic cells during erythroid differentiation.* Exp Hematol, 2004. **32**(12): p. 1156-62.
15. Markova, N.G., N. Karaman-Jurukovska, K.K. Dong, N. Damaghi, K.A. Smiles and D.B. Yarosh, *Skin cells and tissue are capable of using L-ergothioneine as an integral component of their antioxidant defense system.* Free Radic Biol Med, 2009. **46**(8): p. 1168-76.
16. Hartman, P.E., *[32] Ergothioneine as antioxidant*, in *Methods in Enzymology*. 1990, Academic Press. p. 310-318.
17. Melville, D.B., *Ergothioneine**Much of the unpublished work from the author's laboratory reviewed in this article was supported by grants from the National Science Foundation and by research grant E-1745 from the National Institute of Allergy and Infectious Diseases, United States Public Health Service*, in *Vitamins & Hormones*, R.S. Harris, G.F. Marrian, and K.V. Thimann, Editors. 1959, Academic Press. p. 155-204.
18. Fahey, R.C., *Novel thiols of prokaryotes.* Annual Review of Microbiology, 2001. **55**: p. 333-356.
19. Pfeiffer, C., T. Bauer, B. Surek, E. Schömig and D. Gründemann, *Cyanobacteria produce high levels of ergothioneine*. Vol. 129. 2011. 1766-1769.
20. Seebeck, F.P., *In Vitro Reconstitution of Mycobacterial Ergothioneine Biosynthesis.* Journal of the American Chemical Society, 2010. **132**(19): p. 6632-+.
21. Melville, D.B., M.L. Ludwig, E. Inamine and J.R. Rachele, *Transmethylation in Biosynthesis of Ergothioneine.* Federation Proceedings, 1958. **17**(1): p. 274-274.
22. Cheah, I.K., R.M. Tang, T.S. Yew, K.H. Lim and B. Halliwell, *Administration of Pure Ergothioneine to Healthy Human Subjects: Uptake, Metabolism, and Effects on Biomarkers of Oxidative Damage and Inflammation.* Antioxid Redox Signal, 2017. **26**(5): p. 193-206.
23. Grigat, S., S. Harlfinger, S. Pal, R. Striebinger, S. Golz, A. Geerts, A. Lazar, E. Schomig and D. Grundemann, *Probing the substrate specificity of the ergothioneine transporter with methimazole, hercynine, and organic cations.* Biochem Pharmacol, 2007. **74**(2): p. 309-16.
24. Arduini, A., G. Mancinelli, G.L. Radatti, P. Hochstein and E. Cadenas, *Possible mechanism of inhibition of nitrite-induced oxidation of oxyhemoglobin by ergothioneine and uric acid.* Archives of Biochemistry and Biophysics, 1992. **294**(2): p. 398-402.
25. Misra, H.P., *Generation of superoxide free radical during the autoxidation of thiols.* J Biol Chem, 1974. **249**(7): p. 2151-5.

26. Leone, E. and T. Mann, *Ergothioneine in the seminal vesicle secretion.* Nature, 1951. **168**(4266): p. 205-6.
27. Melville, D.B., W.H. Horner and R. Lubschez, *Tissue ergothioneine.* J Biol Chem, 1954. **206**(1): p. 221-8.
28. Hediger, M.A., M.F. Romero, J.B. Peng, A. Rolfs, H. Takanaga and E.A. Bruford, *The ABCs of solute carriers: physiological, pathological and therapeutic implications of human membrane transport proteinsIntroduction.* Pflugers Arch, 2004. **447**(5): p. 465-8.
29. Skwara, P., *Ein neuer Mechanismus des Transporters SLC22A11: Membraninsertion von Estronsulfat gegenüber Translokation von Harnsäure und Glutamat.* 2017, Universität zu Köln (Dissertation).
30. Nakamura, T., K. Yoshida, H. Yabuuchi, T. Maeda and I. Tamai, *Functional characterization of ergothioneine transport by rat organic cation/carnitine transporter Octn1 (slc22a4).* Biol Pharm Bull, 2008. **31**(8): p. 1580-4.
31. Paul, B.D. and S.H. Snyder, *The unusual amino acid L-ergothioneine is a physiologic cytoprotectant.* Cell Death and Differentiation, 2010. **17**(7): p. 1134-1140.
32. Bacher, P., S. Giersiefer, M. Bach, C. Fork, E. Schomig and D. Grundemann, *Substrate discrimination by ergothioneine transporter SLC22A4 and carnitine transporter SLC22A5: gain-of-function by interchange of selected amino acids.* Biochim Biophys Acta, 2009. **1788**(12): p. 2594-602.
33. Tschirka, J., M. Kreisor, J. Betz and D. Grundemann, *Substrate Selectivity Check of the Ergothioneine Transporter.* Drug Metab Dispos, 2018. **46**(6): p. 779-785.
34. Kato, Y., Y. Kubo, D. Iwata, S. Kato, T. Sudo, T. Sugiura, T. Kagaya, T. Wakayama, A. Hirayama, M. Sugimoto, K. Sugihara, et al., *Gene knockout and metabolome analysis of carnitine/organic cation transporter OCTN1.* Pharm Res, 2010. **27**(5): p. 832-40.
35. Sugiura, T., S. Kato, T. Shimizu, T. Wakayama, N. Nakamichi, Y. Kubo, D. Iwata, K. Suzuki, T. Soga, M. Asano, S. Iseki, et al., *Functional expression of carnitine/organic cation transporter OCTN1/SLC22A4 in mouse small intestine and liver.* Drug Metab Dispos, 2010. **38**(10): p. 1665-72.
36. Pfeiffer, C., M. Bach, T. Bauer, J. Campos da Ponte, E. Schomig and D. Grundemann, *Knockout of the ergothioneine transporter ETT in zebrafish results in increased 8-oxoguanine levels.* Free Radic Biol Med, 2015. **83**: p. 178-85.
37. Santiago, J.L., A. Martinez, H. de la Calle, M. Fernandez-Arquero, M.A. Figueredo, E.G. de la Concha and E. Urcelay, *Evidence for the association of the SLC22A4 and SLC22A5 genes with type 1 diabetes: a case control study.* BMC Med Genet, 2006. **7**: p. 54.
38. Taubert, D., N. Jung, T. Goeser and E. Schomig, *Increased ergothioneine tissue concentrations in carriers of the Crohn's disease risk-associated 503F variant of the organic cation transporter OCTN1.* Gut, 2009. **58**(2): p. 312-314.

39. Nakamura, T., S. Sugiura, D. Kobayashi, K. Yoshida, H. Yabuuchi, S. Aizawa, T. Maeda and I. Tamai, *Decreased proliferation and erythroid differentiation of K562 cells by siRNA-induced depression of OCTN1 (SLC22A4) transporter gene.* Pharmaceutical Research, 2007. **24**(9): p. 1628-1635.
40. Guijarro, M.V., A. Indart, O.I. Aruoma, M. Viana and B. Bonet, *Effects of ergothioneine on diabetic embryopathy in pregnant rats.* Food and Chemical Toxicology, 2002. **40**(12): p. 1751-1755.
41. Greene, M.F., *Prevention and Diagnosis of Congenital Anomalies in Diabetic Pregnancies.* Clinics in Perinatology, 1993. **20**(3): p. 533-547.
42. Lucas, M.J., K.J. Leveno, M.L. Williams, P. Raskin and P.J. Whalley, *Early pregnancy glycosylated hemoglobin, severity of diabetes, and fetal malformations.* Am J Obstet Gynecol, 1989. **161**(2): p. 426-31.
43. Viana, M., E. Herrera and B. Bonet, *Teratogenic effects of diabetes mellitus in the rat. Prevention by vitamin E.* Diabetologia, 1996. **39**(9): p. 1041-6.
44. Motohashi, N. and I. Mori, *Thiol-Induced Hydroxyl Radical Formation and Scavenger Effect of Thiocarbamides on Hydroxyl Radicals.* Journal of Inorganic Biochemistry, 1986. **26**(3): p. 205-212.
45. Zhu, B.Z., L. Mao, R.M. Fan, J.G. Zhu, Y.N. Zhang, J. Wang, B. Kalyanaraman and B. Frei, *Ergothioneine prevents copper-induced oxidative damage to DNA and protein by forming a redox-inactive ergothioneine-copper complex.* Chem Res Toxicol, 2011. **24**(1): p. 30-4.
46. Akanmu, D., R. Cecchini, O.I. Aruoma and B. Halliwell, *The Antioxidant Action of Ergothioneine.* Archives of Biochemistry and Biophysics, 1991. **288**(1): p. 10-16.
47. Rifkind, J.M., *Copper and the autoxidation of hemoglobin.* Biochemistry, 1974. **13**(12): p. 2475-81.
48. Rowley, D.A. and B. Halliwell, *Formation of hydroxyl radicals from NADH and NADPH in the presence of copper salts.* Journal of Inorganic Biochemistry, 1985. **23**(2): p. 103-108.
49. Hochstein, P., K.S. Kumar and S.J. Forman, *Lipid peroxidation and the cytotoxicity of copper.* Ann N Y Acad Sci, 1980. **355**: p. 240-8.
50. Aruoma, O.I., M. Whiteman, T.G. England and B. Halliwell, *Antioxidant action of ergothioneine: Assessment of its ability to scavenge peroxynitrite.* Biochemical and Biophysical Research Communications, 1997. **231**(2): p. 389-391.
51. Arduini, A., L. Eddy and P. Hochstein, *The reduction of ferryl myoglobin by ergothioneine: a novel function for ergothioneine.* Arch Biochem Biophys, 1990. **281**(1): p. 41-3.
52. Galaris, D., E. Cadenas and P. Hochstein, *Redox cycling of myoglobin and ascorbate: a potential protective mechanism against oxidative reperfusion injury in muscle.* Arch Biochem Biophys, 1989. **273**(2): p. 497-504.
53. Deiana, M., A. Rosa, V. Casu, R. Piga, M. Assunta Dessi and O.I. Aruoma, *L-ergothioneine modulates oxidative damage in the kidney and liver of rats in*

vivo: studies upon the profile of polyunsaturated fatty acids. Clin Nutr, 2004. **23**(2): p. 183-93.

54. Sheu, C. and C.S. Foote, *Reactivity toward Singlet Oxygen of a 7,8-Dihydro-8-Oxoguanosine (8-Hydroxyguanosine) Formed by Photooxidation of a Guanosine Derivative.* Journal of the American Chemical Society, 1995. **117**(24): p. 6439-6442.
55. Devasagayam, T.P.A., S. Steenken, M.S.W. Obendorf, W.A. Schulz and H. Sies, *Formation of 8-Hydroxy(Deoxy)Guanosine and Generation of Strand Breaks at Guanine Residues in DNA by Singlet Oxygen.* Biochemistry, 1991. **30**(25): p. 6283-6289.
56. Rougee, M., R.V. Bensasson, E.J. Land and R. Pariente, *Deactivation of singlet molecular oxygen by thiols and related compounds, possible protectors against skin photosensitivity.* Photochem Photobiol, 1988. **47**(4): p. 485-9.
57. Krüger, J., Untersuchung der Reaktivität von Ergothionein gegenüber Singulett-Sauerstoff in vitro und intrazellulär. 2016, Heinrich-Heine-Universität Düsseldorf (Dissertation).
58. Stoffels, C., *Ist Ergothionein der physiologische Singulett-Sauerstoff-Quencher? Analyse des Ergothioneinschutzes in 293 Zellen und Identifizierung der in vitro Reaktionsprodukte.* 2017, Universität zu Köln (Dissertation).
59. Redmond, R.W. and I.E. Kochevar, *Spatially resolved cellular responses to singlet oxygen.* Photochem Photobiol, 2006. **82**(5): p. 1178-86.
60. Hayyan, M., M.A. Hashim and I.M. AlNashef, *Superoxide Ion: Generation and Chemical Implications.* Chem Rev, 2016. **116**(5): p. 3029-85.
61. Sies, H., *Oxidative stress: oxidants and antioxidants.* Exp Physiol, 1997. **82**(2): p. 291-5.
62. Freeman, B.A. and J.D. Crapo, *Biology of disease: free radicals and tissue injury.* Lab Invest, 1982. **47**(5): p. 412-26.
63. Cross, C.E., B. Halliwell, E.T. Borish, W.A. Pryor, B.N. Ames, R.L. Saul, J.M. McCord and D. Harman, *Oxygen radicals and human disease.* Ann Intern Med, 1987. **107**(4): p. 526-45.
64. Cadet, J., T. Delatour, T. Douki, D. Gasparutto, J.P. Pouget, J.L. Ravanat and S. Sauvaigo, *Hydroxyl radicals and DNA base damage.* Mutat Res, 1999. **424**(1-2): p. 9-21.
65. Ravanat, J.L., C. Saint-Pierre, P. Di Mascio, G.R. Martinez, M.H.G. Medeiros and J. Cadet, *Damage to isolated DNA mediated by singlet oxygen.* Helvetica Chimica Acta, 2001. **84**(12): p. 3702-3709.
66. Sysak, P.K., C.S. Foote and T.Y. Ching, *Chemistry of Singlet Oxygen .25. Photooxygenation of Methionine.* Photochemistry and Photobiology, 1977. **26**(1): p. 19-27.
67. Tomita, M., M. Irie and T. Ukita, *Sensitized Photooxidation of Histidine and Its Derivatives . Products and Mechanism of Reaction.* Biochemistry, 1969. **8**(12): p. 5149-&.

68. Buettner, G.R. and R.D. Hall, *Superoxide, Hydrogen-Peroxide and Singlet Oxygen in Hematoporphyrin Derivative-Cysteine, Derivative-Nadh and Derivative-Light Systems.* Biochimica Et Biophysica Acta, 1987. **923**(3): p. 501-507.
69. Nakagawa, M., H. Okajima and T. Hino, *Photosensitized oxygenation of Nb-methoxycarbonyltryptamines. A new pathway to kynurenine derivatives.* J Am Chem Soc, 1977. **99**(13): p. 4424-9.
70. Jin, F.M., J. Leitich and C. vonSonntag, *The photolysis (lambda=254 nm) of tyrosine in aqueous solutions in the absence and presence of oxygen. The reaction of tyrosine with singlet oxygen.* Journal of Photochemistry and Photobiology a-Chemistry, 1995. **92**(3): p. 147-153.
71. DeRosa, M.C. and R.J. Crutchley, *Photosensitized singlet oxygen and its applications.* Coordination Chemistry Reviews, 2002. **233**: p. 351-371.
72. Krinsky, N.I., *Singlet Oxygen in Biological-Systems.* Trends in Biochemical Sciences, 1977. **2**(2): p. 35-38.
73. Weldon, D., T.D. Poulsen, K.V. Mikkelsen and P.R. Ogilby, *Singlet sigma: The "other" singlet oxygen in solution.* Photochemistry and Photobiology, 1999. **70**(4): p. 369-379.
74. Macpherson, A.N., A. Telfer, J. Barber and T.G. Truscott, *Direct-Detection of Singlet Oxygen from Isolated Photosystem-Ii Reaction Centers.* Biochimica Et Biophysica Acta, 1993. **1143**(3): p. 301-309.
75. Darmanyan, A.P., W.S. Jenks and P. Jardon, *Charge-transfer quenching of singlet oxygen O-2((1)Delta g) by amines and aromatic hydrocarbons (vol 102A, pg 7420, 1998).* Journal of Physical Chemistry A, 1998. **102**(46): p. 9308-9308.
76. Knör, G. and U. Monkowius, *Photosensitization and photocatalysis in bioinorganic, bio-organometallic and biomimetic systems*, in *Advances in Inorganic Chemistry*, R.v. Eldik and G. Stochel, Editors. 2011, Academic Press. p. 235-289.
77. Ergaieg, K. and R. Seux, *A comparative study of the photoinactivation of bacteria by meso -substituted cationic porphyrin, rose Bengal and methylene blue.* Desalination, 2009. **246**(1-3): p. 353-362.
78. Tada-Oikawa, S., S. Oikawa, J. Hirayama, K. Hirakawa and S. Kawanishi, *DNA Damage and Apoptosis Induced by Photosensitization of 5,10,15,20-Tetrakis (N-methyl-4-pyridyl)-21H,23H-porphyrin via Singlet Oxygen Generation.* Photochemistry and Photobiology, 2009. **85**(6): p. 1391-1399.
79. Lambrechts, S.A.G., M.C.G. Aalders, D.H. Langeveld-Klerks, Y. Khayali and J.W.M. Lagerberg, *Effect of monovalent and divalent cations on the photoinactivation of bacteria with meso-substituted cationic porphyrins.* Photochemistry and Photobiology, 2004. **79**(3): p. 297-302.
80. Bottiroli, G., A.C. Croce, P. Balzarini, D. Locatelli, P. Baglioni, P. Lo Nostro, M. Monici and R. Pratesi, *Enzyme-assisted cell photosensitization: a proposal for an efficient approach to tumor therapy and diagnosis. The rose bengal fluorogenic substrate.* Photochem Photobiol, 1997. **66**(3): p. 374-83.

81. Ryter, S.W. and R.M. Tyrrell, *The heme synthesis and degradation pathways: role in oxidant sensitivity. Heme oxygenase has both pro- and antioxidant properties.* Free Radic Biol Med, 2000. **28**(2): p. 289-309.
82. Min, D., Boff, J., *Chemistry and reaction of singlet oxygen in foods.* Comprehensive Reviews in Food Science and Food Safety, 2002 (1): p. 58-72.
83. Pierlot, C., J.M. Aubry, K. Briviba, H. Sies and P. Di Mascio, *Naphthalene endoperoxides as generators of singlet oxygen in biological media.* Singlet Oxygen, Uv-a, and Ozone, 2000. **319**: p. 3-20.
84. Lafleur, M.V., A.W. Nieuwint, J.M. Aubry, H. Kortbeek, F. Arwert and H. Joenje, *DNA damage by chemically generated singlet oxygen.* Free Radic Res Commun, 1987. **2**(4-6): p. 343-50.
85. Skovsen, E., J.W. Snyder, J.D.C. Lambert and P.R. Ogilby, *Lifetime and diffusion of singlet oxygen in a cell.* Journal of Physical Chemistry B, 2005. **109**(18): p. 8570-8573.
86. Ogilby, P.R., *Singlet oxygen: there is indeed something new under the sun.* Chemical Society Reviews, 2010. **39**(8): p. 3181-3209.
87. Ogilby, P.R. and C.S. Foote, *Chemistry of Singlet Oxygen .42. Effect of Solvent, Solvent Isotopic-Substitution, and Temperature on the Lifetime of Singlet Molecular-Oxygen (1-Delta-G).* Journal of the American Chemical Society, 1983. **105**(11): p. 3423-3430.
88. Wilkinson, F., W.P. Helman and A.B. Ross, *Rate Constants for the Decay and Reactions of the Lowest Electronically Excited Singlet-State of Molecular-Oxygen in Solution - an Expanded and Revised Compilation.* Journal of Physical and Chemical Reference Data, 1995. **24**(2): p. 663-1021.
89. Kramarenko, G.G., S.G. Hummel, S.M. Martin and G.R. Buettner, *Ascorbate reacts with singlet oxygen to produce hydrogen peroxide.* Photochemistry and Photobiology, 2006. **82**(6): p. 1634-1637.
90. Harding, L.B. and W.A. Goddard, *Mechanism of the Ene Reaction of Singlet Oxygen with Olefins.* Journal of the American Chemical Society, 1980. **102**(2): p. 439-449.
91. Yamaguchi, K., T. Fueno, I. Saito and T. Matsuura, *On the Mechanism of Ene Reaction of Electron-Rich Olefins with Singlet Oxygen - Abinitio Mo Calculations.* Tetrahedron Letters, 1980. **21**(42): p. 4087-4090.
92. Davies, M.J., *Singlet oxygen-mediated damage to proteins and its consequences.* Biochemical and Biophysical Research Communications, 2003. **305**(3): p. 761-770.
93. Rawls, H.R. and Vansante.Pj, *A Possible Role for Singlet Oxygen in Initiation of Fatty Acid Autoxidation.* Journal of the American Oil Chemists Society, 1970. **47**(4): p. 121-&.
94. MacManus-Spencer, L.A., D.E. Latch, K.M. Kroncke and K. McNeill, *Stable dioxetane precursors as selective trap-and-trigger chemiluminescent probes for singlet oxygen.* Analytical Chemistry, 2005. **77**(4): p. 1200-1205.

95. Adam, W., S.G. Bosio and N.J. Turro, *Highly diastereoselective dioxetane formation in the photooxygenation of enecarbamates with an oxazolidinone chiral auxiliary: Steric control in the [2+2] cycloaddition of singlet oxygen through conformational alignment.* Journal of the American Chemical Society, 2002. **124**(30): p. 8814-8815.
96. Leach, A.G. and K.N. Houk, *Diels-Alder and ene reactions of singlet oxygen, nitroso compounds and triazolinediones: transition states and mechanisms from contemporary theory.* Chemical Communications, 2002(12): p. 1243-1255.
97. Gollnick, K., *Type II Photooxygenation Reactions in Solution*. Advances in Photochemistry, 1968. **6**: p. 1-122.
98. Bisby, R.H., C.G. Morgan, I. Hamblett and A.A. Gorman, *Quenching of singlet oxygen by Trolox C, ascorbate, and amino acids: Effects of pH and temperature.* Journal of Physical Chemistry A, 1999. **103**(37): p. 7454-7459.
99. Davies, K.J., *Oxidative stress: the paradox of aerobic life.* Biochem Soc Symp, 1995. **61**: p. 1-31.
100. Sies, H. and W. Stahl, *Vitamin-E and Vitamin-C, Beta-Carotene, and Other Carotenoids as Antioxidants.* American Journal of Clinical Nutrition, 1995. **62**(6): p. 1315-1321.
101. Fernandez, V. and L.A. Videla, *Biochemical aspects of cellular antioxidant systems.* Biol Res, 1996. **29**(2): p. 177-82.
102. Nordman, T., L. Xia, L. Bjorkhem-Bergman, A. Damdimopoulos, I. Nalvarte, E.S. Arner, G. Spyrou, L.C. Eriksson, M. Bjornstedt and J.M. Olsson, *Regeneration of the antioxidant ubiquinol by lipoamide dehydrogenase, thioredoxin reductase and glutathione reductase.* Biofactors, 2003. **18**(1-4): p. 45-50.
103. Oumari, M., B. Goldfuss, C. Stoffels, H.G. Schmalz and D. Grundemann, *Regeneration of ergothioneine after reaction with singlet oxygen.* Free Radic Biol Med, 2019. **134**: p. 498-504.
104. Frei, B., L. England and B.N. Ames, *Ascorbate Is an Outstanding Antioxidant in Human-Blood Plasma.* Proceedings of the National Academy of Sciences of the United States of America, 1989. **86**(16): p. 6377-6381.
105. Stephen, R. and T. Utecht, *Scurvy identified in the emergency department: a case report.* J Emerg Med, 2001. **21**(3): p. 235-7.
106. Weinstein, M., P. Babyn and S. Zlotkin, *An orange a day keeps the doctor away: scurvy in the year 2000.* Pediatrics, 2001. **108**(3): p. E55.
107. Jacob, R.A. and G. Sotoudeh, *Vitamin C function and status in chronic disease.* Nutr Clin Care, 2002. **5**(2): p. 66-74.
108. Traber, M.G. and J.F. Stevens, *Vitamins C and E: beneficial effects from a mechanistic perspective.* Free radical biology & medicine, 2011. **51**(5): p. 1000-1013.
109. Winkler, B.S., S.M. Orselli and T.S. Rex, *The redox couple between glutathione and ascorbic acid: a chemical and physiological perspective.* Free Radic Biol Med, 1994. **17**(4): p. 333-49.

110. Pompella, A., A. Visvikis, A. Paolicchi, V. De Tata and A.F. Casini, *The changing faces of glutathione, a cellular protagonist.* Biochem Pharmacol, 2003. **66**(8): p. 1499-503.
111. Maher, P., *The effects of stress and aging on glutathione metabolism.* Ageing Res Rev, 2005. **4**(2): p. 288-314.
112. Sies, H., *Glutathione and its role in cellular functions.* Free Radic Biol Med, 1999. **27**(9-10): p. 916-21.
113. Vivancos, P.D., T. Wolff, J. Markovic, F.V. Pallardo and C.H. Foyer, *A nuclear glutathione cycle within the cell cycle.* Biochemical Journal, 2010. **431**: p. 169-178.
114. Lushchak, V.I., *Glutathione homeostasis and functions: potential targets for medical interventions.* J Amino Acids, 2012. **2012**: p. 736837.
115. Pastore, A., F. Piemonte, M. Locatelli, A. Lo Russo, L.M. Gaeta, G. Tozzi and G. Federici, *Determination of blood total, reduced, and oxidized glutathione in pediatric subjects.* Clin Chem, 2001. **47**(8): p. 1467-9.
116. Lu, S.C., *Glutathione synthesis.* Biochim Biophys Acta, 2013. **1830**(5): p. 3143-53.
117. Couto, N., N. Malys, S.J. Gaskell and J. Barber, *Partition and turnover of glutathione reductase from Saccharomyces cerevisiae: a proteomic approach.* J Proteome Res, 2013. **12**(6): p. 2885-94.
118. Kletzien, R.F., P.K.W. Harris and L.A. Foellmi, *Glucose-6-Phosphate-Dehydrogenase - a Housekeeping Enzyme Subject to Tissue-Specific Regulation by Hormones, Nutrients, and Oxidant Stress.* Faseb Journal, 1994. **8**(2): p. 174-181.
119. Galli, F., A. Azzi, M. Birringer, J.M. Cook-Mills, M. Eggersdorfer, J. Frank, G. Cruciani, S. Lorkowski and N.K. Ozer, *Vitamin E: Emerging aspects and new directions.* Free Radic Biol Med, 2017. **102**: p. 16-36.
120. David, R., *CRC Handbook of Chemistry and Physics, 87th ed Editor-in-Chief. Lide (National Institute of Standards and Technology). CRC Press/Taylor and Francis Group.* Journal of the American Chemical Society, 2007. **129**(3): p. 724-724.
121. James, A.M., H.M. Cocheme, R.A.J. Smith and M.P. Murphy, *Interactions of mitochondria-targeted and untargeted ubiquinones with the mitochondrial respiratory chain and reactive oxygen species - Implications for the use of exogenous ubiquinones as therapies and experimental tools.* Journal of Biological Chemistry, 2005. **280**(22): p. 21295-21312.
122. Slater, E.C., *The Q-Cycle, an Ubiquitous Mechanism of Electron-Transfer.* Trends in Biochemical Sciences, 1983. **8**(7): p. 239-242.
123. Castano, A.P., T.N. Demidova and M.R. Hamblin, *Mechanisms in photodynamic therapy: part one-photosensitizers, photochemistry and cellular localization.* Photodiagnosis Photodyn Ther, 2004. **1**(4): p. 279-93.
124. Pierlot, C., S. Hajjam, C. Barthélémy and J.M. Aubry, *Water-soluble naphthalene derivatives as singlet oxygen (1O2, 1Δg) carriers for biological*

media. Journal of Photochemistry and Photobiology B: Biology, 1996. **36**(1): p. 31-39.

125. Cioffi, N., I. Losito, R. Terzano and C.G. Zambonin, *An electrospray ionization ion trap mass spectrometric (ESI-MS-MSn) study of dehydroascorbic acid hydrolysis at neutral pH.* Analyst, 2000. **125**(12): p. 2244-8.
126. Chaimbault, P., *The Modern Art of Identification of Natural Substances in Whole Plants*, in *Recent Advances in Redox Active Plant and Microbial Products: From Basic Chemistry to Widespread Applications in Medicine and Agriculture*, C. Jacob, et al., Editors. 2014, Springer Netherlands: Dordrecht. p. 31-94.
127. Pitt, J.J., *Principles and applications of liquid chromatography-mass spectrometry in clinical biochemistry.* Clin Biochem Rev, 2009. **30**(1): p. 19-34.
128. Lough, W.J. and I.W. Wainer, *High performance liquid chromatography: fundamental principles and practice*. 1995: cRc press.
129. Meyer, V.R., *Practical high-performance liquid chromatography*. 2013: John Wiley & Sons.
130. Kirkland, J.J., F.A. Truszkowski, C.H. Dilks and G.S. Engel, *Superficially porous silica microspheres for fast high-performance liquid chromatography of macromolecules.* Journal of Chromatography A, 2000. **890**(1): p. 3-13.
131. King, R., R. Bonfiglio, C. Fernandez-Metzler, C. Miller-Stein and T. Olah, *Mechanistic investigation of ionization suppression in electrospray ionization.* Journal of the American Society for Mass Spectrometry, 2000. **11**(11): p. 942-950.
132. Becker, J.S., *Inorganic mass spectrometry: principles and applications*. 2007: Wiley Online Library.
133. Smith, R.D., J.A. Loo, R.R.O. Loo, M. Busman and H.R. Udseth, *Principles and practice of electrospray ionization—mass spectrometry for large polypeptides and proteins.* Mass Spectrometry Reviews, 1991. **10**(5): p. 359-452.
134. Bruins, A.P., *Mechanistic aspects of electrospray ionization.* Journal of Chromatography A, 1998. **794**(1-2): p. 345-357.
135. Mora, J.F.d.l., *The Fluid Dynamics of Taylor Cones.* Annual Review of Fluid Mechanics, 2007. **39**(1): p. 217-243.
136. Forschungszentrum., B.-M. *Electrospryionisation (ESI)*. Cited 20.01.2019; Available from: http://www.bmfz.hhu.de.
137. Shimadzu. *Diagram of Quadrupole MS.* Cited 20.01.2019; Available from: https://www.shimadzu.com/an/lcms/support/intro/lib/lctalk/61/61intro.html.
138. Xiao, J.F., B. Zhou and H.W. Ressom, *Metabolite identification and quantitation in LC-MS/MS-based metabolomics.* Trac-Trends in Analytical Chemistry, 2012. **32**: p. 1-14.

139. Ramirez-Correa, G.A., M.I. Martinez-Ferrando, P.B. Zhang and A.M. Murphy, *Targeted proteomics of myofilament phosphorylation and other protein posttranslational modifications.* Proteomics Clinical Applications, 2014. **8**(7-8): p. 543-553.
140. Theodoridis, G.A., H.G. Gika, E.J. Want and I.D. Wilson, *Liquid chromatography-mass spectrometry based global metabolite profiling: A review.* Analytica Chimica Acta, 2012. **711**: p. 7-16.
141. MassBank. *Massbank-High Quality Mass Spectral Database.* Cited 25.01.2019; Available from: http://www.massbank.jp.
142. Metlin. citated 25.01.2019; Available from: https://metlin.scripps.edu/landing_page.php?pgcontent=advanced_search.
143. Lee, M.S. and Q.C. Ji, *Protein Analysis using Mass Spectrometry: Accelerating Protein Biotherapeutics from Lab to Patient*. 2017: Wiley.
144. Frisch, M.J., G.W. Trucks, H.B. Schlegel, G.E. Scuseria, M.A. Robb, J.R. Cheeseman, G. Scalmani, V. Barone, G.A. Petersson, H. Nakatsuji, X. Li, et al., *Gaussian 16 Rev. A.03*. 2016: Wallingford, CT.
145. Ravanat, J.L., P. Di Mascio, G.R. Martinez, M.H.G. Medeiros and J. Cadet, *Singlet oxygen induces oxidation of cellular DNA.* Journal of Biological Chemistry, 2000. **275**(51): p. 40601-40604.
146. Nair, D.P., M. Podgorski, S. Chatani, T. Gong, W.X. Xi, C.R. Fenoli and C.N. Bowman, *The Thiol-Michael Addition Click Reaction: A Powerful and Widely Used Tool in Materials Chemistry.* Chemistry of Materials, 2014. **26**(1): p. 724-744.
147. Sun, Y.P., H. Liu, L. Cheng, S.M. Zhu, C.F. Cai, T.Z. Yang, L. Yang and P.T. Ding, *Thiol Michael addition reaction: a facile tool for introducing peptides into polymer-based gene delivery systems.* Polymer International, 2018. **67**(1): p. 25-31.
148. Schultz, T.W., J.W. Yarbrough and E.L. Johnson, *Structure-activity relationships for reactivity of carbonyl-containing compounds with glutathione.* SAR QSAR Environ Res, 2005. **16**(4): p. 313-22.
149. Devasagayam, T.P., A.R. Sundquist, P. Di Mascio, S. Kaiser and H. Sies, *Activity of thiols as singlet molecular oxygen quenchers.* J Photochem Photobiol B, 1991. **9**(1): p. 105-16.
150. Rong, Y., A. Al-Harbi, B. Kriegel and G. Parkin, *Structural Characterization of 2-Imidazolones: Comparison with their Heavier Chalcogen Counterparts.* Inorganic Chemistry, 2013. **52**(12): p. 7172-7182.
151. Losito, I. and C.G. Zambonin, *Double electropolymer modified platinum electrode to follow the kinetic process H2O2 plus ascorbic acid. Influence of the reaction on amperometric biosensor applications.* Journal of Electroanalytical Chemistry, 1996. **410**(2): p. 181-187.
152. Tolbert, B.M. and J.B. Ward, *Dehydroascorbic Acid.* Advances in Chemistry Series, 1982(200): p. 101-123.

153. Perone, S.P. and W.J. Kretlow, *Application of Controlled Potential Techniques to Study of Rapid Succeeding Chemical Reaction Coupled to Electro-Oxidation of Ascorbic Acid.* Analytical Chemistry, 1966. **38**(12): p. 1760-&.
154. Narainsamy, K., S. Farci, E. Braun, C. Junot, C. Cassier-Chauvat and F. Chauvat, *Oxidative-stress detoxification and signalling in cyanobacteria: the crucial glutathione synthesis pathway supports the production of ergothioneine and ophthalmate.* Molecular Microbiology, 2016. **100**(1): p. 15-24.
155. Cumming, B.M., K.C. Chinta, V.P. Reddy and A.J.C. Steyn, *Role of Ergothioneine in Microbial Physiology and Pathogenesis.* Antioxid Redox Signal, 2018. **28**(6): p. 431-444.
156. Sheridan, K.J., B.E. Lechner, G.O. Keeffe, M.A. Keller, E.R. Werner, H. Lindner, G.W. Jones, H. Haas and S. Doyle, *Ergothioneine Biosynthesis and Functionality in the Opportunistic Fungal Pathogen, Aspergillus fumigatus.* Sci Rep, 2016. **6**: p. 35306.
157. Liao, C. and F.P. Seebeck, *Convergent Evolution of Ergothioneine Biosynthesis in Cyanobacteria.* Chembiochem, 2017. **18**(21): p. 2115-2118.

Free Radical Biology and Medicine 134 (2019) 498–504

Contents lists available at ScienceDirect

Free Radical Biology and Medicine

journal homepage: www.elsevier.com/locate/freeradbiomed

Original article

Regeneration of ergothioneine after reaction with singlet oxygen

Mhmd Oumari[a], Bernd Goldfuss[b], Christopher Stoffels[a], Hans-Günther Schmalz[b], Dirk Gründemann[a,*]

[a] Department of Pharmacology, University of Cologne, Gleueler Straße 24, 50931, Cologne, Germany
[b] Department of Chemistry, University of Cologne, Greinstraße 4, 50939, Cologne, Germany

ARTICLE INFO

Keywords:
Ergothioneine
Regeneration of ergothioneine
Singlet oxygen
Glutathione
Ascorbic acid

ABSTRACT

Ergothioneine (ET), an imidazole-2-thione derivative of histidine betaine, is generally considered an antioxidant. Important antioxidants are typically regenerated from their oxidized products, to prevent the interceptors from being lost after a single chemical reaction with a reactive oxygen species. However, no mechanism for the complete regeneration of ET has yet been uncovered. Here we define a non-enzymatic multi-step cycle for the regeneration of ET after reaction with singlet oxygen ($^1O_2$). All reaction steps were verified by density functional theory computations. Four molecules of GSH are used per turn to detoxify $^1O_2$ to water. Pure $^1O_2$ was generated by thermolysis at 37 °C of the endoperoxide $DHPNO_2$. Addition of 1 mM ET to 10 mM $DHPNO_2$ and 10 mM GSH increased the production of oxidized GSH (GSSG), measured by LC-MS/MS, by a factor of 26 (water) and 28 (D_2O), respectively. In the same assay, the ring of ET alone was able to drive the cycle at equal speed; thus, the zwitterionic amino acid backbone was not involved. Our data suggest that ET reacts at least 4-fold faster with $^1O_2$ than ascorbic acid. ET must now be viewed as tightly linked with the GSH/GSSG redox couple. The necessary thiol foundation is present in all mammalian and vertebrate cells, and also in all species that generate ET, such as cyanobacteria, mycobacteria, and fungi. Regeneration provides a decisive advantage for ET over other reactive, but non-recoverable, compounds. Our findings substantiate the importance of ET for the eradication of noxious $^1O_2$.

1. Introduction

Certain bacteria and fungi synthesize ergothioneine (ET). Starting from L-histidine, the amino group is completely methylated and a sulfur atom is added at position 2 of the planar imidazole ring [1–3]. ET has several properties that are markedly different from ordinary thiols like the ubiquitous glutathione (GSH). This can be explained by the prominent involvement of a thione tautomer [4–6].

Humans and other vertebrates cannot synthesize ET; it must be absorbed from food. Most of our contemporary food contains very little ET, but some mushrooms [1,7] and cyanobacteria [8] contain much, around 1 mg/g of dried material. After ingestion, ET is rapidly cleared from the circulation and then retained in the body with minimal metabolism.

Due to its highly hydrophilic zwitterionic structure, ET on its own can hardly traverse the phospholipid bilayers of cell membranes; it can be translocated, however, by a dedicated protein, the ET transporter (ETT; human gene symbol *SLC22A4*) [9]. ETT is a powerful sodium-driven uptake transporter of the plasma membrane [10,11]. In all vertebrates, the ability to absorb, distribute, and retain ET depends entirely on the activity of this highly specific transporter [12–16]. Cells lacking ETT practically do not accumulate ET. In the human body, ETT is strongly expressed in certain cells and tissues only: erythrocyte progenitor cells of the bone marrow, the small intestine (ileum), kidney, trachea, cerebellum, and monocytes. Case-control studies have shown that polymorphisms in the *SLC22A4* gene are associated with susceptibility to chronic inflammatory diseases, such as Crohn's disease, ulcerative colitis, and type I diabetes [14,17]. It is unknown, however, how these mutations promote disease.

The mere existence of ETT and its strict evolutionary conservation across all vertebrates imply that ET fulfills a beneficial role, like vitamins and essential nutrients. Numerous functions have been proposed for ET. Mostly, it is considered an antioxidant [17,18]. However, its precise physiological purpose is still unresolved. Why do particular tissues or cells accumulate ET despite a 10-fold excess of GSH, the general antioxidant?

Recently, we have reported that in the skin of unstressed ETT knockout zebrafish, the content of 8-oxoguanine was increased 4-fold

* Corresponding author.
E-mail address: dirk.gruendemann@uni-koeln.de (D. Gründemann).

https://doi.org/10.1016/j.freeradbiomed.2019.01.043
Received 15 November 2018; Received in revised form 24 January 2019; Accepted 30 January 2019
Available online 02 February 2019
0891-5849/

Abbreviations

$^1O_2$	singlet oxygen
AA	ascorbic acid
DFT	density functional theory
DHA	dehydroascorbic acid
DHIT	1,3-dihydroimidazole-2-thione
$DHPNO_2$	*N,N'*-di(2,3-dihydroxypropyl)-1,4-naphthalenedipropanamide 1,4-endoperoxide; ET, ergothioneine
ETT	ergothioneine transporter
GSH	glutathione
GSSG	oxidized GSH
LC	liquid chromatography
MS	mass spectrometry
ROS	reactive oxygen species

vs. wild-type [19]. This led to the hypothesis that the specific purpose of ET could be to eradicate noxious singlet oxygen ($^1O_2$), not only in vertebrates but also in the ET producers. In a subsequent in vitro study, we have shown that ET is much more reactive towards singlet oxygen than GSH [20]. Among the reactive oxygen species (ROS), $^1O_2$ is less reactive than the hydroxyl radical, but more aggressive than the superoxide anion and hydrogen peroxide [21]. This translates into a relatively long intracellular half-life ($t_{1/2} \approx 3$ μs) [22]. The radius of the sphere of activity of $^1O_2$ from its point of intracellular production was estimated at 155 nm [23]. While the hydroxyl radical reacts with almost anything, $^1O_2$ is selective about its reaction partner. For example, the hydroxyl radical attacks all 4 DNA bases, but $^1O_2$ confines itself to guanine [24]. In the human body, $^1O_2$ is generated by sunlit photosensitizers in the skin and eye and as a by-product of enzymatic oxygen conversions by hemoglobin and peroxidases [25].

All important antioxidants such as GSH, ascorbic acid, vitamin E (tocopherols plus tocotrienols), uric acid, and ubiquinol are regenerated to a large part from their oxidized products [26–28]. The efficient recycling of antioxidants are of utmost importance to prevent the interceptors from being lost after a single chemical reaction with a ROS. Only continual turnover results in long-lasting antioxidative protection. An antioxidant effect without regeneration of the protective compound is therefore typically of minimal physiological significance. Conversely, effective regeneration provides strong evidence for the importance of the primary interception reaction.

A mechanism for the extensive regeneration of ET after a reaction with a ROS has never been defined. Here we report a non-enzymatic multi-step cycle for the regeneration of ET after reaction with singlet oxygen.

2. Materials & methods

2.1. Singlet oxygen reaction assays

The endoperoxide $DHPNO_2$ was prepared and used as described [20] to generate pure $^1O_2$ by thermolysis at 37 °C. Standard assays, with a total volume of 100 μl in brown polypropylene reaction tubes (72.706.001, Sarstedt, Nümbrecht, Germany), contained 10 μM ET ± GSH in 10 mM ammonium hydrogen carbonate/ammonia (pH 7.4 or 8.0) or in water. In assays without buffer, all components were checked for neutral pH before mixing and adjusted if necessary by adding concentrated ammonia. Reactions were started by adding ice-cold $DHPNO_2$ (68 mM) solution to a final concentration of 10 mM and then incubated at 37 °C on a shaker (300 rpm). After the indicated times, 10 μl samples were removed, diluted 1:10 or 1:100 with ice-cold buffer or water, and then directly analyzed for ET and ET products by LC-MS/MS. Zero time controls were kept on ice throughout. GSSG generation assays (V = 100 μl) contained 10 mM GSH + 10 mM $DHPNO_2$ ± 1 mM test compound in D_2O.

2.2. LC-MS/MS

Ten microliters of the ice-cold reaction samples were analyzed by HPLC coupled to a triple quadrupole mass spectrometer (4000 Q TRAP, AB Sciex, Darmstadt, Germany). For HPLC (Shimadzu SLC-20AD Prominence HPLC; flow rate 0.2 ml/min, autosampler temperature 4 °C, oven temperature 35 °C), a ZIC-HILIC column (5 μm, 2.1 × 100 mm; Dichrom, Marl, Germany) was used with the following gradient: A, 0.1% formic acid and B, 0.1% formic acid in acetonitrile. Gradient flow was set as: 90% B at 0 min, 90% B at 0.5 min, 10% B at 9 min, 10% B at 10 min, 90% B at 14 min, and 90% B at 15 min. At the MS interface, ions were generated by atmospheric pressure ionization with positive electrospray (ESI). Fragmentation by collision with nitrogen on Q2 was used to record product ion spectra (entrance potential 10 V, declustering potential (DP) 60 V, collision cell exit potential (CXP) 10 V, collision energy (CE) variable). The following fragmentations (scan time 150 ms) were chosen for analyte quantification by selected reaction monitoring (SRM; *m/z* parent:*m/z* fragment): ergothioneine, 230:127 and 230:186 (DP 41 V, CXP 8 V, CE 27 V); GSSG, 307:130 (DP 56 V, CXP 6 V, CE 21 V) and 613:355 (DP 71 V, CXP 14 V, CE 33 V); compound 246, 246:202 (DP 60 V, CXP 10 V, CE 25 V); compound 551, 551:244 (DP 60 V, CXP 10 V, CE 40 V); and compound 553, 553:246 (DP 60 V, CXP 10 V, CE 25 V).

For each analyte, the area of the intensity vs. time peak was integrated. For ET and GSSG, linear calibration curves were constructed (weighting $1/y^2$) from six standards which were prepared using the solvent of the respective experiment. Sample analyte content was calculated from the analyte peak area and the slope of the calibration curve.

2.3. Calculations and statistics

All assays were performed at least three times on separate days. Results are presented, if not indicated otherwise, as the arithmetic mean ± SEM with at least n = 3. For the data shown in Fig. 4, the slopes from linear regression were compared (in 2 groups each, control and sample) using GraphPad Prism version 8.0.1 for macOS, GraphPad Software, San Diego, California, USA. The *P* values (two-tailed) indicate the chance that randomly selected data points would have slopes as different as (or more different than) observed. *P* values < 0.05 were considered significant.

Density functional theory (DFT) computations were performed with the Gaussian 16 package [29]. All minima and transition structures were fully optimized and characterized by frequency computations using the B3LYP/6-31G*-GD3-BJ method. Gibbs-energies (unscaled, 298.150 K, 1 bar) were employed to assess relative stabilities and reaction barriers.

2.4. Materials

Commercial compounds (from Sigma-Aldrich, Munich, Germany, unless noted otherwise) used include: L-ascorbic acid (A92902), L-Cysteine Separopore 6B-CL (201811581, bioWORLD, Dublin, OH, USA), L-dehydroascorbic acid (261556), deuterium oxide (151882), 1,3-dihydro-2H-imidazol-2-one (sc-357477A, Santa Cruz Biotechnology, Heidelberg, Germany), L-(+)-ergothioneine (THD-201, Tetrahedron, Vincennes, France), glutathione (G4251), 1H-imidazole-2-thiol (OR8823, Apollo Scientific, Cheshire, United Kingdom), methimazole (M8506), 4-methyl-1H-imidazole-2-thiol (ST02626, Synthon Chemicals, Bitterfeld-Wolfen, Germany), 3-(5-oxo-2-thioxo-4-

imidazolidinyl)-propanoic acid (CDS002303), L-serine (S4500), L-Serine Separopore 6B-CL (201811621, bioWORLD), and 2-thiohydantoin (T30406). All other chemicals were at least of analytical grade.

3. Results

Ergothioneine (ET) at 10 μM was rapidly oxidized in buffered water by singlet oxygen ($^1O_2$), generated by the thermolysis of $DHPNO_2$ at 37 °C. Addition of 10 mM glutathione (GSH) largely prevented the decline of ET (Fig. 1A). We have shown previously that compound 246:143 is generated much faster than other products made from ET and $^1O_2$ [20]. To avoid an interference from GSH at > 5 mM, we have measured this compound by SRM as 246:202 here. In the control, the content of 246:202 followed the decrease of ET over time (Fig. 1B). In the presence of GSH, 246:202 was reduced. This could indicate that GSH reacts with 246:202 or diminishes the generation of 246:202. If GSH would merely capture most of the $^1O_2$ in this experiment, then all compounds made from ET and $^1O_2$ should decline strongly at high GSH. This was not the case for compounds 264 (Fig. 2B) and 246:202 (Fig. 2C) up to a 1000-fold excess of GSH over ET. Fig. 2A shows the accumulation of compounds 551 and 553 as a function of GSH concentration; both compounds are reaction products of ET and $^1O_2$ and GSH [20] (see Fig. 3 for structures). Compound 551 predominates at low GSH concentrations (0.1–1.0 mM), but disappears at 10 mM GSH or higher. By contrast, the generation of compound 553 depends on higher GSH concentrations; it accumulates maximally around 10 mM GSH and then declines. These profiles suggest that compound 551 reacts with GSH if available in sufficient amounts. The generation of compound 553 probably follows the transformation of 551; it is less efficient than the generation of compound 551, since 100-fold higher GSH levels are necessary. The decline of 553 at very high GSH could mean that this compound also reacts with GSH. Based on the above and our previous findings, a circular reaction scheme (Fig. 3) was devised that defines the regeneration of ET. Supplementary Fig. 1 shows the detailed reactions, with transition states and activation energies from DFT computations.

The proposed regeneration cycle consumes 4 molecules of GSH and generates 2 molecules of oxidized glutathione (GSSG) and 2 molecules of water per turn. The production of GSSG was measured by LC-MS/MS. In control assays made of 10 mM $DHPNO_2$ and 10 mM GSH, the production of GSSG at 37 °C in the time range of 3–12 min was low, at 0.6 ± 1.3 μM min^{-1}. Addition of 1 mM ET markedly increased the production of GSSG to 14 ± 4 μM min^{-1}. When water was replaced by D_2O, both rates increased strongly, because of longer $^1O_2$ life time, to 4.5 ± 1.1 μM min^{-1} (control) and 125 ± 14 μM min^{-1} (+ET). The ratio of rates was similar in H_2O (f = 26) and D_2O (f = 28).

In the GSSG generation assay, ET was compared to several other compounds (Fig. 4). In every experiment, assays with (average relative rate = 1 ± 0.13) and without ET (control, 0.03 ± 0.02) were performed in parallel. It was verified that 10 mM GSH plus 1 mM ET without $DHPNO_2$ hardly generate GSSG (Fig. 4B, rightmost bar). Addition of L-histidine had no effect (0.02 ± 0.04). Stimulation by ascorbic acid (AA) was relatively small (0.15 ± 0.02). After subtraction of the control, ET produced 8 times more GSSG than AA. The regeneration of AA from dehydroascorbic acid (DHA) generates only 1 GSSG per cycle [30]. Thus, under the assumption that losses of AA (from DHA hydrolysis) and ET (from side reactions) are roughly similar, ET reacted at least 4-fold faster than AA with $^1O_2$. If it would take more time to complete the ET cycle than the AA cycle, then the difference would be even greater. The ring of ET, 1,3-dihydroimidazole-2-thione (DHIT), was working exactly as good as ET, as was the 4-methyl ET ring (Fig. 4B). Methylation of the ET ring on one of the 2 nitrogens (drug names: INN thiamazole, USAN methimazole) halved GSSG production (0.58 ± 0.09). Substitution in the ET ring of sulfur with oxygen markedly reduced GSSG generation (0.29 ± 0.08). With 2-thiohydantoin, the GSSG production (0.05 ± 0.03) was on the control level.

The generation of GSSG as a function of GSH concentration could be described by a simple hyperbola (Fig. 5). The half-maximal rate was at 1.8 mM (95% confidence interval, 1.5–2.2).

To prove regeneration of ET, we tried to capture reaction intermediates by means of thiol groups attached to an insoluble matrix. Low background binding of ET was obtained with cross-linked agarose beads that carry L-cysteine covalently linked via its amino group. In the assays, ET was incubated with and without $DHPNO_2$ in the presence of the beads, which were then transferred to mini-columns for washing and elution. After washing, removal of unbound original ET was complete, since the buffer eluates contained no ET (Fig. 6). Without $^1O_2$ in the initial reaction, little ET was released from the columns by GSH. When $^1O_2$ had been present, however, a large amount of ET was released by washing with GSH. This suggests that products from the reaction of ET and $^1O_2$ were indeed captured by the beads. Addition of GSH, but not of serine, stimulated further reaction towards ET. In parallel controls, beads with L-serine ligands also captured some reaction intermediates, but the amount of ET released from Cys beads was almost 3-fold higher than from Ser beads (after subtraction of the background in $^1O_2$-negative assays). These data strongly suggest that ET is indeed regenerated from Cys-attached intermediates by the thiol GSH.

4. Discussion

Numerous functions have been proposed for ET; most of these are related to reactive oxygen species (ROS). However, no mechanism for the complete regeneration of ET after a reaction with a ROS has ever been uncovered. If a specific reaction of ET has continual antioxidative

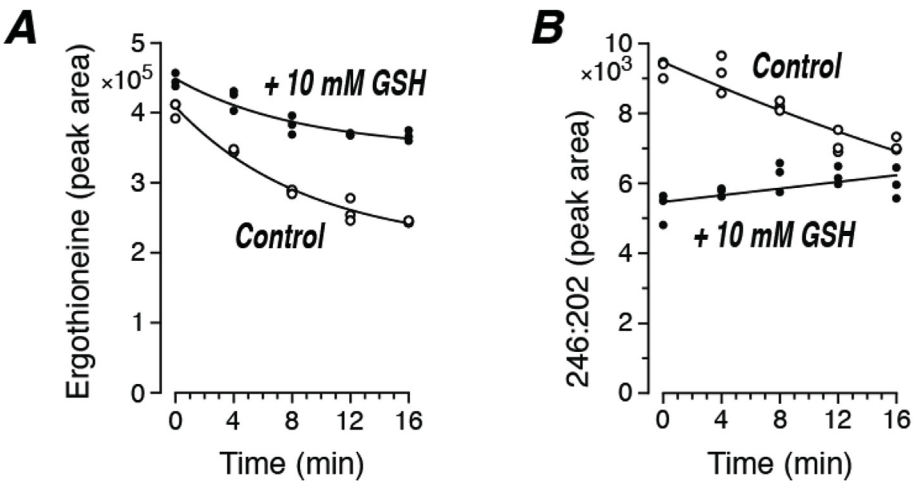

Fig. 1. Addition of GSH diminishes the loss of ET in the reaction with $^1O_2$. 10 μM ET and 10 mM $DHPNO_2$ without (control) or with 10 mM GSH in 10 mM ammonium hydrogen carbonate, pH 7.4, were incubated (V = 50 μl) for the indicated times at 37 °C. Samples were diluted 1:10 with buffer and analyzed directly by LC-MS/MS for ET and compound 246:202. Exponential decay functions and linear regression (GSH in B) were used to describe the data.

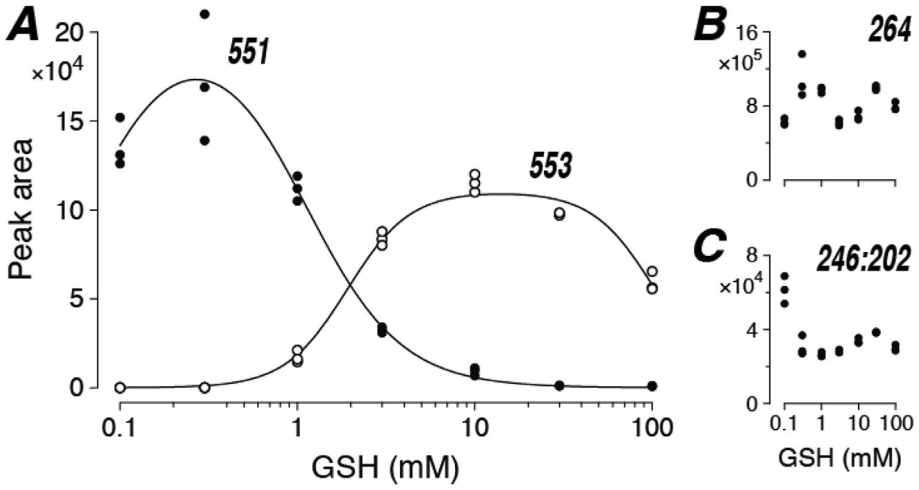

Fig. 2. Generation of products 551 and 553 from the reaction of ET + $^1O_2$ + GSH as a function of GSH concentration. 100 µM ET, 10 mM $DHPNO_2$, and GSH as indicated in 10 mM ammonium hydrogen carbonate, pH 7.4, were incubated (V = 100 µl) for 10 min at 37 °C. Samples were diluted 1:10 and analyzed directly by LC-MS/MS for the analytes 551, 553, 264, and 246:202. Results from a single experiment are shown; each dot represents a sample.

relevance, then there must be regeneration. Here we report a non-enzymatic multi-step cycle for the regeneration of ET after reaction with $^1O_2$. Four molecules of GSH are used per turn to detoxify $^1O_2$ to water. The cycle itself operates without loss, but in our in vitro assays the recovery of ET was slightly reduced by side reactions. Further experiments are required to confirm our findings in living cells, to verify that ET cannot be regenerated after reaction with the other ROS species, and to examine the relevance for humans. It is also unclear at present whether the 2 proposed [20] alternative initial reactions between ET and $^1O_2$ have any relevance compared to the large flow of ET through the cycle shown here.

The data of Fig. 4 strikingly demonstrate (and provide a meaningful answer to our fundamental question from the Introduction) why GSH is no substitute for ET in the reaction with $^1O_2$: there was little production of GSSG from 10 mM GSH (control), although GSSG accounts for 63% of the $^1O_2$ reaction products [31]. In previous reports, GSH and other cysteine-based thiols were also less reactive towards $^1O_2$ than ET, but the difference was not as marked as in our work: f, the ratio of rate constants for ET and GSH, was 13 [31] or 3 (at pH 7.4; GSH was represented here by 2-mercaptopropionyl glycine) [32], whereas our GSSG generation data (Fig. 4) suggest f ≈ 30/2 * 10 = 150. The methods used were very different to our methods: both groups have measured chemiluminescence at 1270 nm, a readout that is proportional to the available $^1O_2$. Sies and coworkers [31] determined their rate constants from Stern-Volmer plots that in turn were based on two points only, the initial steady-state chemiluminescence (= S_0) and the

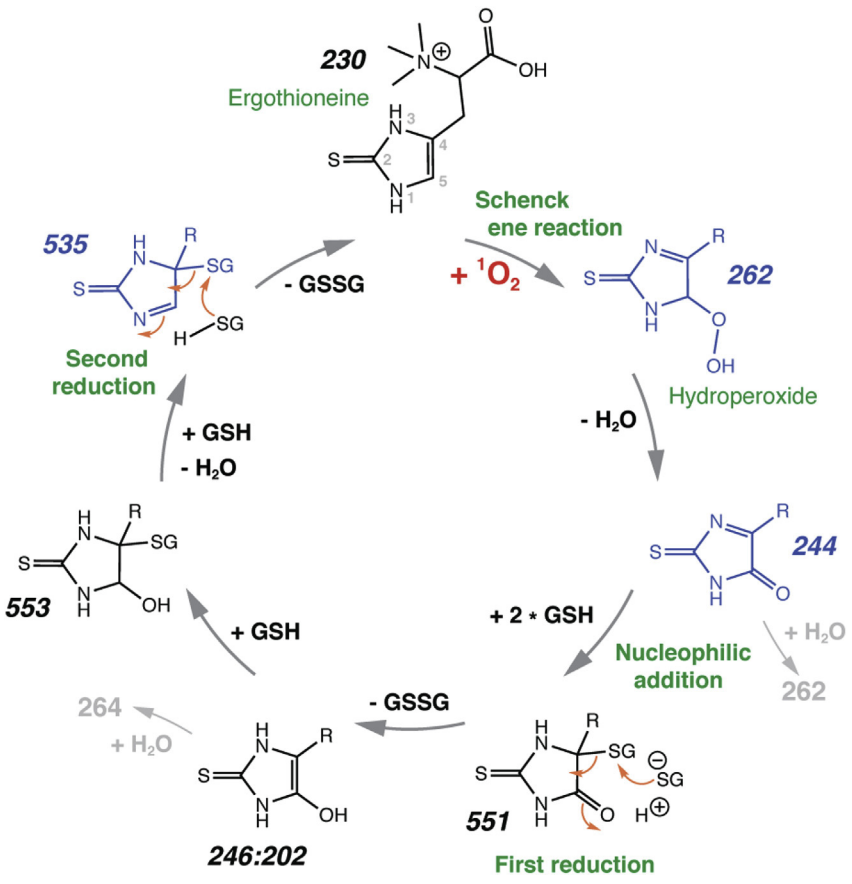

Fig. 3. Regeneration of ET after reaction with singlet oxygen. The simplified scheme (cf. Supplementary Fig. 1) shows products that were detected by LC/MS (black), proposed reaction intermediates (blue), and potential side reactions (grey). The *m/z* values (italic numbers) correspond to acidic LC conditions. R represents the amino acid moiety shown for ergothioneine. (For interpretation of the references to colour in this figure legend, the reader is referred to the Web version of this article.)

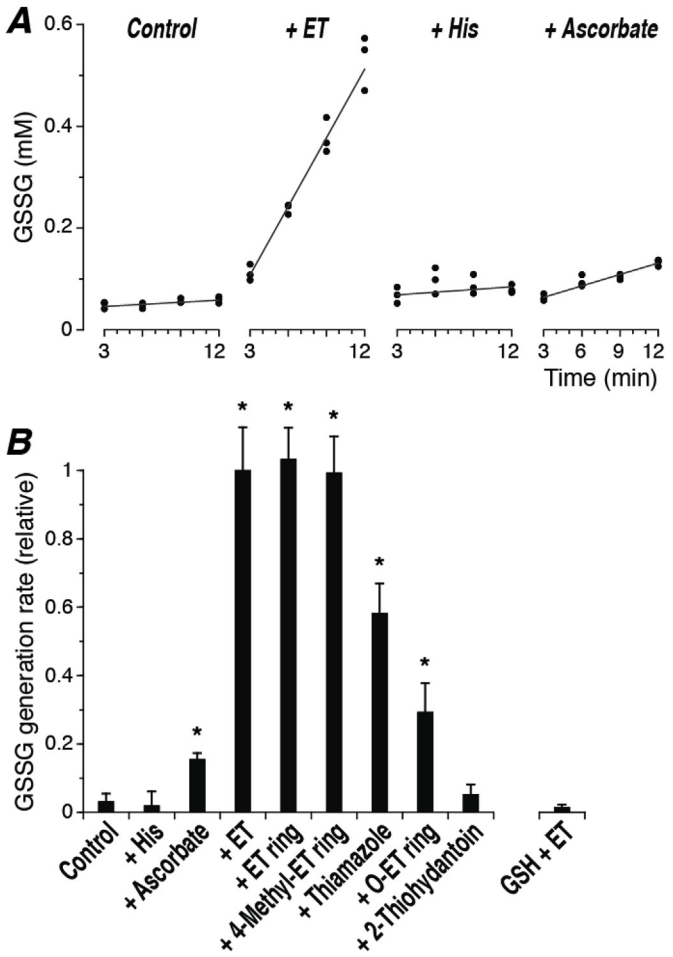

Fig. 4. GSSG generation assays. All assays contained 10 mM GSH and 10 mM $DHPNO_2$ in D_2O. Further compounds were added as indicated to a final concentration of 1 mM. Samples were incubated at 37 °C for 3–12 min, diluted 1:100, and then analyzed directly by LC-MS/MS for GSSG content. (A) Representative results from a single experiment; each dot represents a sample. Data were analyzed by linear regression; the slopes approximate initial GSSG production rates. Since the rate of $^1O_2$ generation from $DHPNO_2$ decreases with a half-life of 23 min, an exponential function ($n = n_{max} * (1 - \exp(- \lambda *t))$) would be more correct; the deviation from linearity is very slight, however, in the chosen time intervall (not shown). (B) Combined results from several experiments. Rates were normalized to the GSSG generation rate in the presence of ET and then averaged (n = 3 or 4). Note that the rightmost bar, GSH + ET, shows an additional control where 10 mM GSH plus 1 mM ET were incubated without $DHPNO_2$. Error bars indicate the SEM; an asterisk denotes that the slope of the sample group was significantly different from the respective control group.

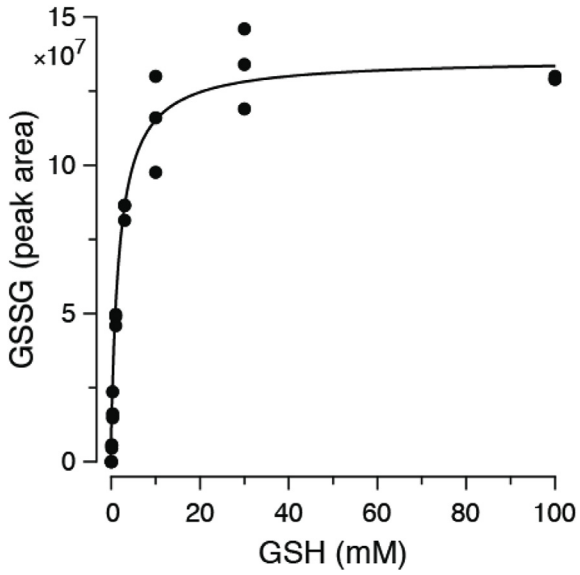

Fig. 5. Generation of GSSG as a function of GSH concentration. Assays contained 0.1 mM ET, 10 mM ammonium hydrogen carbonate pH 7.4, 10 mM $DHPNO_2$, and GSH as shown. Samples were incubated for 10 min at 37 °C and then analyzed directly by LC-MS/MS for GSSG content. Results from a single experiment are shown; each dot represents a sample. The data were analyzed by non-linear regression, using a hyperbola function analogous to the Michaelis-Menten equation.

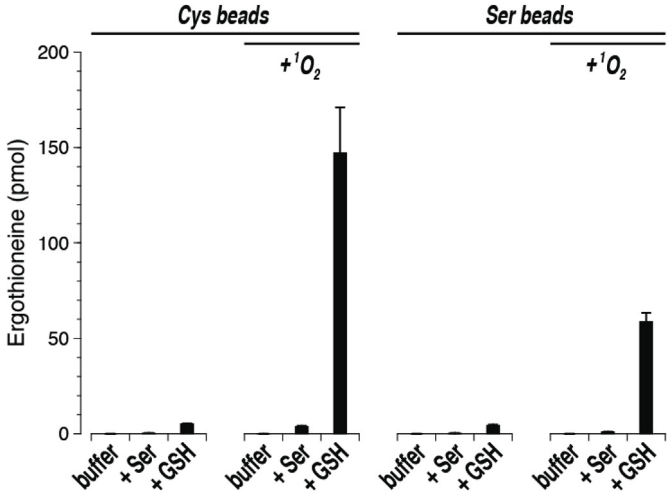

Fig. 6. GSH regenerates ET from reaction products of ET and $^1O_2$ captured by cysteine agarose beads. In polypropylene reaction tubes (72.690.001, Sarstedt, Nümbrecht, Germany), 1 mM ET ± 10 mM $DHPNO_2$ in 10 mM ammonium hydrogen carbonate pH 8.0 buffer (V = 50 µl) was mixed with 100 µl of sedimented Cys beads (Separopore 6B-CL, bioWORLD, Dublin, OH, USA; particle size range, 52–180 µm; approx. 4 nmol L-cysteine per µl of gel; this corresponds to an 8-fold molar excess of thiol groups vs. ET); 0.1 mM GSH was present to diminish disulfide formation between ET and the Cys ligands (not shown). The assays were incubated for 10 min at 37 °C on a shaker (1200 rpm), then the beads were transferred into polypropylene microliter tips (70.762.010, Sarstedt, Nümbrecht, Germany) and onto a small cotton plug. After 3 washes each with 500 µl of 100 mM NaCl buffer, the following solutions were applied in succession to the column (100 µl each, at room temperature): buffer, 10 mM L-serine in buffer, and 10 mM GSH in buffer. The eluates were directly analyzed by LC-MS/MS for ET content. Data shown are median ± median absolute deviation.

end-point chemiluminescence (= S), after all ET or thiol had reacted (Figs. 1 and 2 in the cited reference). This method did not monitor initial rates of reaction; if ET reacts further with initial ET-$^1O_2$ products as suggested by our work, then the reactivity of ET will be underestimated. Rougee et al. [32] have used a photosensitizer for $^1O_2$ production; other ROS were generated simultaneously and may have had an impact on the results.

Because of the regeneration cycle, ET must now be viewed as tightly linked with the GSH/GSSG redox couple. The necessary, almost optimal (Fig. 5), foundation (5–10 mM GSH) is present in all mammalian and vertebrate cells [33], and also (GSH and mycothiol) in all species that generate ET, such as cyanobacteria [34], mycobacteria [35], and fungi [36]. When cyanobacteria established the synthesis of ET for the first time [3], built-in auto-regeneration obviated the need to develop an additional regenerative enzyme. It is clear now that ET will work steadily only in concert with GSH; recycling depends on high thiol levels. In the absence of GSH, we expect ET, by its nucleophilic thiol tautomer, to function as a reductant like GSH, thereby creating ET

dimers and consuming itself. However, in the presence of 0.1 mM GSH, ET disulfide formation was completely abolished [20]. In other words, ET must be accompanied by 10 mM GSH in order to sustain its efficacy against $^1O_2$.

The regeneration of ET by GSH bears some analogy to the non-enzymatic regeneration of ascorbic acid (AA; vitamin C). The oxidized form of AA, dehydroascorbic acid (DHA), is reduced back to ascorbic acid by 2 GSH molecules. The resulting GSSG is then reduced to GSH by NADPH-dependent enzymes [30]. It has been suggested that ascorbate is the most efficient chemical quencher of $^1O_2$. The reaction is rapid, $k = 3 \times 10^8\ M^{-1}\ s^{-1}$ for the reaction of the ascorbate monoanion with $^1O_2$ [37]. The very fast reaction of ascorbate with $^1O_2$ and its high concentration (2–4 mM) in the water space of cells suggested that it could be an important sink for $^1O_2$ in vivo. However, our data indicate that ET is a superior interceptor of $^1O_2$ (Fig. 4A). Judging by the generation of GSSG, the number of ET molecules that reacted with $^1O_2$ was at least 4 times higher than the number of ascorbate molecules. Moreover, the reaction with ET followed by the regeneration cycle completely defuses $^1O_2$. By contrast, the reaction of ascorbate with $^1O_2$ results in, besides DHA, the stoichiometric production of H_2O_2 [38], which poses further oxidative challenge for cells and tissues. Note that in vitro DHA, depending on the reaction conditions, may not be recycled completely [30]. Also in the ET regeneration cycle, some side reactions are possible in vitro, but our results (Fig. 1A) demonstrate that, in the presence of 10 mM GSH, ET levels are largely stable.

It is interesting to estimate the efficiency of ET as an interceptor of $^1O_2$ here. $DHPNO_2$ decays at 37 °C with a half-life of 23 min to release 59% $^1O_2$ [39]. It follows from $N(t) = N_0$ * exp (-lambda *t) and lambda = ln (2)/$t_{1/2}$ that after 12 min, $DHPNO_2$ has decayed by 30% to release 10 mM * 0.30 * 0.59 = 1.8 mM $^1O_2$. With 2 GSSG produced per ET regeneration cycle, it follows from the difference of rates (see Results) that in 12 min in D_2O, 0.72 mM ET was recycled after reaction with $^1O_2$. In other words, an impressive 40% of released $^1O_2$ was quenched chemically by ET. Some, if not all, of the rest was certainly quenched physically (by non-toxic unreactive collisions with the solvent or other molecules).

The GSSG generation assay demonstrates that the aromatic ring of ET (compound DHIT) is fully sufficient for the complete cycle (Fig. 4B); the zwitterionic amino acid backbone is not involved. With thiamazole (= DHIT plus methyl group on one nitrogen), the GSSG production was only at half of the DHIT level. This fits with the Schenck ene reaction (first step) that requires a proton on the nitrogen at position 3. The residual GSSG comes from an attack of $^1O_2$ on the other side of the ring, then using the proton on the position 1 nitrogen. The reaction of the proposed intermediate 244 (Fig. 3) with GSH can be considered as a highly efficient (cf. Fig. 2) nucleophilic addition to the electron-deficient imine substructure. This S=C-N=C (N-thioacyl imine) system resembles α,β-unsaturated ketones in Michael additions [40,41]. Position 4 of the imidazole ring represents a soft electrophilic spot and thus the most likely target for thiols, the softest of the biological nucleophiles [42].

If we explain the drop in 246:202 levels (Fig. 1B) by the reaction of GSH with this compound, then the enol 246:202 is not a side product, but part of the cycle. The corresponding ketone, according to our DFT computations (not shown), is the most stable tautomer. However, the ketone cannot be part of the cycle, because the model compounds 2-thiohydantoin (Figs. 4B) and 3-(5-oxo-2-thioxo-imidazolidin-4-yl)-propionic acid (not shown) failed to drive the production of GSSG. We therefore suggest that the aromatic enol 246:202 is the crucial intermediate to initiate the second reduction (Fig. 3). We presume that the ET ring promotes this step, since a simple enol C=C-OH, like simple C=O functions [42], would not react easily with a thiol under physiological conditions. Because of the higher prevalence of zwitterionic resonance structures with a positive charge on the nitrogens [4], imidazole-2-thiones may activate better (by withdrawing electron density from the C=C bond) than imidazole-2-ones. The 3-fold lower GSSG production by 1,3-dihydroimidazol-2-one (Fig. 4B), with oxygen instead of sulfur, could originate from this step.

It remains uncertain whether GSH prefers position 4 or 5 of the imidazole ring for attachment. Our MS fragmentation data of compound 553 cannot resolve that question [20]. Our DFT computations (see Methods) show that the barriers for the addition of methanethiol to the enol C(4) = C(5)-OH function are similar for the MeS-C-C(H)-OH (38.9 kcal/mol) or HC-C(SMe)-OH (32.9 kcal/mol) products. Since the ET ring (DHIT) was as effective as ET and the 4-methyl ring to drive GSSG production (Fig. 4B), alkyl substitution at position 4 probably does not influence the reaction at this stage. Thus, if there is a preferred attack site, it is governed only by the hydroxyl at position 5, all else being symmetrical in the simple ET ring. The side product 264 (cf. Fig. 3) represents ET with 2 oxygen atoms. This could mean vicinal hydroxyls at positions 4 and 5 [20] or a geminal 5-diol. MS^2 could not distinguish these alternatives, because the observed main fragment at *m/z* 188 is plausible for both variants, representing, after loss of thiourea, either a vicinal enediol or an acrylic acid structure. However, in a MS^3 experiment, the fragment *m/z* 188 yielded a robust fragment at *m/z* 160 (not shown), which must correspond to the loss of CO here. This agrees with the vicinal enediol only. Therefore, compound 264 contains hydroxyls at positions 4 and 5, resulting from an attack of water at position 4 of the enol 246:202. GSH should then, by analogy, attack at position 4; however, we cannot entirely rule out an attack at position 5.

Elimination of water (possibly GSH-assisted) from the MeS-C-C(H)-OH adduct yields a S=C-N=C (N-thioacyl imine) system (compound 535). In the final reduction step, the S=C function helps to accommodate electron density at the imino function.

In conclusion, the ring of ergothioneine (1,3-dihydroimidazole-2-thione) is not only an outstanding reaction partner for singlet oxygen, but it also supports, in concert with a thiol like glutathione, a cycle of regeneration. Four molecules of GSH are used per turn to transform $^1O_2$ to water, without any enzyme involvement. The necessary thiol foundation is present in all species that generate or use ET. Regeneration provides a decisive advantage for ET over other reactive, but non-recoverable, compounds. Our findings substantiate the importance of ET for the eradication of noxious $^1O_2$.

Acknowledgments

This research did not receive any specific grant from funding agencies in the public, commercial, or not-for-profit sectors. We thank Samira Boussettaoui, Simone Kalis, and Kathi Krüsemann for skillful technical assistance. We also thank the computing center of the University of Cologne (RRZK) for providing CPU time on the DFG-funded supercomputer CHEOPS and for support.

Appendix A. Supplementary data

Supplementary data to this article can be found online at https://doi.org/10.1016/j.freeradbiomed.2019.01.043.

References

[1] D.B. Melville, Ergothioneine, in: R.S. Harris, G.F. Marrian, K.V. Thimann (Eds.), Vitamins and Hormones, Advances in Research and Applications, Academic Press, New York and London, 1959, pp. 155–204.
[2] F.P. Seebeck, In vitro reconstitution of mycobacterial ergothioneine biosynthesis, J. Am. Chem. Soc. 132 (19) (2010) 6632–6633.
[3] C. Liao, F.P. Seebeck, Convergent evolution of ergothioneine biosynthesis in cyanobacteria, Chembiochem 18 (21) (2017) 2115–2118.
[4] Y. Rong, A. Al-Harbi, B. Kriegel, G. Parkin, Structural characterization of 2-imidazolones: comparison with their heavier chalcogen counterparts, Inorg. Chem. 52 (12) (2013) 7172–7182.
[5] K. Peckelsen, J. Martens, L. Czympiel, J. Oomens, G. Berden, D. Gründemann, A. Meijer, M. Schäfer, Ergothioneine and related histidine derivatives in the gas phase: tautomer structures determined by IRMPD spectroscopy and theory, Phys. Chem. Chem. Phys. 19 (34) (2017) 23362–23372.

[6] A. Sugihara, K. Uemura, Y. Matsuura, N. Tanaka, T. Ashida, M. Kakudo, Crystal-structure of L-ergothioneine dihydrate, C9H15N3O2S * 2 H2O, Acta Crystallogr. Sect. B Struct. Sci. 32 (Jan15) (1976) 181–185.
[7] M.D. Kalaras, J.P. Richie, A. Calcagnotto, R.B. Beelman, Mushrooms: a rich source of the antioxidants ergothioneine and glutathione, Food Chem. 233 (2017) 429–433.
[8] C. Pfeiffer, T. Bauer, B. Surek, E. Schömig, D. Gründemann, Cyanobacteria produce high levels of ergothioneine, Food Chem. 129 (4) (2011) 1766–1769.
[9] D. Gründemann, S. Harlfinger, S. Golz, A. Geerts, A. Lazar, R. Berkels, N. Jung, A. Rubbert, E. Schömig, Discovery of the ergothioneine transporter, Proc. Natl. Acad. Sci. U.S.A. 102 (2005) 5256–5261.
[10] B.D. Paul, S.H. Snyder, The unusual amino acid L-ergothioneine is a physiologic cytoprotectant, Cell Death Differ. 17 (7) (2010) 1134–1140.
[11] T. Nakamura, K. Yoshida, H. Yabuuchi, T. Maeda, I. Tamai, Functional characterization of ergothioneine transport by rat organic cation/carnitine transporter Octn1 (slc22a4), Biol. Pharm. Bull. 31 (8) (2008) 1580–1584.
[12] P. Bacher, S. Giersiefer, M. Bach, C. Fork, E. Schömig, D. Gründemann, Substrate discrimination by ergothioneine transporter SLC22A4 and carnitine transporter SLC22A5: gain-of-function by interchange of selected amino acids, Biochim. Biophys. Acta Biomembr. 1788 (12) (2009) 2594–2602.
[13] S. Grigat, S. Harlfinger, S. Pal, R. Striebinger, S. Golz, A. Geerts, A. Lazar, E. Schömig, D. Gründemann, Probing the substrate specificity of the ergothioneine transporter with methimazole, hercynine, and organic cations, Biochem. Pharmacol. 74 (2) (2007) 309–316.
[14] D. Gründemann, The ergothioneine transporter controls and indicates ergothioneine activity - a review, Prev. Med. 54 (Suppl) (2012) S71–S74.
[15] D. Nikodemus, D. Lazić, M. Bach, T. Bauer, C. Pfeiffer, L. Wiltzer, E. Lain, E. Schömig, D. Gründemann, Paramount levels of ergothioneine transporter SLC22A4 mRNA in boar seminal vesicles and cross-species analysis of ergothioneine and glutathione in seminal plasma, J. Physiol. Pharmacol. 62 (4) (2011) 411–419.
[16] J. Tschirka, M. Kreisor, J. Betz, D. Gründemann, Substrate selectivity check of the ergothioneine transporter, Drug Metab. Dispos. 46 (6) (2018) 779–785.
[17] I.K. Cheah, B. Halliwell, Ergothioneine; antioxidant potential, physiological function and role in disease, Biochim. Biophys. Acta 1822 (5) (2012) 784–793.
[18] P.E. Hartman, Ergothioneine as Antioxidant, Methods in Enzymology vol 186, Academic Press, 1990, pp. 310–318.
[19] C. Pfeiffer, M. Bach, T. Bauer, J. Campos da Ponte, E. Schömig, D. Gründemann, Knockout of the ergothioneine transporter ETT in zebrafish results in increased 8-oxoguanine levels, Free Radic. Biol. Med. 83 (2015) 178–185.
[20] C. Stoffels, M. Oumari, A. Perrou, A. Termath, W. Schlundt, H.G. Schmalz, M. Schäfer, V. Wewer, S. Metzger, E. Schömig, D. Gründemann, Ergothioneine stands out from hercynine in the reaction with singlet oxygen: resistance to glutathione and TRIS in the generation of specific products indicates high reactivity, Free Radic. Biol. Med. 113 (2017) 385–394.
[21] R.W. Redmond, I.E. Kochevar, Spatially resolved cellular responses to singlet oxygen, Photochem. Photobiol. 82 (5) (2006) 1178–1186.
[22] E. Skovsen, J.W. Snyder, J.D. Lambert, P.R. Ogilby, Lifetime and diffusion of singlet oxygen in a cell, J. Phys. Chem. B 109 (18) (2005) 8570–8573.
[23] P.R. Ogilby, Singlet oxygen: there is indeed something new under the sun, Chem. Soc. Rev. 39 (8) (2010) 3181–3209.
[24] J.L. Ravanat, C. Saint-Pierre, P. Di Mascio, G.R. Martinez, M.H.G. Medeiros, J. Cadet, Damage to isolated DNA mediated by singlet oxygen, Helv. Chim. Acta 84 (12) (2001) 3702–3709.
[25] C. Kiryu, M. Makiuchi, J. Miyazaki, T. Fujinaga, K. Kakinuma, Physiological production of singlet molecular oxygen in the myeloperoxidase-H2O2-chloride system, FEBS Lett. 443 (2) (1999) 154–158.
[26] H. Sies, W. Stahl, Vitamins E and C, beta-carotene, and other carotenoids as antioxidants, Am. J. Clin. Nutr. 62 (6 Suppl) (1995) 1315S–1321S.
[27] T. Nordman, L. Xia, L. Bjorkhem-Bergman, A. Damdimopoulos, I. Nalvarte, E.S. Arner, G. Spyrou, L.C. Eriksson, M. Bjornstedt, J.M. Olsson, Regeneration of the antioxidant ubiquinol by lipoamide dehydrogenase, thioredoxin reductase and glutathione reductase, Biofactors 18 (1–4) (2003) 45–50.
[28] V. Fernandez, L.A. Videla, Biochemical aspects of cellular antioxidant systems, Biol. Res. 29 (2) (1996) 177–182.
[29] M.J. Frisch, G.W. Trucks, H.B. Schlegel, G.E. Scuseria, M.A. Robb, J.R. Cheeseman, G. Scalmani, V. Barone, G.A. Petersson, H. Nakatsuji, X. Li, M. Caricato, A.V. Marenich, J. Bloino, B.G. Janesko, R. Gomperts, B. Mennucci, H.P. Hratchian, J.V. Ortiz, A.F. Izmaylov, J.L. Sonnenberg, Williams, F. Ding, F. Lipparini, F. Egidi, J. Goings, B. Peng, A. Petrone, T. Henderson, D. Ranasinghe, V.G. Zakrzewski, J. Gao, N. Rega, G. Zheng, W. Liang, M. Hada, M. Ehara, K. Toyota, R. Fukuda, J. Hasegawa, M. Ishida, T. Nakajima, Y. Honda, O. Kitao, H. Nakai, T. Vreven, K. Throssell, J.A. Montgomery Jr., J.E. Peralta, F. Ogliaro, M.J. Bearpark, J.J. Heyd, E.N. Brothers, K.N. Kudin, V.N. Staroverov, T.A. Keith, R. Kobayashi, J. Normand, K. Raghavachari, A.P. Rendell, J.C. Burant, S.S. Iyengar, J. Tomasi, M. Cossi, J.M. Millam, M. Klene, C. Adamo, R. Cammi, J.W. Ochterski, R.L. Martin, K. Morokuma, O. Farkas, J.B. Foresman, D.J. Fox, Gaussian 16, Rev. B.01, Wallingford, CT, 2016.
[30] B.S. Winkler, S.M. Orselli, T.S. Rex, The redox couple between glutathione and ascorbic acid: a chemical and physiological perspective, Free Radic. Biol. Med. 17 (4) (1994) 333–349.
[31] T.P. Devasagayam, A.R. Sundquist, P. Di Mascio, S. Kaiser, H. Sies, Activity of thiols as singlet molecular oxygen quenchers, J. Photochem. Photobiol., B 9 (1) (1991) 105–116.
[32] M. Rougee, R.V. Bensasson, E.J. Land, R. Pariente, Deactivation of singlet molecular oxygen by thiols and related compounds, possible protectors against skin photosensitivity, Photochem. Photobiol. 47 (4) (1988) 485–489.
[33] V.I. Lushchak, Glutathione homeostasis and functions: potential targets for medical interventions, J. Amino Acids 2012 (2012) 736837.
[34] K. Narainsamy, S. Farci, E. Braun, C. Junot, C. Cassier-Chauvat, F. Chauvat, Oxidative-stress detoxification and signalling in cyanobacteria: the crucial glutathione synthesis pathway supports the production of ergothioneine and ophthalmate, Mol. Microbiol. 100 (1) (2016) 15–24.
[35] B.M. Cumming, K.C. Chinta, V.P. Reddy, A.J.C. Steyn, Role of ergothioneine in microbial physiology and pathogenesis, Antioxidants Redox Signal. 28 (6) (2018) 431–444.
[36] K.J. Sheridan, B.E. Lechner, G.O. Keeffe, M.A. Keller, E.R. Werner, H. Lindner, G.W. Jones, H. Haas, S. Doyle, Ergothioneine biosynthesis and functionality in the opportunistic fungal pathogen, Aspergillus fumigatus, Sci. Rep. 6 (2016) 35306.
[37] R.H. Bisby, C.G. Morgan, I. Hamblett, A.A. Gorman, Quenching of singlet oxygen by Trolox C, ascorbate, and amino acids: effects of pH and temperature, J. Phys. Chem. 103 (37) (1999) 7454–7459.
[38] G.G. Kramarenko, S.G. Hummel, S.M. Martin, G.R. Buettner, Ascorbate reacts with singlet oxygen to produce hydrogen peroxide, Photochem. Photobiol. 82 (6) (2006) 1634–1637.
[39] C. Pierlot, J.M. Aubry, K. Briviba, H. Sies, P. Di Mascio, Naphthalene endoperoxides as generators of singlet oxygen in biological media, Methods Enzymol. 319 (2000) 3–20.
[40] D.P. Nair, M. Podgorski, S. Chatani, T. Gong, W.X. Xi, C.R. Fenoli, C.N. Bowman, The thiol-michael addition click reaction: a powerful and widely used tool in materials chemistry, Chem. Mater. 26 (1) (2014) 724–744.
[41] Y.P. Sun, H. Liu, L. Cheng, S.M. Zhu, C.F. Cai, T.Z. Yang, L. Yang, P.T. Ding, Thiol Michael addition reaction: a facile tool for introducing peptides into polymer-based gene delivery systems, Polym. Int. 67 (1) (2018) 25–31.
[42] T.W. Schultz, J.W. Yarbrough, E.L. Johnson, Structure-activity relationships for reactivity of carbonyl-containing compounds with glutathione, SAR QSAR Environ. Res. 16 (4) (2005) 313–322.

Free Radical Biology and Medicine 113 (2017) 385–394

Contents lists available at ScienceDirect

Free Radical Biology and Medicine

journal homepage: www.elsevier.com/locate/freeradbiomed

Original article

Ergothioneine stands out from hercynine in the reaction with singlet oxygen: Resistance to glutathione and TRIS in the generation of specific products indicates high reactivity

Christopher Stoffels[a], Mhmd Oumari[a], Aris Perrou[a], Andreas Termath[b], Waldemar Schlundt[b], Hans-Günther Schmalz[b], Mathias Schäfer[b], Vera Wewer[c], Sabine Metzger[c], Edgar Schömig[a], Dirk Gründemann[a,*]

[a] Department of Pharmacology, University of Cologne, Gleueler Straße 24, 50931 Cologne, Germany
[b] Department of Chemistry, University of Cologne, Greinstraße 4, 50939 Cologne, Germany
[c] MS-Platform Biocenter, Cluster of Excellence on Plant Science (CEPLAS), University of Cologne, Zülpicher Straße 47b, 50674 Cologne, Germany

ARTICLE INFO

Keywords:
Ergothioneine
Singlet oxygen
Glutathione
LC-MS
Antioxidant
Imidazole
Hydroperoxide

ABSTRACT

The candidate vitamin ergothioneine (ET), an imidazole-2-thione derivative of histidine betaine, is generally considered an antioxidant. However, the precise physiological role of ET is still unresolved. Here, we investigated *in vitro* the hypothesis that ET serves specifically to eradicate noxious singlet oxygen ($^1O_2$). Pure $^1O_2$ was generated by thermolysis at 37 °C of *N,N'*-di(2,3-dihydroxypropyl)-1,4-naphthalenedipropanamide 1,4-endoperoxide ($DHPNO_2$). Assays of $DHPNO_2$ with ET or hercynine (= ET minus sulfur) at pH 7.4 were analyzed by LC-MS in full scan mode to detect products. Based on accurate mass and product ion scan data, several products were identified and then quantitated as a function of time by selected reaction monitoring. All products of hercynine contained, after a [4 + 2] cycloaddition of $^1O_2$, a carbonyl at position 2 of the imidazole ring. By contrast, because of the doubly bonded sulfur, we infer from the products of ET as the initial intermediates a 4,5-dioxetane (after [2 + 2] cycloaddition) and hydroperoxides at position 4 and 5 (after Schenck ene reactions). The generation of single products from ET, but not from hercynine, was fully resistant to a large excess of tris (hydroxymethyl)aminomethane (TRIS) or glutathione (GSH). This suggests that $^1O_2$ markedly favors ET over GSH (at least 50-fold) and TRIS (at least 250-fold) for the initial reaction. Loss of ET was almost abolished in 5 mM GSH, but not in 25 mM TRIS. Regeneration of ET seems feasible, since some ET products – by contrast to hercynine products - decomposed easily in the MS collision cell to become aromatic again.

1. Introduction

Ergothioneine (ET) is a natural compound that humans and other vertebrates cannot synthesize; it must be absorbed from food. Most of our contemporary food contains very little ET, but many mushrooms [1,2] and cyanobacteria [3] contain around 1 mg/g dried material. After ingestion, ET is rapidly cleared from the circulation and then retained in the body with minimal metabolism. During the biosynthesis of ET, L-histidine is converted to a betaine and a sulfur atom is attached to position 2 of the imidazole ring [1,4]. ET can be considered a derivative of thiourea. Because of the prevailing thione tautomer [5,6], ET has several properties that are markedly different from ordinary thiols like the ubiquitous glutathione (GSH).

Previously, we discovered an ET transporter (ETT; human gene symbol *SLC22A4*) [7]. ETT is a powerful sodium-driven uptake transporter in the plasma membrane [8,9]. Cells lacking ETT do not accumulate ET since phospholipid bilayers are virtually impermeable to this hydrophilic zwitterion. In the human body ETT is strongly expressed in erythrocyte progenitor cells in bone marrow, the small intestine (ileum), trachea, kidney, cerebellum, lung, and monocytes. The ability to absorb, distribute, and retain ET depends entirely on this highly specific transporter [10–13].

Abbreviations: $^1O_2$, singlet oxygen; DHPN, *N,N'*-di(2,3-dihydroxypropyl)-1,4-naphthalenedipropanamide; $DHPNO_2$, DHPN 1,4-endoperoxide; ET, ergothioneine; ETT, ergothioneine transporter; GSH, glutathione; HPLC, high-performance liquid chromatography; HRMS, accurate ion mass measurement at high resolution; LC, liquid chromatography; MS, mass spectrometry; NMR, nuclear magnetic resonance; SRM, selected reaction monitoring; TMPyP, 5,10,15,20-Tetrakis(*N*-methyl-4-pyridyl) – 21,23H-porphyrin tetratosylate; TRIS, tris(hydroxymethyl)aminomethane

* Corresponding author.
E-mail address: dirk.gruendemann@uni-koeln.de (D. Gründemann).

http://dx.doi.org/10.1016/j.freeradbiomed.2017.10.372
Received 25 July 2017; Received in revised form 17 October 2017; Accepted 19 October 2017
Available online 23 October 2017

Case-control studies suggest that polymorphisms in the *SLC22A4* gene are associated with susceptibility to chronic inflammatory diseases, such as Crohn's disease, ulcerative colitis, and type I diabetes [12,14], but it is unknown how these mutations promote disease. The mere existence and evolutionary conservation of ETT imply that ET fulfills a beneficial role, perhaps like a vitamin. In general, ET is considered an intracellular antioxidant [5,14]. However, its precise physiological purpose is still unresolved. Why do we accumulate ET in particular tissues or cells despite a 10-fold excess of GSH, the general antioxidant?

Recently, we have reported that in the skin of unstressed ETT knockout zebrafish, the content of 8-oxoguanine (8OG; alias 8-oxo-7,8-dihydroguanine) was increased 4-fold vs. wild-type [15]. This led to the hypothesis that the specific purpose of ET could be to eradicate noxious singlet oxygen ($^1O_2$).

$^1O_2$ is a member of the ROS (reactive oxygen species) quartet; it is less reactive than the hydroxyl radical, but more aggressive than the superoxide anion and hydrogen peroxide [16]. This translates into a relatively long intracellular half-life ($t_{1/2} \approx 3$ μs) [17]. The radius of the sphere of activity of $^1O_2$ from its point of intracellular production was estimated at 155 nm [18]. While the hydroxyl radical reacts with almost anything, $^1O_2$ is selective about its reaction partner. For example, the hydroxyl radical attacks all 4 DNA bases, but $^1O_2$ confines itself to guanine [19]. In guanine, $^1O_2$ reacts via [4+2] cycloaddition with the imidazole ring to create a 4,8-endoperoxide, an 8-hydroperoxide and, after reduction, an 8-carbonyl [20,21]. Interestingly, a doubly bonded oxygen (carbonyl group) at position 2 of the imidazole ring stimulates reactivity very much: 8OG - which bears obvious similarity in the imidazole ring with ET - reacts at least 100-fold faster with $^1O_2$ than guanine [22].

In the human body, $^1O_2$ can be generated by sunlit photosensitizers in skin and eye. It is clear from the rare human disorder erythropoietic protoporphyria that sunlight does also impinge on erythrocytes in circulating blood, a major site of ET accumulation in all vertebrates. Symptoms include itching, severe pain, swelling, and skin ulcers. Here, sunlight drives $^1O_2$ production from protoporphyrin IX, the iron-free precursor of heme. Binding of Fe^{2+} to the porphyrin ring blocks $^1O_2$ production almost completely [23]. However, if only a small fraction of heme in erythrocytes was degraded to iron-free porphyrin, deleterious $^1O_2$ would be produced. Alternatively, even intact hemoglobin may generate singlet oxygen, because of its peroxidase activity [24–26]. Peroxidases such as myeloperoxidase, eosinophilic peroxidase, lactoperoxidase and thyroid peroxidase are closely related heme proteins. They generate $^1O_2$ as a by-product of enzymatic oxygen conversions [27]. In monocytes and macrophages - another site of prominent ET accumulation - peroxidases produce highly reactive defence molecules (respiratory burst). Here, the collateral production of singlet oxygen [28,29] could also cause cellular damage.

Information on the reaction of ET with $^1O_2$ is scarce. Hartman and coworkers reported conflicting results; at least in an assay with rose bengal, ET was a better quencher than azide [30,31]. Other groups have measured that in simple aqueous solution ET reacts faster than GSH with $^1O_2$ [32,33]. To the best of our knowledge, the reaction products of ET and $^1O_2$, if any, are unknown.

Recently, the reaction of ET in aqueous solution with the oxidants hypochlorite (ClO^-), peroxynitrite ($ONOO^-$), and hydrogen peroxide ± myoglobin was investigated [34]. By LC-MS, 3 products were detected: ET disulfide, ET sulfonic acid, and hercynine (= ET minus sulfur). It was hypothesized that hercynine is generated in a pathway involving hydrolysis of ET disulfide.

The aim of our study was to define by LC-MS the products of ET and $^1O_2$ that are generated in aqueous solution at 37 °C and physiological pH. The reactivity of ET towards $^1O_2$ was compared with hercynine. The responses to the addition of TRIS and GSH were used to devise a model of the reaction pathways.

To generate $^1O_2$ in aqueous solution, photosensitizers like rose bengal, methylene blue, or TMPyP [35] are frequently used. The major drawback of this approach is that superoxide anion, hydrogen peroxide, and hydroxyl radical are generated alongside with singlet oxygen, so results can be ambiguous. A brilliant alternative is based on the reversible binding (Diels-Alder addition) of $^1O_2$ to polycyclic aromatic hydrocarbons like naphthalene and anthracene [36]. The resulting endoperoxides are stable in the cold (≤ 4 °C), but release $^1O_2$ (together with some unreactive triplet oxygen) upon mild warming. A very useful

Table 1
Products from the reaction of ET or hercynine with $^1O_2$.

Compound Code	SRM	Assay	Accurate Mass (Da) Delta (mDa)	Peak Top Elution Time (min)	Full Scan Peak Area
230 early	230:171	hercynine + $^1O_2$	230.1133 0.7	6.1	7.1
230 late	230:153	hercynine + $^1O_2$	230.1134 0.6	7.2	4.2
246:229	246:229	hercynine + $^1O_2$	246.1084 0.5	6.2	3.1
246:143	246:143	ET + $^1O_2$	246.0905 0.7	6.6	−1.9
248	248:188	hercynine + $^1O_2$	248.1241 0.5	7.0	6.2
262	262:245	ET + $^1O_2$	262.0854 0.7	5.4	10
264	264:188	ET + $^1O_2$	264.1012 0.6	6.7	1.3
288	288:212	hercynine + $^1O_2$ + 0.1 mM thiourea	288.1120 1.0	8.5	1.0
333	333:274	hercynine + $^1O_2$ + 5 mM TRIS	333.1767 0.7	6.7	29
365 early 365 late	365:230 365:244	ET + $^1O_2$ + 5 mM TRIS	365.1490 0.4	6.8 7.2	combined 13
519	519:460	hercynine + $^1O_2$ + 0.1 mM GSH	519.1863 1.0	7.9	4.4
535	535:228	hercynine + $^1O_2$ + 1 mM GSH	535.1814 0.8	7.8	6.4
551	551:244	ET + $^1O_2$ + 0.1 mM GSH	551.1583 1.0	7.7	1.7
553	553:246	ET + $^1O_2$ + 1 mM GSH	553.1741 0.9	7.9	0.95

All assays contained 100 μM ET or hercynine plus 10 mM $DHPNO_2$. Full scan peak area (in units of 10^6 counts × min) was calculated as the difference of the area under the curve between 60 min and 0 min samples. SRM states parent and fragment masses. Delta, exact mass of proposed compound minus accurate mass.

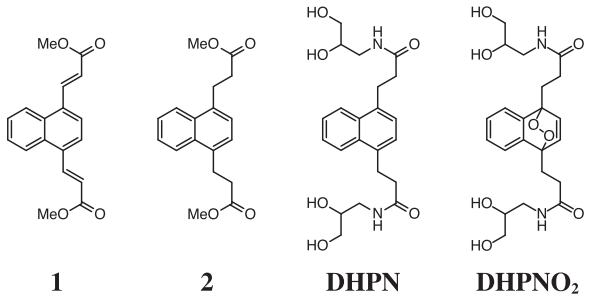

Fig. 1. Synthesis of $DHPNO_2$. Structures of intermediates and products. See Section 2 for details.

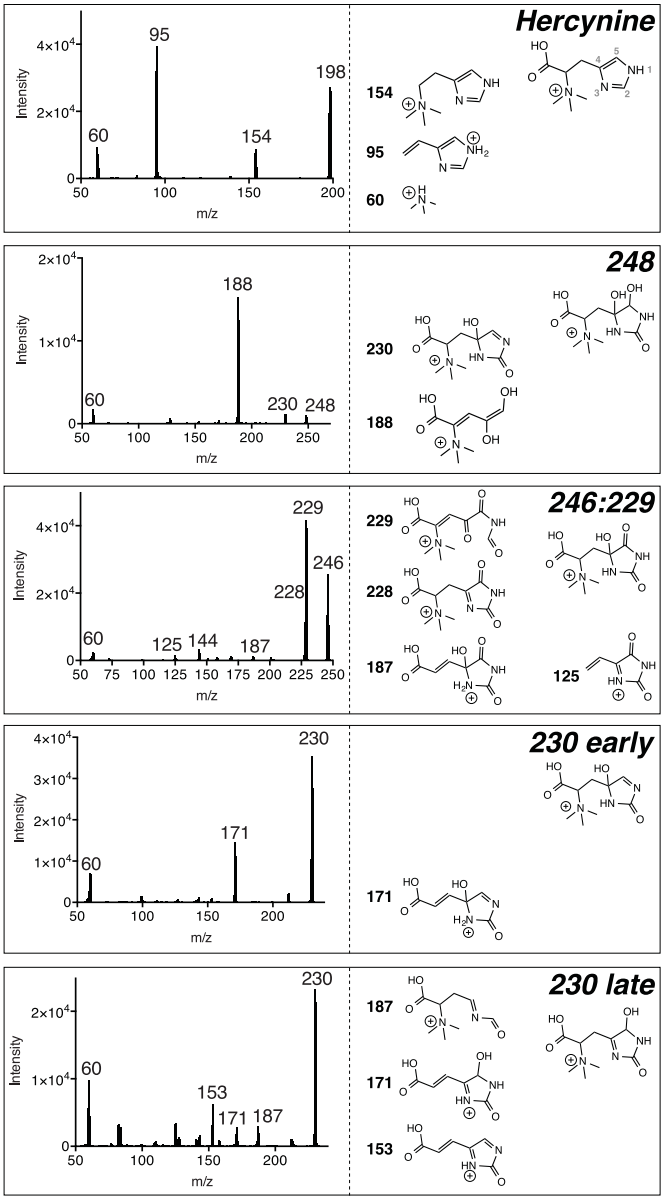

Fig. 2. Products of hercynine and $^1O_2$ in water. For each compound (see Table 1 for compound codes and further details) the product ion spectrum after collision induced fragmentation is shown on the left. Structural interpretations of the main peaks are shown on the right. The imidazole ring numbers are shown for hercynine. A hercynine product at *m/z* 214 was observed by HRMS only (accurate mass = 214.1181 Da; weak fragments at *m/z* 127 and 111) because of high background in the QTRAP machine. With 1-methyl-hercynine, products analogous to the hercynine products were obtained at *m/z* 262, 260, and 244 (not shown).

derivative, developed by Aubry and coworkers [37], is *N,N'*-di(2,3-dihydroxypropyl) − 1,4-naphthalenedipropanamide (DHPN). The corresponding endoperoxide $DHPNO_2$ dissolves well in water (39 mmol/l at 20 °C) and decays with a half-life of 23 min at 37 °C to release 59% $^1O_2$ [36]. Best of all, the non-ionic $DHPNO_2$ can passively penetrate the plasma membrane of living cells to release by thermolysis pure $^1O_2$ in the cytosol [36,37]. In our study, we have used $DHPNO_2$ to ensure the generation of clean $^1O_2$.

2. Material and methods

2.1. Reaction of ergothioneine or hercynine with $^1O_2$

All assays (total volume 100 µl) were incubated in brown polypropylene reaction tubes (72.706.001, Sarstedt, Nümbrecht, Germany) at 37 °C with 100 µM substrate in water. Some assays additionally contained TRIS–HCl pH 7.4 buffer (5 or 25 mM) or GSH (0.1, 1, or 5 mM). Reactions were started by adding ice-cold $DHPNO_2$ stock solution (around 70 mM on average) to a final concentration of 10 or 1 mM. After the indicated times, reactions were stopped by adding 100 µl ice-cold water and then put on ice. Zero time controls were kept on ice throughout. Assays (300 µl) with the photosensitizer TMPyP (100 or 10 µM) were incubated in 12-well polystyrene plates (83.3921, Sarstedt) on a shaker (300 rpm, 20 min, room temperature). UV light was cast 20 cm from above with an upside-down UV table set to 365 nm.

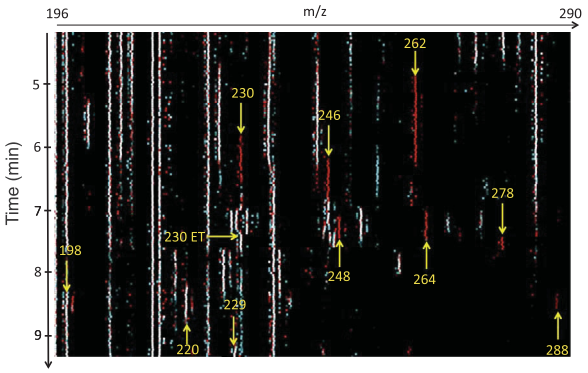

Fig. 3. Difference Shading image of products of ET and $^1O_2$ in water. Notable signals (red indicates an increase, cyan a decrease) are marked with an arrow and the *m/z* value. Sodium echo denotes a (somewhat less intense) peak with an identical elution profile at +22 Da relative to the base signal; this suggests, in the present context, the presence of a carboxyl moiety in the compound. (For interpretation of the references to color in this figure legend, the reader is referred to the web version of this article.)

2.2. LC-MS/MS

10 µl of the ice-cold reactions were immediately analyzed by LC-MS. For HPLC (Shimadzu SLC-20AD Prominence HPLC; flow rate 0.2 ml/min, autosampler temperature 4 °C, oven temperature 35 °C), a ZIC-HILIC column (5 µm, 2.1 × 100 mm; Dichrom, Marl, Germany) was used with the following gradient: A: 0.1% formic acid, B: 0.1% formic acid in acetonitrile; gradient flow: 90% B at 0 min, 90% B at 0.5 min, 10% B at 9 min, 10% B at 10 min, 90% B at 14 min, and 90% B at 15 min. At the interface to the triple quadrupole mass spectrometer (4000 Q TRAP, AB Sciex, Darmstadt, Germany), ions were generated by atmospheric pressure ionization with positive electrospray (ESI).

LC-MS difference shading [7] was used to search robustly for reaction products. In order to compare two samples, e.g. reaction mixtures after 0 and 60 min, full scan data (50–650 Da; declustering potential (DP) 60 V, entrance potential 10 V) were collected on Q1. Then, two gray scale images with axes of *m/z* and time were generated, in which the lowest intensities are rendered black (red green blue model: 0, 0, 0) and the highest intensities are rendered white (255, 255, 255). Finally, a difference image was created, combining for each pixel the red component of the 60 min image with green and blue of the zero time image. Thus, newly made compounds can be spotted as red signals (e.g., 64, 0, and 0), while compounds present in equal amounts in both sets remain in gray tones (e.g., 100, 100, and 100).

Fragmentation by collision with nitrogen on Q2 was used to record product ion spectra (DP 60 V, entrance potential 10 V, collision energy (CE) 25 V, collision cell exit potential (CXP) 10 V). The *m/z* values of parent and fragment used for analyte quantification (SRM, selected reaction monitoring [38]; scan time 150 ms; DP 60 V; CXP 10 V; CE 25 or 30 V) are mostly listed in Table 1. ET dimer, SRM 229:185; ET sulfonic acid, SRM 278:154; hercynine, SRM 198:95; thiourea, SRM 77:60. SRM with DP 41 V and CXP 8 V: ET, SRM 230:127, CE 27 V; compound

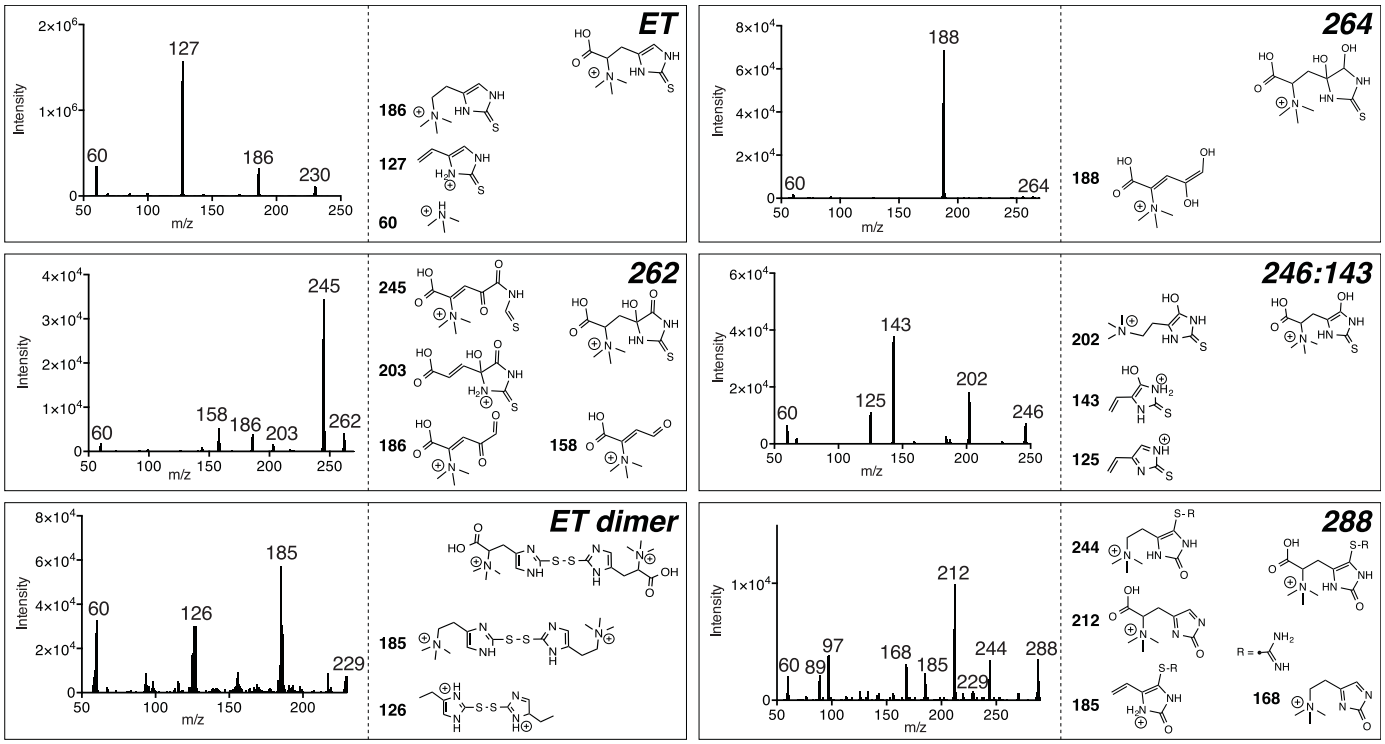

Fig. 4. Products of ET and $^1O_2$ in water. See legend to Fig. 2 and Table 1 for further details. The signal at *m/z* 60 is thought to represent trimethylammonium for all compounds.

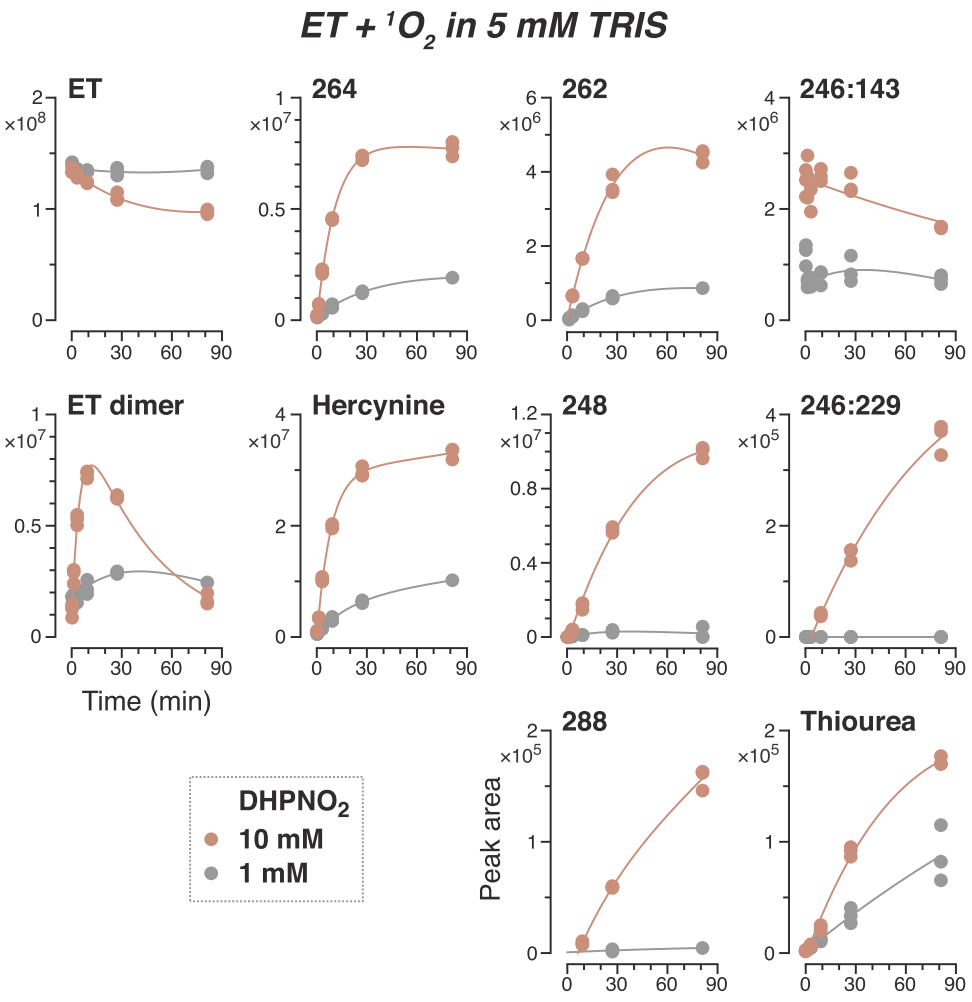

Fig. 5. Relative compound levels as a function of time in assays with ET and $^1O_2$ in 5 mM TRIS. Peak areas were determined by SRM as defined in Table 1. $^1O_2$ was generated from 1 or 10 mM $DHPNO_2$. Each symbol represents a single measurement.

248, CE 15 V; compound 288, CE 25 V. For each analyte, the area of the intensity vs. time peak was integrated.

2.3. Accurate mass LC/MS

Samples were analyzed by quadrupole time-of-flight mass spectrometry and MS/MS on a maXis 4 G instrument (Bruker Daltonics, Bremen, Germany) equipped with an electrospray ionization source, after HPLC separation on a Dionex HPG 3200 system (Thermo Scientific, Dreieich, Germany) as described above. The mass spectrometer was operated in positive-ion mode with the following operating conditions: dry gas (nitrogen): 8 l/min, dry heater: 220 °C, nebulizer pressure: 1.8 bar, capillary voltage: 4500 V. Internal calibration through automation was performed in high precision calibration mode using a reference mass list of sodium formate clusters. The resulting error was below 1 ppm for all reference masses.

2.4. Calculations and statistics

All assays were at least performed three times, on separate days, with 3 replicates per condition. The graphs shown in time courses were estimated by non-linear regression with the function y = scale1 * exp (-kdown * x) - scale2 * exp(-kup * x) where scale1 and scale2 describe maximal deflections and kdown and kup are rate constants. Full scan peak area represents the difference of the area under the curve of 2 samples, e.g. 60 min area minus zero time area in the time interval of peak elution.

2.5. Materials

Ergothioneine (THD-201, Tetrahedron, France), TRIS (AE15.3, Carl Roth, Karlsruhe, Germany), GSH (G4251, Sigma-Aldrich, Munich, Germany), TMPyP (PO890204, Porphyrin Systems, Appen, Germany). All other chemicals were at least of analytical grade.

2.6. Synthesis of hercynine

Hercynine was synthesized from 60 mg α-*N,N*-dimethyl-L-histidine (F3625, Bachem, Bubendorf, Switzerland) and methyl iodide as described [39]. The raw product was dried, dissolved in 1 ml methanol/H_2O/25% (v/v) NH_3 (10:2:1) (= mobile solvent), and applied by gravity flow to a silica gel column (60741, Sigma-Aldrich; length of packed gel cylinder 10 cm, diameter 2.8 cm). Fractions of 2 ml were collected and pooled guided by results from thin layer chromatography (Silica gel 60 F_{254} plastic sheets 20 × 20; 1057350001, Merck, Darmstadt) with iodine staining. The yield of hercynine was 21 mg.

2.7. Synthesis of $DHPNO_2$

A novel 4-step route towards DHPN was developed using a double Heck reaction as the C-C bond forming key step. Products were characterized by FT-IR, ^{1}H NMR, ^{13}C NMR, GC-MS, HRMS, and analytical TLC on Merck silica gel 60 F_{254} plates.

1,4-Dibromonaphthalene was synthesized, based on a published procedure [40], from 1.0 equiv. 1-bromonaphthalene and 1.1 equiv. bromine in dichloromethane at −30 °C under light exclusion and argon. The product was crystallized from n-hexane with an average yield of 70%.

Compound **1** (Fig. 1) was synthesized at 120 °C in dimethylformamide from 1.0 equiv. 1,4-dibromonaphthalene and 2.9 equiv. methyl acrylate in the presence of 2.5 equiv. anhydrous sodium acetate, 0.015 equiv. palladium(II) acetate, and 0.06 equiv. triphenylphosphine. The product was crystallized from n-hexane and ethyl acetate with a yield of 82%.

Compound **2** was obtained by catalytic hydrogenation at room temperature in dichloromethane/methanol (2:1) from 1.0 equiv. of diester **1** and hydrogen gas in the presence of 0.05 equiv. palladium on carbon. After filtration over Celite and solvent evaporation, the yield was > 99%.

DHPN was synthesized, based on patent EP 2551291 A1 (M. Ito and H. Shibata, 2013), at 110 °C in methanol from 1.0 equiv. of diester **2** and 2.3 equiv. 3-aminopropane-1,2-diol in the presence of 0.2 equiv. sodium methoxide. The product was dissolved in water and purified by reversed phase silica column chromatography with a yield of 78%.

$DHPNO_2$ was generated as described [36,41]. In detail, 1.0 g of DHPN was dissolved in 33 ml of 0.2 mg/ml methylene blue in D_2O by slight warming. The solution was filled into an irradiation tube with internal cooling (3 °C) and illuminated for 7 h with a LED lamp (2700 lm, 3000 K; ca. 10 cm distance) under constant O_2 bubbling. After transfer of the mixture to a flask immersed in an ice-water bath, 1.0 g of Chelex ion exchanger was added under stirring and argon bubbling. The suspension was stirred at 4 °C for 20 min and then filtered through a Schott filter (porosity IV). The solid was washed with a

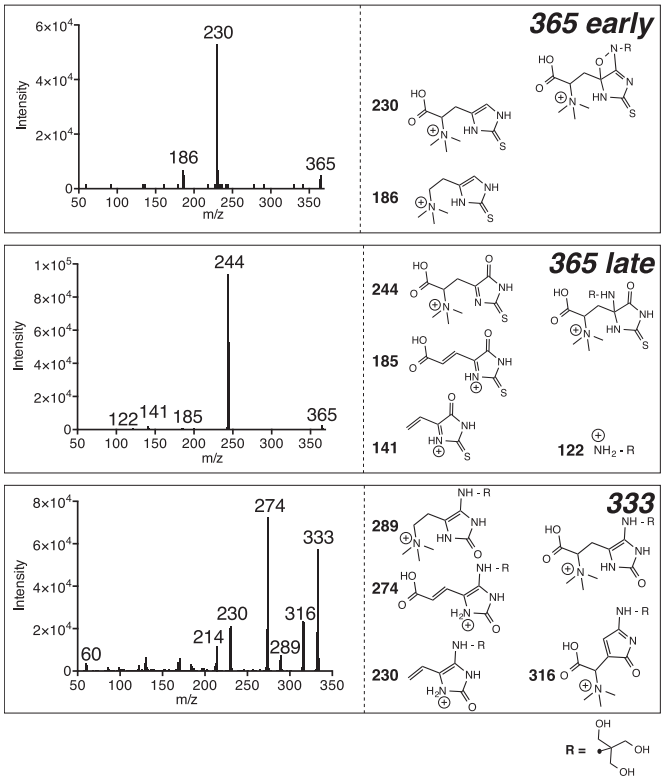

Fig. 6. Products of ET or hercynine and $^1O_2$ made with TRIS. See legend to Fig. 2 and Table 1 for further details.

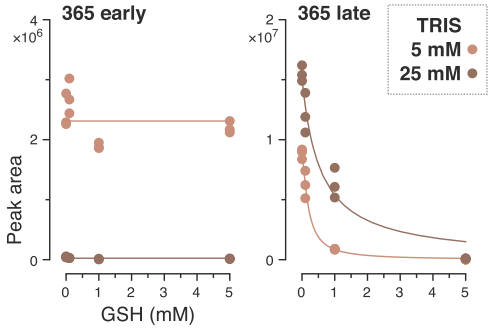

Fig. 7. Relative compound levels as a function of GSH concentration in assays with ET and $^1O_2$ in TRIS. Peak areas were determined by SRM as defined in Table 1. $^1O_2$ was generated from 10 mM $DHPNO_2$; TRIS was used at 5 or 25 mM as indicated.

few ml of D_2O; the combined filtrates were directly frozen in liquid nitrogen. HPLC analysis showed on average 80% conversion of DHPN to $DHPNO_2$.

3. Results

3.1. Reaction products of hercynine and singlet oxygen

100 μM hercynine was incubated at 37 °C with 10 mM $DHPNO_2$ (to generate $^1O_2$) in water. Comparison of 60 min versus zero time control samples by LC-MS difference shading revealed (not shown) products at *m/z* 248, 246, and two products at 230. Plausible structures could be deduced from the respective fragmentation patterns (Fig. 2). Molecular formulas of parent compounds were confirmed by accurate ion mass measurements at high resolution (HRMS). The robust signal at *m/z* 248 (Table 1) thus corresponds to a hercynine derivative with 3 oxygen atoms at positions 2, 4, and 5 of the imidazole ring. Compound 246:229 (Table 1) contains, relative to 248, a carbonyl at position 5. Compound 230 late contains a carbonyl at position 2, a hydroxyl at position 5, and a double bond between positions 3 and 4. Compound 230 early is an isomer of 230 late with the hydroxyl at position 4 and the double bond between positions 1 and 5.

3.2. Reaction products of ergothioneine and singlet oxygen

100 μM ET was incubated at 37 °C with 10 mM $DHPNO_2$ in water. Comparison of 60 min versus zero time control samples by LC-MS difference shading revealed (Fig. 3) intense product peaks (red color) at *m/z* 262 and 264 and additional signals at 248, 246, 230, and 288. The signal at *m/z* 198 (isotope echo at 199; sodium echo at 220; see figure legend) corresponds to hercynine (full scan peak area: 6.0×10^6), the cyan signal at *m/z* 229 to ET disulfide dimer, and the signal at *m/z* 278 to ET sulfonic acid [34].

Based on HRMS and fragmentation data from MS^2 product ion spectra, compound 264 is an ET derivative with 2 hydroxyls at positions 4 and 5 of the ring (Fig. 4). Similarly, compound 262 contains a carbonyl instead of a hydroxyl moiety. Few compounds of this study, like ET and hercynine, show a loss of CO_2 (minus 44) in the fragmentation spectrum. We interpret this to indicate an aromatic ring. Thus, compound 246:143 likely contains an aromatic ring with a hydroxyl at position 5. The products 248 and 230 correspond to the hercynine products described above. Compound 288 was not detected in assays (reaction time 60 min) with 100 μM hercynine and 10 mM $DHPNO_2$; however, a large amount was generated when 100 μM thiourea was added (full scan peak area, calculated here as the area difference between + thiourea and + urea assays: 1.7×10^7). By contrast, no red

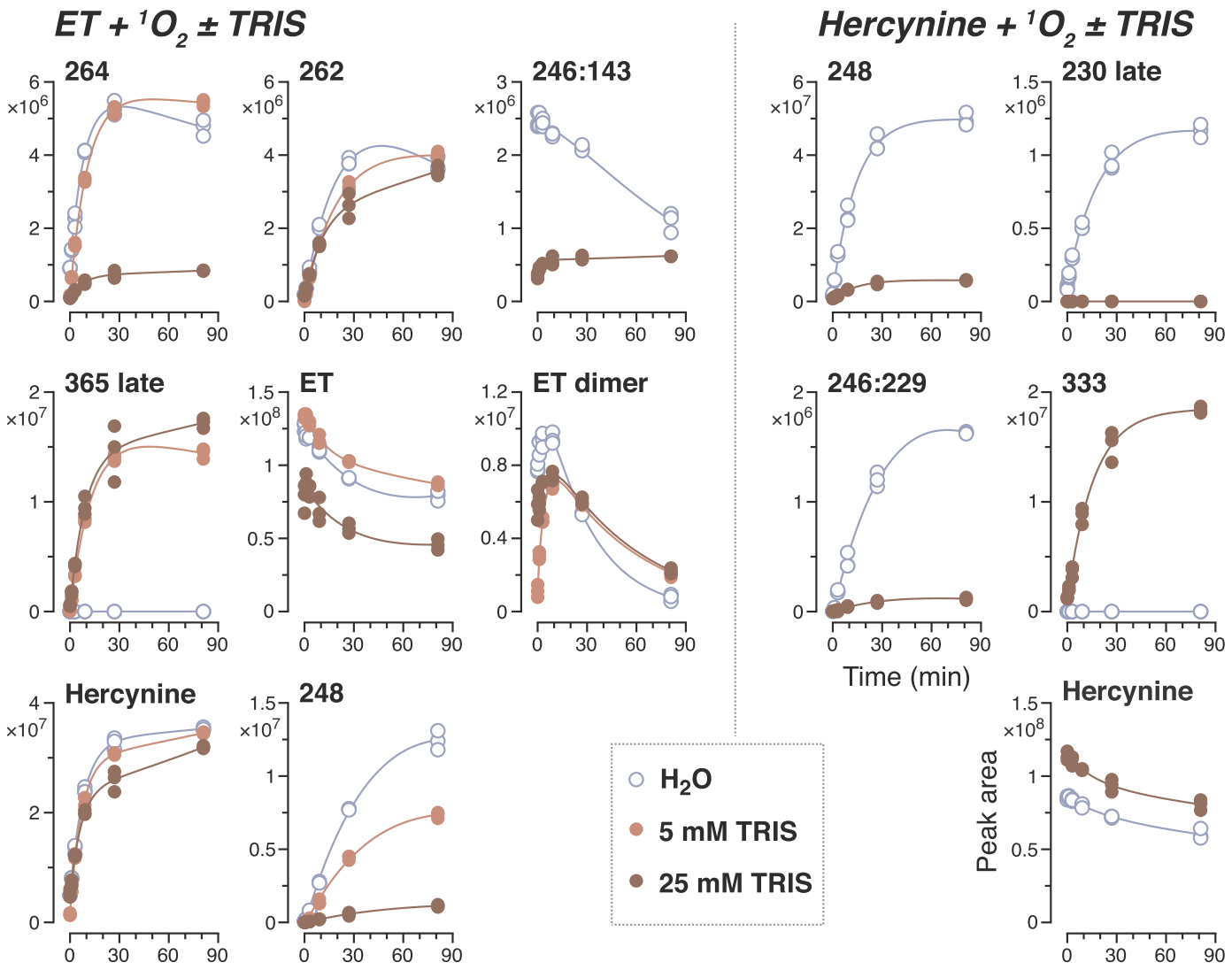

Fig. 8. Relative compound levels as a function of time in assays with ET or hercynine and $^1O_2$ in water ± TRIS. Peak areas were determined by SRM as defined in Table 1. $^1O_2$ was generated from 10 mM $DHPNO_2$. Note that ET peak areas, probably because of ion suppression, were somewhat reduced in the 25 mM TRIS samples.

signals in the range $100 < m/z < 500$ were observed in difference shading when ET + $^1O_2$ + thiourea was compared with ET + $^1O_2$ or with ET + $^1O_2$ + urea.

The above products were also observed when 100 μM ET and 100 μM of the photosensitizer TMPyP were mixed in water and illuminated at 20 °C for 20 min to (predominantly) generate $^1O_2$. These products were not created in the absence of ET or TMPyP. At low $^1O_2$ (10 μM TMPyP), the order of full scan peak areas was 264 > 262 > > 246:143.

The detailed time course of product generation was analyzed by selected reaction monitoring (SRM) (Fig. 5). Here, 100 μM ET and 10 mM $DHPNO_2$ were incubated at 37 °C in 5 mM TRIS to set the pH to 7.4. ET decreased exponentially (measured half-life = 20 min). The compounds 264 and 198 (hercynine) were formed rapidly; the slope of compound 262 was slightly lower. The ET dimer 229 (= disulfide) at first accumulated rapidly but later depletion dominated; the full scan peak area (Fig. 3) was therefore negative: -5.1×10^6. Compound 246:143 was generated even faster, but then also declined. The hercynine product 248 followed the generation of hercynine. With further delay, the hercynine products 246:229 and 288 were generated. The production of all compounds and the depletion of ET were vastly diminished when $DHPNO_2$ was reduced from 10 to 1 mM.

3.3. TRIS intercepts reaction intermediates

In the reactions of $^1O_2$ with ET or hercynine, the generation of some products was inhibited by 25 mM tris(hydroxymethyl)aminomethane (TRIS). At the same time, large peaks for compounds containing TRIS appeared for ET (*m/z* 365) and hercynine (333). Based on HRMS and fragmentation data, the hercynine derivative 333 likely contains (Fig. 6) a stable aromatic ring (judging from the loss of CO_2), an oxygen at position 2, and TRIS probably at position 5. The major fragments of the hercynine derivative 333 suggest that TRIS cannot leave here.

The signal at 365 was resolved to 2 largely overlapping peaks. Compound 365 late broke easily in the collision cell and even in the source of the mass spectrometer, releasing TRIS and a fragment ion at *m/z* 244 (Fig. 6). This compound likely is an ET derivative with TRIS at position 4 and a carbonyl at position 5. Compound 365 early was split almost entirely into TRIS and a fragment ion at *m/z* 230. The latter was identified as ET by disintegration in the ion trap into ions at *m/z* 186 and 127 (compare ET product ion spectrum, Fig. 4). Thus, 365 early is an isomer of 365 late, most likely with interchanged TRIS moiety. Addition of glutathione (GSH) to the ET/TRIS assay (Fig. 7) inhibited the generation of 365 late (IC_{50} at 5 mM TRIS ≈ 0.2 mM). By contrast, production of 365 early was stable.

The detailed time course of generation of products was analyzed by SRM (Fig. 8). Here, 100 μM ET and 10 mM $DHPNO_2$ were incubated in paired assays at 37 °C either in 5 or 25 mM TRIS pH 7.4 or in water. The TRIS product 365 late was generated rapidly and vigorously. The generation of ET product 264, 246:143, and the hercynine product 248 were vastly inhibited by 25 mM TRIS. By contrast, the generation of ET dimer, hercynine, and ET product 262 were hardly affected. In the hercynine assays (Fig. 8), the products 248, 230 late, and 246:229 were strongly reduced by 25 mM TRIS. Again, the TRIS product 333 was generated rapidly and in large amounts.

3.4. Glutathione competition assays

GSH was tested at 0.1, 1, and 5 mM as a reductant and nucleophilic competitor to water in the assays with 100 μM ET and 10 mM $DHPNO_2$. Difference shading revealed small specific peaks at *m/z* 551 and 553. Based on HRMS and fragmentation data, the compound at *m/z* 553 likely is an ET derivative with a hydroxyl at position 5 and GSH at position 4 of the imidazole ring (Fig. 9). Compound 551 contains a carbonyl.

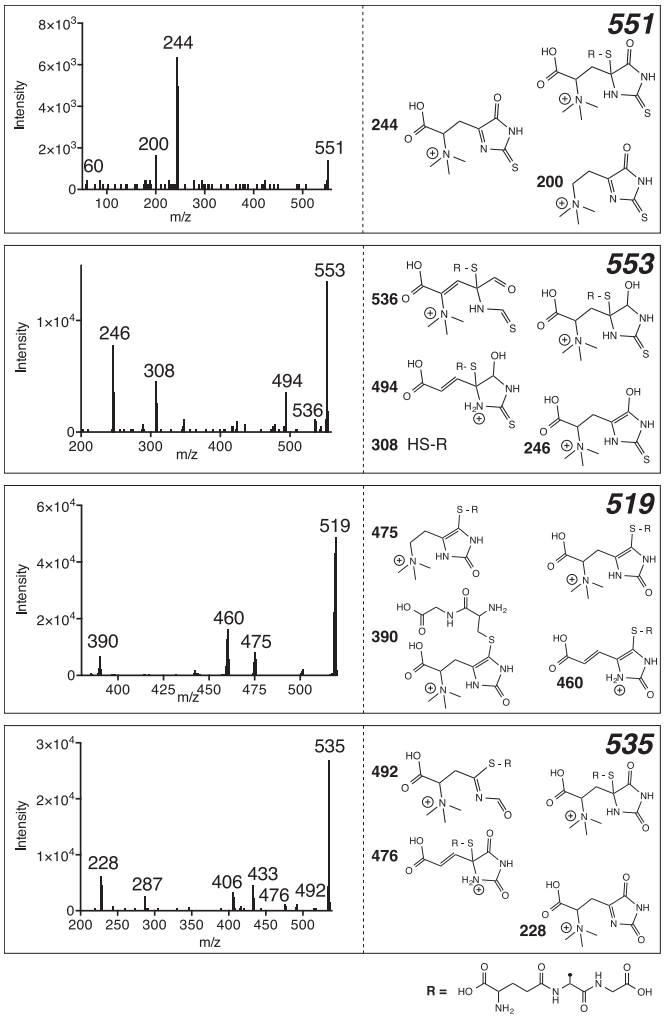

Fig. 9. Products of ET or hercynine and $^1O_2$ made with GSH. See legend to Fig. 2 and Table 1 for further details. Additional doubly charged hercynine product ions were observed at *m/z* 260 (= (519 + 1)/2) in 0.1 mM GSH and at *m/z* 268 (= (535 + 1)/2) in 1.0 mM GSH. In 5 mM GSH, both ions were absent.

In assays with 100 μM hercynine and 10 mM $DHPNO_2$, addition of 1 mM GSH yielded new compounds at *m/z* 519 and 535. Compound 519 likely is an aromatic hercynine derivative with a carbonyl at position 2 and GSH at position 5 of the imidazole ring (Fig. 9). Compound 535 contains a carbonyl at position 2, GSH at position 4, and a carbonyl at position 5.

Precise quantitation by SRM (Fig. 10) of ET products revealed that compound 262 was completely eliminated by 1 mM GSH. Compound 264 was increased from water to 0.1 mM GSH and then remained stable at 1 and 5 mM GSH. ET product 246:143 was reduced with 0.1 mM GSH, but partly restored in 1 mM GSH. Products made from ET, $^1O_2$, and GSH changed markedly with GSH concentration: at 0.1 mM GSH, the sole product was at 551. At 1.0 mM GSH, the major product was 553. At 5 mM GSH, both compounds were reduced. The ET dimer was completely eliminated by 0.1 mM GSH or higher. The initial production of hercynine from ET remained stable, even at 5 mM GSH; the hercynine product 248 declined in the presence of GSH.

In the hercynine SRM assays, 1 mM GSH greatly diminished the production of 230 and 248; the initial production of 246:229 was also reduced. The hercynine/GSH product 519 was generated more rapidly than compound 535; both compounds were stable. At 5 mM GSH, only 535 gave a small signal in difference shading (not shown).

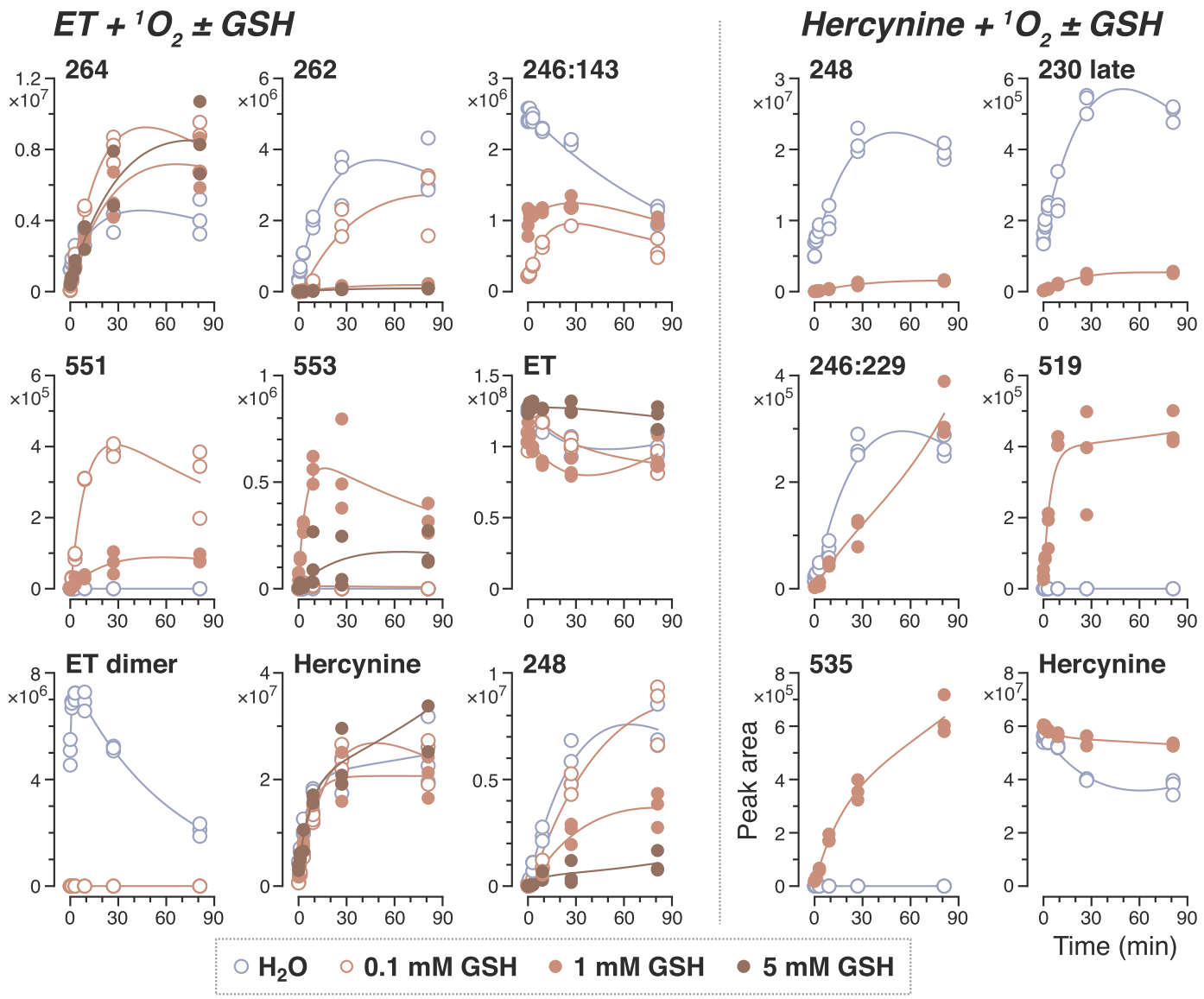

Fig. 10. Relative compound levels as a function of time in assays with ET or hercynine and $^1O_2$ in water ± GSH. Peak areas were determined by SRM as defined in Table 1. $^1O_2$ was generated from 10 mM $DHPNO_2$.

4. Discussion

For proper interpretation of our data, it is important to mind the constraints of the present study: 1.) Generation of $^1O_2$ decreases exponentially with time; the half-life of $DHPNO_2$ at 37 °C is 23 min [36]. Thus, after 76 min the rate of $^1O_2$ generation is down to 10% of the initial rate obtained shortly after mixing in the ice-cold $DHPNO_2$. 2.) The temperature-dependent release of $^1O_2$ from $DHPNO_2$ could promote reactions after assay termination at temperatures above room temperature. This may have been relevant for our zero time samples at the beginning of HPLC separation in LC-MS. We have not used azide as a physical quencher of $^1O_2$ here to stop reactions, since azide as a nucleophile could modify results. 3.) We could not detect unstable intermediates that react very fast. Structures were assembled based on SRM and HRMS data only, so some details remain tentative. NMR studies could refine structures, but it may be difficult to purify many compounds identified in this study in sufficient amounts since they were unstable during storage of samples at −20 °C (data not shown). 4.) A comparison of product amounts is not possible on the basis of the SRM peak area results (Figs. 5, 7, 8, and 10) since the efficiencies of fragment generation could be widely different. In the absence of authentic standards, we resorted to the comparison of full scan peak areas (Table 1). In this mode, ionization efficiencies of related compounds might be roughly similar.

Our reactions products of hercynine and $^1O_2$ (Fig. 2) agree mostly with previous reports on photooxidation products of histidine and derivatives [42,43]. It was suggested that some of the detected products were hydroperoxides [42], but in that study no MS fragmentation was performed. Our fragments look plausible without assuming hydroperoxides in the parent compounds. Moreover, it was calculated that imidazole hydroperoxides should be rather unstable [44].

The *in vitro* reaction of ET and $^1O_2$ at pH 7.4 directly yielded 3 main products: compounds 264, 262, and 246:143 (Table 1, Figs. 3 and 5). In parallel, ET is partly (see below) converted to hercynine which then yields further $^1O_2$ reaction products like 248 and 246:229. Although the initial slope of production of 264 was greater than that of 262 (Figs. 5 and 8), 262 was actually generated about 5 times faster than 264, since the full scan peak area of 262 at 60 min (Table 1) was 8 times higher. The initial increase of 246:143 at 10 mM $DHPNO_2$ was not resolved here, but the markedly lower curve for 1 mM $DHPNO_2$ proves that 246:143 is truly a $^1O_2$ reaction product. The decrease over time indicates a further reaction.

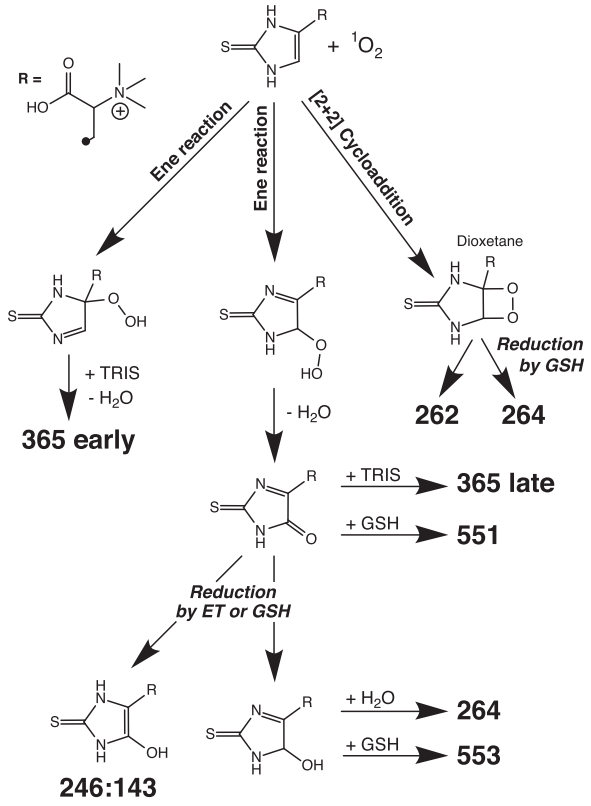

Fig. 11. Reaction of ET with singlet oxygen. The scheme shows the major products and proposed reaction intermediates. See Table 1 for compound codes.

By analogy to previous reports [42] we expect uncharged TRIS to act as a simple amine nucleophile in the addition to imine intermediates [43]. At pH 7.4 and 37 °C, 25 mM TRIS corresponds to 8.1 mM free (uncharged) base (pK_a 37 °C = 7.72). In the ET assays we have discerned a large amount of two TRIS products, 365 early and 365 late. Production of 365 late was inhibited by GSH, whereas 365 early was unaffected (Fig. 7). To explain this striking difference, we propose as reaction intermediates 2 isomeric hydroperoxides (Fig. 11). The compound with the hydroperoxide at position 5 of the ring contains a geminal proton which allows the intramolecular elimination of water [45] to yield an intermediate (M_r = 244) that can react by addition of TRIS or GSH to the imine moiety. The 4-hydroperoxide has no geminal proton; here, reaction with TRIS is possible to yield 365 early, but lack of inhibition suggests that GSH cannot react. Interestingly, in the mass spectrometer collision of 365 early (but not of 365 late) with nitrogen gas regenerated ET (Fig. 6). At the same time, TRIS should be released as a C-nitroso compound. In agreement with our model (Fig. 11), raising TRIS from 5 to 25 mM increased 365 late; however, it is unclear why 365 early was diminished (Fig. 7).

Addition of 25 mM TRIS to the ET assay vastly inhibited the generation of 246:143 and 264 (Fig. 8). These compounds thus probably are following the postulated intermediate (M_r = 244) that leads to the TRIS compound 365 late; reduction by ET (oxidized to the dimer) or GSH (see below) would yield 246:143 directly and 264 indirectly (addition of water to an imine). Amazingly, TRIS even at 25 mM did not inhibit the generation of compound 262 (Fig. 8). This suggests that generation of 262 does not involve an external nucleophilic attack like addition to an imine: both oxygen atoms from the initial attack of $^1O_2$ should be incorporated into this compound. We propose here the intramolecular conversion of a dioxetane intermediate to compound 262 (Fig. 11). In the hercynine assays, 25 mM TRIS vastly diminished the generation of all products (Fig. 8). By contrast to ET product 262, there is no TRIS-resistant hercynine reaction pathway.

TRIS and GSH are both good nucleophiles, but in contrast to TRIS, GSH is also a potent reductant: 25 mM TRIS hardly affected (Fig. 8), but 0.1 mM GSH completely inhibited ET dimer formation (Fig. 10), in agreement with previous reports [46]. The responses to GSH challenge in the ET assay are therefore more complex (Fig. 10). Most importantly, compound 262 is completely gone at 1 mM GSH or higher. However, compound 264 is doubled from water to 0.1 mM GSH and then remains high even at 5 mM GSH. Since 262 was stable with 25 mM TRIS (Fig. 8), only reduction of compound 262 (to yield 264) or reduction of a precursor of 262 would be plausible. Compounds 551 and 553, which incorporate GSH, were rapidly formed (Fig. 10), but then declined - by contrast to the stable TRIS compound 365 late. This probably indicates relatively rapid turnover on top of declining $^1O_2$ levels. Remarkably, at 0.1 mM GSH the production of 551 was high, but production of 246:143 was low. The further increase of GSH attenuated production of 551, but increased 246:143. 553 was high at 1 mM GSH, but lower at 5 mM GSH. The much lower accumulation of GSH products compared to TRIS products (based on full scan peak area data, Table 1) suggests swift decay of ET GSH products. GSH at 5 mM may operate predominantly as a reductant at a step preceding the imine addition steps. We propose reduction of the dioxetane (Fig. 11) to yield compound 264.

Remarkably and by contrast to 25 mM TRIS (Fig. 8), at 5 mM GSH the level of ET was almost stable (Fig. 10). This suggests that GSH inhibits the major processes that cause ET loss in water. Alternatively or additionally, GSH might open up a (reductive) route to regeneration of ET that is not available with TRIS. Note that the production of hercynine from ET continued unabated in 5 mM GSH (Fig. 10). This unidentified path must therefore have minor importance for the depletion of ET in these assays.

In the hercynine assays, 1 mM GSH attenuated the depletion of hercynine (Fig. 10). Fittingly, GSH abolished the generation of 248 and 230 late, and decreased the rate of production of 246:229. Thus, by contrast to the ET product 264, the generation of all hercynine products was inhibited by GSH. This difference reveals an astounding affinity of ET for $^1O_2$: although the thiol in GSH is a notable target for $^1O_2$ itself [47], a 50-fold excess of GSH (5 mM) over ET (0.1 mM) did not inhibit production of compound 264. In other words, $^1O_2$ favors ET over GSH for the initial reaction by at least a factor of 50.

Release of thiourea might be a minor side reaction in the ET + $^1O_2$ assays (Fig. 4), but thiourea corroborates the difference between ET and hercynine: thiourea reacted vigorously with hercynine + $^1O_2$ to yield the stable aromatic compound 288, but no products containing thiourea were detected with ET + $^1O_2$. This may reflect rapid breakdown of ET intermediates after nucleophilic attack of thiourea. Attack via sulfur seems likely, since urea (0.1 mM) did not generate products in the hercynine + $^1O_2$ and ET + $^1O_2$ assays.

Overall, our data demonstrate that the reactivity of ET towards $^1O_2$ is very different from hercynine. While the imidazole ring of hercynine simply offers the reaction paths of imidazole/histidine based on an initial [4+2] cycloaddition, in ET the doubly bonded sulfur at position 2 effectively blocks this position for endoperoxide resolution. We propose that the 4,5-dioxetane (from a [2+2] cycloaddition of $^1O_2$ [48,49]) and two hydroperoxides (from Schenck ene reactions [50]) are the initial products here (Fig. 11). Full methylation of the amino group prevents the subsequent intramolecular reactions known from histidine [42]. The consequences are apparent from the TRIS products: the hercynine product 333 has a stable aromatic ring which resists fragmentation; the ET products 365 early and 365 late break up easily to become aromatic. This hints at a facile route to regenerate ET. Indeed, in our pilot studies, ET was not consumed when $^1O_2$ was generated massively with an illuminated photosensitzer inside living cells. With typical intracellular concentrations of 5–10 mM [51], we expect GSH to be the partner for regeneration here, perhaps by decomposition of the GSH products.

It remains to be seen whether ET provides relevant protection inside living cells under $^1O_2$ attack, in particular in erythrocytes. The typical ET content at 1 mM is not far away from the hemoglobin concentration

of roughly 20 mM (calculated for the monomer). We estimate that ET would make a difference if it was roughly 100-fold more reactive in this cellular context towards $^1O_2$ than the accessible His residues in the hemoglobin tetramers.

In conclusion, the *in vitro* products of singlet oxygen identified here establish fundamental differences between ergothioneine and hercynine. While hercynine like other imidazoles engages in [4 + 2] cycloaddition, ET - because of the doubly bonded sulfur - supports [2 + 2] cycloaddition and Schenck ene reactions. The generation of specific products from ET, but not from hercynine, was resistant to a large excess of TRIS and GSH. This suggests that $^1O_2$ markedly favors ET over GSH (at least 50-fold) and TRIS (at least 250-fold) for the initial reaction. Loss of ET was nearly abolished in 5 mM GSH, but not in 25 mM TRIS. MS fragmentation data hint at a path to regeneration, since some ET products – by contrast to the corresponding hercynine products - decomposed easily to become aromatic.

Acknowledgments

We thank Simone Kalis and Samira Boussettaoui for skillful technical assistance. This research did not receive any specific grant from funding agencies in the public, commercial, or not-for-profit sectors.

References

[1] D.B. Melville, Ergothioneine, Vitam. Horm. 17 (1958) 155–204.
[2] M.D. Kalaras, J.P. Richie, A. Calcagnotto, R.B. Beelman, Mushrooms: a rich source of the antioxidants ergothioneine and glutathione, Food Chem. 233 (2017) 429–433.
[3] C. Pfeiffer, T. Bauer, B. Surek, E. Schömig, D. Gründemann, Cyanobacteria produce high levels of ergothioneine, Food Chem. 129 (4) (2011) 1766–1769.
[4] F.P. Seebeck, In vitro reconstitution of mycobacterial ergothioneine biosynthesis, J. Am. Chem. Soc. 132 (19) (2010) 6632–6633.
[5] P.E. Hartman, Ergothioneine as Antioxidant, Methods in Enzymology 186 Academic Press, 1990, pp. 310–318.
[6] K. Peckelsen, J. Martens, L. Czympiel, J. Oomens, G. Berden, D. Gründemann, A. Meijer, M. Schäfer, Ergothioneine and related histidine derivatives in the gas phase: tautomer structures determined by IRMPD spectroscopy and theory, Phys. Chem. Chem. Phys. 19 (34) (2017) 23362–23372.
[7] D. Gründemann, S. Harlfinger, S. Golz, A. Geerts, A. Lazar, R. Berkels, N. Jung, A. Rubbert, E. Schömig, Discovery of the ergothioneine transporter, Proc. Natl. Acad. Sci. USA 102 (2005) 5256–5261.
[8] B.D. Paul, S.H. Snyder, The unusual amino acid L-ergothioneine is a physiologic cytoprotectant, Cell Death Differ. 17 (7) (2010) 1134–1140.
[9] T. Nakamura, K. Yoshida, H. Yabuuchi, T. Maeda, I. Tamai, Functional characterization of ergothioneine transport by rat organic cation/carnitine transporter Octn1 (slc22a4), Biol. Pharm. Bull. 31 (8) (2008) 1580–1584.
[10] P. Bacher, S. Giersiefer, M. Bach, C. Fork, E. Schömig, D. Gründemann, Substrate discrimination by ergothioneine transporter SLC22A4 and carnitine transporter SLC22A5: gain-of-function by interchange of selected amino acids, Biochim. Biophys. Acta 12 (2009) (1788) 2594–2602.
[11] S. Grigat, S. Harlfinger, S. Pal, R. Striebinger, S. Golz, A. Geerts, A. Lazar, E. Schömig, D. Gründemann, Probing the substrate specificity of the ergothioneine transporter with methimazole, hercynine, and organic cations, Biochem. Pharmacol. 74 (2) (2007) 309–316.
[12] D. Gründemann, The ergothioneine transporter controls and indicates ergothioneine activity - a review, Prev. Med. (54 Suppl.) (2012) S71–S74.
[13] D. Nikodemus, D. Lazić, M. Bach, T. Bauer, C. Pfeiffer, L. Wiltzer, E. Lain, E. Schömig, D. Gründemann, Paramount levels of ergothioneine transporter SLC22A4 mRNA in boar seminal vesicles and cross-species analysis of ergothioneine and glutathione in seminal plasma, J. Physiol. Pharmacol. 62 (4) (2011) 411–419.
[14] I.K. Cheah, B. Halliwell, Ergothioneine; antioxidant potential, physiological function and role in disease, Biochim Biophys. Acta 5 (2012) (1822) 784–793.
[15] C. Pfeiffer, M. Bach, T. Bauer, J. Campos da Ponte, E. Schömig, D. Gründemann, Knockout of the ergothioneine transporter ETT in zebrafish results in increased 8-oxoguanine levels, Free Radic. Biol. Med. 83 (2015) 178–185.
[16] R.W. Redmond, I.E. Kochevar, Spatially resolved cellular responses to singlet oxygen, Photochem. Photobiol. 82 (5) (2006) 1178–1186.
[17] E. Skovsen, J.W. Snyder, J.D. Lambert, P.R. Ogilby, Lifetime and diffusion of singlet oxygen in a cell, J. Phys. Chem. B 109 (18) (2005) 8570–8573.
[18] P.R. Ogilby, Singlet oxygen: there is indeed something new under the sun, Chem. Soc. Rev. 39 (8) (2010) 3181–3209.
[19] J.L. Ravanat, C. Saint-Pierre, P. Di Mascio, G.R. Martinez, M.H.G. Medeiros, J. Cadet, Damage to isolated DNA mediated by singlet oxygen, Helv. Chim. Acta 84 (12) (2001) 3702–3709.
[20] J. Cadet, J.L. Ravanat, G.R. Martinez, M.H. Medeiros, P. Di Mascio, Singlet oxygen oxidation of isolated and cellular DNA: product formation and mechanistic insights, Photochem. Photobiol. 82 (5) (2006) 1219–1225.
[21] J. Cadet, T. Douki, J.L. Ravanat, Oxidatively generated base damage to cellular DNA, Free Radic. Biol. Med. 49 (1) (2010) 9–21.
[22] C. Sheu, C.S. Foote, Reactivity toward Singlet Oxygen of a 7,8-Dihydro-8-Oxoguanosine (8-Hydroxyguanosine) Formed by Photooxidation of a Guanosine Derivative, J. Am. Chem. Soc. 117 (24) (1995) 6439–6442.
[23] H. Ali, J.E. van Lier, Metal complexes as photo- and radiosensitizers, Chem. Rev. 99 (9) (1999) 2379–2450.
[24] E. Nagababu, J.M. Rifkind, Reaction of hydrogen peroxide with ferrylhemoglobin: superoxide production and heme degradation, Biochemistry 39 (40) (2000) 12503–12511.
[25] J. Everse, N. Hsia, The toxicities of native and modified hemoglobins, Free Radic. Biol. Med. 22 (6) (1997) 1075–1099.
[26] J. Everse, M.C. Johnson, M.A. Marini, Peroxidative activities of hemoglobin and hemoglobin derivatives, Methods Enzymol. 231 (1994) 547–561.
[27] C. Kiryu, M. Makiuchi, J. Miyazaki, T. Fujinaga, K. Kakinuma, Physiological production of singlet molecular oxygen in the myeloperoxidase-H2O2-chloride system, FEBS Lett. 443 (2) (1999) 154–158.
[28] H. Tatsuzawa, T. Maruyama, K. Hori, Y. Sano, M. Nakano, Singlet oxygen ((1)Delta (g)O(2)) as the principal oxidant in myeloperoxidase-mediated bacterial killing in neutrophil phagosome, Biochem. Biophys. Res. Commun. 262 (3) (1999) 647–650.
[29] M.J. Steinbeck, A.U. Khan, M.J. Karnovsky, Extracellular production of singlet oxygen by stimulated macrophages quantified using 9,10-diphenylanthracene and perylene in a polystyrene film, J. Biol. Chem. 268 (21) (1993) 15649–15654.
[30] T.A. Dahl, W.R. Midden, P.E. Hartman, Some prevalent biomolecules as defenses against singlet oxygen damage, Photochem. Photobiol. 47 (3) (1988) 357–362.
[31] P.E. Hartman, Z. Hartman, K.T. Ault, Scavenging of singlet molecular oxygen by imidazole compounds: high and sustained activities of carboxy terminal histidine dipeptides and exceptional activity of imidazole-4-acetic acid, Photochem. Photobiol. 51 (1) (1990) 59–66.
[32] T.P. Devasagayam, A.R. Sundquist, P. Di Mascio, S. Kaiser, H. Sies, Activity of thiols as singlet molecular oxygen quenchers, J. Photochem. Photobiol. B 9 (1) (1991) 105–116.
[33] M. Rougee, R.V. Bensasson, E.J. Land, R. Pariente, Deactivation of singlet molecular oxygen by thiols and related compounds, possible protectors against skin photosensitivity, Photochem. Photobiol. 47 (4) (1988) 485–489.
[34] L. Servillo, D. Castaldo, R. Casale, N. D'Onofrio, A. Giovane, D. Cautela, M.L. Balestrieri, An uncommon redox behavior sheds light on the cellular antioxidant properties of ergothioneine, Free Radic. Biol. Med. 79 (2015) 228–236.
[35] S. Tada-Oikawa, S. Oikawa, J. Hirayama, K. Hirakawa, S. Kawanishi, DNA damage and apoptosis induced by photosensitization of 5,10,15,20-tetrakis (N-methyl-4-pyridyl)−21H,23H-porphyrin via singlet oxygen generation, Photochem. Photobiol. 85 (6) (2009) 1391–1399.
[36] C. Pierlot, J.M. Aubry, K. Briviba, H. Sies, P. Di Mascio, Naphthalene endoperoxides as generators of singlet oxygen in biological media, Methods Enzymol. 319 (2000) 3–20.
[37] A. Dewilde, C. Pellieux, C. Pierlot, P. Wattre, J.M. Aubry, Inactivation of intracellular and non-enveloped viruses by a non-ionic naphthalene endoperoxide, Biol. Chem. 379 (11) (1998) (1377-9).
[38] J.F. Xiao, B. Zhou, H.W. Ressom, Metabolite identification and quantitation in LC-MS/MS-based metabolomics, Trends Anal. Chem. 32 (2012) 1–14.
[39] V.N. Reinhold, Y. Ishikawa, D.B. Melville, Synthesis of alpha-N-methylated histidines, J. Med. Chem. 11 (2) (1968) 258–260.
[40] O. Cakmak, I. Demirtas, H.T. Balaydin, Selective bromination of 1-bromonaphthalene: efficient synthesis of bromonaphthalene derivatives, Tetrahedron 58 (28) (2002) 5603–5609.
[41] G.R. Martinez, J.L. Ravanat, M.H.G. Medeiros, J. Cadet, P. Di Mascio, Synthesis of a naphthalene endoperoxide as a source of O-18-labeled singlet oxygen for mechanistic studies, J. Am. Chem. Soc. 122 (41) (2000) 10212–10213.
[42] V.V. Agon, W.A. Bubb, A. Wright, C.L. Hawkins, M.J. Davies, Sensitizer-mediated photooxidation of histidine residues: evidence for the formation of reactive side-chain peroxides, Free Radic. Biol. Med. 40 (4) (2006) 698–710.
[43] H.R. Shen, J.D. Spikes, C.J. Smith, J. Kopecek, Photodynamic cross-linking of proteins - IV. nature of the his-his bond(s) formed in the rose bengal-photosensitized cross-linking of N-benzoyl-L-histidine, J. Photochem. Photobiol. A 130 (1) (2000) 1–6.
[44] J. Mendez-Hurtado, R. Lopez, D. Suarez, M.I. Menendez, Theoretical study of the oxidation of histidine by singlet oxygen, Chemistry 18 (27) (2012) 8437–8447.
[45] E.L. Clennan, A. Pace, Advances in singlet oxygen chemistry, Tetrahedron 61 (28) (2005) 6665–6691.
[46] C.E. Hand, J.F. Honek, Biological chemistry of naturally occurring thiols of microbial and marine origin, J. Nat. Prod. 68 (2) (2005) 293–308.
[47] K. Briviba, H. Sies, Biological singlet oxygen quenchers assessed by monomol light emission, Methods Enzymol. 319 (2000) 222–226.
[48] L.A. MacManus-Spencer, D.E. Latch, K.M. Kroncke, K. McNeill, Stable dioxetane precursors as selective trap-and-trigger chemiluminescent probes for singlet oxygen, Anal. Chem. 77 (4) (2005) 1200–1205.
[49] S. Kai, M. Suzuki, Dye-sensitized photooxidation of 2,4-disubstituted imidazoles: the formation of isomeric imidazolinones, Heterocycles 43 (6) (1996) 1185–1188.
[50] L.B. Harding, W.A. Goddard, Mechanism of the Ene Reaction of Singlet Oxygen with Olefins, J. Am. Chem. Soc. 102 (2) (1980) 439–449.
[51] V.I. Lushchak, Glutathione homeostasis and functions: potential targets for medical interventions, J. Amino Acids 2012 (2012) 736837.